

GIS for Safety & Security Management

GIS Ostrava 2018



conference proceedings

ISBN 978-80-248-4235-6

VŠB - Technical University of Ostrava

Igor IVAN, Jan CAHA and Jaroslav BURIAN (Eds.)

GIS for Safety & Security Management



**GIS Ostrava
2018**

March 21st – 23rd 2018

Auspices

ISPRS - International Society for Photogrammetry and Remote Sensing

CAGI - Czech Association for Geoinformation

ČKS - Czech Cartographic Society

Ivo Vondrák - President of the Moravian-Silesian Region

Tomáš Macura - Mayor of the City of Ostrava

Václav Snášel - Rector of VŠB - Technical University of Ostrava

Editors

Igor Ivan
VŠB - Technical University of Ostrava
Institute of Geoinformatics
17. listopadu 15, 708 33
Ostrava - Poruba, Czech Republic
igor.ivan@vsb.cz

Jan Caha
Mendel University in Brno
Faculty of Regional Development and International Studies
tř. Generála Píky 7, 61300
Brno, Czech Republic
jan.caha@mendelu.cz

Jaroslav Burian
Palacký University Olomouc
Department of Geoinformatics
17. listopadu 50, 771 46
Olomouc, Czech Republic
jaroslav.burian@upol.cz

Technical editing, typesetting: Tomáš Inspektor, Igor Ivan

Production:

Department of Geoinformatics
VŠB - Technical University of Ostrava
17. listopadu 15, 708 33, Ostrava - Poruba, Czech Republic
tomas.inspektor@vsb.cz

GIS Ostrava 2018 – GIS for Safety & Security Management

March 21st – 23rd 2018, Ostrava, Czech Republic

Edition: First edition, 2018

Number of pages: 250

This proceedings is subject of copyright. All rights are reserved, whether the whole or part of the book is concerned, specifically the rights of reprinting, reuse of illustrations, reproducing or transmitted in any form or by any means, including photocopying, microfilming, and recording, or by any information storage or retrieval system, without prior permission in writing from the publisher.
Product or corporate names may be trademarks or registered names, and are used only for identification and explanation, without intent to infringe.

© VŠB - Technical University of Ostrava, 2018

ISBN 978-80-248-4235-6

Preface

Dear Colleagues,

In a turbulent world, many threats and challenges are endangering society. Important questions regarding how geospatial technologies can help to protect people, information, critical infrastructure, property, and environments, can be raised. These questions can include the following: How to build and utilize smart cities to be resilient to possible threats? How to divide the responsibility and development of safe and security management among the state and local governments, rescue and security organizations, and GI community?

Current and future GI-technologies are often requested to provide accurate and up-to-date geospatial data gathered from advanced technologies, including new satellite missions, UAV, UGV, sensor networks, mobile phones, social networks, crowdsourcing, and others. Tracking and predicting mobility of people, means, and sources, effective data collection, and fast processing are key features of future geospatial systems for security management. Such data might provide new valuable insights into many spatial processes. Processing of these highly diverse data sources, as well as big geodata, is still a relatively new topic for GIScience. The utilization of such datasets requires implementation of new techniques for risk and hazard optimization, dealing with uncertainty, improvements of modeling and simulations within the context spatial analyses as well as it requires enhancements of spatial visualizations and cartographic capabilities for event management.

Improvement of GI-technologies should support the collaboration of emergency services, law enforcement, military, and intelligence staff, as well as central and local governance, researchers, and society.

Dr. Igor Ivan

Dr. Jan Caha

Dr. Jaroslav Burian

Scientific Committee

Igor Ivan (VŠB-Technical University of Ostrava, CZE) - chair
Vojtěch Bravenec (Police of the Czech Republic, CZE)
Michael Leitner (Louisiana State University, USA)
Jiří Horák (VŠB-Technical University of Ostrava, CZE)
Martin Raubal (ETH Zurich, CHE)
Petr Kubíček (Masaryk University, CZE)
Harry J.P. Timmermans (Eindhoven University of Technology, NLD)
Hassan Karimi (University of Pittsburgh, USA)
Elena Moltchanova (University of Canterbury, NZL)
Petr Lukeš (Czechgloge, CZ)
Lex Comber (University of Leicester, GBR)
Juha Oksanen (Finnish Geospatial Research Institute, FI)
Gennady Andrienko (Fraunhofer Institute for Intelligent Analysis and Information Systems, GE)
Natalia Andrienko (Fraunhofer Institute for Intelligent Analysis and Information Systems, GE)
Mikhail Kanevski (University of Lausanne, CHA)
Andy Newton (University of Leicester, GBR)
Simon Scheider (Utrecht University, NLD)
Juan Carlos García Palomares (Universidad Complutense de Madrid, ESP)
Ákos Jakobi (Eötvös Loránd University, Budapest, HUN)
Jan Caha (Mendel University in Brno, CZE)
Jaroslav Burian (Palacký University Olomouc, CZE)
David W. Wong (George Mason University, USA)
Jed A. Long (University of St Andrews, GB)
Soora Rasouli (Eindhoven University of Technology, NLD)
Josef Strobl (University of Salzburg, AT)
Carsten Jürgens (Ruhr-Universität Bochum, GE)
Jakub Vorel (Czech Technical University in Prague, CZE)
Marcin Stępnia (Polish Academy of Sciences, PL)
Bin Jiang (University of Gävle, SWE)
Wolfgang Reinhardt (University of the Bundeswehr Munich, GE)
Katarzyna Sila-Nowicka (University of Glasgow, GB)

List of Contributors

Edeko BABINE Sambus Geospatial Nigeria Limited, FCT, Abuja, Nigeria

Vincenzo BARRILE Geomatics Lab, DICEAM, Mediterranea University, loc. Feo di Vito, 89123, Reggio Calabria, Italy

Petr BERGLOWIEC IT4Innovations, VŠB - Technical University of Ostrava, 17. listopadu 15/2172, 708 33 Ostrava-Poruba, Czech Republic

Jan BITTA Department of Environmental Protection in Industry, Faculty of Metallurgy and Material Engineering, VSB - Technical University of Ostrava, 17.listopadu 15/2172, 708 33, Czech Republic

Jan CAHA Department of Regional Development and Public Administration, Mendel University in Brno, Zemědělská 1, 613 00, Brno, Czech Republic

Róbert CIBULA State Geological Institute of Dionýz Štúr, Mlynská dolina 1, 817 04, Bratislava, Slovakia

Jaromír ČAPEK Department of Military Geography and meteorology, Faculty of Military Technologies, University of Defence in Brno, Kounicova 65, 66210, Brno, Czech Republic

Adam DĄBROWSKI Institute of Geoecology and Geoinformation, Faculty of Geographical and Geological Sciences, Adam Mickiewicz University in Poznań, Bogumiła Krygowskiego 12, 61-606, Poznań, Poland

Filip DOHNAL Department of Military Geography and Meteorology, Faculty of Military Technologies, University of Defence, Kounicova 65,662 10, Brno, Czech Republic

Renata ĎURAČIOVÁ Department of Theoretical Geodesy, Faculty of Civil Engineering, Slovak University of Technology in Bratislava, Radlinského 11, 810 05, Bratislava, Slovak Republic

Jitka ELZNICOVÁ Faculty of Environment, J.E. Purkyně University in Ústí nad Labem, Králova výšina 7, 40096, Ústí nad Labem, Czech Republic

Jana FAIXOVÁ CHALACHANOVÁ Department of Theoretical Geodesy, Faculty of Civil Engineering, Slovak University of Technology in Bratislava, Radlinského 11, 810 05, Bratislava, Slovak Republic

Olutoyin FASHAE Department of Geography, University of Ibadan, 200284 Ibadan, Oyo, Nigeria

Antonino FOTIA Geomatics Lab, DICEAM, Mediterranea University, loc. Feo di Vito, 89123, Reggio Calabria, Italy

Shitta HABU Department of Geography, University of Abuja, P.M.B. 117 FCT-Abuja, Nigeria

Jiří HANZELKA IT4Innovations, VŠB - Technical University of Ostrava, 17. listopadu 15/2172, 708 33 Ostrava-Poruba, Czech Republic

Radovan HLADKÝ Department of Applied Geoinformatics and Cartography, Faculty of Science, Charles University, Albertov 6, Prague 2, 128 43

Jiří HORÁK Institute of Geoinformatics, Faculty of Mining and Geology, VŠB-Technical University of Ostrava, 17. listopadu 15/2172, 708 33 Ostrava-Poruba, Czech Republic

Michal HOŠEK Faculty of Environment, J.E. Purkyně University in Ústí nad Labem, Králova výšina 7, 40096 Ústí nad Labem, Czech Republic

Martin HUBÁČEK Department of Military Geography and Meteorology, Faculty of Military Technologies, University of Defence, Kounicova 65,662 10, Brno, Czech Republic

Igor IVAN Institute of Geoinformatics, Faculty of Mining and Geology, VŠB-Technical University of Ostrava, 17. listopadu 15/2172, 708 33 Ostrava-Poruba, Czech Republic

Ákos JAKOBI Department of Regional Science, Faculty of Sciences, Eötvös Loránd University, Pázmány Péter sétány 1/c, H-1117, Budapest, Hungary

Petr JANČÍK Department of Environmental Protection in Industry, Faculty of Metallurgy and Material Engineering, VSB - Technical University of Ostrava, 17.listopadu 15/2172, 708 33, Czech Republic

Jaromír KOLEJKA Institute of Geonics, Drobného 28, 602 00, Brno, Czech Republic

Michal KRUMNIKL IT4Innovations, VŠB - Technical University of Ostrava, 17. listopadu 15/2172, 708 33 Ostrava-Poruba, Czech Republic

Jan KŘENEK IT4Innovations, VŠB - Technical University of Ostrava, 17. listopadu 15/2172, 708 33 Ostrava-Poruba, Czech Republic

Josef LAŠTOVIČKA Department of Applied Geoinformatics and Cartography, Faculty of Science, Charles University, Albertov 6, Prague 2, 128 43

Milan LAZECKÝ IT4Innovations, VSB-TUO, 17. listopadu 15, 708 33 Ostrava-Poruba, Czech Republic

Jan MARTINOVIČ IT4Innovations, VŠB - Technical University of Ostrava, 17. listopadu 15/2172, 708 33 Ostrava-Poruba, Czech Republic

Tereza MATĚJOVÁ Institute of Environmental Engineering, Faculty of Mining and Geology, VŠB-Technical University of Ostrava, 17. listopadu 15/2172, 708 33 Ostrava-Poruba, Czech Republic

Piotr MATCZAK Institute of Sociology, Faculty of Social Sciences, Adam Mickiewicz University in Poznań, Augustyna Szamarzewskiego 89c, 60-568 Poznań, Poland

Tomáš MATYS GRYGAR Faculty of Environment, J.E. Purkyně University in Ústí nad Labem, Králova výšina 7, 40096 Ústí nad Labem, Czech Republic

Milan MUŇKO Department of Theoretical Geodesy, Faculty of Civil Engineering, Slovak University of Technology in Bratislava, Radlinského 11, 810 05, Bratislava, Slovak Republic

Petr NOVÁK Faculty of Environment, J.E. Purkyně University in Ústí nad Labem, Králova výšina 7, 40096 Ústí nad Labem, Czech Republic

Jana NOVÁKOVÁ Institute of Environmental Engineering, Faculty of Mining and Geology, VŠB-Technical University of Ostrava, 17. listopadu 15/2172, 708 33 Ostrava-Poruba, Czech Republic

Chukwudi NWAOGU Department of Geoinformatics, Palacký University, Olomouc, 771 46, Czech Republic

Josua OKEKE Sambus Geospatial Nigeria Limited, FCT, Abuja, Nigeria

Daniel PALUBA Department of Applied Geoinformatics and Cartography, Faculty of Science, Charles University, Albertov 6, Prague 2, 128 43

Irena PAVLÍKOVÁ Department of Environmental Protection in Industry, Faculty of Metallurgy and Material Engineering, VSB - Technical University of Ostrava, 17.listopadu 15/2172, 708 33, Czech Republic

Vilém PECHANEC Department of Geoinformatics, Palacký University, Olomouc, 771 46, Czech Republic

Andrea PÓDÖR Institute of Geoinformatics, Alba Regia Technical Faculty, Óbuda University, Pirosalma u. 1-3, H-8000, Székesfehérvár, Hungary

Tomáš POHANKA Department of Geoinformatics, Palacký University, Olomouc, 771 46, Czech Republic

Jan POPELKA Faculty of Environment, J.E. Purkyně University in Ústí nad Labem, Králova výšina 7, 40096 Ústí nad Labem, Czech Republic

Josef RADA Department of Military Geography and Meteorology, Faculty of Military Technology, University of Defence in Brno, Kounicova 65, Brno 662 10, Czech Republic

Francisco RAMOS Institute of New Imaging Technologies, Universitat Jaume I, Avda. Sos Baynat, 12071, Castellon, Spain

Aleš RUDA Department of regional development and public administration, Faculty of regional development and international studies, Mendel university in Brno, třída gen. Píky 7, 613 00, Brno, Czech Republic

Jan RŮŽIČKA Institute of Geoinformatics, Faculty of Mining and Geology, VŠB-Technical University of Ostrava, 17. listopadu 15/2172, 708 33 Ostrava-Poruba, Czech Republic

Kateřina RŮŽIČKOVÁ Institute of Geoinformatics, Faculty of Mining and Geology, VŠB-Technical University of Ostrava, 17. listopadu 15/2172, 708 33 Ostrava-Poruba, Czech Republic

Tomáš ŘEZNÍK Masaryk University, Faculty of Science, Department of Geography, Kotlarska 2, 611 37, Brno, the Czech Republic

Martin SIKORA Faculty of Environment, J.E. Purkyně University in Ústí nad Labem, Králova výšina 7, 40096 Ústí nad Labem, Czech Republic

Thakur SILWAL Department of National Park and Wildlife Conservation, Institute of Forestry, Tribhuvan University, Pokhara Campus - 15, Hariyokharka, Pokhara, Nepal

Adu SIMON Sambus Geospatial Nigeria Limited, FCT, Abuja, Nigeria

Václav SVATOŇ IT4Innovations, VŠB - Technical University of Ostrava, 17. listopadu 15/2172, 708 33 Ostrava-Poruba, Czech Republic

Vladislav SVOZILÍK Institute of Geoinformatics, Faculty of Mining and Geology, VŠB-Technical University of Ostrava, 17. listopadu 15/2172, 708 33 Ostrava-Poruba, Czech Republic

Kateřina ŠIMKOVÁ Department of Military Geography and Meteorology, Faculty of Military Technologies, University of Defence, Kounicova 65,662 10, Brno, Czech Republic

Přemysl ŠTYCH Department of Applied Geoinformatics and Cartography, Faculty of Science, Charles University, Albertov 6, Prague 2, 128 43

Václav TALHOFER Department of Military Geography and meteorology, Faculty of Military Technoloies, University of Defence in Brno, Kounicova 65, 66210, Brno, Czech Republic

Patrik VETEŠKA IT4Innovations, VŠB - Technical University of Ostrava, 17. listopadu 15/2172, 708 33 Ostrava-Poruba, Czech Republic

Vít VONDRÁK IT4Innovations, VŠB - Technical University of Ostrava, 17. listopadu 15/2172, 708 33 Ostrava-Poruba, Czech Republic

Andrzej WÓJTOWICZ Faculty of Mathematics and Computer Science, Adam Mickiewicz University in Poznań, Umultowska 87, 61-614, Poznań, Poland

Pravesh YAGOL Institute of New Imaging Technologies, Universitat Jaume I, Avda. Sos Baynat, 12071, Castellon, Spain

Content

URBAN FACTORS INFLUENCING SPATIAL DISTRIBUTION OF DISCARDED SYRINGES AND NEEDLES IN OSTRAVA Jiří HORÁK and Igor IVAN	1
DIGITAL SKETCH MAPS DETECTING PLACES OF FEAR OF CRIME Andrea PÓDÖR and Ákos JAKOBI	22
ERROR PROPAGATION IN WATERSHED ASSESMENT. A CASE STUDY OF DELINEATION POLLUTION CONTRIBUTION AREA Kateřina RŮŽIČKOVÁ, Jana NOVÁKOVÁ, Tereza MATĚJOVÁ and Jan RŮŽIČKA	32
DEVELOPMENT OF THE SYSTEM FOR ONLINE TESTING AND EXAMINATION IN THE DOMAIN OF GEOSCIENCES Milan MUŇKO, Jana FAIXOVÁ CHALACHANOVÁ and Renata ĎURAČIOVÁ	43
SPATIO-TEMPORAL VULNERABILITY ANALYSES OF LANDSCAPE AND CLIMATE EFFECTS ON MALARIA PREVALENCE USING GEOSTATISTICAL APPROACH IN SUB-SAHARA AFRICA Joshua OKEKE, Edeko BABINE, Adu SIMON, Chukwudi NWAOGU2 and Vilém PECHANEC	53
EVALUATION OF THE FOREST DISTURBANCES USING TIME SERIES OF LANDSAT DATA: A COMPARISON STUDY OF THE LOW TATRAS AND SUMAVA NATIONAL PARKS Přemysl ŠTYCH, Radovan HLADKÝ, Josef LAŠTOVIČKA and Daniel PALUBA	63
ADOPTING INTERNET OF THINGS CONCEPT TO SENSOR NETWORKS BASED ON GEOSPATIAL MODIFICATION OF LORAWAN AND MQTT Róbert CIBULA and Tomáš ŘEZNÍK	81
GEOMATIC SYSTEM FOR ANALYSIS AND MONITORING OF SHORELINE Vincenzo BARRILE and Antonino FOTIA	93

IMPROVING THE USER KNOWLEDGE AND USER EXPERIENCE BY USING AUGMENTED REALITY IN A SMART CITY CONTEXT Francisco RAMOS and Pravesh YAGOL	103
TRENDS IN COLLECTION OF TERRAIN INFORMATION IN THE CZECH MILITARY GEOGRAPHICAL SERVICE Josef RADA	113
THE SPECIFICS OF ACQUIRING EXPERTS OF GEOGRAPHIC AND METEOROLOGICAL SPECIALIZATIONS IN THE CZECH ARMY Jaromír ČAPEK and Václav TALHOFER	126
SAFETY SPATIAL ANALYSIS OF WILDLIFE ATTACKS IN CHITWAN, NEPAL Aleš RUDA, Jaromír KOLEJKA and Thakur SILWAL	134
THE SELECTION OF EXPERIMENTAL AND CONTROL AREAS IN CRIME ANALYSIS – THE PROBLEM OF SPATIALLY AGGREGATED DATA. Adam DĄBROWSKI, Piotr MATCZAK and Andrzej WÓJTOWICZ	147
THREAT OF POLLUTION HOTSPOTS REWORKING IN RIVER SYSTEMS: EXAMPLE OF THE PLOUČNICE RIVER (CZECH REPUBLIC) Jitka ELZNICOVÁ, Tomáš MATYS GRYGAR, Martin SIKORA, Jan POPELKA, Michal HOŠEK and Petr NOVÁK	159
NATURAL DISASTER VULNERABILITY, MANAGEMENT AND THE ROLES OF LAND USE/LAND COVER: AN ASSESSMENT OF LANDSLIDES USING GIS IN JOS, NIGERIA Chukwudi NWAOGU, Shitta HABU, Onyedikachi OKEKE, Vilém PECHANEC, Tomaš POHANKA and Olutoyin FASHAE	177
AIR POLLUTION DISPERSION MODELLING USING SPATIAL ANALYSES Jan BITTA, Irena PAVLÍKOVÁ, Vladislav SVOZILÍK and Petr JANČÍK	188
IDENTIFICATION OF R PACKAGES FOR SPATIAL DATA HANDLING AND ANALYSES Jan CAHA	200

IDENTIFICATION OF ACTIVE SLOPE MOTION IN CZECH ENVIRONMENT USING
SENTINEL-1 INTERFEROMETRY

Milan LAZECKÝ

212

FLOREON+: INTEGRATION OF DIFFERENT THEMATIC AREAS

Václav SVATOŇ, Patrik VETEŠKA, Jan KŘENEK, Jiří HANZELKA,
Petr BERGLOWIEC, Jan MARTINOVIČ, Michal KRUMNIKL and Vít
VONDRÁK

219

THE INFLUENCE OF MICRORELIEF ELEMENTS ON THE PASSABILITY OF THE
AREA

Martin HUBÁČEK, Filip DOHNAL and Kateřina ŠIMKOVÁ

229

URBAN FACTORS INFLUENCING SPATIAL DISTRIBUTION OF DISCARDED SYRINGES AND NEEDLES IN OSTRAVA

Jiri, HORAK¹; Igor, IVAN²

^{1,2}Department of Geoinformatics, Faculty of Mining and Geology, VŠB-Technical University of Ostrava, 17. listopadu 15/2172, 708 33 Ostrava-Poruba, Czech Republic

jiri.horak@vsb.cz, igor.ivan@vsb.cz

Abstract

Unsafely discarded syringes and needles by injection drug users represent significant health risk, degrade urban quality and provoke social intolerance. We have focused on city scale analysis of available urban factors which may indicate the higher concentration of IDUs and more attractive places for discards. Various residential and facilities characteristics as well as reported offences was expressed as densities and shares around randomly generated points in Ostrava. After the standard EDA and ESDA the method of decision trees was applied to predict high densities of discarded syringes/needles with two types of models – models with a target category and models with a scaled predictor. The average model accuracy for the classified predictor is about 75%. Main influencing factors are pollution offences, hostels (densities or shares), share of family housing and density of housing blocks but each year may emphasize the role of some other specific factors i.e. gambling clubs. According to the testing of different categories it seems hostels are important mainly to explain high occurrence of syringes/needles while pubs and schools influence the small and middle isolated occurrences. The results were verified using comparison of model probabilities for high occurrences, errors classification, distribution of significantly underestimated and overestimated values, and KDE isolines. Explanations of trends, errors and anomalies contribute to formulation of recommendations for further analyses.

Keywords: drug, syringes, decision tree, spatial distribution, urban factors

INTRODUCTION

Illicit drug usage is one of the symptoms of social pathology issues. The monitoring is quite difficult due to the personal sensitivity, stigmatization and frequent isolation which issue in a problem of phenomenon latency – usually we have some evidence only about a part of the drug scene.

The most serious form is the injection usage. The injection drug users (IDU) are at health risk not only for drug itself but also for blood-borne pathogens (mainly HIV, hepatitis B and hepatitis C viruses) due to multiperson use of contaminated needles and syringes. The overall long-term trend in injecting is declining in EU, nevertheless still there are many concerns especially for harm risks i.e. blood-borne infections are often diagnosed relatively late (EMCDAA, 2017a).

Syringes and needles (hereafter needles) used by IDU are discarded safely or unsafely ways. Needles discarded in open spaces by IDUs represent an important sign of social disorder that degrades community quality-of-life and provokes intolerance of much-needed health services,

such as needle exchange programs (NEP) (Montigny, 2008). Even more they represent certain health risks. The anxiety regarding discarded needles is not only that they are unsightly to the community, but that they might be handled by citizens, particularly children, and could lead to needle-stick injuries and HIV or hepatitis infections (Normand et al., 1995).

The NEP (and similar type of programmes) plays a crucial role to decrease the harm and negative impacts caused by uncontrolled needles' discards. The positive effect was confirmed by several studies, e.g. comparison of practices in a city with versus a city without such programme (Tookes et al., 2012). The possibility to improve the needle exchange service delivery by mapping user's needs was addressed by (Davidson et al., 2011). Effects of different types of drug-related litters in UK were studied by Parkin and Coomber (2011). The impact of physical distance from the point of NEP on HIV risk behaviours was proved by Bruneau et al. (2008). The neighbourhood-based measures for accessing NEP, drug-related law enforcement activities and their impacts to drug user health were explored by Cooper et al. (2009). Distance and temporal effects of NEP programme in local urban study was analysed by Montigny et al. (2010). The concerns about the implementation of NEPs that large-scale distribution of free sterile needles might lead to an increased number of discarded and possibly contaminated needles on the street were refused by Doherty et al. (1997).

It is not surprising the collection of discarded needles is one of the important tasks of officers of each municipal police.

What can be expected to influence the location and number of discarded needles? The most important is the number of IDU (not taken into account by Montigny) and environmental and social factors influencing the spaces associated with IDUs behaviour. To the opposite, higher concentration of IDU can reflect higher concentration of residents (roughly 0.6% of world population are regular illicit drug users (Dasgupta, 2017) while in the Czech republic high-risk drug (methamphetamine, opioids) users are about 0.7% of population (EMCDAA, 2017b), but also deprived social status indicated by worse dwelling conditions and by increased crime (mainly offences) due to frequent economic issues of IDU (drug related crime was specified by i.e. Carpentier, 2007). But the research on drug use and violence generally concludes, contrary to popular conceptions, that these relationships are unsystematic and/ or weak (Fagan, 1990, Miczek et al., 1994).

Environmental factors are focused on spaces which are intended to (1) drug acquisition, (2) injection, and (3) needle disposal (Montigny, 2011). Acquisition anchors encompass features of the built environment that represent starting places for the acquisition of drugs or injection equipment. Opportunity spaces encompass locations in which public injection could take place, and the characteristics of these spaces that could modify their suitability for public injection. Disposal options encompass facilities that provide the means to dispose of soiled needles, either safely or unsafely. A fourth construct, that of social controls serves to identify and select variables describing the social environment (influence shown as dotted lines in Fig. 1). These spatial constructs served to identify and select independent variables of the physical environment in Montigny (2008). He focused on detail mapping and analysing the local urban conditions but it requires the well located cases – he evaluates the position accuracy of geocoding better than 5 m.

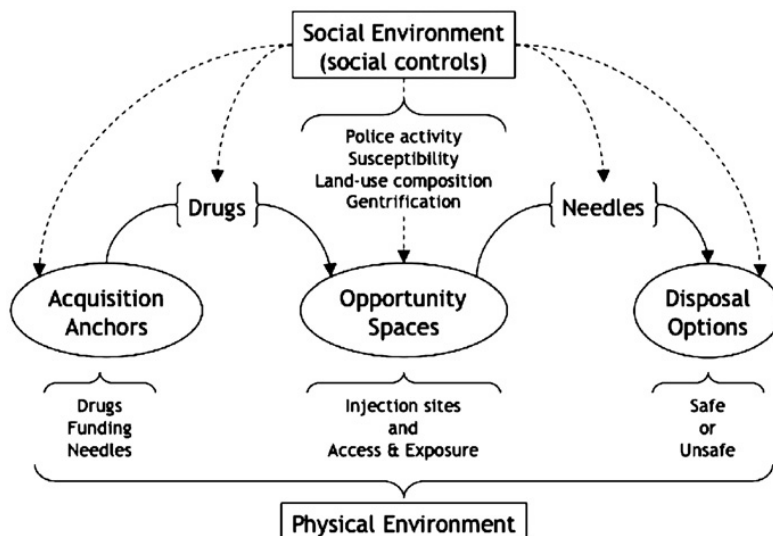


Fig. 1. Conceptual model of the ecology of public injecting and discarding (Montigny, 2011)

In our study we have focused on the Ostrava city. In the Czech Republic 6.4 million syringes were distributed through NEP in 2015 (EMCDA, 2017b) and the number is still growing. The situation in Moravian-Silesian Region (where Ostrava is located) is similar to other regions except to the highest share of students and pupils (Petrášová, Füleová, 2014).

Concerning environmental factors Montigny (2008, 2011) found in the detail urban study discards were more likely to be found near bus stops, pay-phones, adult services, pawnshops and single-room occupancy hotels. Such results cannot be easily transferred due to big differences between Canadian and Czech urban and social environment and we have to modify the set of potential influencing factors. Unfortunately, the low accuracy of geocoded data from municipal police records unable to perform such detail urban study like Montigny and we cannot study local variables and conditions on the micro-level. We have focused on city scale analysis using selected available data sources which provide factors of urban situation which may indirect way indicate the higher concentration of IDUs and more attractive places for discards.

The research is sponsored by TA CR as a part of the fear and crime research focused on identification of safety risk areas in cities with 50k+ population and elimination or reduction of potential negative development factors.

DATA SOURCES

Following data sources have been used:

- Records of collection of discarded syringes and needles (Municipal Police Ostrava), from 2010-2013 years. Records were checked out, summarised (syringes and needles together) and geocoded using a database rule procedure (Horák et al., 2015). The final data set represents point cases with the number of discards organized into 4 years (files).

- Register of buildings and entrances (RBE as a part of RSO, 1.1.2017, CZSO) incl. number of flats, age category, usage and type of building. In the RBE we have found differences in records between entrances of one building according to age, type of usage, number of flats, population etc. It means it is not possible to easily calculate e.g. the number of commercial buildings established between 1970 and 1980 because each part of the building may have different classification. This is why we decided to aggregate data by entrances. Thus hereafter “housing” means number of entrances. The positive side effect is to better deal with buildings of very different size. Obviously it is more fair to substitute large buildings with a set of their parts represented by entrances which may decrease the evident weight difference between block of flats and typical small family housing.
- Number of residents (Census 2011, CZSO) where two categories of residents are distinguished - according to evidence and according to usual state. We have calculated relative differences (change) between them which may indicate large inhabitant movements, important temporal changes and social issues like temporal jobs, overcrowded residences etc. Also the number of residents (usual state) per flat is calculated because a high density of residents may be a symptom of social issues. Overcrowded residences may increase the probability to apply drugs outside and correspondingly increase the occurrence of unsafely discarded needles.
- Register of selected type of facilities – gambling clubs, pubs (all kinds of restaurants, pubs, bars etc. where alcoholic drinks can be served), schools (all kinds except kindergartens), hostels (all kinds of hostels and lodging for temporal residents of workers or socially disadvantaged people), shopping centres, pawnshops. Data is integrated from different sources based on original municipal evidence and completed by field surveys of students.

METHODOLOGY

To analyse spatial distribution of point location of above variables the aggregation of point values inside circles around randomly generated points in the study area was used.

The key question is how large circle diameter to set. The recommended value was taken from an optimisation of the kernel bandwidth. The bandwidth of kernel density estimation for spatial distribution of needles was optimised by Mitana (2016) (fig. 2). The bandwidth of 400 m was recommended for mapping anomalies nevertheless better continuity can be seen for 550 m. For the sake of interpretation simplicity we use a close value of 564 m (diameter of a circle with 1 km² area). Thus the calculated frequencies within 564 m can be interpreted as a density of the phenomenon per 1 km².

Totally 1000 points was randomly generated following the uniform distribution (Complete Spatial Randomness CSR, Bailey, Gattrell 1991) using the function “create random points” in ArcGIS 10.5. To avoid the border issue (the shortage of indicators due to missing locations outside the border) (Horák, 2015) the inner buffer of 564 m was applied (fig. 3 right).

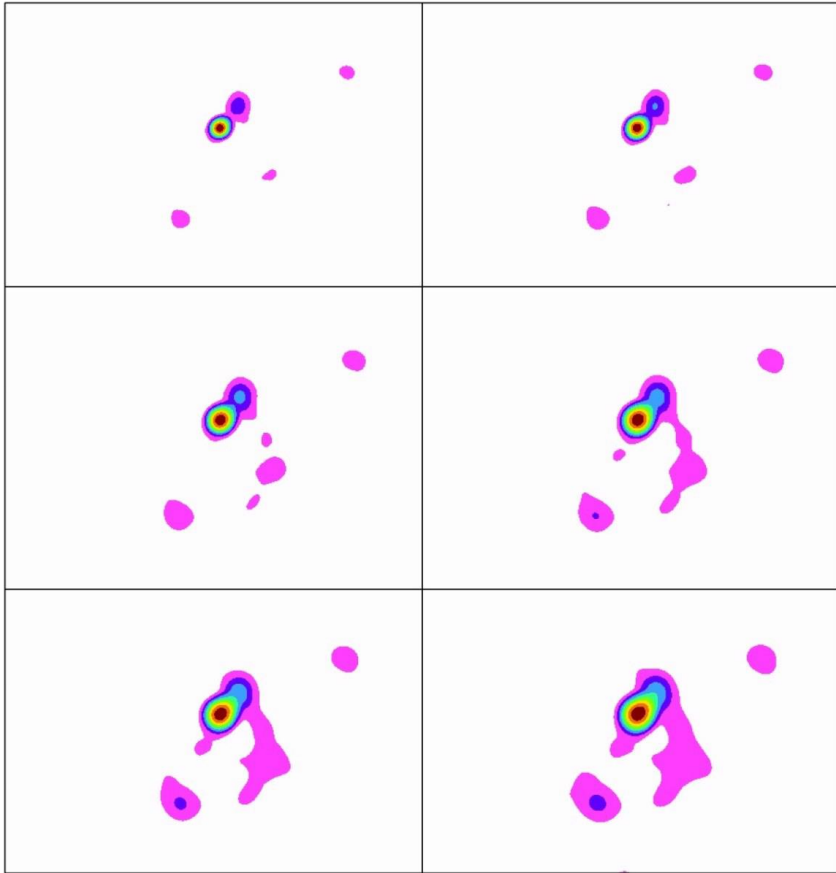


Fig. 2. Kernel bandwidth optimisation for needles distribution (from left and top: 350, 400, 450, 500, 550, 600 m) (Mitana, 2016)

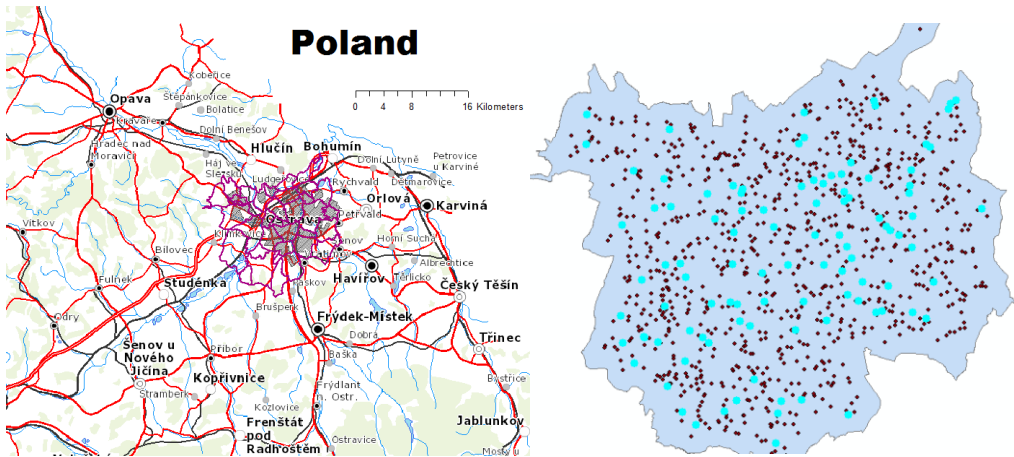


Fig. 3. Ostrava and 1000 randomly generated points

The records of discards cover 4 years and data was aggregated by each year separately. The same set of random points was used for all years.

The housing conditions, facilities and population were left the same for all years – we have no evidence of important changes within this period, thus we consider these changes can be neglected.

Most of variables were summarised inside circles except of residents per flat and the change of population between evidence and usual status where average and variance characteristics of the group were applied.

The final set of variables calculated for each circle:

- Dependent variables – densities of syringes + needles in each year (hereafter syrnee - SYRNEE10, SYRNEE11, SYRNEE12, SYRNEE13),
- densities of offences of disturbing in night time in each year (hereafter disturbing offences; MP10RUS, MP11RUS, MP12RUS, MP13RUS),
- densities of offences of pollution of public space in each year (hereafter pollution offences; MP10ZNE, MP11ZNE, MP12ZNE, MP13ZNE),
- densities of property offences in each year (MP10MAJ, MP11MAJ, MP12MAJ, MP13MAJ),
- densities of buildings established before 1919, in 1920-45, in 1946-60, in 1961-70, in 1971-80, in 1981-90, in 1991-00 and in 2001-11 (D1919, D1945, D1960, D1970, D1980, D1990, D2000, D2011),
- share of buildings established before 1960 (PHOUSOLD),
- densities of family housing, block of flats, hostels, recreational housing, industrial buildings (according to RBE) (DFAMIL, DBLOCK, DHOSTEL, DREKR, DINDUSTR),
- share of family housing, block of flats, hostels, recreational housing, industrial buildings (PFAMIL, PBLOCK, PHOSTEL, PREKR, PINDUSTR),
- densities of residents in evidence (RESIDEV),
- densities of residents usual status (RESIDUS),
- average number of residents per flat (RESFLATAVG),
- average change in residents (between evidence and usual status) in % (RESCHNAVG),
- variance of change in residents (RESCHNVAR),
- densities of pubs, gambling clubs, hostels, shops, schools, pawnshops (PUB, GAMBL, HOSTEL, SHOP, SCHOOL, PAWNSHOP).

Standard EDA and ESDA were performed for all variables using SPSS and GeoDa.

The dependent variable SYRNEE follows almost the power distribution where some small differences can be seen close to its high tail.

The decision tree method requires to establish certain value categories for syrnee where classification accuracy can be evaluated. The 1st option is to use natural breaks in frequency distribution. Unfortunately, it was hard to detect any natural break in frequency which should be used to distinguish “normal” and “abnormal” occurrence of needles (fig. 4).

Therefore we decided to use artificial threshold based on the top decile. The last decile for the whole dataset is 130, but due to the interest to explore the situation in each year we decided to establish the threshold of 110 which satisfies the selection of minimal 10% in each year (the real share of selected cases varies from 10% in 2013 to 13.5% in 2011). This limit was applied in decision trees to create targeted category “high density of syrnee”.

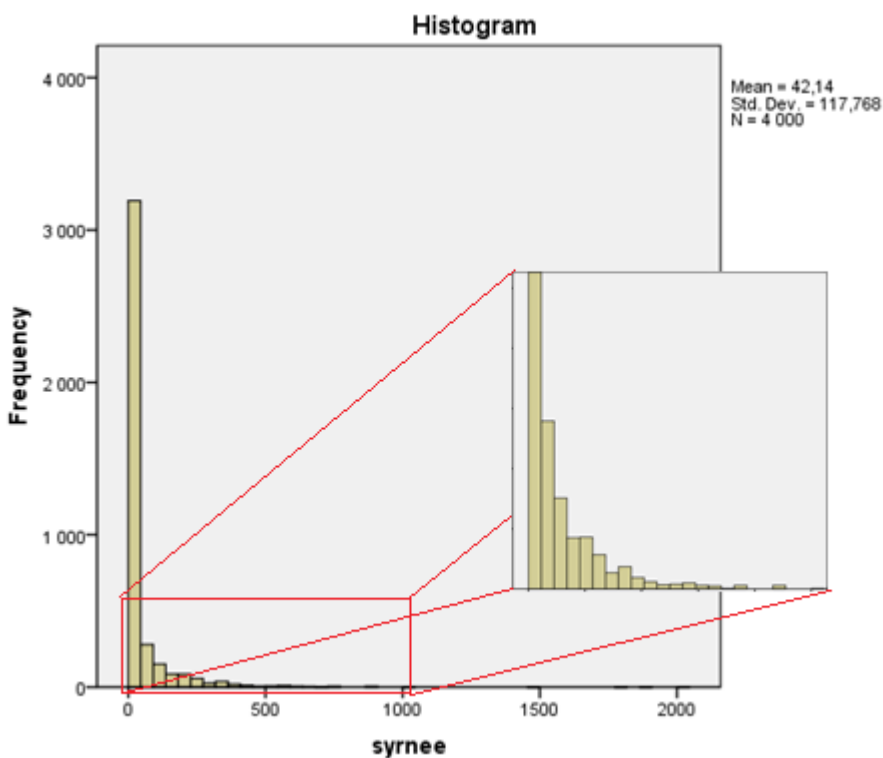


Fig. 4. Distribution of syrnee densities

The spatial distribution of these high values was checked because some exploratory analysis of relationships among variables (fig. 4) showed a possibility to find high values only in 2 localities (especially in 2010) which should create strong spatial deficit of randomness. F.e. fig. 5 indicates strong relationships of hostels and block of flats to the high density of syrnee but these high values are concentrated only in 2 localities which should questioning the common validity of such discover.

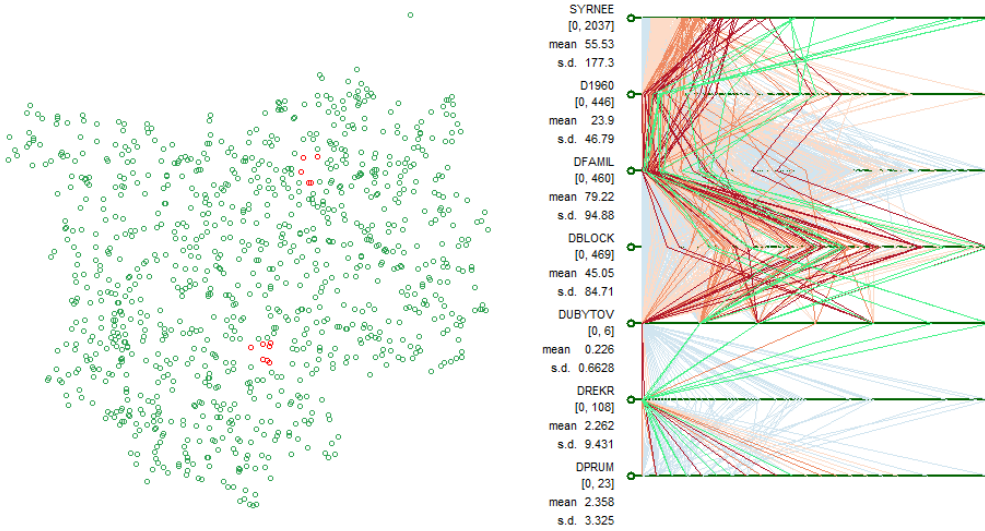


Fig. 5. Parallelogram of selected variables with selection of high syrnee values and corresponding spatial distribution

The spatial distribution of high values (top decile) in all years demonstrates the clustered but not isolated spatial distribution (fig. 6).

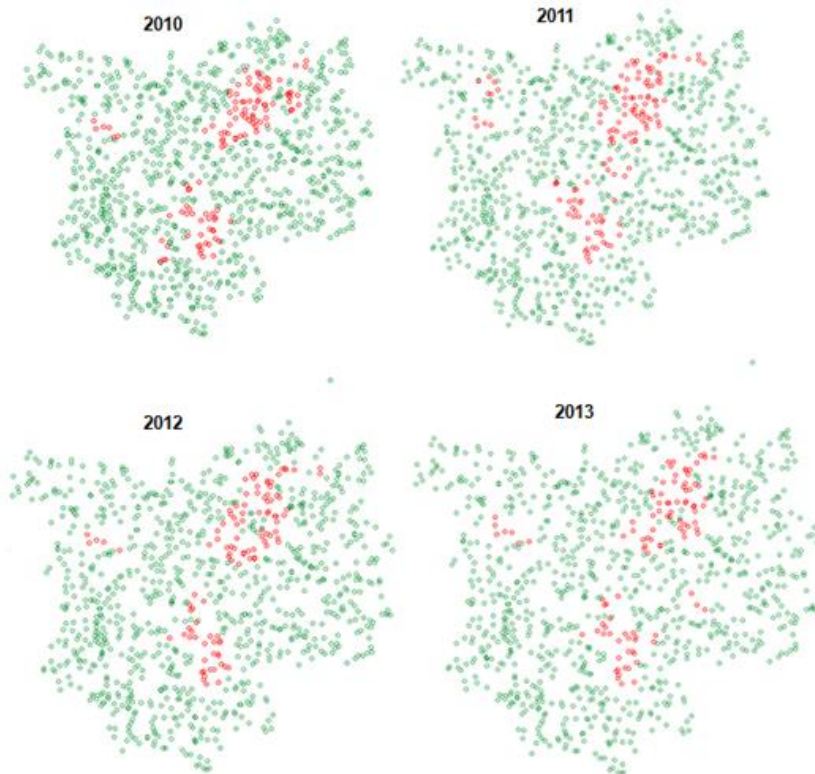


Fig. 6. Distribution of high collection of needles in each year

Concerning independent variables except of RESFLATAVG, RESCHNAVG, PHOUSOLD and PFAMIL all other variables have strong positive skewness and do not satisfy conditions of the normal distribution. Pairwise relationships were explored for the whole dataset 2010-13, especially correlation with syrnee. Nonparametric correlation coefficients were calculated (fig. 7) and the types of relationships were checked by visual inspection of scatter diagrams and maps.

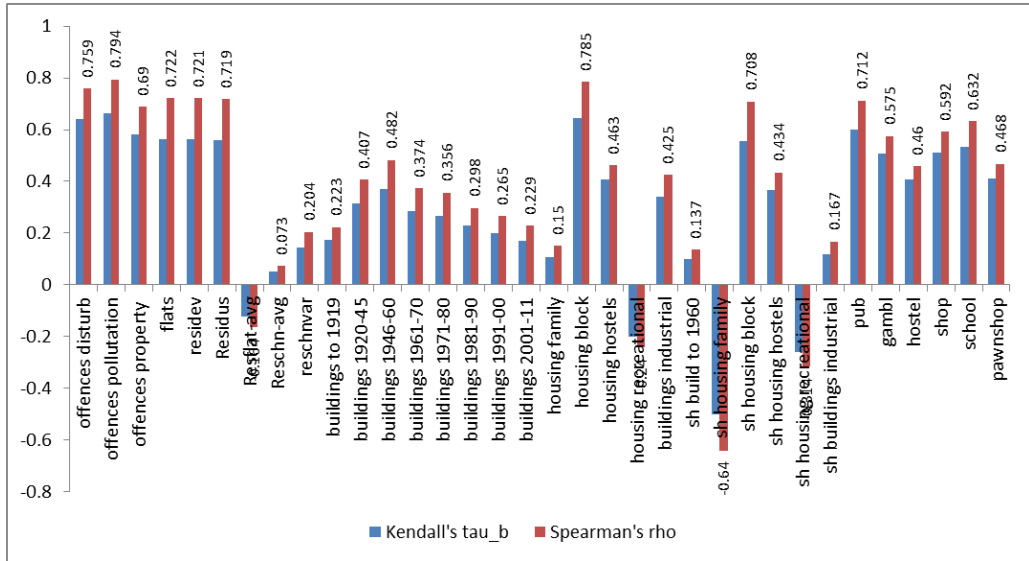


Fig. 7. Pairwise correlation coefficients of syrnee with independent variables (all correlations are significant at the 0.01 level 2-tailed)

Strong positive correlation can be seen for offences especially pollution of public space and disturbing. The reality of the relationship with property offences was not proved by scatter diagrams (fig. 8). Quite strong relationships were confirmed also to the density of flats and residents (which was expected). A small inverse correlation was recorded also to the density of residents in flats (expected but small). Expected but small positive correlation was found for variability in resident changes. The correlations with different age of buildings vary from low to middle values. Higher correlation can be seen for buildings constructed before and after 2nd World War. It indicates the older housing (especially buildings from main after-war construction activities) influences the occurrence of discards. To confirm this hypothesis the share of old buildings (before 1960) was calculated and tested but the correlation is low.

The highest correlation was found for the density of block of flats which is related to the population concentration but also to the social issues of this type of dwellings (high anonymity etc.) (Rochovska et al., 2017). This relationship was confirmed by the high correlation of the housing block share. The share of family housing is highly correlated but not the density of family housing. To the opposite industrial buildings are correlated only for the density and not for the share. A high correlation was discovered also for the density and share of hostels, especially

housing hostels. Surprisingly high correlations were found for pubs and schools which were not finally approved by decision trees.

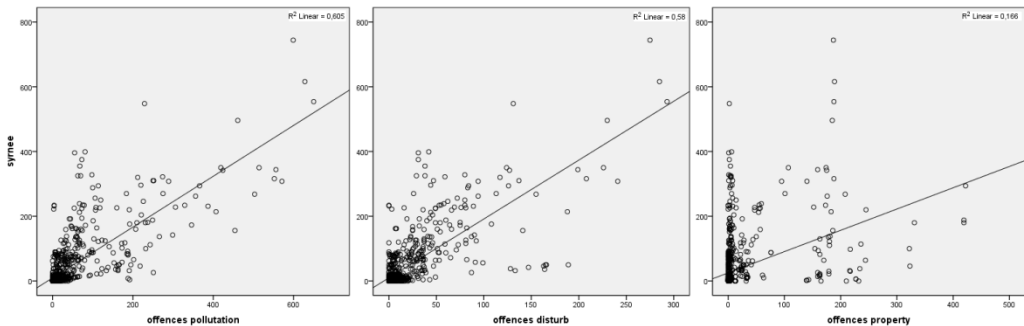


Fig. 8. Relationships between syrnee and different type of offences

For modelling influences of factors the method of decision trees was selected. The decision tree procedure creates a tree-based classification model. It classifies cases into groups or predicts values of a dependent (target) variable based on values of independent (predictor) variables. The decision trees have no assumptions about the type of distribution, the data population can be heterogeneous, and the effect of predictors can be nonlinear (Hendl, 2006). Similarly to Horak et al. (2016) the growing method of exhaustive CHAID was applied.

Two types of models have been tested – models with a target category (classified predictor) and models with a scaled predictor. The first one classified data into two categories – low and high syrnee (density of discarded needles) where the threshold of 110 was applied. The target category for the high values was treated as the category of primary interest in the analysis and it enables to use some classification rule options and gains-related output. It has no effect on the tree model, risk estimate, or misclassification results (SPSS, 2007).

The second models use directly syrnee as a dependent variable. The model attempts to predict directly the density of discards.

The maximal depth of trees for exhaustive CHAID is 3. Significance levels for splitting nodes and merging categories are both 0.05. Models were validated using subdivision of all data into 2/3 for training and 1/3 for testing data sets. The interpretation was made for nodes with their index higher than 100.

RESULTS AND DISCUSSION

The decision tree with classified predictor was calculated in several variants. All significant factors in these categorised models are listed in the following table where the relative importance is expressed in numbers.

Table 1. Evaluation of factors importance in decision trees for categorised models of syrnee

factors	Categorised models						
	2010-2013	2010-2013, no age categories of buildings	2010	2011	2012	2013	2011, no housing block
offences pollution	3	3	3		3	1	
offences disturb						3	3
offences property			1.5				
buildings to 1919	1				1		1.5
buildings 1946-60	1						
buildings 1961-70	1						
buildings 1981-90	1						
buildings 1991-00	1			1			
buildings 2001-11						1	
sh build to 1960		1					
housing block				3			
housing family		1					
sh housing family	2	2					1.5
housing recreational							1
housing hostels	2	2	2	1	1	2	2
sh housing hostels	1	1.5				1	
hostel				2	2		
gambl			2				
school					1.5		
pub		1					
shop						1	
flats		1					
resflatavg			1				
reschnavg							1
Accuracy [%]	75.5	75.5	60.8	76.3	82.2	68.3	73.3

Notes: 1 – the variable listed only in the list of significant variables, 1.5 - more important variable used rarely for delimiting of the group with index higher than 100, 2 - variables frequently used in delimiting groups with index higher than 100, 3 - the most important variable used to tree subdivision on the 1st level

The accuracies for categorised models are high (varied from 61 to 82%).

First, the model for all independent variables and all years were prepared. In the first model a lot of age categories of buildings were included to the set of significant variables but with no clear interpretation. The further model was tested without these age variables. This 2nd model provides the same accuracy as the 1st model but it creates slightly changed set of important variables – new are pubs, flats and the share of old buildings (before 1960). The model internal consistency was tested by subdivision to individual years. Each year demonstrates some specific minor deviations in significant factors used to build the model. The largest differences can be seen for 2011 where the main factor was the density of housing blocks. Nevertheless the exclusion of this variable from the model provides only slightly worse accuracy and the new set of significant variables are more consistent with other years and the overall data set. The other specific factors are gambling clubs significant for 2010, schools significant for 2012, and the substitution of pollution offences by disturbing offences in the role of the primary factor.

To summarize results, we do not see large differences between years. The main factors are pollution offences, disturbing offences (both type of offences partly substitute each other; in 2010 and 2012 the pollution offences are preferred in the model while disturbing offences are preferred in the other years), hostels (expressed in all 3 forms - housing hostels, objects or the share from all buildings), and in some years we can see also a small negative influence of the share of housing family.

That is why the overall decision tree has been created for the full time period. The model accuracy reached 76%. The part of the tree is exemplified in fig. 9. Each statistical significant splitting of the tree is documented by the name of variable (predictor) with adjusted P-value, the values of Chi-square test and degrees of freedom.

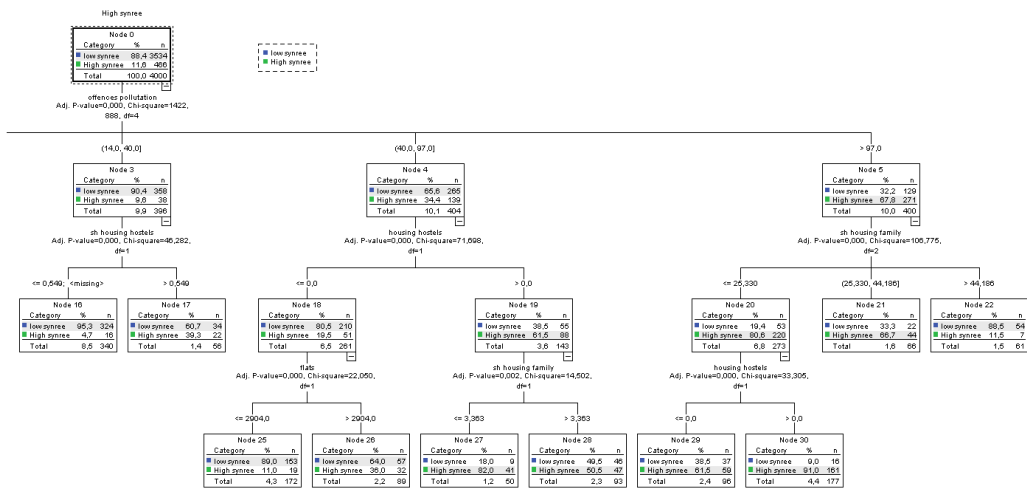


Fig. 9. Part of the overall decision tree for classified syrne (2010-2013)

The most important nodes with their responses, indexes and interpretation are provided in the following table.

Table 2. The most important nodes of the overall decision tree

Node	Node		Gain		Response	Index	interpretation
	N	Percent	N	Percent			
34	177	4,4%	161	34,5%	91,0%	780,8%	very high pollution of-fences, low share of family housing, hostel
31	50	1,3%	41	8,8%	82,0%	703,9%	high pollution offences, hostel, low share of family housing
25	66	1,7%	44	9,4%	66,7%	572,2%	very high pollution of-fences, middle share of family housing
33	96	2,4%	59	12,7%	61,5%	527,5%	very high pollution of-fences, low share of family housing, no hostel
32	93	2,3%	47	10,1%	50,5%	433,8%	high pollution offences, higher share of family housing, hostel
21	56	1,4%	22	4,7%	39,3%	337,2%	middle pollution offences, higher share of hostels
30	89	2,2%	32	6,9%	36,0%	308,6%	high pollution offences, no hostels, high density of flats
28	52	1,3%	11	2,4%	21,2%	181,6%	low pollution offences, very high share of buildings before 1960, pubs >1

On the base of the overall model, the probability of classification to the target category (high value of syrnee) was calculated for each year. To evaluate modelling results we have provided kernel density estimations (KDE) of original records of discarded needles (bandwidth 550 m, ArcGIS kernel density function); different densities are expressed by isolines with 0.00004 interval. The modelled probability of the high syrnee and isolines of KDE of measured discards are portrayed in fig. 10 for 2010 and 2012.

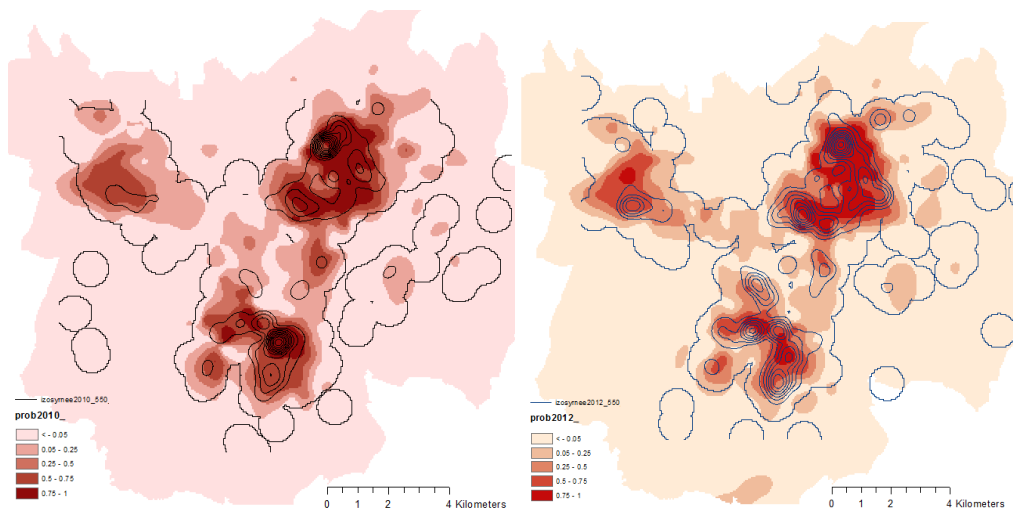


Fig. 10 Comparison of izolines for discarded needles and probability of the high syrnee in the model (2010 left, 2012 right)

We can see relatively well corresponding high value areas. Some shifts are located especially in the western part (Poruba, explained later) and in the central part in 2012 (caused by one anomaly collection).

We have provided internal model validation by comparison of the measured and predicted values of syrnee classifying them into 4 categories (fig. 11) – properly predicted low values (below 110) (LOWPROV), properly predicted high values (above 110) (HIGHPROV), 1st class errors (errors of commission) (ERR I) and 2nd class errors (errors of omission) (ERR II) (Congalton, Green 1993). The situation was analysed for each year. The classified results are accompanied by the value of probabilities of high syrnee classification. The spatial distributions of probabilities in each year are similar because majority of urban factors are the same and differences may be caused only by the different densities of offences.

Probabilities above 50% in 2013 are concentrated in three continual risk areas – the city centrum (Moravian Ostrava) with extension to Přívoz and smaller peninsulas to Mariánské Hory, Hrabůvka and Poruba. Older years provide more risk areas but these 3 areas remain the most important and dominant in each year.

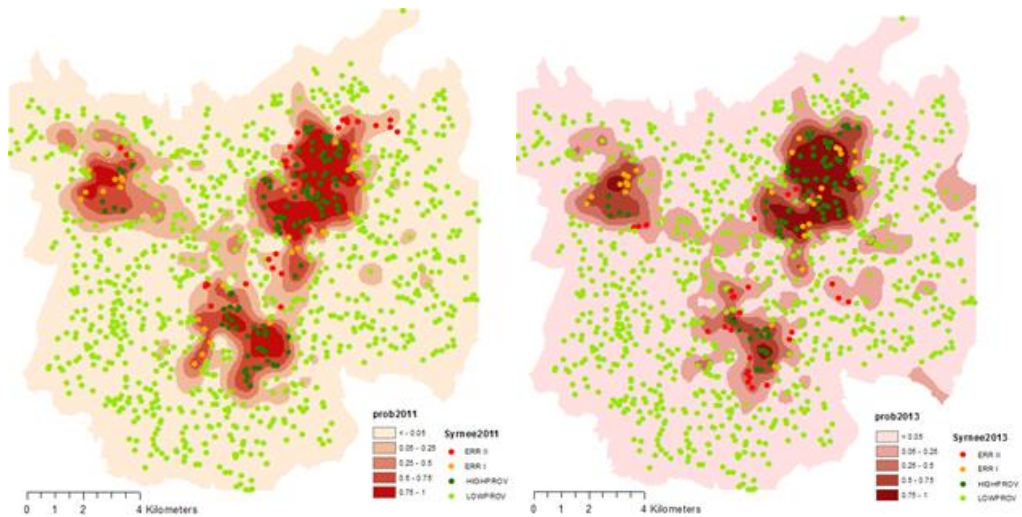


Fig. 11 Probability of high synree classification by the model and validation results (2011, 2013)

The results are relatively satisfactory. Majority of high values of synree are well mapped by the model. Errors are situated mainly on the border of the 3 risk areas. Worse situation can be seen for modelling results in Poruba.

In 2013 nine places in Poruba were false positive (it means the overestimated risk in NW part of Poruba), also in 2012, partly in 2011 and 2010 where only the western part is overestimated. There are 2 main reasons of model overestimation. First, the positive influence of hostels plays the important role in the model and several students' hostels are located here. This fact increases model estimations although student's hostels in reality do not change for the worse. The second reason is these false positive points are located in places where we can meet a natural deficit of discarded needles due to a large areal of the hospital and the university. The overestimated prediction of synree is also supported by the high densities of offences (pollution and especially disturbance), high density of block of flats and middle share of family housing (22%).

To the opposite the risk is underestimated in 2010, 2012 and 2013 in SE part of Poruba. In 2011 the situation is correctly classified and low discards are confirmed here. The reason of overall model underestimation of the risk is the high anomalies occasionally occur in the area (fig. 12 one collection of 78 synree at Ukrajinska Street) combined with unexpectedly low contribution of urban factors like a low level of offences density (mainly low pollution offences) and very high level of the family housing share (55%).

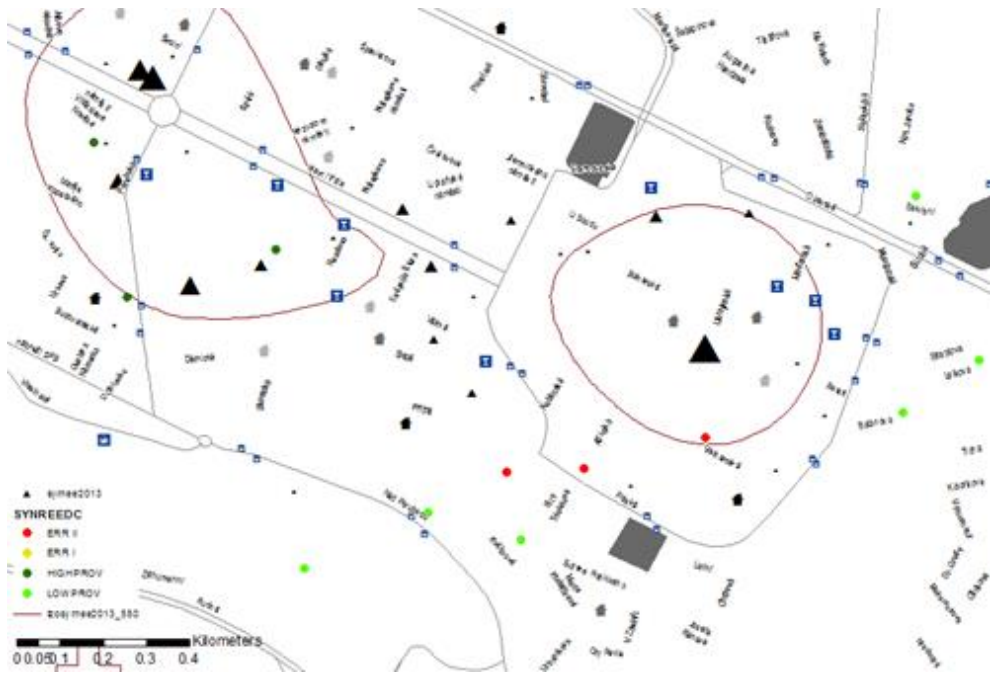


Fig. 12. Three misclassified points due to one anomaly collection of discards and low level of surrounding urban factors

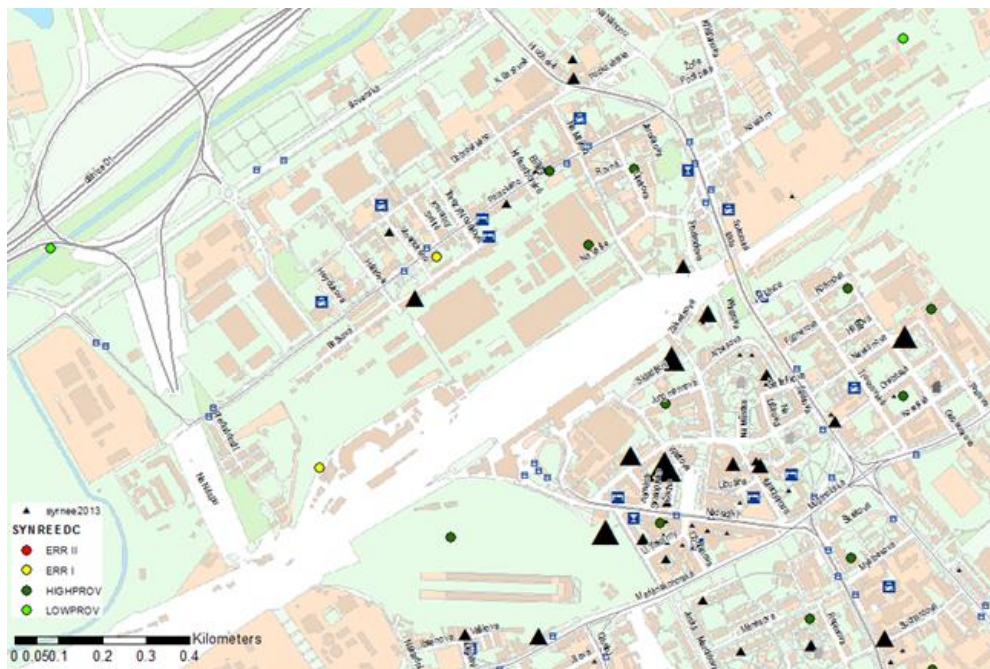


Fig. 13. Low measured synee (overestimated by the model) (yellow points) situated close to large fenced area of the main railway station in Ostrava with the lack of freely available places

To summarise results – overestimation of the categorised model occurs especially close to fenced and controlled places where IDUs cannot discard needles as well as policemen cannot collect it. Mainly large industrial areas may significantly influence results (model overestimation) like factories, railway stations (see fig.13 where the large area of the main railway station in Ostrava causes the model overestimation due to the lack of measured discards), water bodies etc.

The model with the scaled predictor was also evaluated. The highest influence was confirmed for the density and share of pollution offences and hostels. The map of differences (fig. 14) between measured and modelled synree (in 2013) provides similar results as previous maps. Only low occurrences are well estimated. Although the categorised model has classified well the substantial part of high occurrences, the scaled model does not perform such way. The differences are high which is not surprising because abnormal values are difficult to predict by majority of models.

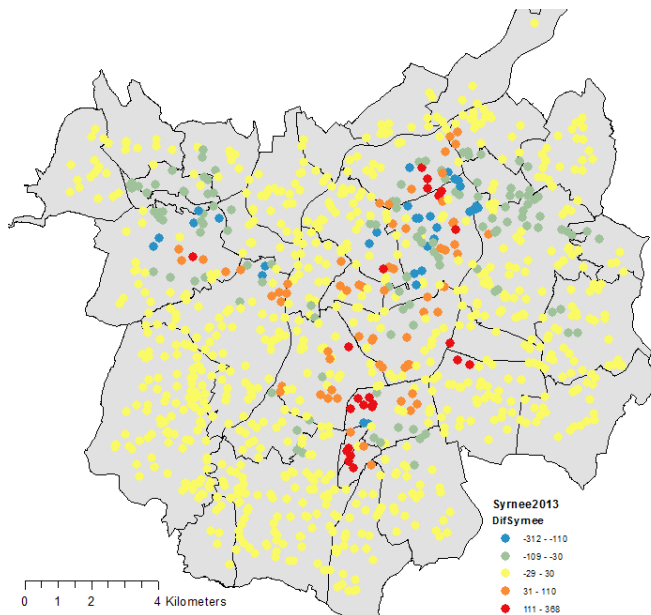


Fig. 14. Differences between measured and estimated synree for the model with scaled predictor

The predicted values show some underestimation of values by the model (fig. 15) which is the result of abnormally high values occurrence. The model provides middle values of R^2 (0.483). The distribution of significantly overestimated and underestimated predicted values is portrayed in fig. 16. In both cases the indicated anomalies do not create clear pattern.

Underestimated values are concentrated in places of two main risk areas but also in two small additional places – f.e. two cases in Kunčičky and four cases close to socially excluded locality “Na Liščině” in Hrušov (NW). The distribution of overestimated (predicted is significantly higher than measured) values is even more regular and it is difficult to discover one or more localities with clear deviation from the model.

It is worth to note that places of under- or overestimated values are practically the same which indicates some data variation in the same place. The current time period of one year may be not enough to provide stabile results or the results are highly influenced by random occasional abnormal collection of discards.

The influence of anomaly high value was experimentally tested. We apply a threshold of 500 and only cases below this limit were included to the decision tree modelling. Obviously, the result indicates better results which is confirmed by higher R^2 for correlation between measured and expected value ($R^2=0.647$). The important factors are pubs while hostels have not such strong impact as earlier. It indicates hostels are important mainly to explain high and very high value of dependent variable while pubs (and schools) influence the small and middle isolated occurrences.

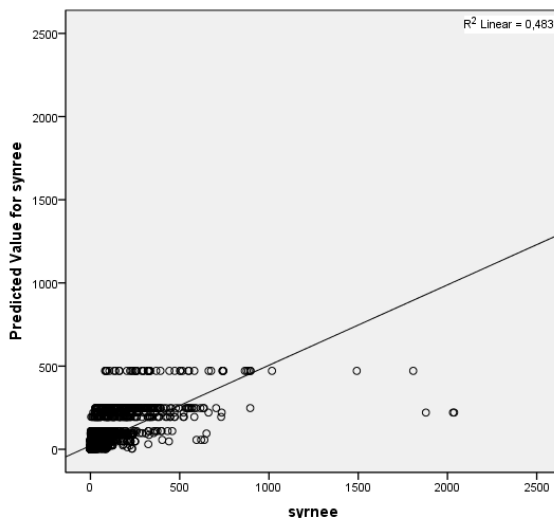


Fig. 15. Predicted versus measured syrnee values (the scaled model, 2010-2013)

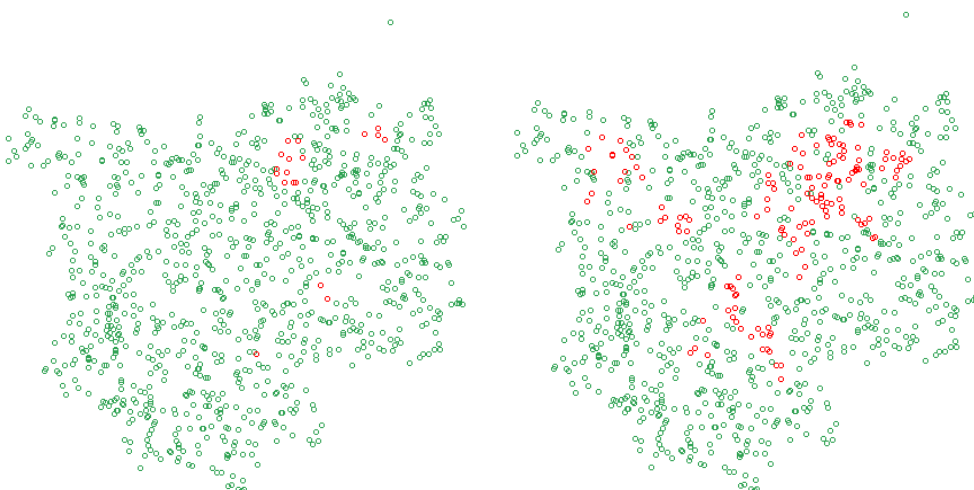


Fig. 16. Distribution of significantly different values - underestimated values (left) and overestimated values (right) by the scaled model

CONCLUSION

Predictions of high densities of discarded syringes and needles at the city scale based on decision trees provide satisfactory results with the average model accuracy about 75%. 24 from the 33 independent variables have been selected as significant variables (indicators) for modelling. Nevertheless, some variables are very close by their meaning and some of them can be mutually exchanged. After validation and model refinement for the overall model (for the full time period 2010-2013) we consider following variables as the main important influences – pollution offences, hostels (densities or share), share of family housing and eventually density of housing blocks. Each year may emphasize the role of some other specific factors i.e. gambling clubs significant for 2010 or schools significant for 2012 which is added to the model to improve the model performance.

The model with the scaled predictor provides similar results concerning main influencing factors. Not surprisingly, the quality of the value prediction is not high ($R^2=0.483$).

The interesting question is the role of offences. By our opinion the selected type of offences (pollution or disturbing) acts like an indicator of the environmental degradation level and does not affect directly.

The modelling results pointed out some problems:

- high abnormal collections of discards. It is recommended to reclassify them or to exclude such values from further processing.
- an inaccurate location unable to reach well designed and satisfactory models. It limits possibilities to provide useful local reasons and discover some of unknown factors or hidden anomalies.
- well classified objects are necessary. I.e. not all hostels are relevant accommodation for temporal workers or socially endangered people (potential risk for drug consumption/distribution).
- area of technological areals have to be excluded otherwise it causes a deficit in aggregated collection of discards.
- A global trend in the drug usage (the time progress of IDUs) should be eliminated. For time-partial analysis (i.e. by each year) the relative frequency (the share of local collection from the all for the given time interval) should be used as a dependent variable.

ACKNOWLEDGEMENTS

The research is supported by the Czech Technology Agency, project No. TJ01000465 Effective Methods of Identification, Assessment and Monitoring of Safety Risk Areas Using Spatial Micro-data. Data is provided by the courtesy of the Czech Statistical Office, Municipal Police Ostrava and Ostrava City Government.

REFERENCES

- Bruneau J, Daniel M, Kestens Y, Zang G, Génereux M. Associations between HIV-related injection behaviour and distance to and patterns of utilisation of syringe-supply programmes. *Journal of Epidemiology and Community Health*. 2008; 62:804–810.
- Cooper HLF, Bossak B, Tempalski B, Jarlais DCD, Friedman SR. Geographic approaches to quantifying the risk environment: drug-related law enforcement and access to syringe exchange programmes. *International Journal of Drug Policy*. 2009; 20:217–226.
- Carpentier, C., 2007. Drugs and crime — a complex relationship European Monitoring Centre for Drugs and Drug Addiction. ISSN 1725-8480. http://www.emcdda.europa.eu/attachements.cfm/att_44774_EN_Dif16EN.pdf
- Congalton Rg., Green K. (1993): A Practical Look at the Sources of Confusion in Error Matrix Generation. *Photogrammetric Engineering And Remote Sensing*. 59(5), 641-644.
- Dasgupta A. (2017): *Alcohol, Drugs, Genes and the Clinical Laboratory*, Elsevier 2017. ISBN: 978-0-12-805455-0
- Davidson P.J., Scholar S., Howe M. (2011): A GIS-based methodology for improving needle exchange service delivery. *Int J Drug Policy*. 2011 Mar; 22(2): 140–144. Available on-line at <https://www.ncbi.nlm.nih.gov/pmc/articles/PMC3070054/>
- Doherty M.C., Garfein R.S., Vlahov D., Junge B., Rathouz P.J., Galai N., Anthony J.C., Beilenson P. (1997): Discarded Needles Do Not Increase Soon After the Opening of a Needle Exchange Program. 1997, *American Journal of Epidemiology*, Vol. 145, No. 8., p. 730-737.
- EMCDDA (2017a): EUROPEAN MONITORING CENTRE FOR DRUGS AND DRUG ADDICTION, 2017. *European Drug Report 2017: Trends and Developments*. Lisbon: ISBN: 978-92-9497-074-9. 90 pp.
- EMCDDA (2017b): EUROPEAN MONITORING CENTRE FOR DRUGS AND DRUG ADDICTION, 2017. *Czech Republic. Country Drug Report 2017*. Lisbon: ISBN: 978-92-9168-972-9. <http://www.emcdda.europa.eu/system/files/publications/4511/TD0416912ENN.pdf>
- Fagan J. Intoxication and Aggression. In: Tonry M, Wilson JQ, editors. *Drugs and Crime*. Chicago, IL: University of Chicago Press; 1990. pp. 241–320.
- Hendl J. (2006): *Přehled statistických metod zpracování dat*. Portál, Praha. 583 pp. ISBN 80-7367-123-9.
- Horák J., Ivan I., Inspektor T., Tesla J.: Sparse Big data problem. A case study of Czech graffiti crimes. LNGC Springer 2017.
- Horák J., Inspektor T., Caha J., Kukuliač P.: Geokódování objektů podle adresy. In sborník „GIS Ostrava 2015 - Současné výzvy geoinformatiky“, Ostrava, 26-28.1.2015. http://gis.vsb.cz/GIS_Ostrava/GIS_Ova_2015/sbornik/papers/gis2015541c4ad4ce8fc.pdf
- Horák J., *Prostorová analýza dat (Spatial Data Analysis)*, VŠB-TU Ostrava, 6th issue, 2015.

- Miczek KA, De Bold JF, Haney M, Tidey J, Vivian J, Weertz M. Alcohol, drugs of abuse, aggression, and violence. In: Reiss AJ Jr, Roth JA, editors. *Understanding and Preventing Violence*. Washington, D.C: National Academy Press; 1994. pp. 377–570.
- MITANA (2016): *Prostorová analýza drogové problematiky v Ostravě (Spatial Analysis of Drug Scene in Ostrava)*. Diploma thesis, VSB-TU Ostrava, 2016.
- Montigny, L. D. A. K., 2011. A spatial analysis of the physical and social environmental correlates of discarded needles. In: MOON, G. *Health & Place* [online]. Montreal [cit. 2012-11-03]. ISRC 757–766. Dostupné z: <http://www.sciencedirect.com/science/article/pii/S1353829211000219>
- Montigny, L. D., Moudon A.V., Leigh B., Young K. (2010): *Assessing a Drop Box Programme: A Spatial Analysis of Discarded Needles*. *International Journal of Drug Policy*, Volume 21, Issue 3, Pages 208-214 (May 2010)
- Normand J, Vlahov D, Moses LE, eds. *Preventing HIV transmission: the role of sterile needles and bleach*. Panel on Needle Exchange and Bleach Distribution Programs. Washington, DC: National Academy Press, 1995:136, 216-17, 226.
- Parkin S., Coomber R. (2011): *Injecting drug user views (and experiences) of drug-related litter bins in public places: A comparative study of qualitative research findings obtained from UK settings*. *Health & Place* 17 (2011) 1218–1227
- Petrášová B., Füleová A. (2014): *Incidence, prevalence, zdravotní dopady a trendy léčených uživatelů drog v České republice v roce 2013: výroční zpráva. (Incidence, prevalence, health impacts and trends of attended drug users in the Czech Republic in 2013: year report)*. Prague, Hygienic station, Year report, 2014.
- Rochovska A., Majo J., Kacerova M., Ondos S. (2017): *Friendly neighbourhood, the importance of the environment for a healthy seniors' community*. *GEOGRAPHIA CASSOVIENSIS*, 11(2), 184-200.
- Tookes H.E., Kral A.H., Wenger L.D., Cardenas G.A., Martinez A.N., Sherman R.A., Pereyra M., Forrest D.W., LaLota M., Metsch L.R. (2012): *A comparison of syringe disposal practices among injection drug users in a city with versus a city without needle and syringe programs*. *Drug and Alcohol Dependence* 123 (2012) 255– 259.

DIGITAL SKETCH MAPS DETECTING PLACES OF FEAR OF CRIME

Andrea, PÓDÖR¹; Ákos, JAKOBI²

¹ Institute of Geoinformatics, Alba Regia Technical Faculty, Óbuda University,
Pirosalma u. 1-3, H-8000, Székesfehérvár, Hungary

podor.andrea@amk.uni-obuda.hu

² Department of Regional Science, Faculty of Sciences, Eötvös Loránd University,
Pázmány Péter sétány 1/c, H-1117, Budapest, Hungary

jakobi@caesar.elte.hu

Abstract

This study aims to prove the usefulness of digital sketch maps in identifying criminally problematic areas in a city environment. In our research we collected fear of crime data of citizens by using a web application, which provided a tool for users to mark areas on a map, where they feel safe or feel fear. The collected sketch map data were aggregated and processed by GIS tools, making it possible to statistically evaluate, verify and compare safe or unsafe places marked by the respondents with official police statistics. According to the results, some kind of a prejudice and preconception can be connected to our test city's certain locations, where minority or homeless people are frequently living. The study also confirmed that there are places, where citizens' opinion and police statistics coincide.

Keywords: fear of crime, crime mapping, digital sketch maps, mental maps, Hungary

INTRODUCTION

Already in the 1960's the strengthening of urban violence raised the interest of studying fear of crime in Britain and USA (Zedner 1997). Since then there have been many efforts to formulate the meaning of fear of crime. Ferraro and LaGrange for example defined this phenomenon as a negative emotional manifestation that is triggered by crime or related symbols (Ferraro and LaGrange 1987). Their research study aimed to decide whether personal attributes, like gender or age, have an effect on fear of crime, namely for example older people are more scared of such topics than young. Additionally, it is important that beside personal factors also the environment has influence on anxiety and sense of fear. According to Doran and Burgess (2012) many of the researches on this subject underpin the fact that fears of crime are concentrated in areas, which can be described with definite environmental characteristics. Also the paper of Lederer and Leitner (2012) in Linz concluded that fear of being a victim of burglary can be attributed to certain geographical hot spots and is connected with definite statistical features and even with areas having less technical protection.

In this paper our goal is to prove on a Hungarian example that geographical applications such as digital sketch mapping and GIS analyses may contribute to identify hot spots and other environmental factors related to the citizens' fear of crime. In the literature one could find best practices and recent advances in detecting environmental and location factors related to fear of

crime by the application of big datasets, however those are not suitable for all kind of analyses. Geolocated data acquired from Twitter was applied for example to detect population having a heightened crime risk for burglaries and robberies (Kounadi et al. 2017), however Twitter in Hungary is not so intensively used by locals to get enough data for detecting the places of fear of crime. Furthermore, since the Hungarian police have not carried out any systematic survey on the issue of fear of crime, we decided to develop an own and simple web application to compile data from mental maps, which would possibly measure – to a certain degree – the level and the location of fear of crime.

Many research studies claim that fear of crime is strongly related to prejudice (Skogan, 1995) and preconceptions have an essential role in judging the crime situation. According to numerous studies, prejudice is present also in Hungarian society (Váradi, 2014), therefore it is worth to consider such factors in our current research, too. For example in 2013, a study on the town of Kalocsa, Bács-Kiskun County, Hungary (Pődör and Dobos, 2014) revealed that there is a correlation between the level of fear of crime and the presence of Gipsy minorities, although official crime statistics did not confirm this result (note that it is illegal to register the offender's ethnicity in crime statistics in Hungary).

All in all our recent study aims to compare results gained from our web-application with the official crime data. We assume that the difference between the official data and the results of our fear of crime surveys points out areas of deeper sociological problems in the urban environment.

THE STUDY AREA

To test our application we have chosen Székesfehérvár, a medium large Hungarian city as the study area, which can model the average circumstances of Hungarian cities. In this city with 98,000 residents, crime statistics reflects that usually there are cca. 6-7,000 crimes registered per year. According to the report of Székesfehérvár Police Department, from the year 2015 to 2016 the total number of crimes have been decreased significantly. This last year showed statistically the best results of the past seven years, namely the number of crimes decreased from 3025 to 1958, with less robberies and thefts (from 1076 to 740) or car crashes (37 to 22). According to the report this improvement might be connected to the deployment of surveillance systems throughout the city during this period.

The analysed city is definitely not homogenous, we assumed that the perception of fear of crime has some connections with different types of urban zones. The city can be divided into 18 parts as defined by the town's integrated urban development plan. Additionally, since industry has a key role in the life of the city, there are 3 big industrial parks located in Székesfehérvár (Figure 1.). The urban areas can be characterized as follows:

- *Centre*: This major zone covers the areas of “Belváros” (1), “Vasút-környék” (16), and “Víziváros” (6). The buildings here were mainly built in the 18th century or earlier.
- *Block house areas*: These particularly important parts of Székesfehérvár are characterized by socialist block houses, which were largely built in the '70s and '80s, as

a response to new needs of intensive industrialization. Areas of “Palotaváros” (3), “Tóváros” (2), “Szedreskert” (4) and “Almássy-telep” (8) are included here.

- *Garden city areas*: The here located family-owned houses make up a large proportion of Székesfehérvár’s total number of residential buildings. Such houses could also be found in several places scattered around the city centre. Garden city areas are typically large and distant parts of the city, where the most well-to-do people are living. Areas of “Felsőváros” (5), „Ráchegy” (10), and “Őreghegy” (11) are included here.
- *Sparsely built-up rural-like areas*: Houses and surroundings here are identical to rural areas. These are typically in districts like “Alsóváros” (15), „Maroshegy” (12), „Feketehegy” (13), „Órhalmi szőlők” (17) and „Kisfalud” (18).

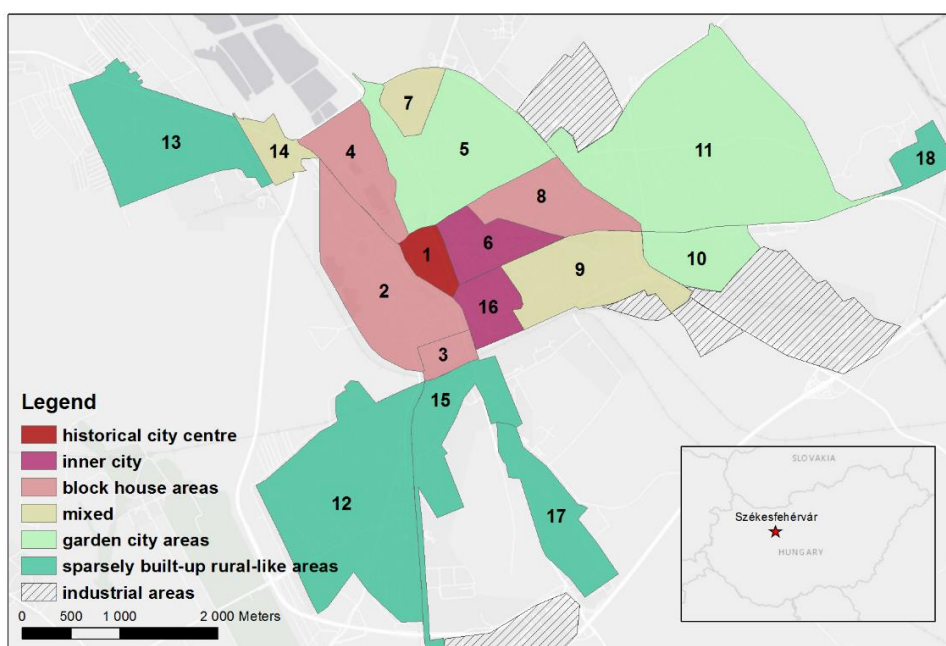


Fig. 1. Urban zones in Székesfehérvár

METHODS

In order to measure peoples’ perception and subjective level of fear of crime associated with certain places or parts of the city, we used mental mapping techniques. Mental mapping is a well-known research method to discover how people see and perceive certain places in their mind (Lynch, 1960, Down and Stea, 1973, Gould and White, 1993). Mental maps can be used for several purposes: urban planning, anti-segregation, behavioural geography, etc. (Letenyeyi, 2005). Though, it is important to note that individual perception of an area may depend on a large number of factors like the mode of travelling, age, education, etc., therefore mental maps can have different visual forms and can reflect different outcomes.

Mental and sketch maps have been used by many studies (Boschmann and Cubbon, 2014) to interpret an environment qualitatively in terms of feelings such as fear, desire or stress. Mental maps are tools for behavioural geography to understand human behaviours based on peoples' perceptions of their spatial environment, whereas sketch maps have been used in participatory and qualitative geographic information systems to depict spatial narratives of groups or individuals (Boschmann and Cubbon, 2014). Matei (2005) used mental maps for example to reveal the role of media in shaping urban spaces in relation with fear of crime in Los Angeles. He used 215 mental maps taken from seven neighbourhoods across the city and processed them by the application of GIS tools. The results proved that people's fear is associated with a concentration of certain ethnicities in a given area.

Mapping the fear of crime and the so-called emotional mapping have much in common, as fear is mainly and clearly related to emotions. Several research papers deal with emotional mapping (e.g., Pánek et al. 2016), in which the web applications collect the emotional perception of urban space. A more complex research project (Resch et al., 2015) uses technical and human sensors and georeferenced social media posts, from which the researchers extract contextual emotional information.

From a methodological perspective based on Lynch's works (1960) a determinative study on mental maps was carried out by Stanley Milgram (1992), who applied the free recall technique, in which respondents had to draw mental maps on a blank paper. The only problem with this method was that different people saw the same places differently, so it was hard to compare the result maps with each other and it was difficult to extract information out of them. Recently, various and new data collection techniques were developed in mental mapping, such as purely quantitative survey methods, qualitative and non drawing-based interviewing techniques, free recall data collection methods based on freely drawn maps, oriented recall-map drawing techniques with supplemented interviews, and data collection methods based on existing maps and images.

To collect comparable mental map data on people's opinion on places of fear of crime in our research a web-based application was developed. The application was based on the latter mental mapping procedure (namely data collection was based on existing maps) and was available both as a website and as a mobile phone application. For base map of the application Google Maps were chosen, as it is commonly used among Hungarian citizens, so map reading abilities did not influence the completion of the mental map survey. To distribute our online survey application and to reach the participants we used mainly social media channels (Facebook, Viber). Due to this fact, the survey sample is somewhat distorted, since respondents naturally should have online and map reading competencies. We consider our survey, therefore, as a model experiment.

The web-application for data collection

As mentioned above, a web application was developed in order to collect fear of crime data in forms of digital sketch maps. The application itself utilised the Google native web API with an additional drawing function created through Drawing Manager (the webpage is available at <http://bunmegelozes.amk.uni-obuda.hu/>). The respondents was allowed to use the webpage

without registration. Technically the web application was based on MySQL DataBase Management System and PHP.

First, a short questionnaire was asked to fill out by the respondents, on which they had to indicate their home address postcode, age, gender and the usual mode of transport, as – according to Doran and Burgess (2012) – these facts influence the perception of fear of crime significantly. After giving responses to the questions, the users could have found a short explanation of how to use the map application. By following the instructions, they could indicate places where they feel safe (practically the users could draw a simple, green-coloured polygon on the map around safe areas), and also they could indicate places where they feel fear of crime (by drawing simple, red-coloured polygons on the map).

Each drawings of the respondents resulted a digital sketch map layer in our database, which then have been aggregated and transformed to a 200x200m grid in order to be able to perform basic GIS calculations to evaluate the results. In Hungary also other social data are available in such grid forms, so for later analyses it seemed to be reasonable to choose the same grid system.

RESULTS

Altogether, we have collected digital sketch map data between August-September 2017 from 160 respondents, of them 96 were women, and 64 were men, that is to say 60% of the respondents were women. The average age of the participants was 36.4 years, the average age of women and men was almost the same. 30% of the respondents was coming from the age group of 21-30, 23% were from the group 31-40, 20% were between the ages 41-50, while 14% are from the age group of 51-60. Only 5 respondents were older than 60 years and 14 of the participants in the survey were younger than 21 years. If we look at the gender distribution, we may notice that the majority of male participants (39%) were coming from the age group of 21-30. On the contrary, the age distribution of female respondents was more balanced: the age group of 41-50 represented itself with the highest number. Concerning the reported mode of transport, the majority of respondents (71 people, 45%) mentioned walking. It is interesting, that the majority of walkers were women (50 people), while on the contrary the majority of those, who mentioned car driving as the mode of transport were men.

Places considered to be safe or unsafe

Since each individual respondents could have drawn as many polygons of safe and unsafe areas as he or she wanted, we collected a large number of polygon data. Altogether 447 polygons were indicating unsafe places, of them 168 were drawn by male and 279 by female respondents. On the other hand 404 polygons were depicting safe places, out of those 243 were marked by female and 160 by male participants.

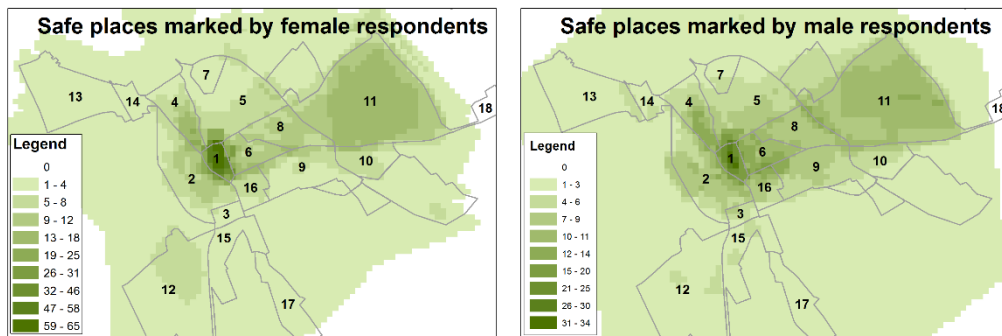


Fig. 2. Places marked as safe

As mentioned above, the drawn polygons were overlapped and aggregated in each part of the city to a 200x200m grid. The value of the grid cells, consequently, represented the total number of the counted polygons at a certain location. Concerning the total number of drawn polygons, women drew much more polygons and they were more decisive concerning safe places. The maximum number of women drawn overlapping polygons, which covered the same places was 65, on the contrary the highest number of identical places indicated by men was 34. Both groups identified the historical inner city (1) as the safest urban district (Figure 2.). This part of the city is densely populated, having typically highly qualified, but not too affluent inhabitants. There are many offices, public institutions and schools in this area, while also street lighting or surveillance cameras are densely installed. The respondents marked also garden city areas as very safe, which is not surprising, since these are the places, where the most affluent people are living (11), moreover one could find strong communities here having neighbourhood watch in operation (5). Among the reported safe locations also some mixed (4) or block building areas (2) could have been identified, where public lighting and surveillance cameras are keeping the place safe even with the opportunity for residents of doing late night sport activities. Concerning gender differences we found in general that women and men mark more or less the same places as safe. It is interesting though, that female respondents defined almost the whole historical city centre as safe, but male respondents indicated just the main street with exclusive shops and theatres on their sketch maps.

Generally speaking, the respondents specified more unsafe places than safe ones. Three main or typical areas were mentioned as unsafe: the train station (16), Alba Plaza, which is a crowded shopping mall with a nearby busy bus station and the city park near the city centre (1-2) (Figure 3.). According to the results, only some residential areas were left blank on the map. The maximum number of overlapping polygons reached as high as 84 in case of women, while it was only 44 in the case of male participants. Consequently, we might draw the conclusion that this topic is addressing the interest rather of female respondents. By comparing the two maps, we found that they are differing more from each other than it was in the case of safe area maps. Anyway, the most fearful places were quite identical for both genders.

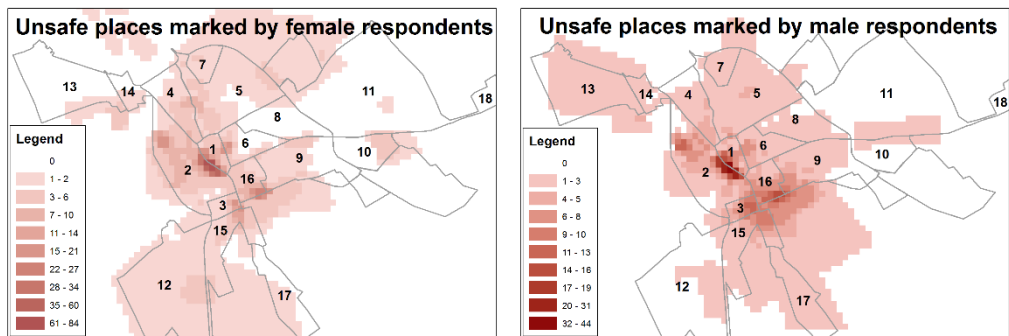


Fig. 3. Places marked as unsafe

Unsafe places, where people possibly feel fear of crime could also be in correlation with places, where higher concentration of socially disadvantaged population is observable (3). This is the case also in areas of municipal social housing (2), as well as in zones, where public lighting is poor, or homeless shelters are possible to see (e.g. edge zone of 4-5), in areas with somewhat larger share of ethnic minorities (12) or in certain parts of the city with very few or no population (3).

To make our analysis clearer, we provided the respondents the possibility in the questionnaire to make some comments about their fear. The most important causes and fearful things they mentioned were: theft, harassment, molestation, beggars, minority people, homeless, dog attack, bad public lighting, empty spaces and drunken people. Most of them (18 people: 17 women and 1 man) mentioned theft as primary reason of fear. They also indicated places in relation with the fear of theft, which were mainly connected to the main bus station and the shopping mall nearby. The second most often mentioned cause of fear was in relation with harassment or molestations, which were mentioned 14 times (12 women, 2 men). The mentioned places connected to this type of fear were typically the train and bus stations and the main shopping mall.

In order to have a comprehensive outcome we compiled sketch maps containing safe places with those marking unsafe places. As a result, a grid map was created, where grid values were showing the difference between the number of sketch maps mentioning a certain location as safe and the number of cases mentioning it as unsafe. Therefore, where the map returned positive values it meant that more safe polygons were overlapping than unsafe ones (see green pixels on Figure 4.), while negative values represented more unsafe overlapping polygons than safe ones (see red pixels).

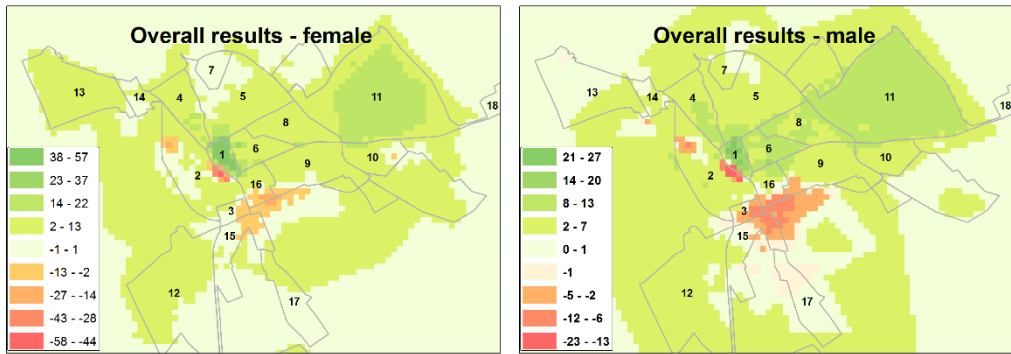


Fig. 4. Overall results

The maps mirrored evidently that both male and female participants have in common that unsafe places are: the main shopping mall and nearby bus station (1), areas with municipal social housing and with Gypsy minority population (some parts of zone 2 and 3), as well as the main train station and its surroundings (16). On the other hand, a noteworthy difference between places marked by male and female participants is that the extremes, namely the range of values is much larger on the combined result map of female respondents (with values between -58 and 57), than on the male's map (with values between -23 and 27), which is a consequent of the different sample sizes.

Comparing results with official data

In Hungary, official crime statistics data are available at the police.hu website, which provides data with a delay of 30 days. The website offers also mapped data by showing the location of each crime event represented as a point symbol. Event locations of the following crime types are observable on the map: violent crimes against persons, theft, car and motor theft, breaking up of cars, burglary, vandalism, robbery, violence and disruption, as well as offence against properties. Based on this service we collected data for the period of 01.09.2016-01.09.2017, and after that the address level data were aggregated to a 200x200m grid similarly to our previously mentioned analysis.

According to the official data, the most infected areas with the highest number of offences were located around the main bus station and the shopping mall (1) and near the northern edge of the historical centre (1), where public events are usually attracting a lot of people (Figure 5.). Also the area around the main train station (south edge of zone 16) and some neighbourhoods with homeless shelters were frequently affected (4-5). Grid cells with 6-8 offences were typically connected to locations offering entertainment services, while cells with 1 to 4 offences were typically locations near supermarkets, traffic junctions or major housing estates. Interestingly, industrial zones had no recorded crime events during the observed period.

By comparing unsafe places marked by the citizens and locations of officially registered crime events we could discover some coincident places such as the main shopping mall, the central bus station or the train station. However, we could also identify places, which were marked as unsafe by the respondents, but did not appear in the official police statistics such as some areas with relatively large share of Gypsy minority (3), or districts with municipal social housing estates (4).

It is also remarkable that the historical city centre is usually considered to be safe, although most of the offences happen there.

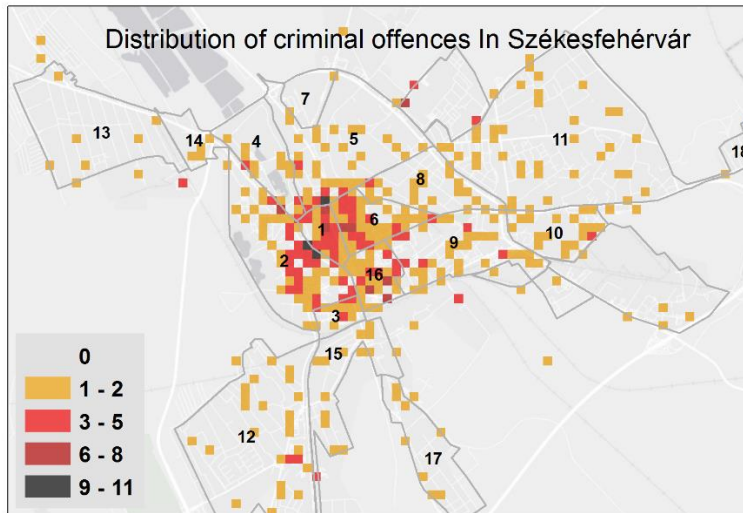


Fig. 5. Spatial distribution of official police data about criminal offenses

CONCLUSIONS

Although the presented methodology is not as complex as some other applications (Pánek et al. 2016, Resch et al. 2015), this study still confirmed that critical places could be efficiently detected with the assistance of this tool. The application happened to be suitable for some tasks of criminal investigations or could be used by police departments for deeper crime analysis, as well as by municipalities for implementing new surveillance camera systems or for local law enforcement strategies. This study verified that fear of crime is strongly related to prejudice. Generally speaking, unsafe places were marked around crowded entertainment locations, or in the neighbourhood of socially backward areas, where, on the contrary, police statistics did not indicate high crime rates. Some places however, such as traffic junctions, bus and train stations were both mentioned by citizens and recorded as event locations in police crime statistics.

REFERENCES

- Boschmann, E. E., & Cubbon, E. (2014). Sketch maps and qualitative GIS: Using cartographies of individual spatial narratives in geographic research. *The Professional Geographer*, 66(2), 236-248.
- Doran D. J. & Burgess M. B. (2012). *Putting Fear of Crime on the Map: Investigating Perceptions of Crime Using Geographic Information Systems*. New York, NY: Springer.
- Downs, R. M. & Stea, D. (1973). Cognitive maps and spatial behaviour: process and products. In: R. M. Downs & D. Stea (Eds.), *Image and Environments*. Chicago: Aldine.

- Ferraro, K. F. & LaGrange, R. L. (1987). The measurement of fear of crime. *Sociological Inquiry*, 57, 70-101.
- Gould, P.; & White, R. (1993). *Mental Maps*. New York: Rutledge. p. 93.
- Hungarian Police Department, Official statistics about the numbers of crime: <http://www.police.hu/a-rendorsegrol/statisztikak/bunugyi-statisztikak> (Accessed 05.10.2017)
- Kounadi, O., Ristea, A., Leitner, M., & Langford, C. (2017). Population at risk: using areal interpolation and Twitter messages to create population models for burglaries and robberies. *Cartography and Geographic Information Science*, 1-16.
- Lederer, D. & Leitner, M. (2012). Erfassung der stadtteilspezifischen Kriminalitätsfurcht und Verortung von Kriminalitätsfurchträumen in Linz. In: J. Strobl, T. Blaschke & G. Griesebner (Eds.), *Applied Geographic Information Technology*. Berlin/Offenbach: Wichmann.
- Letenyey, L. (2005). Preparing mental maps. In: Letenyey László, *Településkutatás I*, 147-185. Budapest: Ráció. [in Hungarian]
- Lynch, K. (1960). *The Image of the City*. Cambridge MA: MIT Press.
- Matei, S., Ball-Rokeach, S. & Qiu Linchuan, J. (2001). Fear and misperception of Los Angeles urban space: a spatial-statistical study of communication-shaped mental maps. *Communication Research* 28 (4), 429–463.
- Milgram, S. (1992): Psychological maps of Paris. In: J. Sabini & M. Silver (Eds.), *The Individual in a Social World: Essays and Experiments*. New York: McGraw-Hill.
- Pánek, J., Pászto, V. & Marek, L. (2016). Mapping emotions: spatial distribution of safety perception in the city of Olomouc. In: *GIS Ostrava 2016 – The Rise of Big Spatial Data. Springer Lecture Notes in Geoinformation and Cartography*, 211-224.
- Pődör A. & Dobos, M. (2014). Official crime statistics versus fear of crime of the citizens in a hungarian small town. In: R. Vogler, A. Car, J. Strobl & G. Griesebner (Eds.), *GI_Forum 2014 – Geospatial Innovation for Society*. Berlin: Herbert Wichmann. pp. 272-275.
- Resch, B., Summa, A., Sagl, G., Zeile, P. & Exner, J.-P. (2015). Urban emotions – geo-semantic emotion extraction from technical sensors, human sensors and crowdsourced data. In: G. Gartner & H. Haosheng (Eds.), *Progress in Location-Based Services 2014*, Cham, Switzerland: Springer. pp. 199-212.
- Skogan, W. G. (1995). Crime and the racial fears of white Americans. *The Annals of the American Academy of Political and Social Science*, 539(1) 59-71.
- Váradi, L. (2014). *Youths Trapped in Prejudice, Politische Psychologie*. Wiesbaden: Springer Fachmedien .
- Zedner, L. Victims. In M. Maguire, R. Morgan, & R. Reiner (Eds.), *The Oxford Handbook of Criminology* (2nd ed., pp. 577–612). Oxford, England: Clarendon Press.

ERROR PROPAGATION IN WATERSHED ASSESMENT. A CASE STUDY OF DELINEATION POLLUTION CONTRIBUTION AREA

Kateřina, RŮŽIČKOVÁ¹; Jana, NOVÁKOVÁ²; Tereza, MATĚJOVÁ²; Jan, RŮŽIČKA¹

¹Institute of Geoinformatics, HGF, VŠB – TU Ostrava, 17. listopadu 15, 708 33, Ostrava, Czech Republic

katerina.ruzickova@vsb.cz

²Institute of Environmental Engineering, HGF, VŠB – TU Ostrava

Abstract

Solving of an environmental pollution is one of our primary effort. It is important to find the source of the pollution to stop this demotion in a case that it is not self-evident. Dripping water chemicals are usually invisible so we use hydrological analysis in GIS to clarify invisible processes. These analyses are very sensitive to a digital terrain model accuracy. The paper describes the evaluation of a watershed assessment with a respect to uncertainty of a digital terrain model (DTM) and its precision. There is used sequential Gaussian geostatistical simulation to simulate probable variations of a DTM and the Monte Carlo simulation to delineate a watershed area. Elevation data from LiDAR scanning were used and two levels of terrain accuracy were set. The result showed, that high errors can leads to less stable solution a can significantly devalue watershed delineation.

Keywords: uncertainty, DTM, watershed, water flow, Monte Carlo simulation, Gaussian geostatistical simulation

INTRODUCTION

There are more uncertain aspects, which should be solved during a calculation of contributing areas/watersheds in hydrogeological analysis. Uncertainty is increasing during the whole process of watershed delineation – it starts with phase of data capturing thru DTM generation, hydrological analysis and result interpretation at the end. The well-defined and measurable part of uncertainty are errors (Chrisman, 1991). Poorly defined part of uncertainty in form of vagueness and ambiguity is not such a big problem in working with spatial-elevation data in comparing with working with attribute-classified data (Oksanen, 2006). Output error of terrain analysis is a function of input error and model error. This error propagation could be solved by analytical method or Monte Carlo simulation. For applications in hydrological field using D8 flow directions algorithm is more suitable Monte Carlo simulation (O'Callaghan & Mark, 1984).

The Monte Carlo simulation is based on a generation of random (potential) elevation errors with a specific range/distribution, which are added to original elevation data. The whole geospatial analyse is done with these adjusted elevations. With higher number of simulation repetitions of this process there are more variations for input elevations and analyse results afterwards. Finally, all the results are statistically evaluated together (Fisher, 1991; Heuvelink, 1998).

Random functions for creation model of DTM error are used and it changes the character of the watershed analysis into the stochastic process. Random field has spatial context, because there is spatial dependence of elevations and its errors. Conditional simulation, where the error model respect existing observations, is beneficial. Geostatistics offers a number of simulation methods, which can be applied in DTM error propagation analysis – e.g. the simulated annealing, spatially autoregressive model, spatial moving averages and sequential Gaussian simulation (Goovaerts, 1997).

Sequential Gaussian simulation generate MultiGaussian field of equally probable DTM solutions. It is based on simple kriging. Each node of modelled locality is visited sequentially and evaluated with the “location-specific mean and variance of conditional cumulative distribution function (CCDF). Finally, a random value is drawn from the CCDF, the value is added to the dataset, and the procedure is repeated until all nodes have been visited” (Oksanen, 2006 based on Goovaerts, 1997).

Elevation source datasets can be evaluated with a different error according the type of a landscape. The error is usually smaller in open areas and is higher in urban areas and forests in a case of aerial sensed elevations. So is necessary to work with different inaccuracy in different areas according the landuse. Accuracy of elevation dataset is a part of metadata; which producers provides with datasets.

During a hydrological modelling the hydrological correctness of a DTM must be solved (Kenny at al., 2008). Hydrological algorithms are very sensitive to sinks in a DTM, because they may cause interruption of water flow over the terrain. Usually we cannot distinguish which sinks in a DTM are real and which were artificially created during an interpolation (Lidberg at al. 2017). To prevent stop of a flow in sinks, all sinks are commonly filled (Samanovic at al. 2016). The regulation of filling can be used e.g. according the size of the sink.

A base step of a hydrological processing is a flow direction calculation. There are more possibilities how to execute the process. Geographic information system (GIS) tools offer an assessment of a single flow direction (SFD (D8)) or a multi-flow direction (MFD) (Pei at al. 2010). It can influence results of all hydrological characteristic. MFD is thought as a better and a more realistic model of a flow, but not all GIS software can do it and use its results as an input for a next processing.

STUDY AND AREA DESCRIPTION

The surrounding of abandoned riverbed was analysed as a solved area. There were measured high concentrations of inorganic phosphorus at this old riverbed, which overcrossing permissible limits. It is placed inside Natural conservation area Poodří (**Fig. 1**). High values of phosphorus cause water eutrophication, which degrades environmental ecosystems. In this view the task is one of the applications for safety and security management in GIS. The source of the phosphorus can be fertilizer, cleaning and laundry agents etc. Water area is shallowed there with a deep deposit and very weak or minimal flow. The neighbourhood pounds do not evince so high level of a pollution. But they are used up and there are higher water exchanges. The goal of the analysis

was delimiting area from which the pollution can be imported into an abandoned riverbed via a surface flow. Uncertain evaluation of the analysis was elected to prevent omitting some parts of potential contributing area which can be omissible during processing deterministically. We also consider to be beneficial to get most probable areas, where we can start with searching of water pollution firstly.

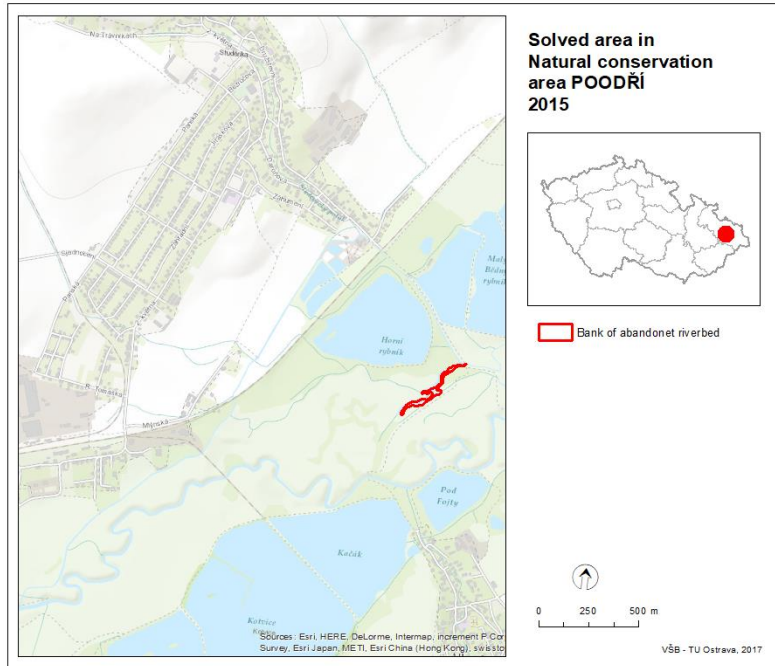


Fig. 1. Solved area

The solved area is relatively flat (**Fig. 2**), so the effect of an uncertain evaluation can be more significant in comparison with a more roughness countryside, because a hydrological analysis is sensitive to a terrain accuracy.

This study is going to present a processing of an uncertainty in contributing area assessment in a local area. Especially in a hydrological analysis a small error in terrain elevations (e.g. a small hillock) can cause a water outflow to another direction and so it can significantly influence the result.

Accuracy of used elevation data were evaluated by comparing with more master data-source as it mentioned in next chapter. A subsidiary goal of this study was also comparing the results with using a different level of terrain elevation error settings.

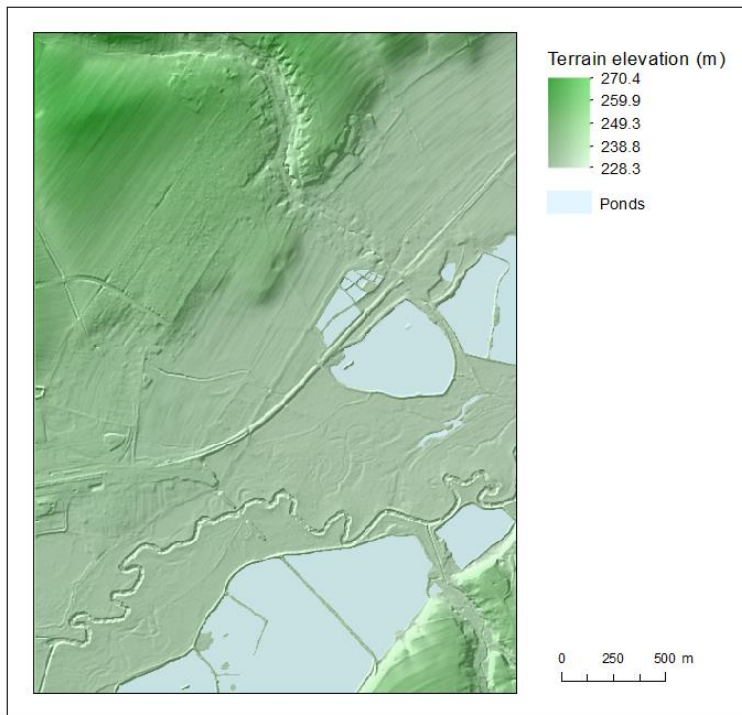


Fig. 2. Terrain in solved area

DATA

There were used data from an aerial laser scanning. Dataset DMR5G, which was acquired and pre-processed by State Administration of Land Surveying and Cadastre. It is irregular point dataset. Declared error (RMSE) of this model is 0,18 m in open area and 0,3 m in area with continuous vegetation and built-up area. Its accuracy was also evaluated by comparison with geodetical verification measurement - according type of landuse as **Tab.1** presents (Brazdil, 2016).

Table 1. Accuracy of DMR5G (elevation points) data (Brazdil, 2016)

Landuse	Systematic error (m)	RMSE (m)	Maximal error (m)
Communication hardline	-0,11	0,18	0,66
Reinforced (urban) area	-0,09	0,13	0,37
Fertile ground	-0,07	0,14	0,56
Meadow and pasture	-0,03	0,21	0,42
Wood, bush and alley	-0,06	0,13	0,46
Mean error	-0,07	0,14	0,49

The elevation points of water levels were removed from measured data by producer. Instead of them a sparse network of interpolated elevation points was added into the dataset in these areas.

Landuse data were derived from topographic map, orthophotos and field survey.

METHOD

Firstly, the area classification according the landuse was done. Ones just the classification into open and area, which was build-up or wooded. At the second go of classification all categories enumerated at **Tab. 1** were classified. According the landuse categories the value of mean error was assigned to each elevation point. Stand-alone lakes and ponds layer were created and water level elevation information was added to these polygons.

For geostatistical Gaussian simulation the simple kriging with elevation points was done to get geostatistical layer in advance. **Fig. 3** presents Cross validation of DTM elevation.

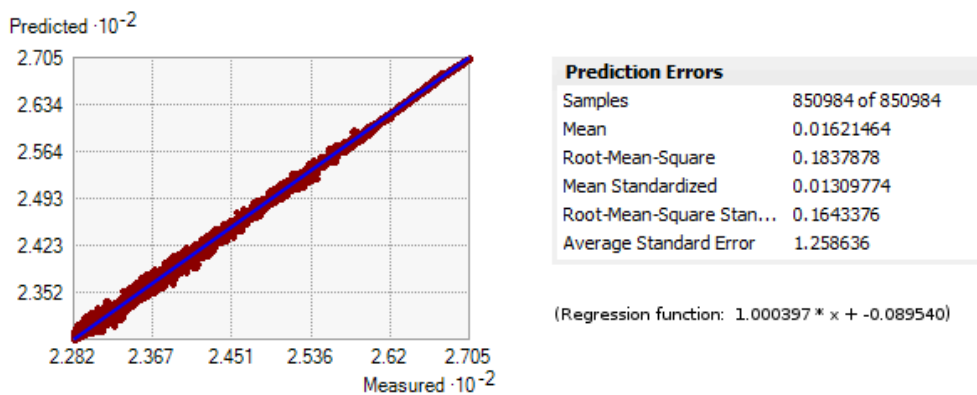


Fig. 3. DTM cross validation

Afterword stochastic modelling via sequential conditional geostatistical Gaussian was used to generate number of realizations of DTM with respect to elevation error according the landuse. Simulation was adjusted as conditional to respect original points elevation with corresponding error. The used tool (for geostatistical Gaussian simulation) in ArcMap requires to set standard deviation error, which was not a part of metadata of elevation dataset. In comparing values of standard deviation and RMSE in different elevation data, we found that standard deviation has usually slightly smaller value than RMSE (DHI GRAS, 2014). We account with RMSE then. We cannot regard it as exactly right error, but relative footing can go. In this view we will later evaluate the results. According the report about used elevation data we can assume a normal distribution of error. This process was done twice – one for elevation error distinction differently for open and build-up (or wooded) area; and second time with different error for each landuse category according **Tab. 1**. So-called for lower and higher accuracy of elevations. There were generated 2 sets of DTMs realisations, each with 100 variations.

Standard deviation of elevations between 100 DTM variations reach up to maximum value 6,65m for set of DTMs with higher accuracy of elevations (errors in **Tab.1**). But high values of this deviation occur only inside ponds. After removing values in ponds, the maximum value of

standard deviation decreased on value 0,34m (**Fig. 4**). We processed ponds elevation separately, because there were not original data and we wanted to assure exactly horizontal water level before hydrological analysis. Similar result we obtained with a simulation, where were set higher values of errors (0,18 m in open areas and 0,3 m in other areas). The maximum standard deviation come up to 3,43m and without water areas up to 0,37m.

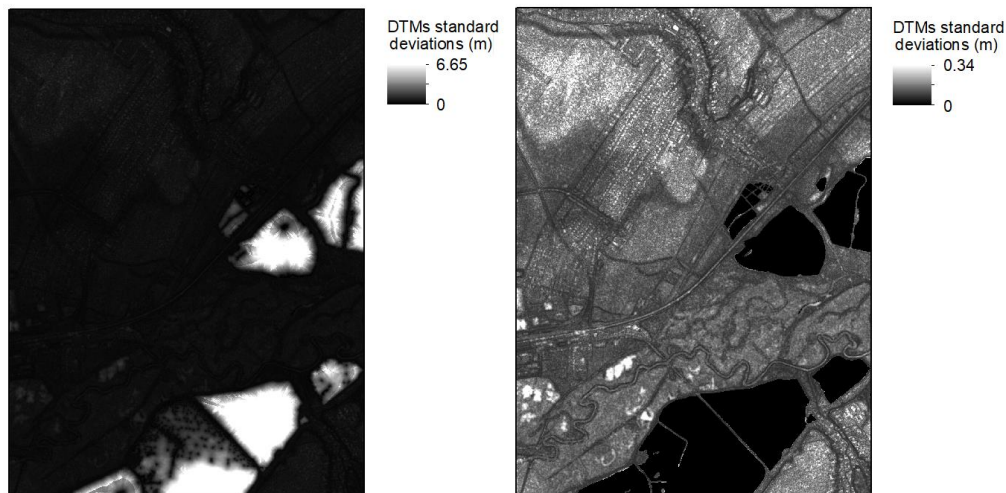


Fig. 4. DTMs standard deviation (left – for the whole DTMs; right – just for places outside the ponds)

Monte Carlo simulation of watershed delineation was processed afterwards for both sets of DTMs separately. Within the scope of this simulation, the sequence of operations focused on deriving contribution flow area into pour point was processed. **Fig. 5** presents the whole process.

At first, DTMs were adjusted to ensure horizontal levelling surfaces of lakes and ponds. The elevations in ponds were removed and set to required value. The average filtration of DTMs was done in order to smooth continuity between water levels and the surrounding terrain. The DTMs were finalized with filling the sinks.

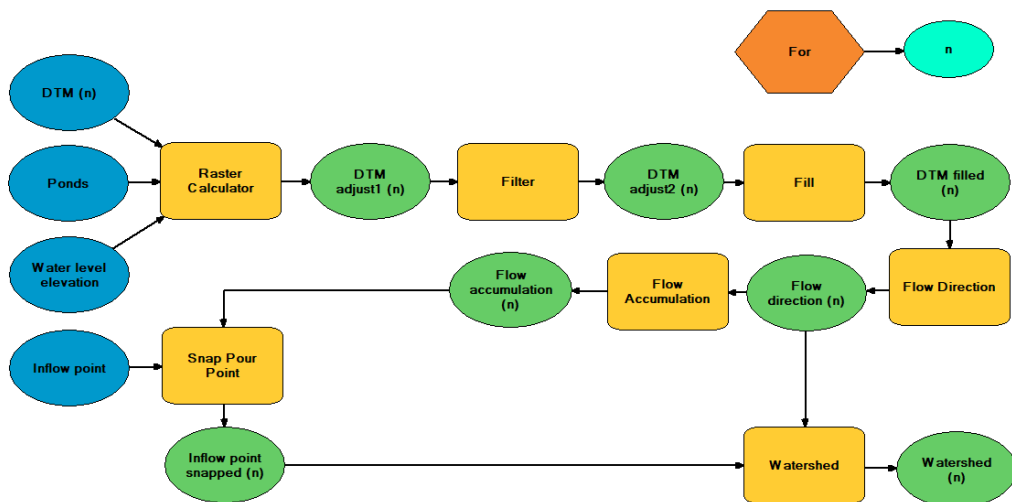


Fig. 5. Process of contributing area delineation

A hydrologic analysis started with calculation of flow directions. A single flow direction (D8) was used. It was the basic for an evaluating of a flow accumulation. Position of pour point was fitted to hydrological topology. Finally, the watershed for the pour point was allocated.

All the possible watersheds were submitted into summarization for each of two DTMs set. Also deterministic evaluation of watershed without any elevations uncertainty was accounted to compare it with result of stochastic processing. It was analogical procedure but with the one DTM with exactly fixed elevations.

RESULTS

Practical modelling of the whole study outcome with one result for deterministic processing and two results for uncertain stochastic processing (for higher and lower elevation accuracy). A blue line in **Fig. 6** presenting determination of simple deterministic watershed evaluation. A red scale represents the result of an uncertain (stochastic) elaboration. The most probable (the most frequent) watershed extent (reddest) matches with result of simple evaluation in the main. But the uncertain assessment offers also more extended area (lighter red), which is not so much probable (it has low frequent), but it can include more extend possibilities. During finding the source of a pollution in the study area the bigger area is desired, because we can be sure, that we will not neglect any possible contributing part of a watershed.

In relation to terrain in studied area we can recognize specific elements of the surface that often act as a borders for basins. These are the river on the south and the railway, which goes thru the area from south-west to north-east. The railway blocks the inflow from north part of terrain, but there is a culvert, which allow the water goes throw the subgrade.

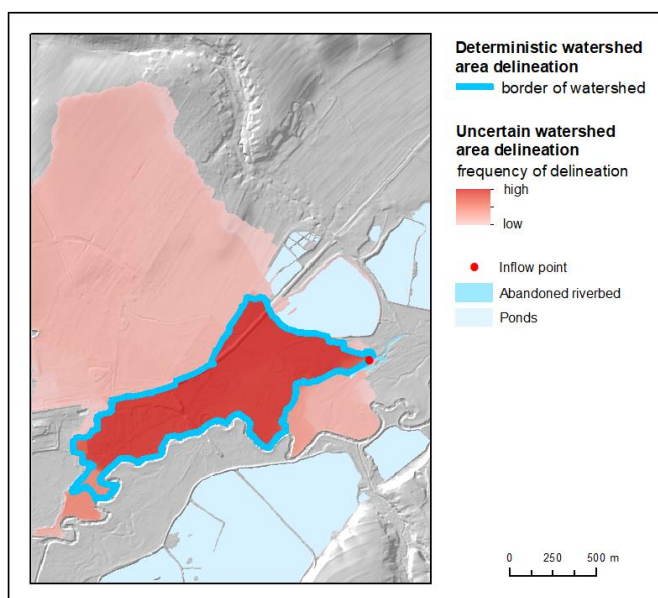


Fig. 6. Contributing area – deterministic and stochastic-uncertain evaluation (for higher elevation accuracy in this case)

In a relation to evaluation with different settings of error levels (elevation accuracy) we have got a predictable result. Smaller errors of elevations lead to more consistent solution in comparison with higher ones. This is noticeable in **Fig. 7.**

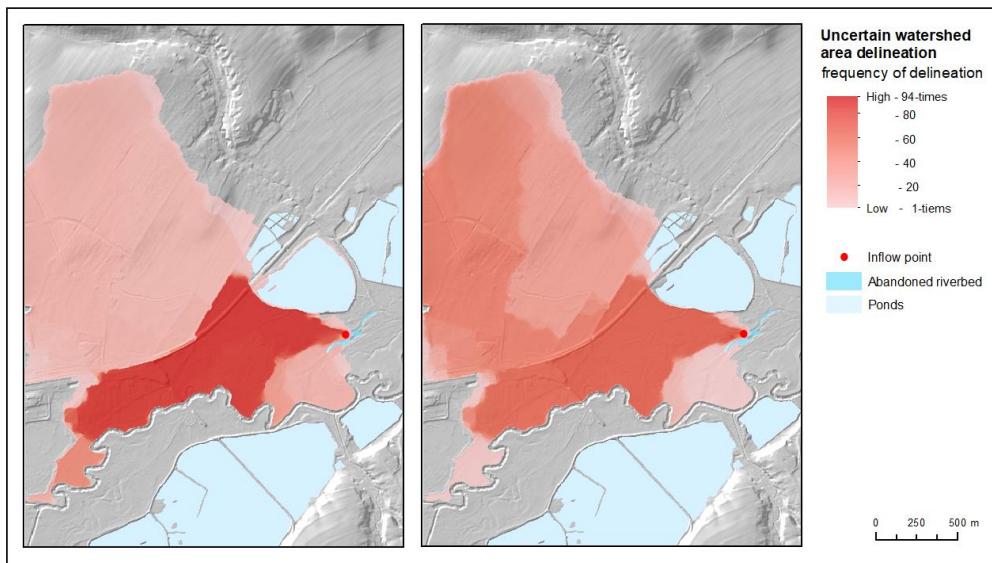


Fig. 7. Uncertain contributing area (left – with elevation errors 0,13-0,21m, right – with elevation errors 0,18-0,3m)

Variability of stochastic watershed delineation was studied also via standard deviation in **Fig. 8.** There is significant, that with subsumption of higher errors the watershed delineation more times does delineate neither deterministic delineation.

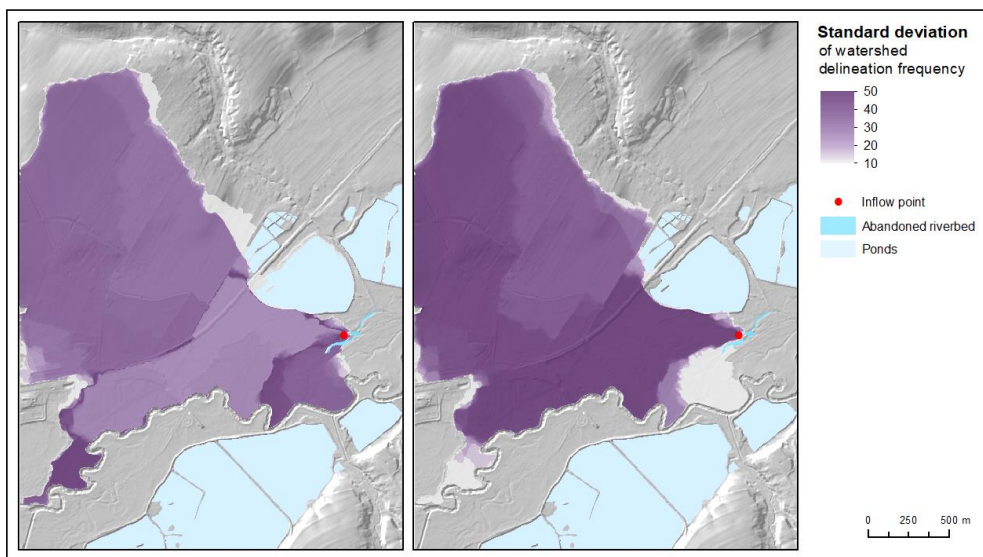


Fig. 8. Standard deviation of watershed delineation frequency (left – with elevation errors 0,13-0,21m, right – with elevation errors 0,18-0,3m)

Uncertain results for two levels of elevation accuracy are compared also by histograms of watershed area in **Fig. 9**. Blue dash line in **Fig. 9**. present value of deterministically evaluated watershed area. With higher error values we received more diffused solution. The uncertain delineation sometimes failed in comparison with result of deterministic contributing area. There occur the terrain obstacles near inflow point, which can be heightened by adding higher elevation error into DTM, so the inflow starts in very short distance from inflow point or it does not start at all. The inflow from further places is blocked by those obstacles. It causes delineation of very small contributing areas. It is evident on histogram (**Fig. 9**, right side), where the most contributing areas is close to zero. The maximum extent is almost the same in both uncertain cases. But this effect cannot be generalised. It is done by morphology of currently used DTM.

Our results of evaluations of uncertainty are necessary to interpret as a relation between smaller and higher amount of uncertainty in input (elevation) data. We do not know accurate elevation error in input data. The variability of results was statistically processed on values of contributing area. **Fig. 9** presents a graphical representation of this evaluation. The result of deterministic contributing area delineation (without uncertainty of elevation data represented by blue borderline in **Fig. 6**) was 64.8250 ha. There is also used blue line (dashed) in graphs for an easier comparison. It is noticeable that bigger uncertainty in input DTM caused bigger variance in results. We did not consider as suitable to remove distance areas (outlier's values in box-plot for smaller uncertainty in DTM), because they are valid result of analyse. The result area values have not normal distribution (according the Shapiro-Wilk test), so there was not possible to use standard comparing two variances. We decided to use exact binomial test (Clopper-Pearson test) about the probability, that the uncertain contributing area reach over the value of deterministic contributing area. The probability of overcrossing deterministic contributing area (64.8250 ha) was 73% for a smaller uncertainty in DTM and 37% for a bigger uncertainty in DTM. The probability 73% for a smaller uncertainty in DTM was confirmed for significance at the 5% level (p -value < 0.001), but probability 37% for a bigger uncertainty in DTM cannot be affirmed (p -value = 0.996).

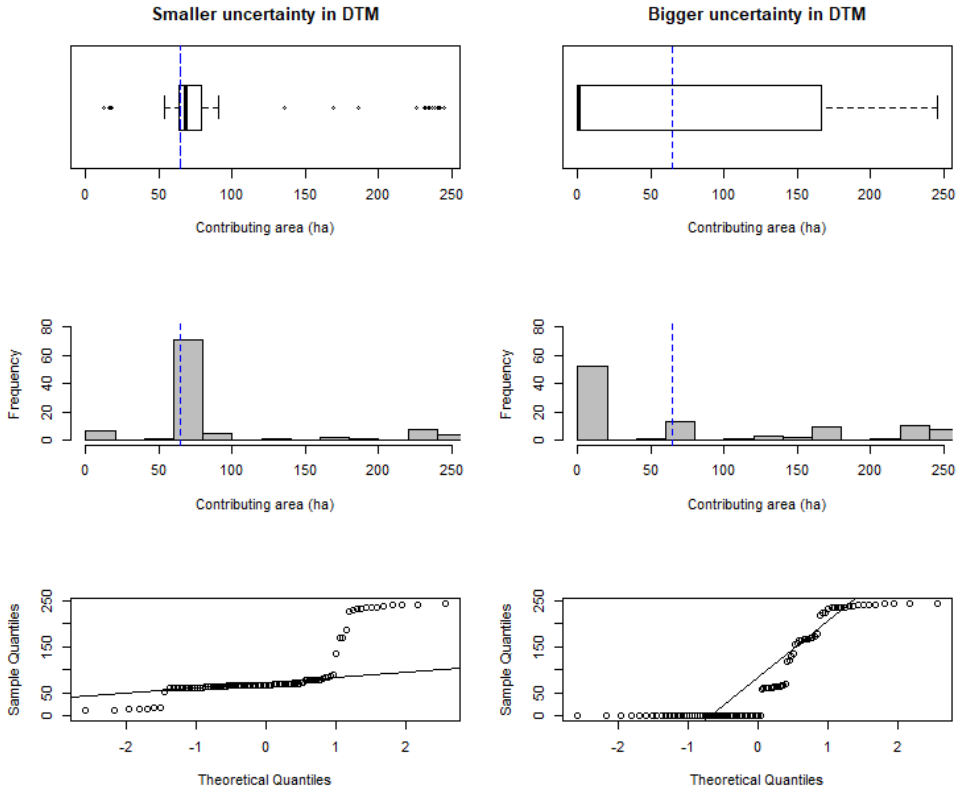


Fig. 9. Statistical evaluation of results of contributing area (blue dashed line represents result of deterministic delineation of contributing area (64.8250ha)).

CONCLUSION

An uncertain stochastic watershed can be more extensive and its borders are inexplicit in comparison with a deterministic solution. It faces the consequences with errors of input elevation data and inaccuracies of the process of the evaluation. There are places where we can be sure, that there is a watershed (the most frequent places) and there are places, where the watershed can rarely reach (less frequent). The proposed solution tries to cover all possible watershed areas. The deterministic evaluation may produce smaller watershed area and some edge parts of the watershed can be aside.

On the other hand, a bigger uncertainty in source (elevation) data brings the risk that an inflow will be artificially blocked, despite of used algorithms tried to increase autocorrelation of terrain elevations based on filtering.

ACKNOWLEDGEMENT

This article was prepared within the project SP2017/13 Analýza a modelování forem fosforu, i tzv. BAP v malých vodních nádržích.

REFERENCES

- Brázdil, K. (2016) *Technická zpráva k digitálnímu modelu reliéfu 5. generace*. Pardubice: Zeměměřičský úřad. Available at: http://geoportal.cuzk.cz/Dokumenty/TECHNICKA_ZPRAVA_DMR_5G.pdf (Accessed: 20 December 2017).
- DHI GRAS (2014) *EU-DEM Statistical Validation*. Available at: <http://ec.europa.eu/eurostat/documents/4311134/4350046/Report-EU-DEM-statistical-validation-August2014.pdf/508200d9-b52d-4562-b73b-edb64eedfb93> (Accessed: 21 December 2017) pp. 27.
- Driemel, A., Haverkort, H., Loeffler, M., Silveira, R. (2011) Flow Computations on Imprecise Terrains. *Algorithms and data structures*. LNCS, Vol. 6844, pp. 350-+. ISBN:978-3-642-22299-3.
- Chrisman, N. (1991) The error component in spatial data. In Maguire DJ, MF Goodchild & DW Rhind (eds). *Geographical Information systems – Vol.1: Principles*. Longman Scientific and Technical, Avon, UK. pp. 165-174.
- Fisher, P. F. First experiments in viewshed uncertainty: The accuracy of the viewshed area. *Photogrammetric Engineering and Remote Sensing*. Vol. 57, No.10, pp. 1321-1327.
- Garrigues, S., Allard, D.; Baret, F. (2007) Using First- and Second-Order Variograms for Characterizing Landscape Spatial Structures from Remote Sensing Imagery. *IEEE Transactions on Geoscience and Remote Sensing*. Vol. 45, Iss. 6, pp. 1823 – 1834.
- Goovaerts, P. (1997) *Geostatistic for Natural Resources Evaluation*. Oxford University Press, New York, 483 p.
- Heuvelink, G.B.M. (1998) *Error propagation in Environmental Modelling with GIS*. Taylor and Francis. London. 127 p.
- Kenny, F., Matthews, B., Todd, K. (2008) Routing overland flow through sinks and flats in interpolated raster terrain surfaces. *Computers & Geosciences*. Vol. 34, Iss. 11, pp. 1417-1430.
- Lidberg, W., Nilsson, M., Lundmark, T., Agren, A, M. (2017) Evaluating preprocessing methods of digital elevation models for hydrological modelling. *Hydrological processes*. Vol. 31, Iss. 26, pp. 4660-4668. ISSN: 0885-6087.
- O'Callaghan J.F. and Mark, D.M. (1984) The extraction of drainage networks from digital elevation data. *Computer Vision, Graphic and Image Processing*. Vol. 28, pp. 323-344.
- Pei, T., Qin, C-Z., Zhu, A-X., Yang, L., Luo, M., Li, B., Zhou, Ch. (2010) Mapping soil organic matter using the topographic wetness index: A comparative study based on different flow-direction algorithms and kriging methods. *Ecological indicators*. Vol. 10, Iss. 3, pp. 610-619.
- Samanovic, S., Medak, D., Gajski, D. (2016) Analysis of the pit removal methods in digital terrain models of various resolutions. *International Archives of the Photogrammetry Remote Sensing and Spatial Information Sciences*. Vol. 41, Iss. B2, pp. 235-239.

DEVELOPMENT OF THE SYSTEM FOR ONLINE TESTING AND EXAMINATION IN THE DOMAIN OF GEOSCIENCES

Milan, MUŇKO¹; Jana, FAIXOVÁ CHALACHANOVÁ¹; Renata, ĎURAČIOVÁ¹

¹Department of Theoretical Geodesy, Faculty of Civil Engineering, Slovak University of Technology in Bratislava, Radlinského 11, 810 05, Bratislava, Slovakia

milan.munko@stuba.sk, jana.chalachanova@stuba.sk, renata.duraciova@stuba.sk

Abstract

There are currently numerous systems used in online testing and examination. Some of them focus on a high complexity and require complicated control; on the other hand, simple examination systems do not always meet specific user requirements. For example, online testing in the domain of geosciences requires the use of specific figures and ensure that information and figures from various licensed software are not published outside the workplace. Therefore, we have developed the open source System for Online Testing and Examination (SOTE) in the domain of geosciences that meets the requirements of examination at the Faculty of Civil Engineering of Slovak University of Technology. The SOTE system is based on open source technologies Python, Django and PostgreSQL. Usage of the system does not require any third-party technology or software and tests can be defined using the standardized JSON file created by common text editors. The system has been used and improved over the three years of its use to test these subjects: Geoinformatics, Information technology, Database systems in GIS, Spatial modelling in GIS, and Web technologies. Although the system has been designed and developed for specific conditions, it is available and can be used in other use cases as well.

Keywords: online examination system, system security, GIS, Python, PostgreSQL

INTRODUCTION

Currently, several software environments can be used for online testing and examination. These include online systems for e-learning and testing (<https://www.onlineexambuilder.com>, <https://www.classmarker.com>), as well as various special university systems (Sunder et al., 2017; Zhao and Li, 2012; <https://is.stuba.sk>; <https://moodle.uniba.sk>). The Academic information system (AIS) of Slovak University of Technology (STU) in Bratislava (<https://is.stuba.sk>) is one of them. It allows the teachers to online test and examine all subjects taught at university. Unfortunately, it is not entirely appropriate to test subjects in the domain of geosciences. The reason is, for example, that online testing of these subjects requires the use of figures created in various licensed software environments that may not be published outside the workplace. In addition, the AIS test system does not have easy and user-friendly control and requires study of documentation, which is why it is not widely used for testing in the domain of geosciences at Faculty of Civil Engineering of Slovak University of Technology (FCE STU).

Another alternative for electronic testing is open source learning platform Moodle (Modular Object-Oriented Dynamic Learning Environment) provided under the GNU GPL license (GNU's Not Unix General Public License). Moodle is based on a single robust, secure and integrated

system to create personalised learning environments (<https://moodle.org>). The key features of the Moodle are file and user's management, included text editor, activities planning, notifications, track progress, secure authentication and authorization, full course creation, external resourcing, backup, reporting, messaging, etc. Moodle is very extensive system with many functions, which is extensible by plugins and add-ons. But for the purposes of simple electronic testing, without needing of complex environment, it is wasted to use such complicated system as the Moodle is. Several papers deal with the consideration the effectiveness of the modern educational technologies, and with the identification the factors affecting the effectiveness of the Moodle system (Aikina et al., 2015; Damnjanovis et al., 2015; Horvat et al., 2015).

Although there are several e-learning and testing systems, due to our own system security requirements and the specificity of geosciences, we have developed our own testing system to test subjects in the domain of geosciences.

The functional and system requirements are based on the usual technical possibilities of system management, as well as on the university testing rules, especially at the FCE STU. The most important requirements are listed below.

Functional requirements:

- Random generation of the questions from the separated sections (e.g. 3 questions from the Section 1; 5 questions from the Section 2, etc.).
- Set the number of points for each question.
- Use the figures in the questions and answers (it is very important for testing and examination in the geosciences domain).
- Possibility to set multiple correct answers.
- Possibility to set number of points for all correct answers, even penalisation for incorrect answers.
- Ease of use for teachers and students.
- Possibility to test multiple subjects in the same time.
- The ability to record the results as well as the correct and incorrect answers for each question and student.
- Record upload time.
- Record the time of submission of the answers.
- Automatic check of the correct answers.
- Automatic evaluation.
- Possibility to see an exam result immediately (because of tests of subjects in the field of GIS at FCE STU in Bratislava usually include the practical part, which can be attended only by students who have successfully passed the test).

System requirements:

- Web application.
- Open source software.
- No need to install other software on the client side (only need a laptop or PC with a web browser and internet connection).

- For each subject, storage of all the questions, its choices and the correct answer in database.
- Storage of the details of the students and examination such a student name, his/her answers, date of examination, start and end time, etc.
- Security of the system (preventing unauthorized access to test questions and test results).
- All tests and results should be hosted in our own infrastructure.
- Access restrictions.

The main goal of the development and implementation of a system for online testing is to make examination process as safe and as simple as possible for both students and teacher. The main objective is to be able to perform examination with instant examination results in controlled environment. A lot of GIS related subjects is examined in two phases. First theoretical exam is used to reduce number of students that are not properly prepared for second practical part. Therefore, a teacher needs a system that provides him/her a way to get examination results in real time.

MATERIALS AND METHODS

Based on the above-mentioned requirements, we have developed the new System for Online Testing and Examination (SOTE). We used open source technologies, namely Python, Django, and PostgreSQL.

Overview of Technologies

To develop the system, Python 3 programming language (www.python.org) we used. Python is an interpreted high-level programming language for general-purpose programming. Python has a design philosophy that emphasizes code readability, and a syntax that allows programmers to express concepts in fewer lines of code, notably using significant whitespace. It provides constructs that enable clear programming on both small and large scales. Python is widely used and supported in most mainstream GIS software such as ArcGIS with their own Python interface ArcPy or in almost all open source projects such as QGIS or GrassGIS.

Django is a high-level Python Web framework that encourages rapid development and clean, pragmatic design (<https://www.djangoproject.com>). Django helps developers avoid many common security mistakes, such as SQL injection, cross-site scripting, cross-site request forgery and clickjacking. Its user authentication system provides a secure way to manage user accounts and passwords.

All data associated to the SOTE system are stored in PostgreSQL (<https://www.postgresql.org>). This database system is well known in GIS environment and is the most used open source relational database.

To create a new test and describe test questions and answers, the JSON format is used. It is readable both by computer and human. Another advantage of the JSON format is its simple syntax. In comparison with XML, JSON does not have opening and closing tags, it only needs matching braces. The JSON file is a standard text file, therefore can be open and edited in any text editor. This allows teachers of different subjects to easily and quickly create new tests.

RESULTS

Realisation of the SOTE system

The SOTE system is run on Ubuntu Server 16.04 LTS with 8 CPU and 16 GB RAM. However, this server is not dedicated only for the SOTE system, but various systems are hosted on this machine. One of the biggest advantages of this system is its low resource usage. The SOTE system can share the minimum resources needed for a host operating system to run. It is accessible through standardized TCP interface in the intranet or through the internet. The administrator can set up port on which system listens and therefore set up access restrictions (let this port be accessible from whole internet, limit it only to local IP addresses or even limit it to only named IP addresses).

The system blocks backward button on the browsers, therefore students are not allowed to return to first screen and regenerate the block of questions. Test is also protected by temporary password, which is valid only during the exam and when the teacher closes the submission of answers, password will be reset.

Using the system from the administrator's point of view

The administrator's interface of the online testing system is shown in (Fig. 1). The administrator can manage tests and test results (Fig. 1 top), add new users (Fig 1 middle), and also activate and deactivate tests, set password, and add new tests (Fig 1 bottom).

Using the system from the teacher's point of view

The teacher needs only text editor to prepare a test in the JSON format and a web browser and an internet connection to set up and start the examination. Each test can be run or paused with a defined password (Fig. 2). The teacher can view the results report during the testing, or within the specified time interval (Fig. 3). The elaborated test is shown in Fig. 4. The correct answers denoted by a student are marked using dark green colour. The correct answers that were not denoted by the student, are marked using pale green colour. The incorrect answers denoted by a student are marked using red colour.

The screenshot displays the Django administration interface. At the top, there is a dark blue header with the text "Django administration" on the left and "WELCOME, ADMINISTRATOR. VIEW SITE / CHANGE PASSWORD / LOG OUT" on the right. Below the header, the page is divided into two main sections. The left section, titled "Site administration", contains three blue-bordered boxes. The first box, "AUTHENTICATION AND AUTHORIZATION", lists "Groups" and "Users", each with a green "+ Add" button and a yellow pencil "Change" icon. The second box, "SKUSKA_ADMIN", lists "Tests" with a green "+ Add" button and a yellow pencil "Change" icon. The third box, "SKUSKA_TEST", lists "Results" with a green "+ Add" button and a yellow pencil "Change" icon. The right section, titled "Recent actions", contains a "My actions" list with four entries: "DSGIS: DSGIS t10 Test" (with a yellow pencil icon), "DSGIS: DSGIS t10 Test" (with a yellow pencil icon), "DSGIS: DSGIS t10 Test" (with a yellow pencil icon), and "DSGIS: DSGIS t10 Test" (with a green "+ Add" icon). The last entry in the list is "IT: 8_2017" (with a yellow pencil icon).

Django administration WELCOME, ADMINISTRATOR. [VIEW SITE](#) / [CHANGE PASSWORD](#) / [LOG OUT](#)

Home > Authentication and Authorization > Users > Add user

Add user

First, enter a username and password. Then, you'll be able to edit more user options.

Username:
Required. 150 characters or fewer. Letters, digits and @/./+/-/_ only.

Password:

Password confirmation:
Enter the same password as before, for verification.

Django administration WELCOME, ADMINISTRATOR. [VIEW SITE](#) / [CHANGE PASSWORD](#) / [LOG OUT](#)

Home > Skuska_Admin > Tests > Add test

Add test

Test name

Test file

Subject

Active

Passwd:

Fig. 1. User interface for the administrator of the SOTE system

Spatial modelling in Gi	SM in GIS	<input type="text"/>	<input checked="" type="checkbox"/>
DSGIS	Test DSGIS 4	<input type="text"/>	<input type="checkbox"/>
DSGIS	DSGIS t10	<input type="text"/>	<input type="checkbox"/>

Fig. 2. User Interface for the teacher – running the test

Spatial modelling in GIS: SM in GIS

Examination start: YYYY-MM-DD HH:MM

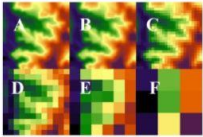
Examination end: YYYY-MM-DD HH:MM

Search

	Show Test	Show Results	Manage Tests	Log out
Time of submission	Student name	Points	Result	
Jan. 14, 2018, 6:02 p.m.	Student AB	1.0	Failed	
Jan. 14, 2018, 5:59 p.m.	Student XY	3.0	Passed	

Fig. 3. User Interface for the teacher – search for the test results

Which of the maps A to F listed in the following figure will have the largest data volume?: [1, 0]

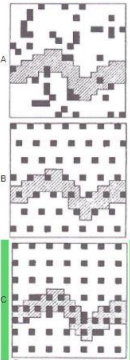


A

F

All maps will have the same volume

Which of the following figures shows the systematic distribution of samples with preferences?: [1, 0]



A

B

C

Verification of the model is: [1, 0]

replacing the real system with its model

changing the structure of the model

verifying compliance of the model and the real system with the assumption of the same entry conditions

Fig. 4. User Interface for teacher – view of the elaborated test

Creation of a new test

The advantage is that each test is written in a simple JSON format. The sample of the test is shown in Fig. 5. Questions can be organized into the sections, and number of questions that should be picked into the test from each section is defined (Fig. 5, row 7). Correct answers are marked by logical value of 1 (Fig. 5, rows 14 and 26), and incorrect answers are marked by logical value of 0 (Fig. 5, rows 15 - 16 and 24 - 25). It is also possible to set the number of points for a correct and incorrect answers (Fig. 5, row 10). Questions (Fig 5, row 12) as well as answers (Fig. 5, rows

24 - 26) may include pictures also. The minimum number of correct answers needed to pass the test is defined as “granted” value (Fig. 5, row 4).

```
1 {
2   "name": "Exam from subject: Spatial Modelling in GIS",
3   "grade": {
4     "granted": 2
5   },
6   "sections": [{
7     "number_of_questions": 3,
8     "questions": [{
9       "id": 1,
10      "points": [1, 0],
11      "question": "Which of the maps A to F listed in the following figure will have the largest data volume?:",
12      "picture": "PMvGIS/raster_objem.JPG",
13      "answers": [
14        ["A", 1],
15        ["F", 0],
16        ["all maps will have the same volume", 0]
17      ]
18    },
19    {
20      "id": 2,
21      "points": [1, 0],
22      "question": "Which of the following figures shows the systematic distribution of samples with preferences?",
23      "answers": [
24        ["A", 0, "PMvGIS/vzork_nah.JPG"],
25        ["B", 0, "PMvGIS/vzork_syst.JPG"],
26        ["C", 1, "PMvGIS/vzork_syst_pref.JPG"]
27      ]
28    }
29  ]
30 }
```

Fig. 5. The example of the test creation in the JSON file

Using the system from the student's point of view

The student can take the exam on a device with an internet connection and a web browser. He can start testing after entering its name and password (Fig. 6). After answering all the questions and submitting the test (Fig. 7), the student immediately gets the result (Fig. 8).

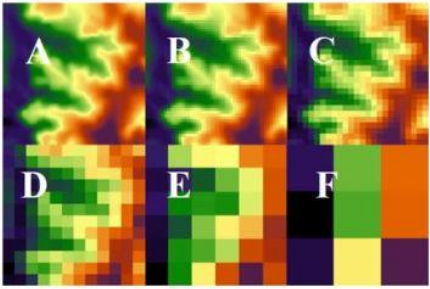
The image shows a web form for a student to start a test. It consists of three input fields stacked vertically. The first field is labeled 'Student name' and has a magnifying glass icon on the left. The second field is labeled 'Spatial modelling in GIS: SM in GIS' and has a dropdown arrow on the right. The third field is labeled 'password' and has a lock icon on the left. Below these fields is a blue button with the text 'Start test' in white.

Fig. 6. User Interface for the student – entering the name and password

Student XY

Exam from subject: Spatial Modelling in GIS

Which of the maps A to F listed in the following figure will have the largest data volume?:

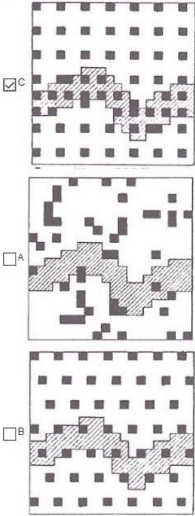


- all maps will have the same volume
- A
- F

Verification of the model is:

- replacing the real system with its model
- verifying compliance of the model and the real system with the assumption of the same entry conditions
- changing the structure of the model

Which of the following figures shows the systematic distribution of samples with preferences?



Submit Reset

Fig. 7. User Interface for the student – answering the questions



Fig. 8. User Interface for student – possible test results

CONCLUSIONS AND DISCUSSION

In this paper, we presented the custom developed open source testing and examination system that can perform automatic multiple simultaneous testing, can be installed on private protected environment and adjusted according to specific needs of its user. This software was successfully tested in the environment of FCE STU in examinations related to GIS lectures and exercises. The SOTE system provides various possibilities of settings of the tests, supports the questions with multiple correct answers or with use of images (gif files). Usage of this system does not require any third-party technology or software and new tests can be defined using the standardized JSON files created by common text editors. The SOTE software is available in compliance with GPL v3.

The system has been used and improved over the three years of its use to test following subjects: Geoinformatics, Information technology, Database systems in GIS, Spatial modelling in GIS, and Web technologies. Summarized data such as the number of students, the total number of questions per subject, and the number of questions in one test are presented in Table 1.

Table 1. The tested subjects and its characteristics

Subject	Number of students	Total number of questions	Number of questions in the test
Geoinformatics	65	43	15
Information technologies	144	850	10
Database systems	66	96	12
Spatial modelling in GIS	39	50	10
CAD systems in geodesy	68	30	10

Based on the three-year use of the above described testing and examination system, we can say that its biggest advantages are:

1. The system allows to safely and online test students.
2. Tests are randomly generated from the given database of questions that is safely stored on own server; the teacher defines how many questions are picked.
3. Questions can be grouped into the sections, then given number of questions from particular section is randomly picked to the test.
4. The system supports tests with multiple correct answers.
5. The system allows to use pictures in both questions and answers.
6. The teacher is able to select either to penalize or ignore incorrect answers.

7. The system is open source, available on <https://github.com/mmunko/skuskovy-system>.

ACKNOWLEDGEMENT

This work was supported by Grant No. 1/0682/16 of the VEGA Grant Agency of the Slovak Republic.

REFERENCES

- Aikina, T. Y., Sumtsova, O. V. and Pavlov, D. I. (2015) Implementing Electronic Courses Based on Moodle for Foreign Language Teaching at Russian Technical Universities, *International Journal of Emerging Technologies in Learning*, Volume 10, No 3, 2015, pp. 58–61.
- ClassMarker. <https://www.classmarker.com>, cited 14.1.2018.
- Damjanovic, V., Jednak, S. and Mijatovic, I. (2015) Factors affecting the effectiveness and use of Moodle: students' perception, *Interactive Learning Environments*, Volume 23, Issue 4, August 2015, pp. 496–514.
- Django. <https://djangoproject.com>, cited 14.1.2018.
- E-learning of Comenius University. <https://moodle.uniba.sk>, cited 14.1.2018.
- Horvat, A., Dobrota, M., Krsmanovic, M. and Cudanov, M. (2015) Student perception of Moodle learning management system: a satisfaction and significance analysis, *Interactive Learning Environments*, Volume 23, Issue 4, August 2015, pp. 515–527.
- Moodle. <https://moodle.org>, cited 14.1.2018.
- Online Exam Builder. <https://www.onlineexambuilder.com>, cited 14.1.2018.
- Planet PostgreSQL. <https://postgresql.org>, cited 14.1.2018.
- Sunder, S., Singh, S. and Raina, C. K. (2017) Online Examination System, *International Journal of Scientific Research in Computer Science, Engineering and Information Technology*, Volume 2, Issue 6, pp. 375–377.
- The Academic information system of Slovak University of Technology in Bratislava. <https://is.stuba.sk>, cited 14.1.2018.
- The Python Software Foundation. <https://python.org>, cited 14.1.2018.
- Zhao Q. and Li, Y. (2012) Research and Development of Online Examination System. In: *Proceedings of the 2012 2nd International Conference on Computer and Information Application (ICCIA 2012)*, Atlantis Press, Paris, France, pp. 936–938.

SPATIO-TEMPORAL VULNERABILITY ANALYSES OF LANDSCAPE AND CLIMATE EFFECTS ON MALARIA PREVALENCE USING GEOSTATISTICAL APPROACH IN SUB-SAHARA AFRICA

Joshua, OKEKE¹; Edeko, BABINE¹; Adu, SIMON¹; Chukwudi, NWAOGU^{2*}; Vilém, PECHANEC²

¹Sambus Geospatial Nigeria Limited, FCT, Abuja, Nigeria

okaykaygeoinfo@gmail.com; sadu@sambusgeospatial.com; ebabine@sambusgeospatial.com

²Department of Geoinformatics, Palacký University, Olomouc, 771 46, Czech Republic

cnwaogu@gmail.com; vilem.pechanec@upol.cz

Abstract

Malaria is an important disease that has a global distribution and significant health burden especially in the tropics and subtropics. The spatial limits of its distribution and seasonal activity are sensitive to land use-land cover (LULC), climate factors, and the capacity to control the disease. This study analyzed the spatio-temporal pattern of malaria incidence in Ife central local government of Osun state, Nigeria. Both spatial and non-spatial data were collected for the study. The spatial data included satellite imagery, GPS data of the waste dumpsites, and the administrative map of the area. The non-spatial data were demographic, climatic, and malaria incidence data. ArcGIS, SPSS, and Jmulti packages were used for the data processing and analyses which included, geospatial index and factor weighting such as kriging, and the regression analysis. The results revealed that malaria prevalence, open spaces, and dumpsites were higher in the central and southern parts, as compared with the northern part of the study area. The study further showed that higher rainfall had substantial malaria incidents. Thus, malaria prevalence increased with increasing rainfall. However, malaria cases increased with moderate temperature, but decreased as temperature became higher. Rainfall indicated a strong significant relationship with malaria incidence/prevalence. High malaria prevalence was recorded from 2007 to 2010, but declined rapidly between 2011 to 2015. Human measures to fight the disease might have been responsible for this decline. Further studies are recommended to ascertain the role of socio-economic factors in the spatio-temporal pattern of malaria in the study area as this would help for the sustainable eradication of the disease.

Key words: diseases, Anopheles mosquito, land use-land cover, waste dumpsites

INTRODUCTION

Malaria is an important disease that has a global distribution and significant health burden especially in sub-Saharan Africa (SSA). The spatial limits of its distribution and seasonal activity are sensitive to climate, landscape factors, and the capacity to control the disease. Several studies have revealed that the risk of malaria incidence has spatio-temporal and climatic variations (Arab et al., 2014; Mohammadkhani et al., 2016). Understanding the space-time, environmental dynamism and distribution of malaria epidemic areas is essential in finding sustainable solution to curbing the disease (Souza-Santos et al., 2008). This is because geographical distribution of

diseases reflects the environmental and socioeconomic conditions that influences the risk and susceptibility. Globally, an estimated population of 3.2 billion persons are still endangered by malaria with about 438 000 casualties yearly (WHO, 2015). Majority of the developing countries especially those within the tropics remain at risk of malaria (Hagenlocher and Castro 2015) in spite momentous improvement made in ameliorating the morbidity and mortality through increasing malaria control programs (Carter et al., 2000; Hardy et al., 2015). For example, in 2015, an estimation of 214 million new malaria incidents were reported (WHO, 2015). This calls for crucial need to employ GIS as a geospatial technology to analyse spatial trends of malaria and delineate disease vulnerability areas for sustainable planning and management (Saxena et al., 2012). The integration of GIS and spatial statistical tools (Saxena et al., 2012) has been reported as successful approaches used in simulating malaria risk in various regions of the world (Reid et al., 2010; Gwitira et al. 2018).

Despite the global and national fight against malaria and the huge expenditure to combat the disease, literature reveals that malaria still constitute a serious public health problem in Nigeria (Nwaneri et al.2017). This could primarily be attributed to paucity of information on spatio-temporal variability and the associated physical features of malaria. Comprehensive empirical studies that identify the malaria hot-spots in Nigeria are inadequate. Other studies on malaria disease in Nigeria have focused on specific interest of the medical professionals (Okogun, 2003) than the spatial trend. The need to investigate the existence of the spatial patterns of malaria cases is to aid in planning interventions for the control of its burden and in the determination of underlying processes that may have given rise to its occurrence (Nick et al. 2017). Significantly, recent researches on malaria in Nigeria showed that scarcely has GIS tools been used in assessing the epidemics (Nick et al. 2017). Thus, this study aimed at analysing the spatial pattern of malaria prevalence in south-western Nigeria, based on LULC and climatic indices of vulnerability. Open drainages, bushes, waste dumpsites, landscape/habitat and wet seasons constitute potential malaria breeding sites and period. Understanding the favourable landscape features and seasonality of malaria transmission are not only important in malaria risk mapping but also for timely and spatially targeted malaria control methods such as indoor residual spraying (Mabaso and Ndlovu, 2012). Therefore, adequate mapping will help develop a geospatially oriented database that will consolidate strategic plans towards eradicating malaria in the area. We therefore hypothesized that land LULC and climate are significant determinants for malaria prevalence. In this context, addressing the following relevant questions will help to achieve the objective(s) of the study: (i) what are the prevailing landuse-landcover types, and is there any relationship between land use and malaria prevalence? (ii) how varied is the climate, and does it contribute to malaria cases? (iii) can the combination of GIS and statistical tools be used for sustainable assessment and control of morbidity and mortality from malaria in the study area?

MATERIALS AND METHODS

Study area

Ife Central is a Local Government Area (LGA) in Osun State, Nigeria. It lies between latitude 7°48'24"N - 7°42'42"N and longitude 4°31'7"E - 4°36'49"E. It has an area of 111 km² and a

population of 167,254 from the latest Nigerian Population Commission 2006 census. It has mean monthly rainfall and temperature which ranged from 76 cm to 285 cm and 23 to 30°C respectively. However, this study is limited to the urban part of the Ife central LGA (Fig.1).

Data collection and analyses

There data-set used for this study included secondary and primary data of both spatial and non-spatial attributes. The XY coordinates of the selected waste dumpsites was obtained with a handheld GPS. High-resolution Ikonos Image and administrative map were sourced from National Airspace Research and Development Agency (NARSDA, Ile-Ife). Demographic data was sourced from NPC. Climatic data was collected from NIMET Ibadan, whereas reported cases of malaria of Ife Central between the duration of 9 years (2007-2015) sourced from National Bureau of Statistics, Abuja.

The administrative map was used in extracting the study area extend on the Ikonos image. Field survey with hand held GPS was used to collect data on the locations of the dumpsites, and other land use. These were geo-rectified with the image and subsequently used to map all the ecological features relevant to the study. Thereafter, the shape-file layers (drainage, bushes, settlements/housing pattern, and open spaces) were digitized and their various attribute tables created. The geospatial database was performed in ArcGIS 10.1 environment, while SPSS and Jmulti were used to analyse the malaria and climatic data.

The geospatial index was built by applying grids to the data in the spatial column. The geospatial grid index created was two-dimensional and spans the various LULC classes. This method was used in assigning the factor weights to each index with its own distinct cell size. The LULC were weighed based on their suitability for mosquitoes as breeding sites. The weights were determined by applying geostatistical analyses such as Kriging, inverse distance weight tools in ArcGIS incorporation with MCE module (Weighted Overlay).

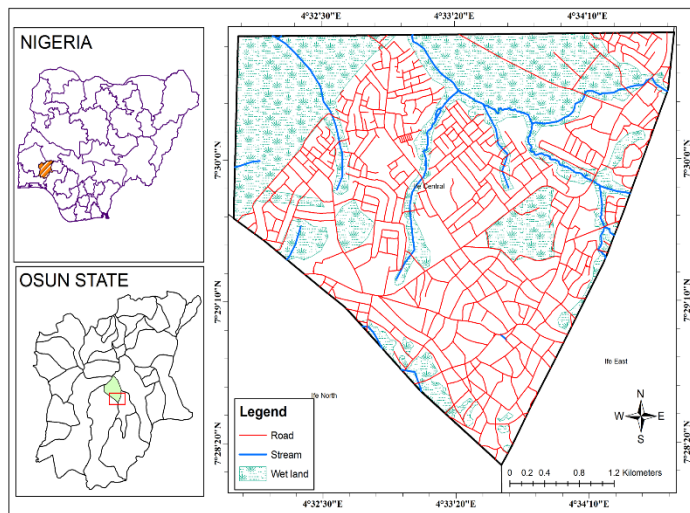


Fig. 1. Map of the study area showing roads, streams, and wetlands.

The values from the geospatial indexing and factor weighting were derived using the geostatistical analyses as earlier mentioned. The result was classified into very low prevalence, low prevalence, medium prevalence, high prevalence and severely high prevalence to malaria.

Regression analysis was used to determine the relationship between the malaria incidents, monthly rainfall and temperature.

Table 1. LULC classes (ecological factors) ranking

S/No.	Classes (factors)	weight
1	Open Drainage	5
2	Bushes (vegetation)	3
3	Built-up (Housing Layout)	2
4	Waste Dump	4
5	Open space	1

RESULTS AND DISCUSSION

Landscape (LULC) and malaria incidents

The result revealed interactions between the population density/built-up (Fig. 2), Landuse-landcover (Fig. .3 and Fig. .4) and prevalence of malaria (Fig. 5). The malaria incidents tend to be common in the central area dominated by medium and high density as compared with either the low-density areas in the southern or northern part (Fig. 6). This could be explained by the reason that open drainage and waste dump sites weighed highest as agents of malaria (Table 1), and the central part of Ife has higher density of rivers and streams, and more waste dump sites relative to the southern part. For instance, about 70% of the southern Ife is dominated by high density population yet, the incident of malaria is not high (Fig.. 7). This indicated that other factors such as drainage, and sanity condition have more significant relationships with malaria occurrence than population density. Many authors have previously reported positive association between poor environment and malaria epidemics in the tropics (Hanafi-Bojd et al., 2012). The central part of our study area has more waterbodies, and rivers and streams were revealed as breeding places for Anopheline mosquitoes (Hanafi-Bojd et al., 2012).

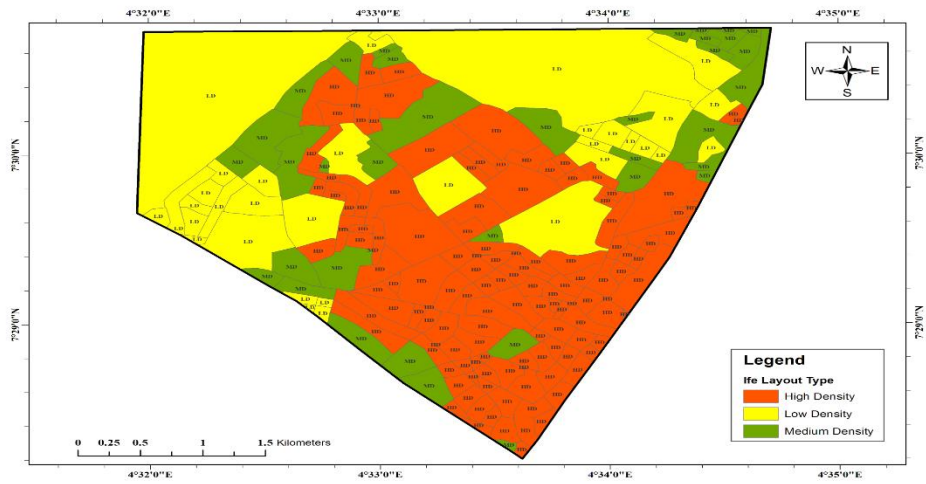


Fig. 2. Built-up areas (housing layouts).

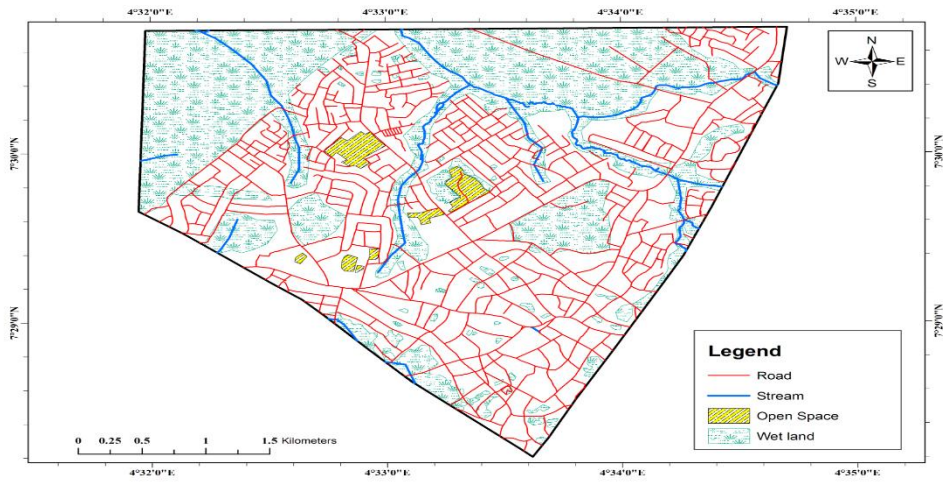


Fig. 3. Landuse-land cover (ecological Factors)

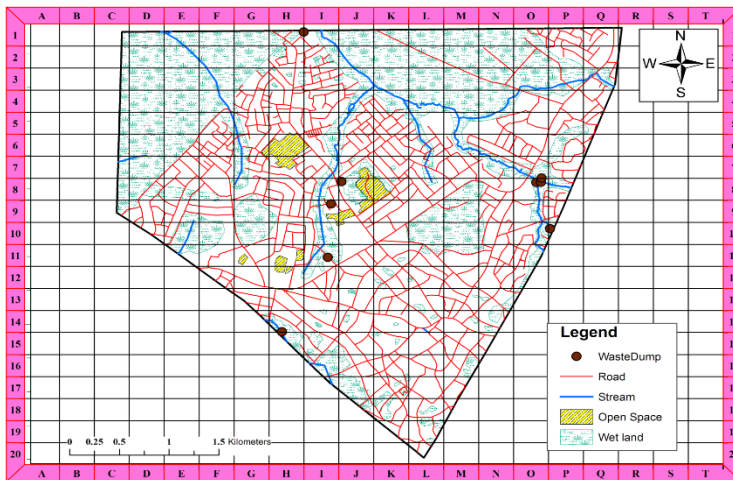


Fig. 4. Geospatial Indexing showing the land use

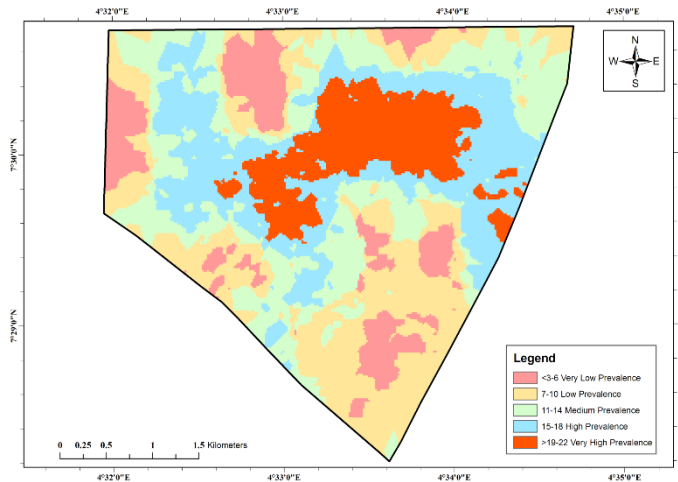


Fig. 5. Malaria vulnerability areas

Climate and malaria prevalence

Malaria occurrences increased with moderate temperature but decreased as temperature became higher (Fig. 7b), whereas the epidemics increased as rainfall increases (Fig.7a). 2007 showed the highest malaria incidence with 22% while, 2012 recorded the lowest malaria incident (3%) and the lowest mean rainfall (93.4 cm).

Malaria occurrences decreased significantly between 2012 to 2015. Generally, the average rainfall tends to decrease by more than 100% from 252.8 cm in 2007 to 100.2 cm recorded in 2015 while, the average temperature fluctuated. The months with the highest rainfall (May, June, July and September) recorded the highest number of malaria cases (Fig. 7c). A significant relationship was recorded between mean annual rainfall and malaria incidence, while temperature

was not significantly correlated with malaria cases (Fig. 7d), though extreme temperature range led to a decrease in malaria cases (Fig.7b). Recent studies revealed the significant relationship between climate and malaria prevalence across the world (Akinbobola and Omotosho, 2012; Mabaso and Ndlovu, 2012; Hanafi-Bojd et al., 2012). In consistent with our findings several authors have reported rainfall as the main determinant of malaria cases in West Africa (Akpalu and Codje, 2013). Open drainages especially polluted water which exist after heavy rainfall provide breeding grounds for the female mosquitoes (Koenraadt et al., 2004; Lindbade et al, 2000), thus, an explanatory reason that rainfall is an agent of malaria occurrence in Ife central, Nigeria. In relation to temperature, our study revealed that temperature promoted malaria cases but extreme temperature reduced the incidents. This might be attributed to the death of the Anopheles breeds at either egg, pupa or larva stage due to intensive heat (Lindsay and Birley,1996; Lindsay et al., 1991). Generally, more than 60% of the study area had low and very low prevalence of malaria and very high prevalence are covered less than 6% of the entire study area (Fig. 8).

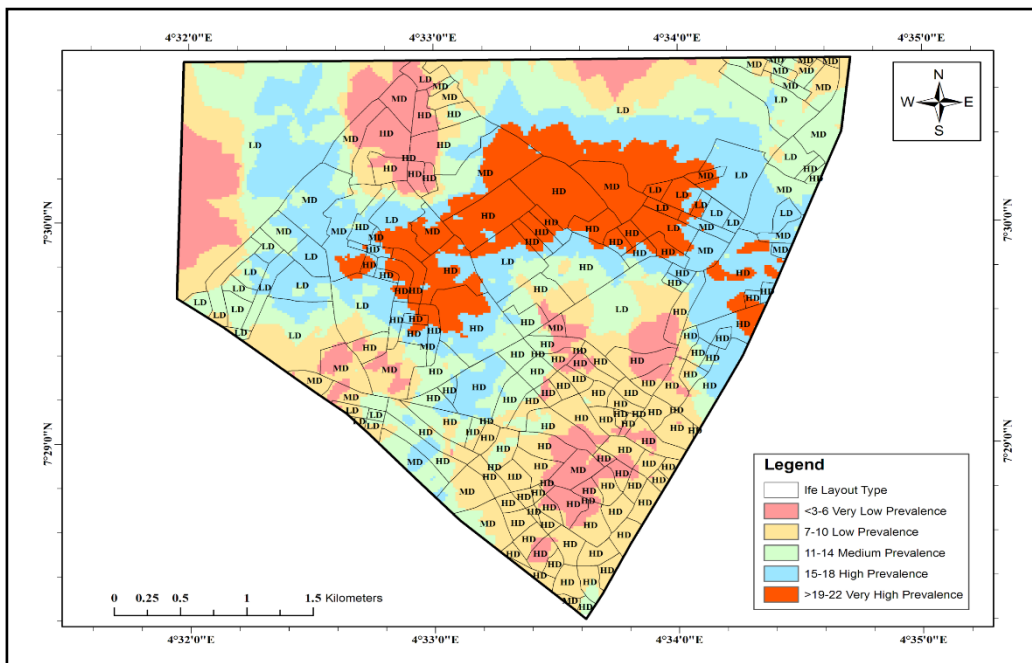


Fig. 6. Overlay: Built-up (housing Layouts) and Malaria vulnerability areas

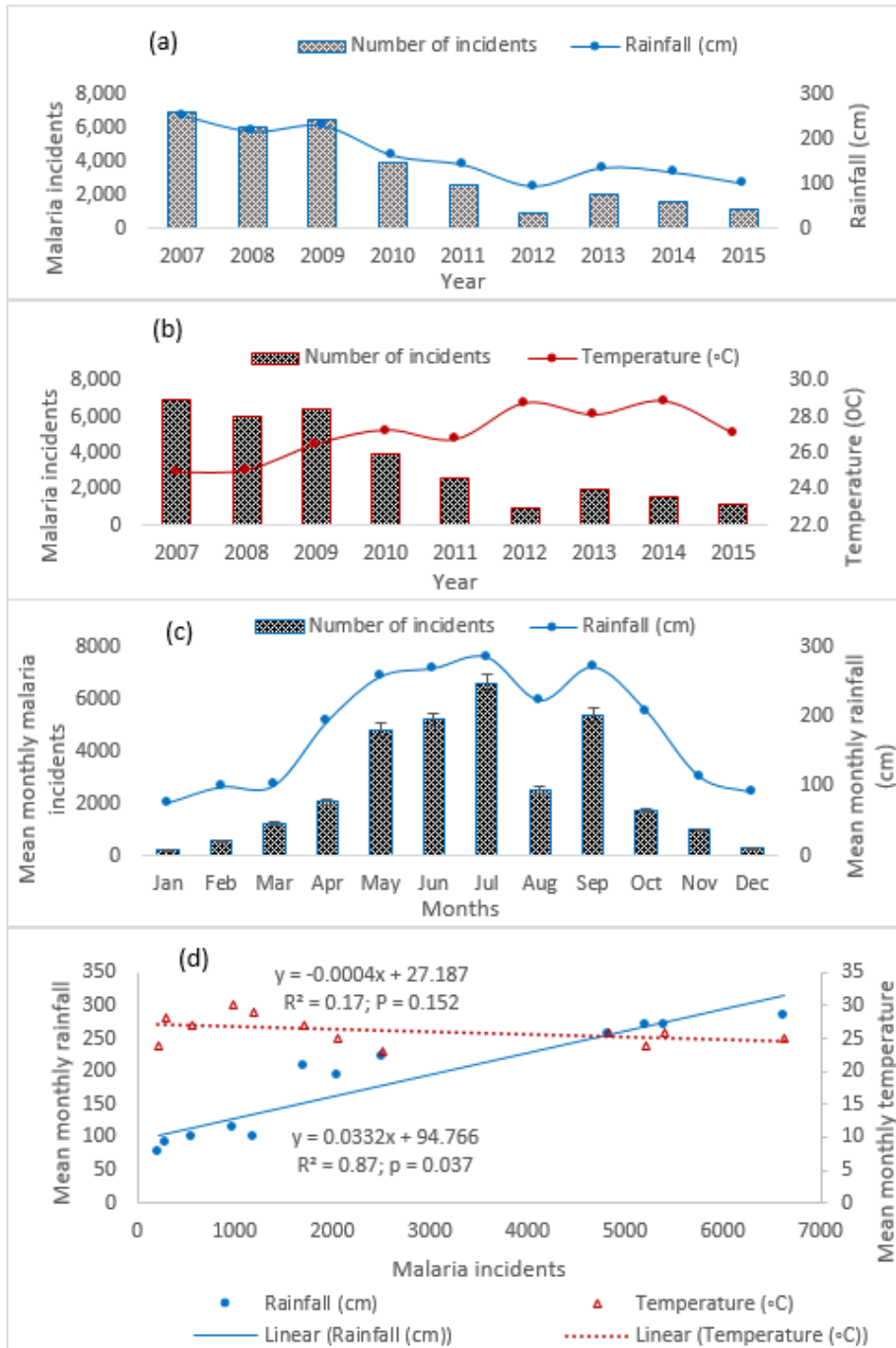


Fig. 7. Malaria incidence and (a) mean annual rainfall (b) mean annual temperature (c) Mean monthly malaria incidents and rainfall (d) relationships with rainfall and temperature in the study from 2007 to 2015. Monthly difference is significant at $p < 0.05$; The bar (in Fig 7c) represents the standard error of the mean for nine years.

CONCLUSION

High population density, uncleared bushes, dump-wastes and poor drainages have substantial effect on malaria incidence in the study area. Malaria occurrence increased with temperature but decreased as temperature became higher. Rainfall showed a strong significant relationship with malaria incidence. Year 2007 to 2010 had high malaria cases which declined rapidly from 2012 to 2015 and human measures to fight the disease might have been responsible for this decline. GIS have proved to be a good tool to be applied in the study of malaria spatial distribution and prevalence in Nigeria. Environmental sanitary measures should be adopted as this will reduce the epidemics.

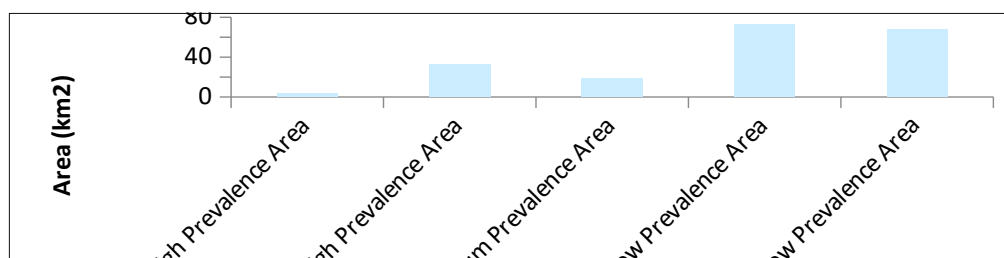


Fig. 8. Incidence of malaria and total area covered in Ife Central

ACKNOWLEDGEMENTS

We appreciate the support from the Department of Geoinformatics, Palacký University, Olomouc, Czech Republic, and Sibus Geospatial Limited, Nigeria. Effort of the blind reviewers, their kind corrections, and remarks were also acknowledged.

REFERENCES

- Akinbobola, A., Omotosho, J.B. (2012) Predicting malaria occurrence in Southwwest and north Central Nigeria using meteorological parameters. *Int. J. Biometeorol.* 1-8.
- Akpalu, W., & Codjoe, S. N. A. (2013) Economic analysis of climate variability impact on malaria prevalence: the case of Ghana. *Sustainability* 5: 4362-4378.
- Arab, A., Jackson, M. C., & Kongoli, C. (2014) Modelling the effects of weather and climate on malaria distributions in West Africa. *Malaria J.*13: 126.
- Carter, R., Mendis, K.N., Roberts, D.R. (2000) Spatial targeting of interventions against malaria. *Bull. World Health Organ.* 78, 1401–1411.
- Gwitira, I., Murwira, A., Zengeya, F.M., Shekede M.D. (2018) Application of GIS to predict malaria hotspots based on *Anopheles arabiensis* habitat suitability in Southern Africa. *Intern. J. Applied Earth Obs. Geoinf.* 64,12-21. doi.org/10.1016/j.jag.2017.08.009
- Hagenlocher, M., Castro, M.C. (2015) Mapping malaria risk and vulnerability in the United Republic of Tanzania: a spatial explicit model. *Popul. Health Metrics* 13.

- Hanafi-Bojd, A.A., Vatandoost, H., Oshaghi, M.A., Haghdoost, A.A., Shahi, M., Sedaghat, M.M., Abedi, F., Yeryan, M., Pakari, A. (2012) Entomological and epidemiological attributes for malaria transmission and implementation of vector control in southern Iran. *Acta Trop.* 121, 85–92
- Hardy, A., Mageni, Z., Dongus, S., Killeen, G., Macklin, M.G., Majambare, S. et al. (2015) Mapping hotspots of malaria transmission from pre-existing hydrology, geology and geomorphology data in the pre-elimination context of Zanzibar, United Republic of Tanzania. *Parasites Vectors* 8.
- Koenraadt, C. J. M., Githeko, A. K., & Takken, W. (2004) The effects of rainfall and evapotranspiration on the temporal dynamics of *Anopheles gambiae* s.s and *Anopheles arabiensis* in a Kenya village. *Acta Tropica*, 90(2): 141-153.
- Lindblade, K. A., Walker, E. D., Onapa, A. W., Katunga, J., & Wilson, M. L. (2000) Land use change alters malaria transmission parameters by modifying temperature in a highland area of Uganda. *Tropical Medicine and International Health*, 5(4): 263-274.
- Lindsay SW, Birley MH. 1996 Climate change and malaria transmission. *Ann. Trop. Med. Parasitol.* 90, 573.
- Mabaso, M. L. H., Ndlovu, N. C. (2012) Critical review of research literature on climate-driven malaria epidemics in sub-Saharan Africa. *Public Health* 126: 909-919.
- Mohammadkhani M, Khanjani N, Bakhtiari B, Sheikhzadeh K. (2016) The relation between climatic factors and malaria incidence in Kerman, South East of Iran. *Parasite Epidemiol. Control* 1: 205–210.
- Nick, S; Azfar, H.S; Martin-Hughes, R; Fowkes, F.J.I; Kerr, C.C; Pearson, R et al. (2017) Maximizing the impact of malaria funding through allocative efficiency: using the right interventions in the right locations. *Malaria J.* 16, 368. <https://doi.org/10.1186/s12936-017-2019-1>
- Nwaneri, D. U; Sadoh, A. E.; Ibadin, M.O. (2017) Impact of home-based management on malaria outcome in under-fives presenting in a tertiary health institution in Nigeria. *Malaria J.* 16:187. DOI 10.1186/s12936-017-1836-6
- Okogun, O. (2003) Epidemiology therapeutic agents and cost of management of paediatric malaria in a Nigerian Tertiary Hospital. *Data Sci J.* 11: 15-20.
- Reid, H., Haque, U., Clements, A.C.A., Tatem, A.J., Vallely, A., Ahmed, S.M., Islam, A., Haque, R., 2010. Mapping malaria risk in Bangladesh using bayesian geostatistical models. *Am. J. Trop. Med. Hyg.* 83, 861–867.
- Saxena, R., Kumar, A., Jeyaseelan, A.T., Baraik, V., 2012. A spatial statistical approach to analyze malaria situation at micro level for priority control in Ranchi district, Jharkhand. *Indian J. Med. Res.* 136, 776–782.
- Souza-Santos, R., de Oliveira, M. V. G., Escobar, A. L., & Ventura, S. L. 2008. Spatial heterogeneity of malaria in Indian reserves of Southwestern Amazonia, Brazil. *Intern. J Health Geographics*, 7:55.

EVALUATION OF THE FOREST DISTURBANCES USING TIME SERIES OF LANDSAT DATA: A COMPARISON STUDY OF THE LOW TATRAS AND SUMAVA NATIONAL PARKS

Premysl STYCH¹, Radovan HLADKY^{1,2}, Josef LASTOVICKA¹, Daniel PALUBA¹

¹Department of Applied Geoinformatics and Cartography, Faculty of Science, Charles University, Albertov 6, Prague 2, 128 43

stych@natur.cuni.cz

²Administration of the Low Tatras National Park, State Nature Conservation of the Slovak Republic (NAPANT)

rado.hladky@gmail.com

Abstract

The work is focused on the evaluation of forest vegetation changes from 1992 to 2015 in the Low Tatras National Park in Slovakia and Sumava National park in the Czechia using the time series of Landsat images. The study area was damaged by wind and bark beetle calamities, which strongly influenced the health state of the forest vegetation at the end of the 20th and beginning of the 21st century. The analysis of the time series was based on the six selected vegetation indices in different types of localities selected according to the type of forest disturbances. The Landsat data CDR was normalized using the PIF method and the results of Time Series were validated by in-situ data. The results confirmed the excellent abilities of the vegetation indices based on SWIR bands (e.g., NDMI) for the purpose of evaluating the individual stages of the disturbance (especially bark beetle calamity). Usage of the Landsat data CDR in the research of long-term forest vegetation changes has a high relevance and perspective due to the free availability of the corrected data.

Keywords: Time series, Landsat, Vegetation Indices, the Low Tatras, Bark Beetle Disturbance, Sumava

INTRODUCTION

Thanks to the long history and rich data archives, EO provides unique information for the purpose of observing the dynamic phenomena on the Earth's surface. Thanks to free access to the data archives of satellite imagery and technologies for their processing, we have acquired new possibilities for studying dynamic changes in the landscape (Wulder et al., 2012, Woodcock et al., 2012a). The most recent issue of the EO image analysis is to determine the state and changes of the forest cover on a continental or even global level. One of the most significant outputs is the worldwide database of status and changes of forest areas from Hansen et al. (2010) or the database of changes in forest areas for Eastern Europe from Potapov et al. (2015). The basic data source for these research areas is the Landsat Thematic Mapper, Enhanced Thematic Mapper Plus (TM / ETM +), and, most recently, the Operational Land Imager (OLI).

The Time Series (TS) methods are very often used to evaluate vegetation changes. For TS purposes, a whole range of satellite data can be used. Due to the availability of the free archive,

Landsat's satellite imagery is one of the most commonly used data type (Wulder et al., 2015). Neigh et al. (2014) took advantage of the Landsat data to deal with the development of the forest of Wisconsin and Minnesota. Using the algorithm, it tries to map insect disturbances using time series methods. Woodcock et al. (2012a, 2012b) and Zhu et al. (2012, 2014, and 2015) systematically address changes in forest areas, both in North and South America (e.g., in Brazil and Colombia).

The tracking of the dynamics of forest vegetation changes in the Central European area has, so far, been dealt with by a large number of authors. After 1990, several studies were carried out to evaluate forest damage caused by industrial emissions in the so-called Black Triangle area (traditional industrial area between the Czech Republic, Germany and Poland), see e.g., Entcheva et al. (1999), Campbell et al. (2004) as well as Albrechtova and Rock (2003). The systematic investigation of the use of vegetation indices in the field of deforestation and the evaluation of the consequences of disturbances in Sumava National Park (in the Czech Republic) has long been dealt with by Hais et al. (2009a, 2009b) and Hais et al. (2016). Hajek and Svoboda (2007) evaluate the death of the spruce forest at Trojmezna in the Sumava National Park. They use a time series of aerial photographs to assess the extent of the forest's death due to the attack by the bark beetle. The evaluation of the impact of calamity events on the state and development of forest areas in Sumava was also the focus of Zemek et al. (2003). Also, in the area of the Krkonose National Park (in the Czech Republic) several studies were carried out with the use of DPZ, e.g. Kupkova et al. 2017. The evaluation of the changes in forest vegetation on the territory of Slovakia is devoted to several studies, e.g., Hostert et al. (2016), Griffiths et al. (2013) or Tucek (2001) and in Poland with focus on the area of High Tatras (e.g., Kozak et al, 2007, Kozak, 2010). The complex assessment of the changes in the forest areas and their consequences in the Carpathian region has been addressed by several Landsat studies, for example, Kuemmerle et al. (2007) or Butsic et al. (2016).

This work is focused on the evaluation of the changes of forest areas in selected localities of the Low Tatras National Park and Sumava National Park using TS methods. The creation of TS is based on Landsat images. Changes in the forest vegetation induced by various disturbance processes are evaluated on the basis of the selected vegetation indices, their tentative capabilities being tested and validated by comparing in-situ data. An important part of this study is the evaluation of the data, methods and results achieved for landscape and nature management and nature conservation institutions.

The main objectives of this work are:

1. The evaluation and comparison of changes in the forest areas in the selected localities of the Low Tatras National Park and Sumava National Park using TS methods which use Landsat data
2. To evaluate the suitability of individual vegetation indices for detection of different types of biotic and abiotic disturbances
3. To validate and interpret the results using in-situ data

4. The discussions and recommendations on the suitability of the EO for nature conservation and management of the Low Tatras National Park and Sumava National Park.

2 OBSERVED AREA

The Low Tatras are among the most important mountain regions of Slovakia. The national park has its own territory of 73 km². The dominant land cover is the forest, we can find extensive forest ecosystems. In many parts of the Low Tatras, spruce forests dominate. Their development takes place under the influence of natural and anthropogenic factors. The integrity of forest ecosystems has been disturbed by several abiotic events (wind, snow, frost, avalanches), biotic agents (sub-insects) or anthropogenic influences (e.g., air pollution).



Fig. 1. The Tatras Tatra (Rupicapra rupicapra tatrica) was artificially launched in the Low Tatras in 1969-1976 (photo by R. Hladky)

On November 19th, 2004, from 15:00 to 24:00, a windstorm passed through the area of the Low Tatras with a maximum speed of about 175 km/h. The territory of the Low Tatras National Park and its protection zone was damaged and extensive forest stands in several areas and localities were destroyed. The wind storm in November 2004 hit the territory of NAPANT very strongly and, as a result, led to the reproduction of European bark beetle (*Ips typographus*). During the summer of 2007, extremely favourable conditions for grafting of subcortical insects were created in almost all non-native and natural spruces in Slovakia. The observed sites of this study are located in the Dumbier part of the Low Tatras (Western Carpathians), in the Mlyinna valley. It is about a 7 km long valley. After the windy calamity in 2004, the valley area was affected by biotic bark beetle calamity, culminating mainly in 2009 (mass pine devastation) with the peak of forest decay occurring in 2012. The sites of interest were categorized according to the type of disturbance. The first site represents the territory with the wind disturbance, the second represents the beetle disturbance prevailing and the third site has been low affected by disturbances (Table 1).

Table 1. Overview of selected localities in NP Low Tatras

ID	Type of disturbance	Year
1	Wind calamity	2004
2	Bark beetle calamity	2006-2009
3	Without disturbance	-

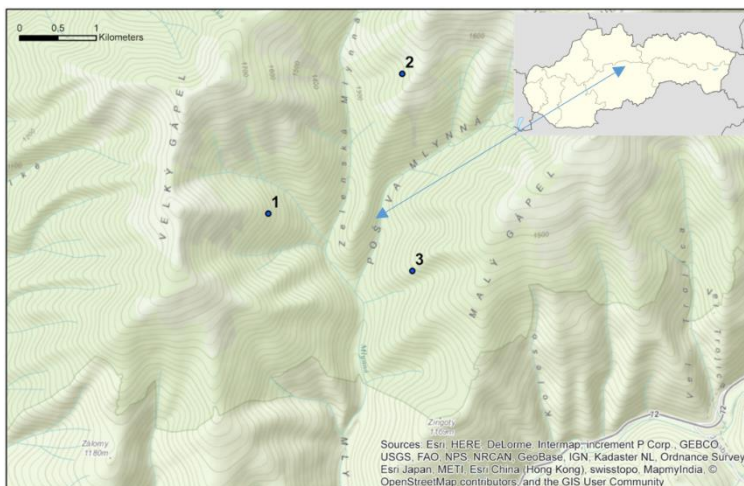


Fig. 2. Map of the used localities in the Low Tatras (source: own work)

Sumava is an extensive mountain range on the border of the Czechia, Austria and German Bavaria. The Sumava (Bohemian) Forest together with the neighbouring Bavarian Forest creates the most extensive forest landscape in Central Europe, called the "Green Roof of Europe" (figure 3). The area of the park is more than 900 km². Sumava forests dominantly consist from spruce.

During 90th last century the bark beetle calamity occurred in the Czech part of Sumava NP with the culmination 1995-2001. The strong impact on forest vegetation had the Kyrill orcas in 2007. In 2008 there was a sharp rise of bark beetle affected areas forest and continued to grow until the year 2010. In the period from 2011 until 2014 there was a slight decline of intensity of disturbance with stabilization after 2014. The first site of interest of this study represents the territory with the wind and bark beetle disturbance, the second represents the bark beetle disturbance and third site is with low disturbances (Table 2).

Table 2. Overview of selected localities in NP Sumava

ID	Type of disturbance	Year
4	Bark beetle calamity with wind and non-natural recovery	since 2007
5	Bark beetle calamity and natural recovery	since 2008
6	Without disturbance	-

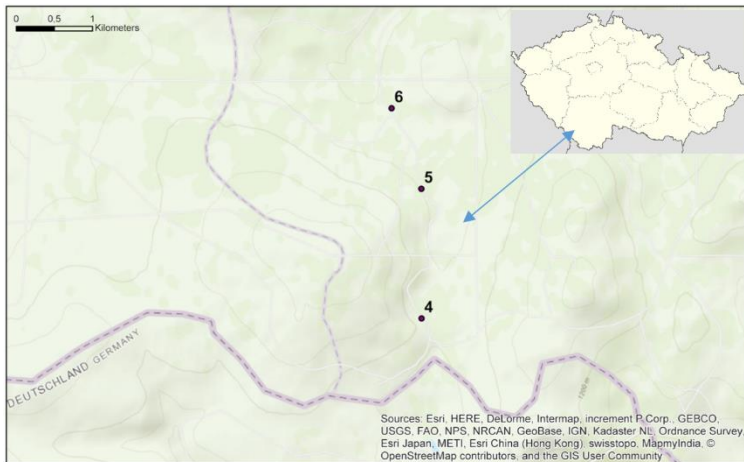


Fig. 3. Map of the used localities in the Sumava (source: own work)



Fig. 4. Forest affected by bark beetle and wind disturbance in Sumava (source: R. Hladky)

DATA

The satellite data and in-situ data were used to process the study. Landsat CDR satellite imagery were used as remote sensing data. The distributed Landsat CDR data is preprocessed with geometric and atmospheric corrections using the Climate Data Record (CDR) database, for more information on the methodologies see e.g., Zhu, Wang and Woodcock (2015), Zhu and Woodcock (2014).

A sufficient number of usable Landsat satellite images (data of Landsat 4 – 8 missions) were found for our areas of interest. For Low Tatras NP, 11 images were finally selected (see Table 3) and for Sumava NP 11 images selected as well (see Table 4). A crucial condition for the selection

of the data was their no cloud and no significant haze infection. An important aspect of the selection was also the date of acquisition. According to many authors, e.g., Griffiths (2013) and Vogelmann et al. (2012) the summer to the first autumn phase is an appropriate time for the assessment of the forest vegetation. Based on these works, it was decided to select data in the months of July to September.

Table 3. Overview of used Landsat images in the NP Low Tatras

Name	Date	Sensor
LC81880262013219LGN00	7-Aug-2013	Landsat 8
LC81880262015193LGN00	12-Jul-2015	Landsat 8
LE71880261999221SGS01	9-Aug-1999	Landsat 7
LE71880262001242SGS00	30-Aug-2001	Landsat 7
LT51880261994183XXX02	2-Jul-1994	Landsat 5
LT51880262005245KIS00	2-Sep-2005	Landsat 5
LT51880262006200KIS01	19-Jul-2006	Landsat 5
LT51880262007203MOR00	22-Jul-2007	Landsat 5
LT51880262009240KIS00	28-Aug-2009	Landsat 5
LT51880262011198MOR00	17-Jul-2011	Landsat 5
LT41880261992202XXX02	20-Jul-1992	Landsat 4

In-situ data, using for validation of the results from Landsat data analysis, was obtained from the administration of national parks and from own field survey. The information obtained from national parks included the field records of foresters, information from forest management plans and archive records of nature conservation documentation. The forest management plan is legislatively enshrined in the Forest Law on Forest Economic Planning (Forest Law No. 326/2005, Slovakia) and it provided data on the status of forests and their past management: area and category of forest, age of the stock and the age, stocking, representation of individual trees, average height, stockpile and method of management and proposal of economic measures.

Table 4. Overview of used Landsat images in the NP Sumava

Name	Date	Sensor
LC81920262013215-SC20160702161259	3-Aug-2013	Landsat 8
LC81920262015221-SC20160702161912	9-Aug-2015	Landsat 8
LE71920262002209-SC20160702153836	28-Jul-2002	Landsat 7
LT51920261994211-SC20160702152112	30-Jul-1994	Landsat 5
LT51920261998222-SC20160702151843	10-Aug-1998	Landsat 5
LT51920262004223-SC20160702151849	10-Aug-2004	Landsat 5
LT51920262005241-SC20160702151622	29-Aug-2005	Landsat 5
LT51920262006196-SC20160702151531	15-Jul-2006	Landsat 5
LT51920262007231-SC20160702151832	19-Aug-2007	Landsat 5
LT51920262009236-SC20160702151537	24-Aug-2009	Landsat 5

DATA PROCESSING

In order to determine the state and changes of vegetation from satellite images, the key information is in the spectral properties of the vegetation species studied. Each species of vegetation has specific spectral characteristic based on it we can detect species and evaluate its qualitative characteristics (e.g., health status) (see Higham et al., Albrecht, Rock, 2003). The time series analyses monitor the changes in vegetation over long periods of time, and are often used for estimating spectral characteristics of studied objects or based on the vegetation indices.

In order to ensure compatibility, the Landsat data source was used. As mentioned above, the geometric, atmospheric and radiometric corrections did not need to be performed on the CDR data because the images are already corrected and converted to Surface Reflectance (i.e., surface reflectance), see Woodcock et al., 2012a. On the other hand, it is clear from many studies that a significant problem in creating time series is to ensure compatibility between the types of data that are often taken by multiple types of sensors (Chen et al., 2005). A different sensor type and a different acquisition time may have a large influence on the result of time series analyses. For this reason, relative radiometric normalization was used for the data used to eliminate the influence of different acquisition times, the different phenological phases of vegetation and the influence of different spectral and radiometric characteristics of different sensors. Thanks to normalization, we can reduce the effects of different time and place of acquisition, different positions of the Sun, and different radiometric and spectral differences. PIF Linear Based was selected for the normalization purposes based on the recommendations of the most relevant studies (Chen et al., 2005, Song et al., 2001) and testing of relative radiometric normalizations in the previous study (Lastovicka et al., 2017). For process of normalization of the CDR Landsat data, custom applications were developed in the MATLAB environment. The developed application was inspired by the TimeSync web application. The application allows working with any type of satellite data in off-line mode. Thanks to the relatively standardized MATLAB encryption, this application is transferable to a wide range of software and operating systems (more info Lastovicka et al., 2017).

After the data normalization process, selected vegetation indices were calculated and time series curves created. For the purpose of creating the time series, above mentioned applications was used. The calculations considered the central pixel values of the site and its surroundings (3x3 pixels).

On the basis of several elaborated studies, e.g., Song et al. (2001), Chen et al. (2005), Rouse et al. (1973), Birth and McVey (1968), Jin and Sader (2004), Wang et al. (2010) or Deering et al. (1975), it was decided to use the list of vegetation indices bellow:

- 1) The Normalized Difference Vegetation Index (NDVI):
$$NDVI = \frac{NIR - RED}{NIR + RED}$$
- 2) The Simple Ratio Index (SR):
$$SR = \frac{NIR}{RED}$$

- 3) The Normalized Difference Moisture Index (NDMI):
$$\text{NDMI} = (\text{NIR} - \text{SWIR}) / (\text{NIR} + \text{SWIR}).$$
- 4) The FMI (Foliar Moisture Index):
$$\text{FMI} = (\text{NIR}) / (\text{RED} * \text{SWIR}).$$
- 5) The Wide-band Normalized Difference Infrared Index (wNDII):
$$\text{wNDII} = (2\text{NIR} - \text{SWIR}) / (2\text{NIR} + \text{SWIR}).$$
- 6) The Transformed Vegetation Index (TVI):
$$\text{TVI} = \sqrt{(\text{NIR} - \text{RED}) / (\text{NIR} + \text{RED}) + 0.5}.$$

Unmasking and calculation of the vegetation indices was calculated in ENVI 5.3. ArcMap was the software which was used to create maps. The final database created for the time series analysis included calculations of 6 vegetation indices from the Landsat CDR standardized data by a PIF Linear Based method.

RESULTS

The result part is focused on the description and interpretation of the value of the vegetation indices in the 6 different case studies in the Low Tatras and Sumava National Parks that have been under different development influencing the forest areas (damage from wind calamity, bark beetle and forest vegetation without any significant influence). The results describe and interpret the values of the studied vegetation indices during the observed period (1992 – 2015) and evaluate their suitability for the assessment of forest changes. The results should indicate the applicability of different vegetation indices or their combinations for detection of different types of disturbances.

Location 1

A significant part of the Low Tatras National Park was damaged by the wind calamity of Elizabeth, which took place on 19.11.2004. The first site represents the area heavily damaged by this event, followed by the natural regeneration of the vegetation in the following years after the calamity.

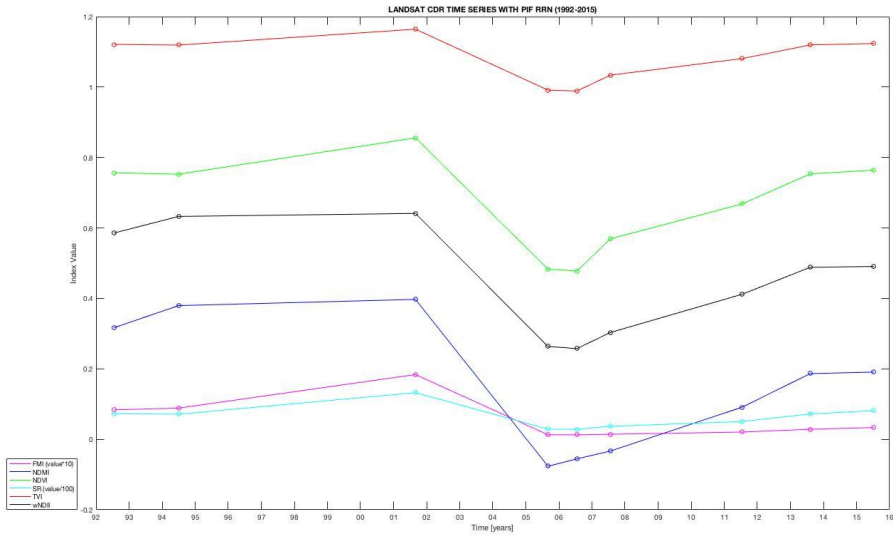


Fig. 5. Time series of vegetation indices for areas affected by wind turbulence (locality 1) (source: own work)

The results of the development of individual monitored indices are documented in Figure 1. The evolution of the values of the monitored indices shows that the wind calamity occurred in 2004 significantly affected the state of forest vegetation. The examined indices strongly reflected this wind calamity. It can be seen from Figure 5 that the most significant change (decrease) is in the values of the following vegetation indices NDVI, NDWI and wNDII; the decline in the curve is more significant for the FMI, SR and TVI indices. The area gradually began to be covered by the ascending deciduous woods, especially the *Sorbus aucuparia*. These young deciduous trees helped with regeneration of the vegetation cover in the damaged area.

Location 2

The second observed site is a site affected by the strongly expanding, devastating bark beetle after 2007. The forest vegetation after the attack was dying and left to spontaneous development. TS graph of the vegetation indices in this area can be seen in Figure 6.

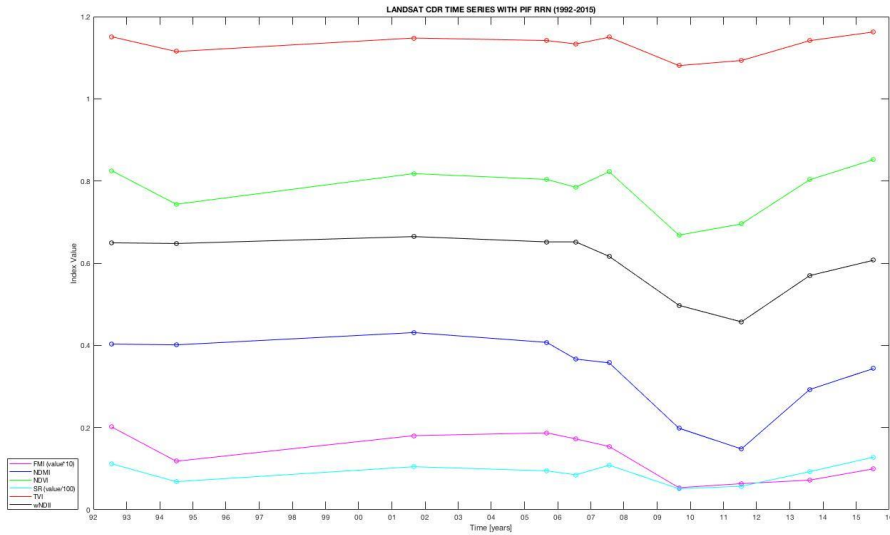


Fig. 6. Time series of vegetation indices for the area affected by bark beetle (locality 2) (source: own work)

In Figure 2, we can see some obvious trends. At this initiation phase of the bark beetle calamity, the vegetation indices wNDII, NDMI and FMI declined, while values of NDVI, SR and TVI indices slightly increased in the period 2005 - 2007. In the period 2007-2009, the location is characterized by a significant degradation of spruce forest. All the monitored indices responded by the decrease of values continuing until 2012. Then the natural regeneration of the territory with the dominance of deciduous trees began, successively occupied the deforested areas in the territory of the calamity. This was mainly reflected by the NDMI, wNDII and NDVI indices.

Location 3

The last observed locality in the Low Tatras represents a place where, unlike the two previous localities, there have been no significant changes in vegetation during observed period. The time series of vegetation indices can be seen in Figure 7.

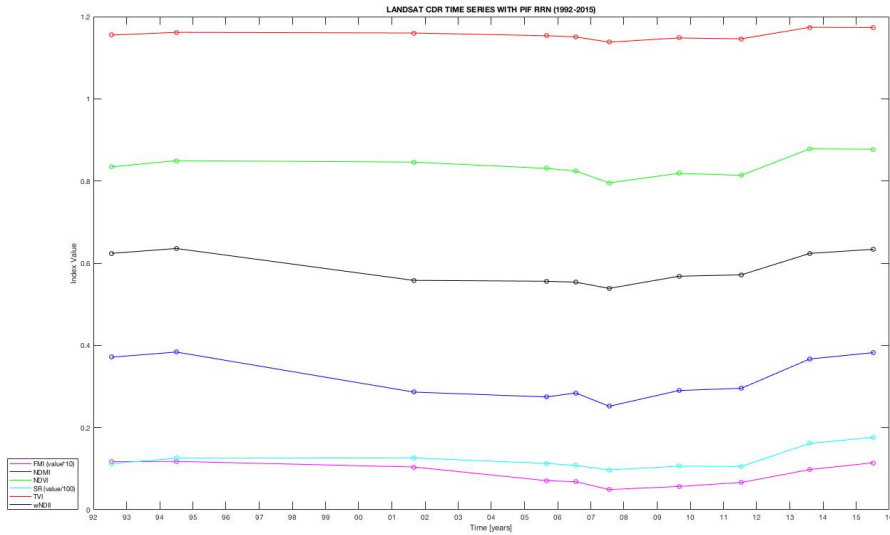


Fig. 7. Time series of vegetation indices for non-intrusive territory (locality 3) (source: own work)

It can be seen from the figure that relatively small value changes occurred in the observed area. Insignificant oscillations are evident mainly in the wNDII and NDMI indices, as well as the FMI. A slight fluctuation was recorded in the TVI index, less in the NDVI and SR indices. In the terms of interpretation, it is necessary to realize that changes in the index values may reflect specific, local conditions, e.g. weather conditions: precipitation x drought (Jensen 2007).

Location 4

The first site from Sumava is a site that has been hit by wind calamity. After disturbing tree structures, the forest was much more affected by bark beetle attack. The result can be seen in Figure 8. Here is especially the steep fall down of curves after 2008, caused by the disturbance of trees by the wind and the subsequent bark beetle. The destruction process is so much faster than in the following location 5.

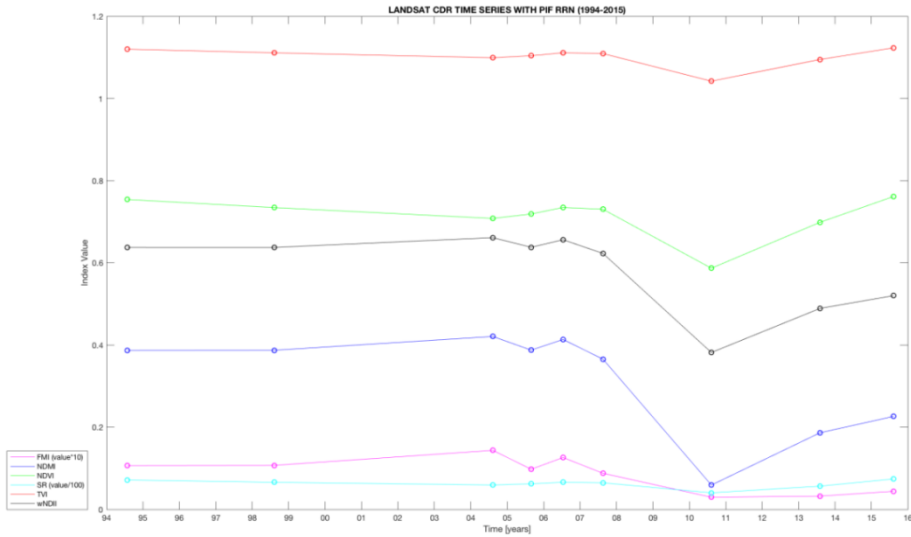


Fig. 8. Time series of vegetation indices for the area affected by bark beetle and wind (locality 4) (source: own work)

Location 5

The second location from Sumava is similar with locality 2 from the Low Tatras region. This is the place where the biotic disturbance has occurred, i.e. bark beetle calamity. Figure 9 shows the results of the time series analyses. The NDMI and wNDII indices reflected the whole disturbance event with decreasing the value. The NDVI, SR, and TVI indices had similar trends in the first years of the calamity (decrease) and then the invasive vegetation (shrubs and smaller trees) was reflected by these indices and the gradual increase or oscillation of values were documented.

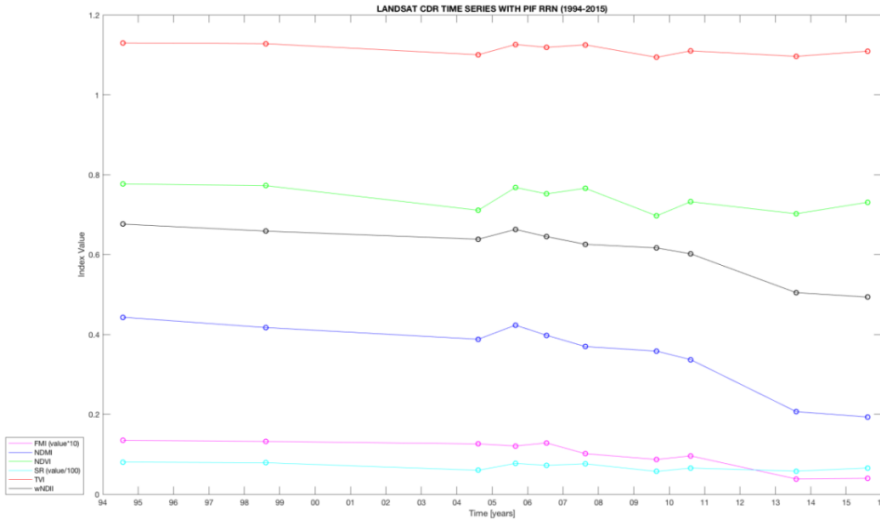


Fig. 9. Time series of vegetation indices for the area affected by bark beetle (locality5) (source: own work)

Location 6

The last site of interest is similar with the locality 3 in the Low Tatras: without any significant disturbance. This location is covered by spruces forest with an approximate age of 50 years according to in-situ data. In Figure 10 we can see a development with oscillation of values without any significant breaks.

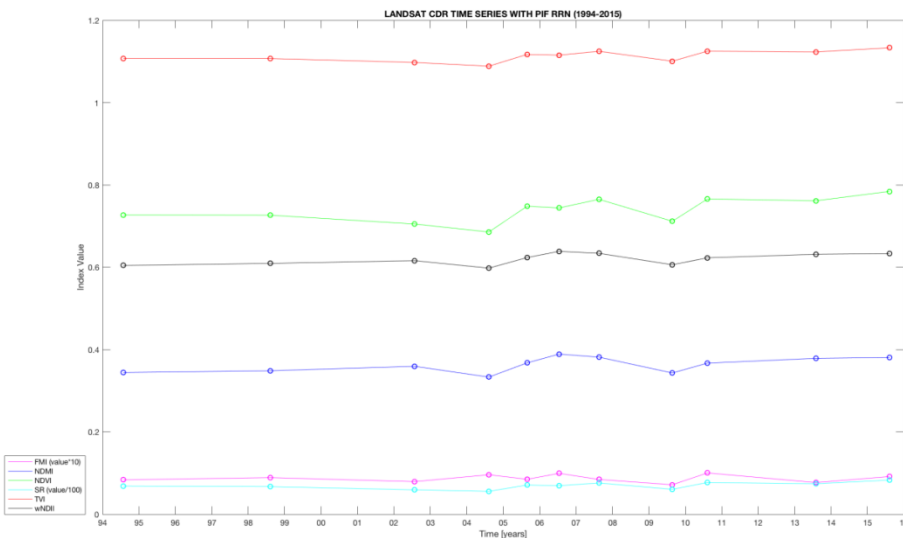


Fig. 10. Time series of non-disturbed vegetation (locality 6) (source: own work)

DISCUSSION AND CONCLUSIONS

The forest in the Low Tatras National and Sumava Parks has been severely affected by the wind calamity and subsequently by bark beetle insects. For selected locations, that differed in the type of disturbance, the calculation of vegetation indices and the comparison/evaluation of their trajectories were performed. The aim was to determine the suitability of individual vegetation indices for detection of different types of biotic and abiotic disturbances using TS analysis. Based on the results of this study is obvious, that each type of disturbance, whether biotic or abiotic, has a specific development and different consequences on the state (health) of vegetation/spectral expression. In the case of wind disaster, a large part of the forest vegetation is devastated in the quick period. This corresponds to a large impact decrease in the reflectance of near-infrared radiation (Cohen et al., 2002). A forestry intervention or succession of new vegetation causes an increase in the reflection in the green and especially in the near infrared part of the spectrum in a relatively short time after the disturbance. A wind calamity has a strong effect on the vegetation, however a recovery in the following years is quick, both spontaneous way and forest-controlled way. If it is compared two sites affected by wind calamities in Low Tatras and Sumava, similar result can be seen. The vegetation indices based on the use of the SWIR band (e.g. NDMI index) show similar trends as well (see Hais et al., 2016). Bark beetle calamity has a much more complicated progress with a specific effect on vegetation. The several generations of beetles gradually occupy the forest with a strong culmination phase. It can be three generations of beetles in one year, which greatly disturb the resistance of the forest stand. Our results confirmed a high sensitivity of the vegetation indices wNDII, NDMI or FMI based on the SWIR band in the case of the bark beetle disturbance. These vegetation indices were able to reflect all the phases of the disturbance using the time series analysis. The reflectivity of the healthy forest vegetation in the SWIR is lower than in the NIR. However, during the disturbance/damage the SWIR reflectivity has a tendency to be increasing. It is clear from the results that this aspect played an important role (compare the NDMI or wNDII vegetation indices used SWIR band with the vegetation indices based on NIR). An important result of this study is that the NDMI and wNDII vegetation indices can detect all the stages of the bark calamity (before, during and after culmination) and are, thus, suitable indicators in monitoring the health status of forest vegetation in such specific/environmentally complex processes as a bark beetle calamity with its causes and consequences.

Freely available Landsat data is a very useful data source for TS analysis of disturbances (Hais et al., 2009b). On the other hand, it is necessary to pay attention to the compatibility of data coming from various sensors of Landsat missions. Although Landsat CDR Data contains atmospheric and radiometric corrections, it is still useful to perform radiometric normalization (Lastovicka et al., 2017). The use of satellite data provides the progressive opportunities to monitor and evaluate the state and changes of forest vegetation for the purpose of the protection and management of national parks. Suggestions for a potential research can be found in a compare study of forest changes in the National Park of Sumava in the Czech Republic and the Bavarian Forest National Park in Germany.

ACKNOWLEDGEMENT

We would like to thank the support of Grant Agency of Charles University (GAUK), Project ID 512217,(2017-2019): “Hodnoceni vlivu disturbance na lesni ekosystemy v Cesku a na Slovensku pomoci metod DPZ”.

REFERENCES

- ALBRECHTOVA J., ROCK B. N. (2003): Dalkovy pruzkum krusnohorskych lesu. Vesmir, c. 82. Downloaded from: <http://www.vesmir.cz/clanek/dalkovy-pruzkum-krusnohorskych-lesu>
- BIRTH, G., G. MCVEY (1968): Measuring the Color of Growing Turf with a Reflectance Spectrophotometer. *Agronomy Journal* 60 (1968): 640-643.
- BUTSIC, V., MUNTEANU, C., GRIFFITHS, P., KNORN, J., RADELOFF, V.C., LIESKOVSKY, J., MUELLER, D., KUEMMERLE, T. (2016): The effect of protected areas on forest disturbance in the Carpathian Mountains from 1985 to 2010, *Conservation Biology*, 31, pp. 570-580.
- CAMPBELL, E.,P.K.,ROCK, B.N., MARTIN, M.E., NEEFUS, C.D.,IRONS, J.R., MIDDLETON, E.M., ALBRECHTOVA, J. (2004): Detection of initial damage in Norway spruce canopies using hyperspectral airborne data. *International Journal of Remote Sensing* 25/24, pp. 5557-5584.
- CHAVEZ, P. (1996): Image-based atmospheric corrections - Revisited and improved. *Photogrammetric Engineering and Remote Sensing*, 62, pp. 1025–1036.
- CHEN, X., VIERLING, L., DEERING, D. (2005): A simple and effective radiometric correction method to improve landscape change detection across sensors and across time. *Remote Sensing of Environment*, 98, pp. 63-79.
- DEERING, D. W., ROUSE, J. W., HAAS, R. H., and SCHELL, J. A. (1975): Measuring Forage Production of Grazing Units from Landsat MSS Data. 10th International Symposium on Remote Sensing of Environment 2: pp. 1169-1178
- DORIC, R. (2013): Možnosti objektovo orientovanej klasifikacie pri monitoringu lucnej vegetacie a manazmentovych zasahov v Krkonoskom narodnom parku. Diplmova prace, vedouci diplomove prace: RNDr. Lucie Kupkova, Ph.D. Univerzita Karlova v Praze, Katedra aplikovane geoinformatiky a kartografie, 78 p.
- DU, Y., TEILLET, P., CIHLAR, J. (2002): Radiometric normalization of multitemporal high-resolution satellite images with quality control or land cover change detection. *Remote Sensing of Environment*, 82, pp. 123–134.
- ENTCHEVA P, ROCK BN, MARTIN M, ALBRECHTOVA J, SOLCOVA B, TIERNEY M, IRONS J. (1999): Remote Sensing Assessment of Forest Stress in the Western Bohemian Mountains of Central Europe – Applications of ground and airborne spectrometry (GER2600 and ASAS). Fourth International Airborne Remote Sensing Conference and Exhibition/21 Canadian Symposium on Remote Sensing, Section H: Forestry; Ottawa, Canada; June 21–2, pp. 128-143.
- FOREST LAW NO. 326/2005, Slovakia

- GRIFFITHS, P., KUEMMERLE, T., KENNEDY, R., ABRUDAN, I., KNORN, J., HOSTERT, P. (2012): Using annual time-series of Landsat images to assess the effects of forest restitution in post-socialist Romania. *Remote Sensing of Environment*, 118, pp. 199–214.
- GRIFFITHS, P., KUEMMERLE, T., BAUMANN, M., RADELOFF, V., ABRUDAN, I., LIESKOVSKY, J., MUNTEANU, C., OSTAPOWICZ, K., HOSTERT, P. (2013): Forest disturbances, forest recovery, and changes in forest types across the Carpathian ecoregion from 1985 to 2010 based on Landsat image composites. *IEEE Journal of Selected Topics in Applied Earth Observations and Remote Sensing*.
- HAI, M., LANGHAMMER, J., JIRSOVA, P., DVORAK, L., (2009a): Deforestation Development Dynamics in Central Part of the Sumava Mountains between 1985 and 2007 Based on Landsat TM/ETM+ Satellite Data. *Acta Universitatis Carolinae - Geographica*, 45, 1-2 p.
- HAI, M., JONASOVA, M., LANGHAMMER, J., KUCERA, T. (2009b): Comparison of two types of forest disturbance using multitemporal Landsat TM/ETM+ imagery and field vegetation data. *Remote sensing of Environment*, Elsevier, 113, 4.
- HAI, M., WILD, J., BEREC, L., BRUNA, J., KENNEDY, R., BRAATEN, J., BROZ, Z. (2016): Landsat Imagery Spectral Trajectories—Important Variables for Spatially Predicting the Risks of Bark Beetle Disturbance. *Remote Sensing* 2016, 8(8), pp. 687.
- HAJEK, F., SVOBODA, M. Vyhodnoceni odumirani horskeho smrkoveho lesa na Tromezne (NP Sumava) metodou automaticke klasifikace leteckych snimku. *Silva Gareta*, kveten 2007, roc. 13, c. 1: s. 69–81.
- HANSEN, M.C., STEHMAN, S. V, POTAPOV, P. V. (2010): Quantification of global gross forest cover loss. *Proceedings of the National Academy of Sciences*, 107, pp. 8650–8655.
- HOSTERT, P. et al. (2016): Mapping Clearances in Tropical Dry Forests Using Breakpoints, Trend, and Seasonal Components from MODIS Time Series: Does Forest Type Matter? *Remote Sensing*, 2016, 8, 657 p.
- JENSEN, J. (2007): *Remote Sensing of the Environment: An Earth Resource Perspective*. Pearson Prentice Hall, 2007. University of Minnesota. 592 p. ISBN: 0131889508.
- JIN, S., SADER, S. (2004): Comparison of time series tasselled cap wetness and the normalized difference moisture index in detecting forest disturbances. *Remote Sensing of Environment*, 94, pp. 364–372.
- JU, J., MASEK, J. (2016): The vegetation greenness trend in Canada and US Alaska from 1984–2012 Landsat data. *Remote Sensing of Environment*, 176, pp. 1–16.
- KENNEDY, R., YANG, Z., COHEN, W. (2010a): Detecting trends in forest disturbance and recovery using yearly Landsat time series: 1. LandTrendr — Temporal segmentation algorithms. *Remote Sensing of Environment*, 114, pp. 2897–2910.
- KENNEDY, R., YANG, Z., COHEN, W. (2010b): Detecting trends in forest disturbance and recovery using yearly Landsat time series: 2. TimeSync — Tools for calibration and validation. *Remote Sensing of Environment*, 114, pp. 2911–2924.
- KENNEDY, R., YANG, Z., COHEN, W., PFAFF, E., BRAATEN, J., NELSON, P. (2012): Spatial and temporal patterns of forest disturbance and regrowth within the area of the Northwest Forest Plan. *Remote Sensing of Environment*, 122, pp. 117–133.
- KOZAK J., ESTREGUIL C., TROLL M., (2007): Forest cover changes in the northern Carpathians in the 20th century: a slow transition. *Journal of Land Use Science* 2, pp. 127-146

- KUEMMERLE, T.; HOSTERT, P.; RADELOFF, V.C.; PERZANOWSKI, K.; KRUHLOV, I. (2007): Post-socialist forest disturbance in the Carpathian border region of Poland, Slovakia, and Ukraine, *Ecological Society of America, Ecological Applications*, 17, pp. 1279-1295.
- KOZAK J. (2010): Forest Cover Changes and Their Drivers in the Polish Carpathian Mountains Since 1800. [in:] *Reforestation Landscapes Linking Pattern and Process* [eds.] H. Nagendra, J. Southworth, *Landscape Series 10*, Springer, pp. 253-273.
- LASTOVICKA, J., HLADKY, R., STYCH, P., HOLMAN, L. (2017): Evaluation of forest disturbances in the Low Tatras National Park using time series of satellite images. 17th International Multidisciplinary Scientific GeoConference SGEM 2017.
- MAIN-KORN, M., COHEN, W., KENNEDY, R., GRODZKI, W., PFLUGMACHER, D., GRIF-FITHS, P., HOSTERT, P. (2013): Monitoring coniferous forest biomass change using a Landsat trajectory-based approach. *Remote Sensing of Environment* 139, s. 277–290.
- MARCINKOWSKA, A., ZAGAJEWSKI, B., OCHTYRA, Adrian, JAROCIŃSKA, A., EDWIN RACZKO, R., KUPKOVA, L., STYCH, P., MEULEMAN, K. (2014): Mapping vegetation communities of the Karkonosze National Park using APEX hyperspectral data and Support Vector Machines. *MISCELLANEA GEOGRAPHICA – REGIONAL STUDIES ON DEVELOPMENT*, 18(2), pp. 23-29.
- MOTOHKA T., NASAHARA K. N., OGUMA H., TSUCHIDA S. (2010): Applicability of Green-Red Vegetation Index for Remote Sensing of Vegetation Phenology. *Remote Sensing*, c.2, pp. 2369-2387.
- NEIGH, C.S.R., BOLTON, D.K., DIABATE, M., WILLIAMS, J.J., CARVALHAIS, N. (2014): An automated approach to map the history of forest disturbance from insect mortality and harvest with Landsat time-series data. *Remote Sens.* 6, pp. 2782–2808.
- OUBRECHTOVA, V. (2012): Vyuziti umelych neuronovych siti v klasifikaci Land Cover. Diplomova prace. Diplomova prace, vedouci diplomove prace: RNDr. Premysl Stych, Ph.D. Univerzita Karlova v Praze, Katedra aplikovane geoinformatiky a kartografie, 70 p.
- POTAPOV, Peter V. a kol (2015): Eastern Europe's forest cover dynamics from 1985 to 2012 quantified from the full Landsat archive. *Remote Sensing of Environment*. 2015/159, pp. 28-43.
- ROUSE, J., HAAS, R., SCHELL, J., DEERING, D. (1973): Monitoring Vegetation Systems in the Great Plains with ERTS. Third ERTS Symposium, NASA (1973): pp. 309-317.
- SHA, Z., BAI, Y., XIE, Y., YU, M., ZHANG, L. (2008). Using a hybrid fuzzy classifier (HFC) to map typical grassland vegetation in Xilin River Basin, Inner Mongolia, China. *International Journal of Remote Sensing* 8: pp. 2317–2337.
- SCHOTT, J., SALVAGGIO, C., VOLCHOK, W. (1988): Radiometric scene normalization using pseudoinvariant features. *Remote Sensing of Environment*, 26, pp. 1–16.
- SONG, C., WOODCOCK, C., SETO, K., LENNEY, M., MACOMBER, A. (2001): Classification and Change Detection Using Landsat TM Data: When and How to Correct Atmospheric Effects? *Remote Sensing of Environment*, 75, pp. 230-244.
- TEILLET, P., MARKHAM, B., IRISH, R. (2006): Landsat cross-calibration based on near simultaneous imaging of common ground targets. *Remote Sensing of Environment*, 102, pp. 264–270.

- TRAN, T., BEURS, K., JULIAN, J. (2016): Monitoring forest disturbances in Southeast Oklahoma using Landsat and MODIS images. *International Journal of Applied Earth Observation and Geoinformation*, 44, pp. 42–52.
- TUCEK, J. (2001): Príspevok k hodnoteniu zdravotného stavu lesov na základe rôznych materiálov DPZ, *Acta Facultatis Forestalis*, XXXXII, 2001, pp. 341–354.
- VOROVENCII, I., MUNTEAN, M. (2014): Relative radiometric normalization methods: overview and an application to Landsat images. *RevCAD*, 17, pp. 193–200.
- VOGELMANN, J., XIAN, G., HOMER, C., BRIANTOLK, B. (2012): Monitoring gradual ecosystem change using Landsat time series analyses: Case studies in selected forest and rangeland ecosystems. *Remote Sensing of Environment*, 2012, 122, pp. 92–105.
- WANG J., SAMMIS T., GUSTCHICK V. (2010): Review of Satellite Remote Sensing Use in Forest Health Studies. New Mexico State University. 15 p.
- WULDER, M., MASEK, J., COHEN, W., LOVELAND, T., WOODCOCK, C. (2012): Opening the archive: How free data has enabled the science and monitoring promise of Landsat. *Remote Sensing of Environment*, 122, pp. 2–10.
- WULDER, M., WHITE, J, LOVELAND, T., WOODCOCK, C., BELWARD, A., COHEN, W., FOSNIGHT, E., SHAW, J., MASEK, J., ROY, D. (2015): The global Landsat archive: Status, consolidation, and direction. *Remote Sensing of Environment*. Downloaded from: <http://dx.doi.org/10.1016/j.rse.2015.11.032>
- WOODCOCK, C., ROY, D., WULDER, M., LOVELAND, T., ALLEN, R., ANDERSON, M., HELDER, D., IRONS, J., JOHNSON, D., KENNEDY, R., SCAMBOS, T., SCHAAF, C., SCHOTT, J., SHENG, Y., VERMOTE, E., BELWARD, A., BINDSCHADLER, R., COHEN, W., GAO, W., HIPPLE, J., HOSTERT, P., HUNTINGTON, J., JUSTICE, C., KILIC, A., KOVALSKYY, V., LEE, Z., LYMBURNER, L., MASEK, J., MCCORKEL, J., SHUAI, Y., TREZZA, R., VOGELMANN, J., WYNNE, R., ZHU, Z. (2012a): Landsat-8: Science and product vision for terrestrial global change research. *Remote Sensing of Environment*, 2014, 145, pp. 154–172.
- WOODCOCK, C., WULDER, M., MASEK, J., COHEN, W., LOVELAND, T. (2012b): Opening the archive: How free data has enabled the science and monitoring promise of Landsat. *Remote Sensing of Environment*, 2012, 122, pp. 2–10.
- ZAGAJEVSKI, B., SOBCZAK, M. (eds.) (2005): *Imaging Spectroscopy. New quality in environmental studies*. EARSeL & Warsaw University, Faculty of Geography and Regional Studies, Warsaw, pp. 852, ISBN 83-89502-41-0.
- ZEMEK F., CUDLIN P., BOHAC J., MORAVEC I., HERMAN M. (2003): Semi-natural forested landscape under a bark beetle outbreak: a case study of the Bohemian forest (Czech Republic). *Landscape Research*, 28: pp. 279–292.
- ZHU, Z., WOODCOCK, C. (2012): Object-based cloud and cloud shadow detection in Landsat imagery. *Remote sensing of Environment*, 2012, 118, pp. 83–94.
- ZHU, Z., WANG, S., WOODCOCK, C. (2015): Improvement and expansion of the Fmask algorithm: cloud, cloud shadow, and snow detection for Landsat 4–7, 8, and Sentinel 2 images. *Remote Sensing of Environment*, 159, pp. 269–277.
- ZHU, Z., WOODCOCK, C. (2014): Continuous change detection and classification of land cover using all available Landsat data. *Remote sensing of Environment*, 2014, 144, pp. 152–171.

ADOPTING INTERNET OF THINGS CONCEPT TO SENSOR NETWORKS BASED ON GEOSPATIAL MODIFICATION OF LORAWAN AND MQTT

Róbert, CIBULA¹; Tomáš, ŘEZNÍK²

¹State Geological Institute of Dionýz Štúr, Mlynská dolina 1, 817 04, Bratislava,
Slovakia

robert.cibula@geology.sk

²Masaryk University, Faculty of Science, Department of Geography, Kotlarska 2,
611 37, Brno, the Czech Republic

tomas.reznik@sci.muni.cz

Abstract

Internet of Things is a phenomenon originating from industry. It offer several benefits also for the geospatial community, such as appropriate collection and transmission of field-based sensor information. In addition, geospatial techniques are strong in analysis and visualization capabilities. Bridging Internet of Things and geospatial techniques opens a way to build advanced (Web) GIS applications with real-time data at low costs.

This paper therefore briefly describes the processes that are preceding the design of a sensor monitoring network in cooperation with GIS (Geographic Information System) and IoT (Internet of Things). It comprises the basics of information transfer from sensor device to a backend system (GIS). The LPWAN (Low Power Wide Area Network) is used for the data transmission from an IoT device to up to few kilometres distant Internet source. MQTT (Message Queue Telemetry Transport) technology was used to exchange information between heterogeneous systems over the Internet.

Keywords: sensor networks, LPWAN, LoRaWAN, MQTT, IoT

INTRODUCTION

Appropriate collection, transmission, analysis and visualization of data/information is a crucial task for any field of study and/or application domain. However, its capabilities are limited by the chosen technologies. In order to correctly establish the information system based on the construction of the sensor network, it is necessary to gain new knowledge by adopting a number of materials and practical skills.

The domain of sensor networks has been intensively discussed in the geospatial domain within last years (Al-Fuqaha, A., Guizani, M., Mohammadi, M., Aledhari, M., Ayyash, M,2015)(Zanella, A., Bui, N., Castellani, A., Vangelista, L., Zorzi, M,2014). Nevertheless, the adoption of Internet of Things (IoT) concept and the technology have not been properly re-used in the geospatial domain. Some examples are information gathering applications in large-scale wireless mesh networks in (Kamimura, A., Tomita, K. 2017), the development of actual field deployment of a Zigbee wireless sensor network for landslide detection system in (Kapoor, S., Pahuja, H. and Singh, B., 2016), and IoT transmission platform based on wireless sensor network

and GPRS (General Packet Radio Station) network in (Li, J., Li, C. K., Li, K., & Liu, Y., 2014). IoT principles applied in cell-phone tracking were described by (Řezník, T., Horáková, B., Szturc, R. (2015), and cataloguing of sensor networks by (Řezník, T., Chudý, R., Mičietová, E., 2016). The OGC (Open Geospatial Consortium) family of standards SWE (Sensor Web Enablement; (Sawant, S., Durbha, S.S., Jagarlapud, A., 2017) (Zambrano, A.M., Perez, I., Palau, C., Esteve, M., 2017) requires a wider bandwidth and significantly more power at the end device. Thus, it could be evaluated as a concept/technology with low costs/performance ratio and more complicated design in comparison to IoT.

To prepare a landslide area monitoring project it is necessary to understand the chosen technology and to have practical experience with it. To date the most used information exchanges are in embedded systems for industrial automation. Embedded systems control manufacturing process with M2M (machine to machine) data exchange. M2M is defined as data communication among devices without the need for human interaction (Ratasuk, R., Vejlgard, B., Mangalvedhe, N., Ghosh A., 2017). ICT (Information and Communications Technology) has not used embedded device so often until recently. The term IoT was first used in 2008/2009 (Postscapes, <https://www.postscapes.com/internet-of-things-history/>, 2017). ICT (Information and Communication Technology) adopts the IoT development from the world of industry. For example, MQTT (Message Queue Telemetry Transport) was originally developed by the IBM company for the industrial sector. Nowadays, it is used in the open source community.

Embedded systems have advantage in comparison to planned systems. They have a lot of energy and they are usually close to the managed system. Thus, for sending and receiving information, they can be either wired or use energy-intensive wireless connection (Wi-Fi, etc.). Planned sensors (inclinometers, groundwater level gauges, etc.) will be quite distant from electric power. It is therefore necessary to build wireless network which should have small energy requirements. Response for this problem is: LPWAN use (Low Power Wide Area Network).

The recent times have also brought about the phenomenon of social networks connecting people with similar interests, where they exchange information and create Knowledge Sharing (Martinez M.G., 2015). The advantage of such a group is when there are members with similar or identical professions. Users of social networks provide a valuable feedback to the developed (IoT) applications that is being used during all the development phases.

The great development of IoT has resulted in the extension of open source hardware and software components, such as Arduino (Arduino, <https://www.arduino.cc>, 2018), ESP8266 (Espressif, <http://espressif.com/>, 2018), ESP32 (Espressif, <http://espressif.com/>, 2018), and many more. It is also necessary to mention the microcomputer devices Raspberry Pi (The Raspberry Pi Foundation, <https://www.raspberrypi.org/> 2018), Odroid (Hardkernel <http://www.hardkernel.com/>, 2018), Beagle (The BeagleBoard.org Foundation, <https://beagleboard.org/>, 2018), Orange Pi (Shenzhen Xunlong Software CO., Limited, <http://www.orangepi.org/>, 2018), etc. They open interesting opportunities for expansion to the ICT community; and they have created a number of solutions that help to develop IoT. Spread of the new technologies has brought cost reduction, and this in turn has allowed for further

expansion. Open source hardware solutions based on the SoC (System on Chip) architecture have also emerged, bringing wider deployment of IoT.

For the sake of brevity and clarity, the article will focus on transmitting information from the sensor using LPWAN and then transmitting information in the internet environment using MQTT. This protocol is very simple to implement. It needs small amount of transmission band. It implements back-end system of LPWAN providers. Other aspects of the sensor network, such as the different parts of the back-end information processing system in LPWAN networks, database management systems, application servers, and, last but not least, the front-end portion that presents data to the user are beyond the scope of this paper.

METHODOLOGY

The conceptual part of the work consisted of technical information analyses on LPWAN and MQTT technologies.

The proof-of-concept part aimed at tests of LPWAN, LoRa and LoRaWAN technologies. Such systems allow to build their own infrastructure. It is also possible to use an open source back-end system.

An MQTT broker was installed to create an end device to test the functionality.. The ability to create a real application was also tested.

LPWAN

LPWAN is a wireless technology that allows long-distance connection with minimal power consumption (Petajajarvi, J., Mikhaylov, K., Roivainen, A., Hanninen T, Pettissalo, M., 2015). Unlike 3G/4G or WiFi, these systems do not focus on enabling high data rates per device or on minimizing latency (Song, Y., Lin, J., Tang, M., Dong, S., 2017). In Slovakia, the following major LPWAN technologies are available: the narrow-band Internet of Things (NB-IoT) (Ratasuk, R., Vejlggaard, B., Mangalvedhe, N., Ghosh A., 2017), Sigfox (Sigfox, <https://www.sigfox.com/en>, 2017) and Long Range (LoRa) technology (Mikhaylov, K., Petäjäjärvi, J., Haenninen, T., 2016).

NB-IoT

NB-IoT (NarrowBand IoT) is a new narrow-band IoT system built from existing LTE (Long-Term Evolution) functionalities. The technology standard was announced by the 3rd generation partnership project (3GPP) in 2016, which promises to provide improved coverage for a massive number of low-throughput low-cost devices with low device power consumption in delay tolerant applications (Song, Y., Lin, J., Tang, M., Dong, S., 2017).

The demodulated spectrum is much wider than individual transmissions so that multiple uplinks can occur simultaneously. The base station carries the complexity of decoding multiple narrow-band channels simultaneously without knowing the exact frequency of these channels. The advantages of NB-IoT technology include its enhanced indoor coverage, which is targeted at an MCL (Maximum Coupling Loss) of 164 dB, and its ability to connect a massive number of low-

throughput devices with an adapted data rate. As indicated by the 3GPP guideline, the design objectives of NB-IoT technology include low-cost devices, high coverage (a 20 dB improvement over the GPRS), long device battery life (more than 10 years), and massive capacity (more than 52,000 devices per channel per cell). Latency is relaxed, although a delay budget of 10 s is the target for exception reports (Song, Y., Lin, J., Tang, M., Dong, S., 2017).

Sigfox

Sigfox is a proprietary standard for long range IoT networks (De Poorter, E. and Hoebeke, J. and Strobbe, M. and Moerman, I. and Latré, S. and Weyn, M. and Lannoo, B. and Famaey, J., 2017). Sigfox utilizes the UNB (Ultra Narrow Band) modulation to achieve high sensitivity (Sigfox, <https://www.sigfox.com/en>, 2017). Sigfox operates in publicly available band to exchange radio messages over the air. It uses a standard radio transmission method called binary phase-shift keying (BPSK), and it takes very narrow chunks of spectrum (100 Hz, resulting in 8000 channels), and changes the phase of the carrier radio wave to encode the data. This allows the receiver to only listen in a tiny slice of spectrum which mitigates the effect of noise. This results in a great sensitivity, which allows for long-range communication (30–50 km in rural areas and 3–10 km in urban areas) at low bitrate (100 bps), provided there is no interference (De Poorter, E. and Hoebeke, J. and Strobbe, M. and Moerman, I. and Latré, S. and Weyn, M. and Lannoo, B. and Famaey, J., 2017). Each message is transferred at 100 or 600 bits per second a data rate, depending on the region (In Europe 868MHz). Long distances can be achieved while being very robust against the noise (Sigfox, <https://www.sigfox.com/en>, 2017). An uplink message has up to 12-bytes payload and takes an average 2 s over the air to reach the base stations which monitor the spectrum looking for UNB signals to demodulate. The payload allowance in downlink messages is 8 bytes. Max Frequency of sending data is 140 messages per day (Sigfox, <https://www.sigfox.com/en>, 2017). Map of the Sigfox signal coverage for the Czech Republic and Slovakia (proof-of-concept areas) is depicted in Fig. 1.

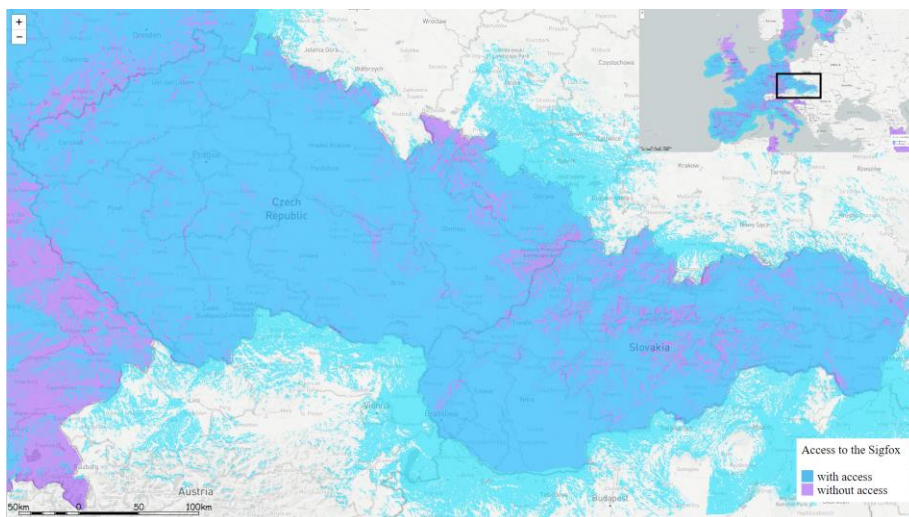


Fig. 1. View coverage for Sigfox network access in Czech Republic and Slovakia (Sigfox, <https://www.sigfox.com/en>, 2017)

LoRa / Lorawan

LoRa/LoRaWAN technology allows you to build your own entire infrastructure. From the collection of information by the IoT device from sensors, sending it to its own gate, built from its own technological background for processing to the presentation of information. For this reason, it is very useful to understand LoRa technology.

LoRa operates in the 868, 433 MHz radio spectrum in Europe, and it either uses GFSK (Gaussian Frequency-Shift Keying) or its proprietary LoRaWAN modulation scheme which employs a version of Chirp Spread Spectrum (CSS) with a channel bandwidth of 125 KHz. The payload can range from 2 to 255 bytes. (Margelis, G., Piechocki, R., Kaleshi, D. and Thomas, P., 2015).

The network follows a hierarchical star based topology, with devices being either end-points, gateways, or the network server. Data rates can range from 0.3 Kbps up to 50 Kbps when channel aggregation is employed. The end-points are further divided in three types:

Class A: Devices where downlink occurs only after an uplink transmission.

Class B devices where downlink occurs in scheduled time slots.

Class D devices that continuously listen for downlink transmissions. Power consumption is proportional to the time devices spend listening, and therefore the correct configuration of an end-point depends of the longevity expectations of the device as well as expectations for real-time downlink capabilities.

Activation of the devices to network can happen in two ways:

Over-The-Air: The end-point device sends a join request containing an address that identifies the owner of the device, and an address that uniquely identifies the endpoint.

Activation by Personalization: The end-device already contains the necessary information to join the LoRa network, including the Network and Application Session Keys, and so the process of join request/join accept messages is bypassed (Margelis, G., Piechocki, R., Kaleshi, D. and Thomas, P., 2015).

The data rate and maximum packet size roughly depend on the distance to the nearest gateway and the type of data to be sent, and are also defined in the specification for each region. Like for the European 863-870 MHz band, the application packet size varies between 51 bytes for the slowest data rate, and 222 bytes for faster rates. Beware that the LoRaWAN protocol adds at least 13 bytes to the application payload. To avoid network congestion, LoRaWAN defines some maximum transmit duty cycles 212 and maximum transmit times (dwell times). These depend on many factors including the region and the type of operation (like sending data, or broadcasting a request to join a network). For the European 863-870 MHz ISM (industrial, scientific and medical) Band the specification limits the duty cycle to 1% for data. The LoRaWAN enforces a per sub-band duty-cycle limitation. Each time a frame is transmitted in a given sub-band, the time

of emission and the on-air duration of the frame are recorded for this sub-band. [0]. For setting transmission parameters (Spreading Factor, Bandwidth), LoRaWAN uses abstraction called Data rate. Table 1. It is very useful in programming.

Table 1. Table LoRaWAN Data Rate.

DataRate	Modulation	SF	BW	bit/s
0	LoRa	12	125	250
1	LoRa	11	125	440
2	LoRa	10	125	980
3	LoRa	9	125	1'760
4	LoRa	8	125	3'125
5	LoRa	7	125	5'470
6	LoRa	7	250	11'000
7	FSK 50 kbps			50'000

MQTT

MQTT is a Client Server publish/subscribe messaging transport protocol. It is light weight, open, simple, and designed so as to be easy to implement. These characteristics make it ideal for use in many situations, including constrained environments such as for communication in Machine to Machine (M2M) and Internet of Things (IoT) contexts where a small code footprint is required and/or network bandwidth is at a premium (Al-Fuqaha 2015).

Table 2. MQTT QoS (Quality of Service) definitions

QoS value	Description
0	At most once delivery
1	At least once delivery
2	Exactly once delivery

Every endpoint has to connect to MQTT broker as publisher or subscriber to defined topic. QoS (Quality of Service) was established for the MQTT broker to guarantee performance, availability and capacity. It is possible to set one value from Table 2.

PROOF-OF-CONCEPT VERIFICATIONS LORA, LORAWAN AND MQTT

Three proof-of-concept tests were conducted to verify applicability of technologies for geospatial IoT-based sensor networks. All devices for the verification tests were developed by the authors from the commercial off-the-shelf components.

LORa PROOF-OF-CONCEPT VERIFICATION

In 2014/2015 in Bratislava, we have built some LoRa gateways to test the sending and receiving of LoRa technology. Testing was successful, but the disadvantage was the custom protocol for reading and sending data. This caused poor interoperability of the created system. A great advantage was a low price of the system. Fig. 2 shows a map of LoRa gateways placed in Bratislava.

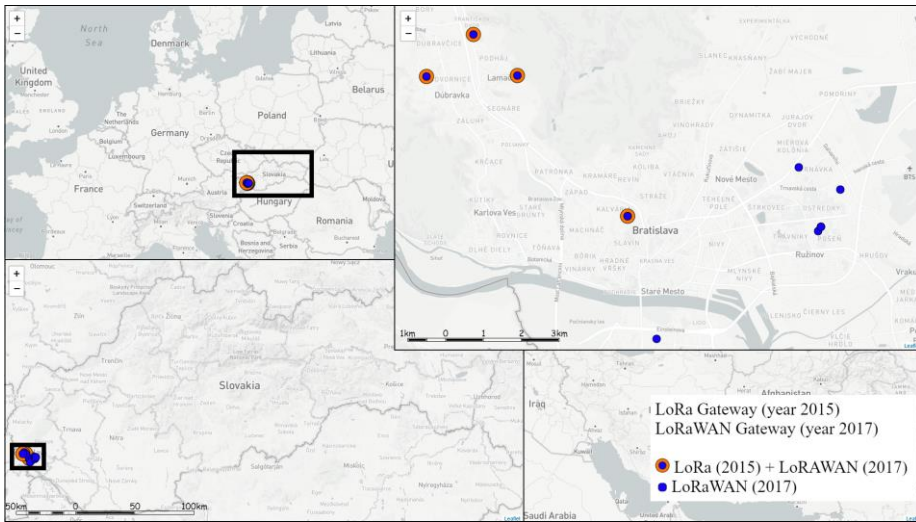


Fig. 2. LoRa (2015) and LoRaWAN (2017) gateways placed in Bratislava



Fig. 3 LoRa GW (without Raspberry Pi).



Fig. 4 LoRa device (measure temp)

Fig. 4 depicts a LoRa device based on ATmega328P (Arduino CPU) with LoRa modem RF96. Fig. 3 shows a LoRa gateway (without Raspberry Pi). On connected Raspberry Pi there is Semtech packet forwarder for further data processing.

LoRaWAN PROOF-OF-CONCEPT VERIFICATION

LoRaWAN gateway with Semtech packet forwarder, see Fig. 5, was built for the test of LoRaWAN deployment according to The Things Network (TTN) approach. MQTT broker was configured on TTN. Arduino Pro with DRF1272F LoRa modem was used as an IoT device. Arduino-LMIC library was used to develop LoRaWAN device software stack. The memory capabilities of the Arduino modem were extremely limited which was considered as a disadvantage for the proof-of-concept tests. The use of RHF76-052 is a possible solution for this problem. LoRaWAN stack is included and communication between Arduino can be by SPI (Serial Peripheral Interface). Disadvantage is price for module. Another IoT device was used LoPy (Fig. 6), which is an easier solution for testing. LoPy was identified as the best candidate to make acquaintance with LoRaWAN technology. It is important to note that the device has not been tested for a long time.



Fig. 5. LoRaWAN gateway built on iC880A concentrator with Raspberry Pi 3.



Fig. 6. Lopy (module with Micro-python LoRaWAN)

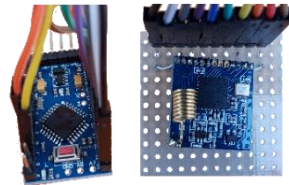


Fig. 7. Arduino mini pro with DRF1272F.

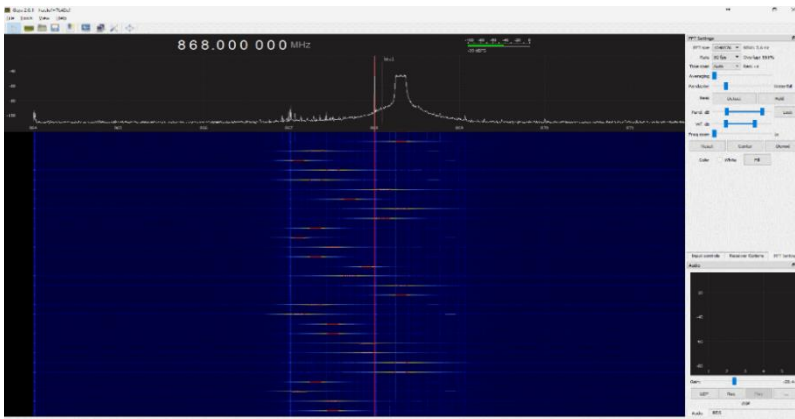


Fig. 8. Radio Frequency analysis of authors LoRaWAN device in 868 MHz with peak when sending data.

For graphical analysis of wireless frequency band, SDR (Software defined Radio) was used. IoT device communication is clearly displayed in Fig. 8. In the picture it is possible to see how the broadcasting channel will be changed for each sent message (uplink). When sending a message

to the device (downlink), the same band on which the device was broadcasted is used. It is also possible to see the peak when sending data.

MQTT PROOF-OF-CONCEPT VERIFICATION

WebGIS application usually gets information from backend on events, which happened on client (identity, zoom, and so on). In this case, when launching WebGIS application, they first subscribe to backend for data of specific topics. When the data changes or is added, the backend actively sends the data to the client who then processes them. This approach allows the client to get data at different stages of processing (from source to analysed data) without active involvement. To test this method, we used the MQTT broker, NodeMCU (type of ESP8266 (Espressif, <http://espressif.com/>, 2017), and a simple WebGIS application written with the Leaflet, MQTT.js, jQuery libraries.

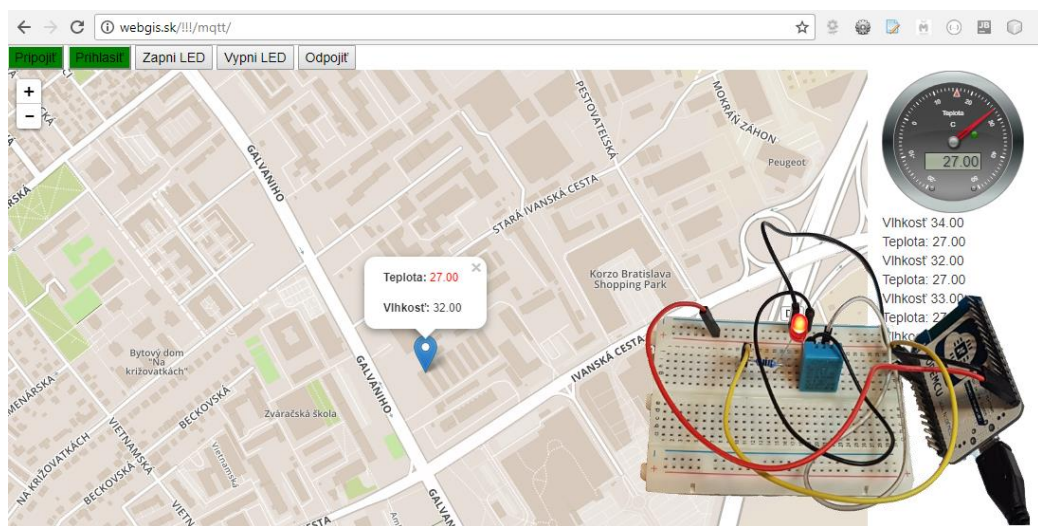


Fig. 9. Temperature from IoT device sent to WebGIS application by MQTT

NodeMCu is MQTT publisher of temperature and humidity and subscriber for switching LED light. WebGIS application is MQTT publisher for switching LED light and subscriber for temperature and humidity messages. The MQTT broker receives and sends MQTT message.

The result of this solution is: WebGIS application switching LED light and showing temperature and humidity of point on the map.

Another test of MQTT was used in attendance system to conference. IoT device has RFID (Radio Frequency IDentification) reader and sends MQTT message to broker. Data from RFID reader are synchronized in six android devices and four windows PC (Personal Computers) and two servers via MQTT messages. For collection and analysing data the system is very useful and works in real time.

DISCUSSION AND CONCLUSIONS

The conducted tests demonstrated the applicability of combined LoRaWAN and MQTT technologies for transmission of the IoT data to a GIS for a range up to several kilometers. Moreover, such a sensor-based GIS is capable of analysing and displaying information for a long period of time without the need to replace the battery thanks to the LPWAN technology. The durability aspect is crucial for the domain of safety and security management to ensure the continuity of sensor measurements. The Internet part of the developed system used the MQTT to share information between heterogeneous networks. From the interoperability point of view, sent and received MQTT messages are also available in the GeoJSON (Geo JavaScript Object Notation) format and are very simple to implement on a light/cheap device for collecting information and analysing in GIS as well to publish in a WebGIS application.

IoT is nowadays commonly designated as a "smart" IoT sensor. Such denotations may be misleading since it is a device without any logic (a "dummy" one). An IoT device is very complex (CPU, memory etc.). However, sensor data are not processed. A device reads the data from the sensor and sends it for processing. It generates large amount of data. For instance, it means that only the 10 minutes temperature readings equal to 6 messages per hour, 144 per day, 1,088 per week, and 53,424 per year.

Adding an application logic to an IoT sensor is simple. Nevertheless, changing the application logic of a sensor requires uploading a new version of firmware in the device. Such an update is also a very expensive one for tens/hundreds/thousands of devices. Besides, the Over the Air (OTA) update may be problematic itself in the LPWAN. This basic limitation is typical for any IoT-based system architecture. In the end, data processing needs to be combined on the levels of sensors, gateways and/or backend system.

ACKNOWLEDGEMENT

This project has received funding from the Masaryk University under grant agreement No MUNI/A/1419/2016 entitled "Integrated Research of Environmental Changes in Earth's Sphere II".

REFERENCES

- Al-Fuqaha, A., Guizani, M., Mohammadi, M., Aledhari, M., Ayyash, M. Internet of Things: A Survey on Enabling Technologies, Protocols, and Applications (2015) IEEE Communications Surveys and Tutorials, Volume 17, Issue 4, pp. 2347-2376.
- Arduino, <https://www.arduino.cc/>.
- Bandyopadhyay, S. and Bhattacharyya, A. (2013) Lightweight Internet protocols for web enablement of sensors using constrained gateway devices, 2013 International Conference on Computing, Networking and Communications (ICNC), San Diego, CA, pp. 334-340.
- Banks, A. and Gupta, R. (2015) MQTT Version 3.1.1 Plus Errata 01.. 10 December 2015. OASIS Standard Incorporating Approved Errata 01. <http://docs.oasis->

open.org/mqtt/mqtt/v3.1.1/errata01/os/mqtt-v3.1.1-errata01-os-complete.html. Latest version: <http://docs.oasis-open.org/mqtt/mqtt/v3.1.1/mqtt-v3.1.1.html>.

- De Poorter, E. and Hoebeke, J. and Strobbe, M. and Moerman, I. and Latré, S. and Weyn, M. and Lannoo, B. and Famaey, J. (2017) Sub-GHz LPWAN Network Coexistence, Management and Virtualization: An Overview and Open Research Challenges. *Wireless Personal Communications*. pp. 1-27.
- Espressif, <http://espressif.com/>.
- Hardkernel co., Ltd, <http://www.hardkernel.com/main/main.php>.
- Kamimura, A., Tomita, K. (2017) A self-organizing network coordination framework enabling collision-free and congestion-less wireless sensor networks, In *Journal of Network and Computer Applications*, Volume 93, Pages 228-244.
- Kapoor, S., Pahuja, H. and Singh, B. (2016) Real time monitoring & alert system for landslide, 2016 2nd International Conference on Contemporary Computing and Informatics (IC3I), Noida, pp. 584-589.
- Li, J., Li, C. K., Li, K., & Liu, Y. (2014) Design of landslide monitoring and early warning system based on internet of things. *Applied Mechanics and Materials*, Volume 511-512, pp. 197-201.
- Margelis, G., Piechocki, R., Kaleshi, D. and Thomas, P. (2015) Low Throughput Networks for the IoT: Lessons learned from industrial implementations, *IEEE 2nd World Forum on Internet of Things (WF-IoT)*, Milan, 2015, pp. 181-186.
- Martinez M.G. (2015) Solver engagement in knowledge sharing in crowdsourcing communities: Exploring the link to creativity, In *Research Policy*, Volume 44, Issue 8, 2015, pp. 1419-1430.
- Mikhaylov, K., Petäjajarvi, J., Haenninen, T. (2016) Analysis of capacity and scalability of the LoRa low power wide area network technology. In: *Proceedings of the 22th European Wireless Conference on European Wireless*; 2016 May 18–20; Oulu, Finland, pp. 1-6.
- Petajarvi, J., Mikhaylov, K., Roivainen, A., Hanninen T, Pettissalo, M. (2015) On the coverage of LPWANs: Range evaluation and channel attenuation model for LoRa technology. In: *Proceedings of the 14th International Conference on ITS Telecommunications*; 2015 Dec 2–4; Copenhagen, Denmark. Piscataway: The Institute of Electrical and Electronics Engineers, Inc.; pp. 55–59.
- Postscapes, <https://www.postscapes.com/internet-of-things-history/> (November 2017).
- Ratasuk, R., Vejlggaard, B., Mangalvedhe, N., Ghosh A. (2017) NB-IoT system for M2M 466 Y. Song et al. / *Engineering* 3, 460–466 communication. In: *Proceedings of the 2016 IEEE Wireless Communications and Networking Conference Workshops*; 2016 Apr 3–6; Doha, Qatar. Piscataway: The Institute of Electrical and Electronics Engineers, Inc.; 2016. pp. 428–32.
- Řezník, T., Horáková, B., Szturc, R. (2015) Advanced methods of cell phone localization for crisis and emergency management applications, *INTERNATIONAL JOURNAL OF DIGITAL EARTH* Volume: 8 Issue: 4 pp. 259-272 Published: APR 3 2015.
- Řezník, T., Chudý, R., Mičietová, E. (2016) Normalized evaluation of the performance, capacity and availability of catalogue services: a pilot study based on INfrastrutture for SPatial InfoRmation in Europe *INTERNATIONAL JOURNAL OF DIGITAL EARTH* Volume: 9 Issue: 4 pp. 325-341 Published: APR 2016.

- Sawant, S., Durbha, S.S., Jagarlapud, A. (2017) Interoperable agro-meteorological observation and analysis platform for precision agriculture: A case study in citrus crop water requirement estimation, In *Computers and Electronics in Agriculture*, Volume 138, pp. 175-187.
- Shenzhen Xunlong Software CO.,Limited, <http://www.orangeapi.org/>.
- Sigfox, <https://www.sigfox.com/en> (November 2017).
- Song, Y., Lin, J., Tang, M., Dong, S. (2017) An Internet of Energy Things Based on Wireless LPWAN, In *Engineering*, Volume 3, Issue 4, 2017, pp. 460-466.
- Sornin, N. (Semtech), Luis M. (Semtech), Eirich T. (IBM) and Kramp T. (IBM) and O. Hersent (Actility) LoRaWan Specification V1.0.2 July, 2016 LoRa Alliance.
- The BeagleBoard.org Foundation, <https://beagleboard.org/>.
- The Raspberry Pi Foundation, <https://www.raspberrypi.org/>.
- The Things Network, <https://www.thethingsnetwork.org/forum/t/limitations-data-rate-packet-size-30-seconds-uplink-and-10-messages-downlink-per-day-fair-access-policy/1300> (November 2017).
- Zambrano, A.M., Perez, I., Palau, C., Esteve, M., (2017) Technologies of Internet of Things applied to an Earthquake Early Warning System, In *Future Generation Computer Systems*, Volume 75, pp. 206-215.
- Zanella, A., Bui, N., Castellani, A., Vangelista, L., Zorzi, M. Internet of things for smart cities (2014) *IEEE Internet of Things Journal*, Volume 1, Issue 1, art. no. 6740844, pp. 22-32.

GEOMATIC SYSTEM FOR ANALYSIS AND MONITORING OF SHORELINE

Vincenzo, BARRILE¹; Antonino, FOTIA¹

¹ Geomatics Lab, DICEAM, Mediterranea University, loc. Feo di Vito, 89123, Reggio Calabria, Italy

vincenzo.barrile@unirc.it antonino.fotia@unirc.it

Abstract

The paper describes and analyses the temporal evolution of the shoreline of Reggio Calabria, focusing on the waterside overlooking the waterfront and considering, as a time interval, the last 30 years. To locate the coastline at different time periods were analysed satellite images from Google Earth, maps provided by the Basin Authority of the Calabria region, orthophotos are taken from the open data section of the National Geoportal and was also carried out a survey using a UAV. The coastal bathymetric survey by means of a single-beam echo sounder and LIDAR sensor on UAV is carried out following the profile lines. All these data were introduced in a GIS to check the difference and the contribution of erosion and nourishment.

Keywords: GIS, Shoreline, UAV, Bathymetric, LIDAR.

INTRODUCTION

Coastal areas are one of the most populated territories in the world. In fact, 37% of the world's population lives within 100 km of a coast, while about 50% live within 200 km. In particular, in Calabria, recent studies have shown that only 30% of the coastal area is not subject to coastal erosion, a very small percentage.

This phenomenon is mainly due to a deficit of sediments, caused by natural and anthropogenic factors. Regarding the natural factors, we are reminded of the subsidence, which involves the lowering of the seabed due to soil compaction, or the raising of the mean sea level produced by climate change. In addition to these natural causes, unfortunately, are added anthropogenic causes that tend to amplify this phenomenon, making coastal erosion even more destructive. The biggest problem is linked to the reduction of river solid contributions to the sea, which are not enough to ensure the equilibrium of the beaches. In fact, in the last few years, we have witnessed the building of dams for hydroelectric purposes, for lamination of floods, or for irrigation, which has blocked the natural sediment transport. To this, we must add the indiscriminate excavations of riverbeds and the building of embankments. Likewise, the construction of massive infrastructures (such as ports, harbors, breakwaters, etc.) and the urbanization of the coast, with the consequent destruction of coastal dunes and the increase of building near the shorelines, has modified or blocked the longshore sediment transport.

To understand and reduce the problem of coastal erosion, it is useful to study all phenomena which are involved in coastal dynamics in particular wave and weather climate analysis, and the contribution of longshore and river sediment transport. Moreover, it is very important to know

the past and present management plans, the tourist use of the coast, and any structures built near the shore and their effects on neighbouring coasts.

Furthermore, it is useful to carry out periodic monitoring of the shoreline (through bathymetric surveys of the seabed, topographical surveys of the emerged beach, and size analysis of sediments). Technological advances led to the emergence of Unmanned Aerial Vehicles (UAV), with which it is possible to perform surveys in areas that are difficult to access.

ANALYSIS OF THE COASTLINE

Site description

The presence of numerous streams characterizes the municipal territory of Reggio Calabria. So most of the coastal strip consists of flat territories of alluvial nature and of short extension, generated precisely by the deposition of sediments transported by various streams. The shoreline studied, from the geomatics point of view by the authors, and from the hydrologic/hydraulic point of view by G. Barbaro, V. Fiamma, V. Barrile, G. Foti and G. Ielo, 2017, is located in the city centre, between the streams Annunziata and Calopinace, it is inclined about 228° from the north and has a wide beach, between 20 and 30 m on average (G. Barbaro, V. Fiamma, V. Barrile, G. Foti and G. Ielo). From the sedimentological point of view, it is characterized by pebbled sand, while from the climatic point of view it is characterized by a Mediterranean climate and is subject to prevailing winds blowing from northwest and southwest.

UAV operation for coastline

The drone model used is the DjiPhantom 2 Vision Plus, equipped with a GoPro HERO3 + Silver Edition camera capable of taking 10 Megapixel photos and shooting Full HD 1920 x 1080p at 30 fps and 720p at 60 fps. The angle of the field of view, depending on the image format chosen, is 110° or 85°.

The drone is also equipped with a small GPS antenna to determine the real-time position of the device and allow scheduled flight by waypoints, and a remote and real-time transmission system of the scene. The ground station allows the operator to control the device. It is constituted by the controller, useful for drone guidance, and monitor, which illustrates the shooting scene and other information about the status of the device. (Dai F, Dong S, Kamat V, Lu M. 2011)

Before starting the flight, we performed a calibration of the GPS and gyroscope, through the forward and reverse movements and the UAV rotation. On the ground, targets were subsequently detected with kinematics GPS rover RTK mode, in order to georeference better the images taken by the UAV and the 3D model generated. (Nahangi M, Haas C.T. 2014)

The images were taken at different altitudes (20 and 30 m), for getting a global coverage of the area to build an orthophoto (Dai F, Rashidi A, Brilakis I, Vela P. 2013). Because of the prohibitive weather conditions for the device, and the presence of wind gusts above 30 km/h, it was not possible to reach higher elevations and extend the duration of the flight to investigate a wider area.

The overlap respect to flight direction was at 70% and at 60% overside (between strips).

The flights were done both as autonomous and manual mode. They were done in different time and different places, to cover overall an area long 1,5 km. For the work in question (the 3D reconstruction in Fig. 1) the software used was Agisoft Photoscan.

Though Agisoft PhotoScan is also able to complete the reconstruction and georeferencing activities without GCP, 10 GCP were used because necessary to obtain top quality results, both in terms of geometric precision and accuracy of georeferencing. (Barrile V, Lamari D, Gelsomino V, Sensini P. 2016)

The workflow is completely automatic both as regards the orientation of the images and for the generation and reconstruction of the model. This condition led to an optimization of processing times ensuring good performance of the machine/software complex. (Barrile V, Critelli M, Lamari D, Meduri G.M, Pucinotti R, Ricciardi A. 2015)

The phases of the elaboration and the setting of individual processing are showing in the following tab.1:

Table 1. Workflow and parameters used in Agisoft Photoscan.

First step: Align photo	
Align photos (photo alignment) consisting of identifying the binding points. The points chosen in the various photos must have characteristics in common in order to be adequately superimposed;	
Accuracy	High
Pair preselection	Disabled
Key point limit	40000
Build mesh (preliminary step to insert GCPs)	
Surface type	Arbitrary
Face count	High
Source data	Sparse cloud
Interpolation	Enabled
Point classes	All
Second step: Import GCPs	
Through this phase are imported the coordinates of the GCPs in the scene	
Measurement accuracy (for GCPs)	
Camera accuracy (m)	10
Marker accuracy (m)	0.05
Scale bar accuracy (m)	0.001
Projection accuracy (pix)	0.1
Tie point accuracy (pix)	4
Third step: Build dense cloud	
Through this phase a dense cloud is constructed using dense image matching algorithms;	
Quality	High

Depth filtering	Aggressive
Fourth step: Build mesh which consists in generating a polygonal model based on the newly created dense cloud;	
Surface type	Arbitrary
Face count	Medium (136012)
Source data	Dense cloud
Interpolation	Enabled
Point classes	All
Generate 3D Model – Export DEM Through this phase, we obtain the 3D representation of the work under investigation.	
Classification of ground points (geometrical filtering)	
Parameter	Value
Max angle (deg)	0.5
Max distance (m)	0.1
Cell size (m)	1



Fig. 1. 3D model of the shoreline object of studies

The dense clouds produced from UAV imagery had a density of 1-3 points per cm^2 with more of 7 million points in a cloud. The point cloud generated were georeferenced by matching control points in the cloud to surveyed ground control points. The resulting accuracy was dependent on the accuracy of the GCP survey and in this case, it is approximately 20-30 mm. (Bhatla A, Choe S, Fierro O, Leite F. 2012) (Dai F, Feng Y, Hough R. 2014)

Bathymetric Data Collecting

The coastal bathymetric survey by means of a single-beam echosounder is carried out following the profile lines, generally placed orthogonally to the coast, integrated by further routes perpendicular to the previous ones that are used for control.

The survey was carried out at sea completely calm and in the absence of wind. The sounding sections were traveled by a low draft boat that moved at low and constant speed along the predetermined routes.

For the bathymetric survey, an automatic-digital data acquisition system was used, with the positioning of the vessel in real time using GPS technology with correction of the coordinates via a radio modem. This system has allowed to realize the survey of the lines without any alignment and to have an instantaneous correction of the dimensions.

The onboard GPS has transmitted in real time, at very high frequencies, the coordinates (East, North and altitude) to the navigation software.

The operator on the boat directing the boat has followed the instructions on the video of the computer, where is indicated the trace that represents the theoretical line to be detected and the instant position of the boat.

Data acquisition begins once the boat is brought into alignment with the section to be detected. The off-route, the speed in knots, the steering angle, the distance from the start and the end of the route, the event number and other useful values for the survey are also visible.

This technology offers significant advantages; in fact, calculating the GPS, as well as the coordinates, also the absolute dimension of the transducer in real time and with centimeter precision, it becomes possible, in conjunction with the data coming from the echo sounder, to automatically correct all the oscillations of the marine surface (tides, waves, raised due to the mass of water pushed by the wind) during the relief.

With this methodology, as we have seen, it is not necessary to make the tidal and atmospheric pressure corrections for the reduction at sea level afterward, plus all the vertical oscillations are automatically taken into consideration.

The echo sounders used are of the hydrographic type with an accuracy of 1-2 cm. The frequency adopted is generally around 200 KHz; a good compromise to guarantee an accurate survey of the seabed with little interference from the water column. The instrument emission cone is usually very narrow to guarantee a high geometric resolution. A frequency of at least one pulse (beam) per second is required. To ensure congruence between depth and planimetric measurements, the echo sounder is positioned on the axis of the receiver for the planimetric position or alternatively, the relative offsets are calculated. At the beginning and end of the survey, the echo sounder was calibrated. The adjustment of the instrument speed according to the speed of the ultrasounds in water is carried out by the "Bar Check" method (measurement of the immersion depth of a bar or metal disk lowered below the transducer and suspended by a graduated cable).

We then proceed to the digital correction of the errors on the navigation software.

Cause of financial availability, in this type of surveys no motion sensors are used to correct roll and pitch and calculate the translator's changes in height. The reliefs are made with perfectly calm sea, and at shallow depths, thus mitigating the problem from a geometric point of view, and therefore the error committed is considered tolerable.

By executing the survey directly in digital format all the data are recorded on the onboard PC.

The reliefs by means of single-beam, especially in the sandy bottoms, do not always need a centimeter accuracy on the position. Often, as seen, DGPS instruments of sub-metric precision are sufficient for obtaining excellent results.

In this case, the tide during the survey is generally measured by reading on a graduated rod, leveled by a well-known landmark, and positioned in a calm sea area.

Table 2. HydroStar 4300

HydroStar 4300 – Survey echo sounder	
Frequency	30/200 kHz
Output power	Up to 800 W
Depth resolution	1 cm
Accuracy	+/- 0.25% of water depth
Beam angle	24°/8°

Advances in sensor technology have led to the miniaturization of LiDAR systems and, at the same time, advances in UAV technology today allow the transport of high loads and longer flight times.

The LIDAR systems used has a wavelength of 532 nm, useful to penetrate the water (if it is clear and not troubled) to measure the seabed.

The bathymetric LIDAR sensors can be simplified into four main components:

- the GPS receiver for the position of the aircraft
- the inertial platform (IMU) for rolling, stepping and yawing
- the laser scanner that emits the signal
- the sensor that reads the return signal

Knowing the position and orientation of all these components it is possible to make accurate measurements which are then recorded by the LIDAR system. Some of these sensors can measure more than 100,000 points per second, returning more than 10 points per square meter in shallow water. (Golparvar-Fard M, Bohn J, Teizer J, Savarese S, Peña-Mora F. 2011)

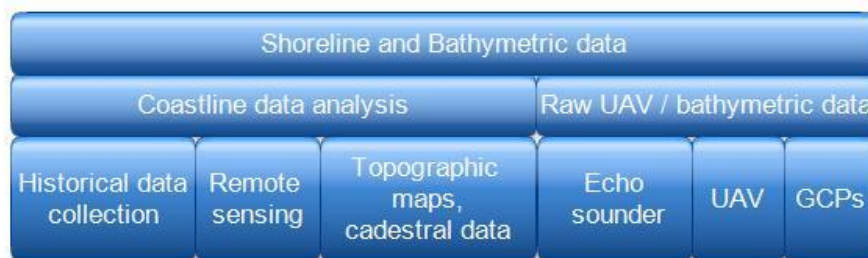


Fig. 2. Flow Chart Shoreline and bathymetric data.

HISTORICAL EVOLUTION OF THE COASTLINE

We acquired and processed, by using the QGIS, the maps of interest or the shapefiles of the coastline near the promontory of Reggio Calabria. Maps, in different scales, are of the years: 1954 (Cassa del Mezzogiorno CASMEZ Cartography 1:5.000), 1985 (IGM Cartography 1:25000), provided by the Basin Authority of the Calabria Region, 1988, 1995, 1998, 2000, 2006, 2008 and 2012 aerial photographs (orthophotos 1:1000) taken from the Open Data section of the Geoportale Nazionale; and flight by UAV of May 24, 2016 (spatial resolution of orthophotos of 5 cm). Clearly the precision of the shoreline, manually reported in the GIS, got the same precision of the maps.

In general, the starting point for achieving a performing GIS is the perfect overlapping of the different map layers that are often made with different reference systems (Datum and Coordinate Systems) for which they need preventative and appropriate georeferencing operations to make them superimposable and, therefore, comparable.

To georeferenced all the maps, we used 4 GCPs that coincided with 4 spots in common at all maps.

Specifically, after acquiring maps, orthophotos and images obtained by processing the UAV flight, to limit and reduce map deformations, and to report in a single coordinate system the area under investigation we used some function of rotation and scale variation. Below are the cartography, orthophotos and the image acquired by the UAV.

To evaluate the advances and retreats of the stretch of coastline and the change of the bathymetric lines object of study, which extends for about 2 km, it has been discretized into 9 different sections placed at an average distance of about 100 meters from each other. It was implemented on QGIS a function that automates the process of calculating the distance between the different coastlines within each section, using as the starting point the 'field calculator' in the program attribute table. (Luhmann T, Tecklenburg W. 2001) (Zhu Z, Brilakis I. 2009)

Specifically, starting with the functions:

```
geom_to_wkt(shortest_line($geometry,geometry(get_feature(Layer,attribute,value))))
```

and

```
length(geom_from_wkt("shortline"))
```

it has been implemented, according to the flowchart below, a function that can determine the distance from a given point starting from a reference vector line in a given coordinate system. (McCoy A, Golparvar-Fard M, Rigby E. 2014)

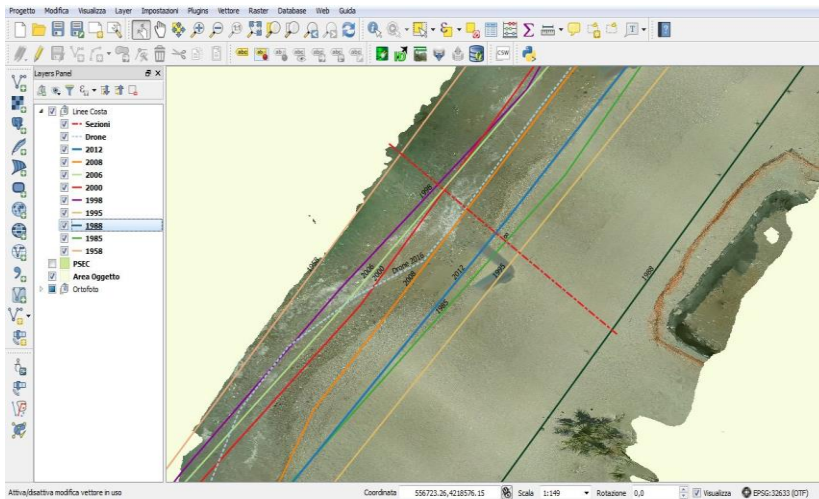


Fig. 3. Comparison of coastlines

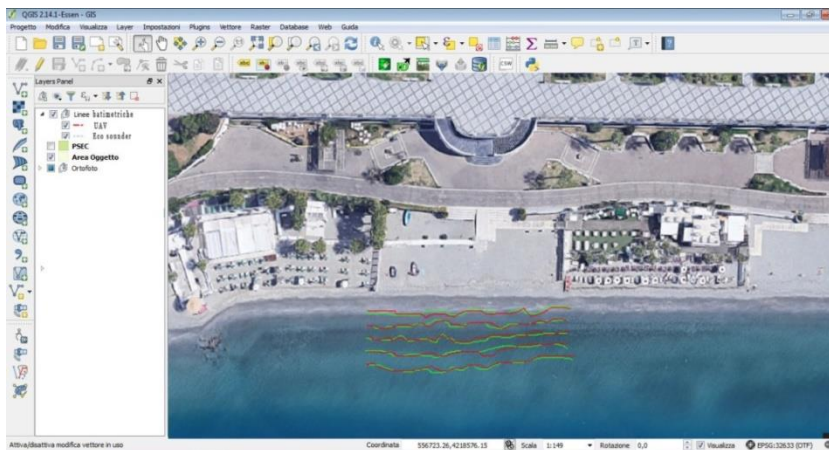


Fig. 4. Comparison of bathymetric lines

From the analysis of the Fig. 5 it can be observed that erosion is present in almost all the time intervals analyzed. It is also possible to observe that most of the coastline variations measured in each period are less than 10 m taken as a reference the coastline in the map of 1954 that anyway, compared with the other cartographies considered, did not have the same degree of accuracy. In relation to the bathymetric lines, instead, this was only an initial experiment and we do not have today the repeatability of the measurements to have an accuracy. Therefore we had measured 4 points in a simple and manual way. The recorded measurements differed, on average and in both cases, from those made of about 7 cm.

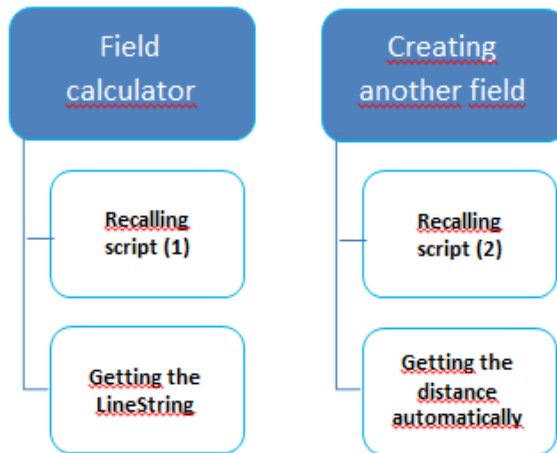


Fig. 5. Flow Chart

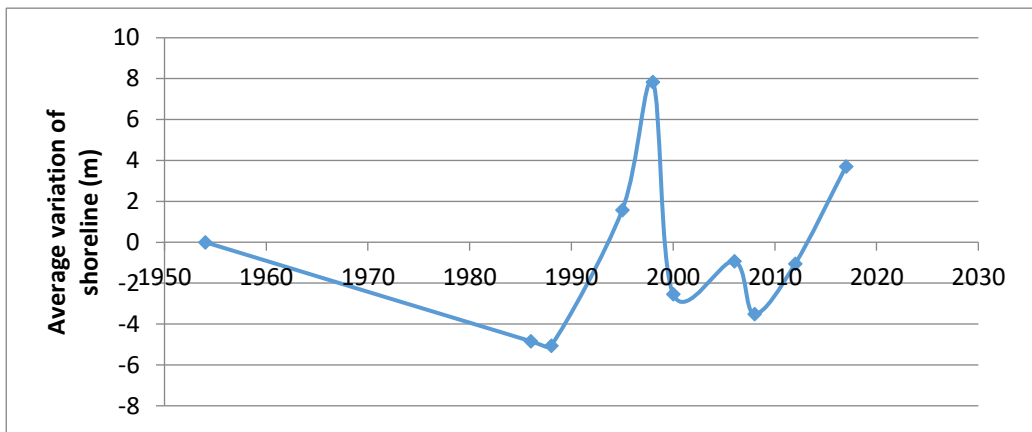


Fig. 6. Coastline variations during the years.

CONCLUSION

The shoreline evolution of the coast in front of the promenade of Reggio Calabria in the last thirty years was analyzed using satellite imagery from Google Earth, cartography data provided by the Calabria Basin Authority (ABR), aerial photos taken from open data section of the National Geoportal, and also from survey data gathered by using an Unmanned Aerial Vehicle (UAV). The coastline under consideration is strategically important for tourism and the landscape. In fact in the summer many coastline bathing facilities contribute to the economic development of Reggio Calabria.

Continuous monitoring through open source systems such as QGIS well can act as an alarm bell to find some possible solutions to prevent potential problem of coastal erosion consists in retention of the river material currently located in the riverbed, and in increased monitoring of climatic activity.

REFERENCES

- Barrile V, Critelli M, Lamari D, Meduri G.M, Pucinotti R, Ricciardi A. (2015), “*Applicazione di Sistemi di Scansione 3D e Fotogrammetrici al caso di un Ponte in C.A.*”, Atti 16° Convegno Aipnd Milano 21-23 Ottobre 2015
- Barrile V, Lamari D, Gelsomino V, Sensini P. (2016), “*Modellazione 3D tramite Droni per Monitoraggi e Controlli*”, 61° Convegno Nazionale Sifet, 8-10 Giugno 2016, Lecce
- Bhatla A, Choe S, Fierro O, Leite F. (2012), “*Evaluation of accuracy of as-built 3D modeling from photos taken by handheld digital cameras*”, Autom. Construct. 28 116–127
- Dai F, Dong S, Kamat V, Lu M. (2011), “*Photogrammetry assisted measurement of interstory drift for rapid post-disaster building damage reconnaissance*”, J. Nondestr. Eval. 30 (3) 201–212
- Dai F, Feng Y, Hough R. (2014), “*Photogrammetric error sources and impacts on modeling and surveying in construction engineering applications*”, Visual. Eng. 2 (1)
- Dai F, Lu M. (2010), “*Assessing the accuracy of applying photogrammetry to take geometric measurements on building products*”, J. Construct. Eng. Manage. 136 (2) 242–250
- Dai F, Rashidi A, Brilakis I, Vela P. (2013), “*Comparison of image-based and time-of-flight-based technologies for three-dimensional reconstruction of infrastructure*”, J. Construct. Eng. Manage. 139 (1) 69–79
- Golparvar-Fard M, Bohn J, Teizer J, Savarese S, Peña-Mora F. (2011), “*Evaluation of image-based modelling and laser scanning accuracy for emerging automated performance monitoring techniques*”, Autom. Construct. 20 (8) 1143– 1155
- Luhmann T, Tecklenburg W. (2001), “*Hybrid photogrammetric and geodetic surveillance of historical buildings for an urban tunnel construction*”, International Workshop on Re-creating the Past Visualization and Animation of Cultural Heritage
- McCoy A, Golparvar-Fard M, Rigby E. (2014), “*Reducing barriers to remote project planning: comparison of low-tech site capture approaches and image-based 3D reconstruction*”, J. Architect. Eng. 20 (1)
- Nahangi M, Haas C.T. (2014), “*Automated 3D compliance checking in pipe spool fabrication*”, Adv. Eng. Inform. 28 (4) 360–369
- Zhu Z, Brilakis I. (2009), “*Comparison of optical sensor-based spatial data collection techniques for civil infrastructure modeling*”, J. Comput. Civil Eng. 23 (3) 170–177

IMPROVING THE USER KNOWLEDGE AND USER EXPERIENCE BY USING AUGMENTED REALITY IN A SMART CITY CONTEXT

Francisco, RAMOS¹; Pravesh, YAGOL²

^{1,2}Institute of New Imaging Technologies, Universitat Jaume I, Avda. Sos Baynat, 12071, Castellon, Spain

¹*francisco.ramos@uji.es*; ²*shr_pravesh@hotmail.com*

Abstract

The idea of Virtuality is not new, as research on visualization and simulation dates back to the early use of ink and paper sketches for alternative design comparisons. As the technology has advanced so the way of visualizing simulations as well, but the progress is slow due to difficulties in creating workable simulations models and effectively providing them to the users (Simpson, 2001).

Augmented Reality and Virtual Reality, the evolving technologies that has been haunting the tech industry, receiving excessive attention from the media and growing tremendously are redefining the way we interact, communicate and work together (Shamalinia, 2017). From consumer application to manufacturers these technologies are used in different sectors providing huge benefits through several applications.

In this work, we demonstrate the potential of Augmented Reality in a smart city context. Initially we present an overview of the state of the art software and technology for AR in different domains of smart cities, and outline considerations from a user study about the effectiveness and user performance of AR technique: real environment with augmented information, everything in the context of a smart city. The evaluation results from the participants show promising results, providing opportunities for improvements and implementation in smart cities.

Keywords: Augmented Reality, Virtual Reality, Smart City

INTRODUCTION

A smart city uses technological infrastructure in every aspect of our lives in order to provide solutions to the citizens to make their life easier (Musa, 2016). The way of communication of information is changing with the advancement in technology, which is a basic strategy of Smart Cities for transforming the city infrastructure and services with Information and communication technologies (ICT), as the driving force for changing the way smart cities compete (Bakici, Almirall, & Wareham, 2013). Comprehensively a city cannot be considered of being smart unless technology enhanced, ICT driven spatial enabled solutions are implemented for better urban performance contributing to smart operations of cities (Roche, Nabian, Kloeckl, & Ratti, 2012). The implementation of smart city is the optimization of the urban system with the use of new generation information technology, making the system more consummate, smart, coordinated and developed, while improving the livelihood of the people enhancing their intelligence and live harmoniously (Lv, Yin, Zhang, Song, & Chen, 2016). The usage of mobile applications has become essential for the cities to become smart city, with the rapidly evolving mobile technology.

As the technology has advanced so has the way of visualizing simulations and information. Virtual Reality and Augmented Reality are great examples of such visualization methods which is booming in this digital era, either by being immersed in simulated virtual environment or adding new dimension of interaction between digital devices and the real world. Both methods have something similar, though slightly different and equally significant in their own ways providing experiences and interaction being detached or blending together with the real world, making real and virtual alike. The process of replacing and supplementing the real world according to the needs, is what makes these methods more desirable and increasingly popular. From consumer application to manufacturers these technologies are used in different sectors providing huge benefits through several applications. Major achievement in emergence of low cost or freely available headsets has made possible the creation of such virtual exhibition within the reach of many with even modest budget (Monaghan, O'Sullivan, O'Connor, Kelly, Kazmierczak and Comer, 2011).

AR IN SMART CITIES

“Augmented Reality” the term coined by researcher Tom Caudell, at Boeing in 1990, for guiding factory workers with improved diagrams and marking devices (Caudell and Mizell, 1992). Advancement in mobile technologies and accessibility of online applications AR system provides service without restraining individuals' whereabouts to an especially equipped area, adding a layer of information whenever desired, having potential to revolutionize the way of presenting information to the people. AR has been used in many domains such as medical, robotics, military, Navigation, traveling, education, entertainment, marketing, tourism, urban planning, manufacturing, product assembly and repair, architecture etc.

In Medical Sector AR has been used in wide range of medical practice ranging from pre-operative imaging training and education to image guided surgery (J. Der Lee, Lee, Hsieh, Wu, & Lee, 2015) decreasing risks associated with long procedure times (Cheung, Wedlake, Moore, Pautler and Peters, 2010). In battlefield, AR provides training solution with Advance Helmet Mounted Display (AHMD) by overlaying actual, augmented and simulated visible environment (Sisodia, Riser, Bayer and McGuire, 2006). Tourism is another blasting industry where the use of AR has an imperative role in redefining the concept of traditional tourism, such as mobile AR applications of guided tour to enhance perception of the reality (Shang, Siang, Zakaria and Emran, 2017). Research shows that Education with AR has proven to be extremely useful in increasing the students' motivation in learning process (Chang, Chang, Hou, Sung, Chao and Lee, 2014).

Navigation in simulated environments has been tried and tested and is still in research phase. AR navigation provide better and faster support route decision making and are visually more demanding (Kim and Wohn, 2011). The use of AR in asset repair system providing pinpointing repair areas has allowed field technicians to quickly and efficiently query and update repair and customer-based information. Augmented Reality in games produces a real time 3D display effect by superimposing virtual information on to the real world involving teenagers more into sports and exercise (Zhao, Chen, Wang and Zhang, 2016). Introduced in July 2016, Pokémon Go, a

mobile location based social game, is by far the most popular AR game involving physical activity of gamer in the real world with potential and documented health benefit.

ARUJI: A MOBILE AUGMENTED REALITY GUIDE

AR UJI is a Native app, a prototype of an AR guiding app for the students and visitors around the university of Jaume I and available in android devices. Generally, the system provides basic functionality of a location based Augmented Reality application using ArcGIS point feature layers in order to easily locate services around the user location through the lenses of the mobile’s camera by displaying information about the POI as a pop up with icons or media designating the POI and some quick info.

System Architecture

When the user open the AR UJI application, it request data from the hosted services published or shared in ArcGIS Online platform by the provider of the app. The ArcGIS online platform validates the request and provides access to data to be downloaded in the form of ArcGIS point feature layers, which visualizes the content into an augmented reality environment in the mobile device. The point feature layer contains all the information about the feature, ensuring its availability in offline mode. The basic difference in using the inbuilt AuGeo app from the AuGeo template and ARUJI app is that, in AuGEO users need to sign in using the ArcGIS account and set all the variables after signing in and download the data required to run the application. But, the ARUJI app runs without user to sign in to the ArcGIS account as the credentials are stored within the application. Moreover the variables are set to user preferred values, appropriate for the users with the data ready for use.

System Design

Once the feature layer is downloaded it can be used in offline mode. The application prepares for the compass calibration of the mobile and determines the user location which is the most essential requirement determining the accuracy of the application. The higher the compass calibration and accurate location determination, more the accuracy of the location of the point features. The services available in UJI are categorized in the following as seen in the table. Each categories are further divide to its possible elements as available inside the University.

Table 1. Categories and its elements for use in the ARUJI app.

Categories	Elements
Food	Café, Restaurant, Canteen, Vending Machines
Bank	Bank, ATM
Shop	Retail store, Printing, Optics
Transport	Bus Stop, Bicicas Station
Health Service	Dental Clinic, Clinic
Building	Department, Office, Library, Info Centre, Gallery

The main window of the application supports two distinct types of functionality. First, users can receive more information from the displayed POIs by selecting in the screen of their mobile

device (such as opening hours, phone number, etc.). Second, users can navigate to the 2D map view mode by click the circular radar at the bottom left corner of the screen for navigational directions to the selected POI.

Naturally, marker based and geo based AR are prone to “occlusion problem”, i.e. the real world as well as the AR contents itself may visually conceal the display AR contents obscuring valuable information (Yovcheva, Buhalis, & Gatzidis, 2013; Kourouthanassis, Boletsis and Lekakos, 2013). Indeed the AR UJI app is no exception, with possibility of displaying POI icons on top of each other for distant POIs. However, these occlusion problems can be solved to some extent with extra options provided to the user. The user can configure the maximum extent for displaying the POIs from the user location, excluding POIs far away causing extra noise in the display screen. Furthermore, the user can zoom in the camera for precise display of POIs. In addition, user can select or unselect the properties that is displayed in the data popups, reducing the size of the popups therefore, minimizing the popups overlapping.

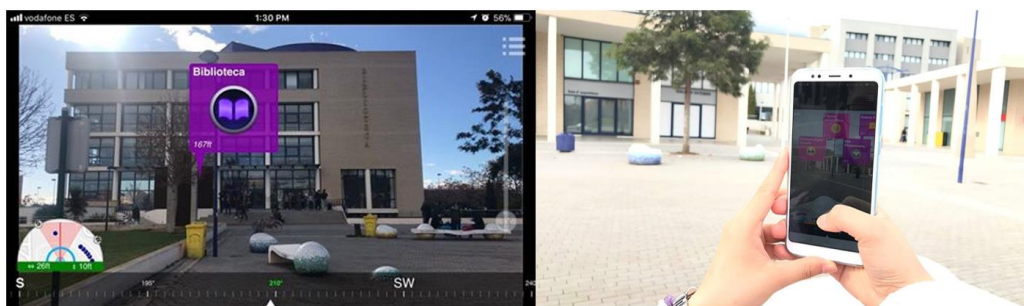


Fig. 1. AR UJI app

USER EVALUATION

Study Design

It's not exaggeration to say map apps like Google maps and Apple maps for searching places and facilities around, is the most popular trend. With the rise of AR and VR in the tech industry, what will be the impact of these technologies to the trending map apps? The problems and difficulties associated with the spatial knowledge and skills of the students were being acknowledged in the unfamiliar urban dynamics and existing issues with the linguistic difference, in order to provide a solution with AR guided maps service.

The study comprise of independent variable as the type of View (2D Map view and the AR view) and dependent variables as Effectiveness, Efficiency and Satisfaction. As the study included only one independent variable, a basic design was approached (Lazar, Feng, & Hochheiser, 2010) with two conditions in the experiment (with and without AR view), i.e. experimenting with Map View and AR View. The effectiveness was determined by the successful completion of the task with and without using the ARUJI application on a basis of Likert scale 1-5 (1: Not at all, 5: Very much). The Efficiency was determined by the time taken for successfully completion of the task with Map View (Google Maps) and AR View (ARUJI). For this two task where defined, to be

performed with AR UJI app and another 2D map app (majority of Google Maps). The satisfaction in using the ARUJI app in this study was determined directly as well as indirectly through the questionnaire. In the indirect determination of satisfaction the questionnaire was classified into five factors namely, ease of Use (successfulness), Clarity of information, controllability, helpfulness and fun. The questionnaires also involved a more direct approach in the sense that the respondents were asked explicitly about the comfortability and satisfaction in using the ARUJI app compared to other mapping apps.

User Sampling

A convenient sampling methodology was adopted for inviting prospective users of AR UJI. The participants consisted of 20 random individuals and groups from different countries who were new to the University, and having experience in using mobile applications, in order to avoid biasness and ensure credibility of the results. Table 2 provides the information of the demographics of the participants.

Table 2. Sample Demographics

Dimension	Value	Total	Percentage %
Gender	Male	10	50
	Female	10	50
Age	< 18	1	5
	19 – 25	9	45
	26 – 35	10	50
	35 +	0	0
Education	University Graduate	10	50
	Post Graduate	10	50

Procedure

Initially, the objectives of the study was explained to the randomly approached participants, and a Samsung Galaxy Tab SM-T700 was used for testing purpose. The users were given tasks to locate services and facilities around them with their choice of app and later perform the same task with the AR UJI app. As a final request, the participants were asked to fill in the questionnaires for evaluation to measure the performance, usability, controllability, comfortability, clarity in information, helpfulness and satisfaction in using the application.

The questionnaires were developed using the 5 point Likert scale, for better understandability and the results can be easily quantifiable. The 5 point Likert scales was preferred as possible over a binary choice (Yes/No) or a 3 point Likert scale, as it provides only direction rather than providing level of perception. Also the 10 point Likert scale was not favorable for participants, creating difficulties in choosing the options giving insignificant results (Dillman, Smyth and Christian, 2014). The questionnaires are segmented into 3 phases as: (i) General statistics, including general questions related to the user, (ii) Knowledge in AR, to measure user’s knowledge in AR technologies and the use of existing AR apps, and (iii) ARUJI app, questions related to the user’s findings about the app regarding the easiness, difficulties, understanding, controls, information provided, discomforts and helpfulness of the proposed system.

Results

The results were derived from the responses to the questionnaires. Almost all of the participants relied on 2D apps like google maps, apple maps and Maps.me for searching and navigating around, with maximum adhering to Google Maps. It was found that, 95 % (Fig. 4) of the participants never heard of AR apps similar to AR UJI, providing augmented reality solutions for searching places and information. Remaining 5% participants have used Google AR translate for translating languages on boards while searching for places. This portrays that there has been lack of knowledge about such AR apps, related to navigation and tour guide. Fig. 2 (Left) shows the graph of AR applications used by the participants, are mostly related to entertainment and education domain, which can be justified from the graph in Fig. 2 (Left), which shows the reason for using such AR app.

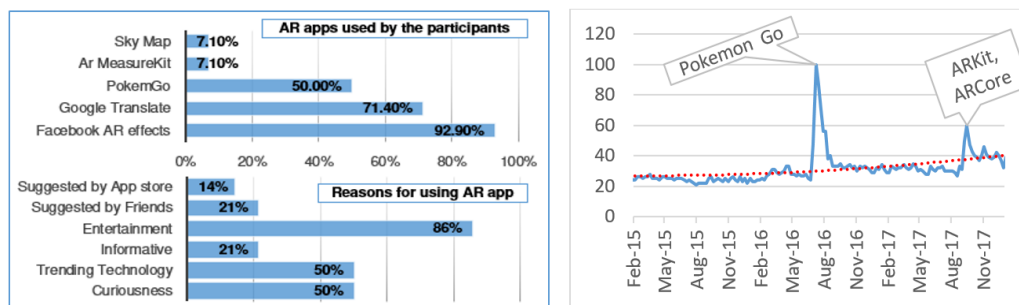


Fig. 2. (Left) AR apps used by participants and reasons for using them, (Right) Google Search Trends of Augmented Reality apps (*Source: Google Trends*).

More than 80% of the participants used AR applications, as it was fun and full of entertainment. Half of them were using it due to curiosity and for being a technology in trend. Least of them, about 17% used AR apps to gain information. It is possible that AR solutions has not yet been well presented in these scenarios in order to see its popularity in such sectors. This facts can be further supported by the graph in Fig. 2 (Right), which shows the search trends in AR applications is in decreasing trend for many years until it hyped drastically after the lunch of Pokemon GO in July 6th 2016, which remained for some months and declined to its previous state. But the interest in AR apps can be seen increasingly progressive and picked up the pace after the release of ARKit for iOS and Google ARCore near the end of 2017. This clearly depicts the reason for non interest in AR apps among users, due to lack of AR developing platforms and its support in mobile devices. The recent development in AR sector with its support in mobile devices has led in the rise of interest in AR apps, but is still limited to specific domains such as entertainment. Thus with the recent launches of ARKit and ARCore, 2018 will be a momentous year for AR technology, becoming a mainstream commercial application.

The effectiveness of the application is measured from the successful completion of both the tasks (Task1 & Task 2) in Map View and AR View was 100%. All the participants were able to complete the task without any problems. The participants found the AR View more effective in finding information and services of nearby surroundings more than the Map View, with some participants commenting AR View to be more fun and astonishing experience in mapping sector.

The participants have valued, more the interface with information in the popups providing better perceptions of the surrounding vicinity compared to that conveyed by Map View.

The efficiency is measured by the time taken to complete the tasks using the Map View and AR View which can be seen in the graph (Fig. 3) below. For Task 1, it can be indubitably said that AR View is more efficient than the Map View. However, Task 2 illustrates few fluctuations where Map View proves more efficient. This is due to the nature of the task and users ability of fast reaction to the question. The efficacy in typing and with the concise keyword might have been the reason behind the efficiency of Map View in some observations. The average time taken by AR View to complete both the task is slightly less than that of the Map View with a difference of around 2 secs. Hence, AR View is slightly efficient than the Map View in locating services around the surrounding area.

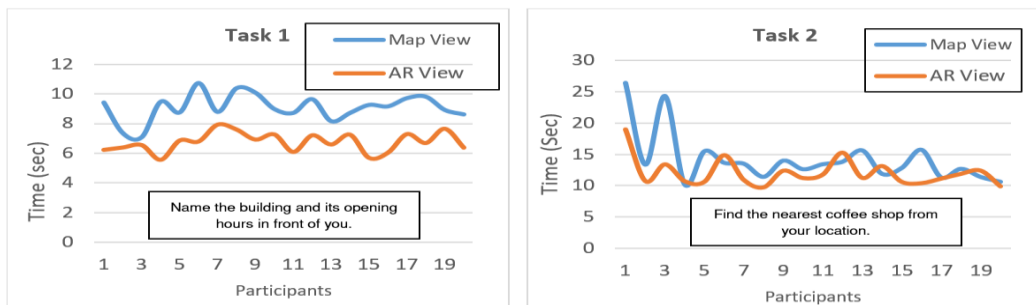


Fig. 3. Time taken to complete the tasks using Map View and AR view.

The satisfaction of the users were evaluated in two phase, indirectly and directly. Firstly, the participants were asked questions related to ease of use, controllability, clarity, and successful maneuver of the application that served as an indirect means of evaluating satisfaction. In Fig. 4 (left), we can see that almost all the participants are somewhat clear about the information displayed in the app, and able to control and successfully get information from the app, with minority of the participants i.e. 20% trying a bit hard in controlling and finding problem in clarity of the displayed information. This is mainly due to fast movement of the mobile and relative slow processing of the mobile, which effects in the oscillations of the popups causing difficulty in controlling the app.

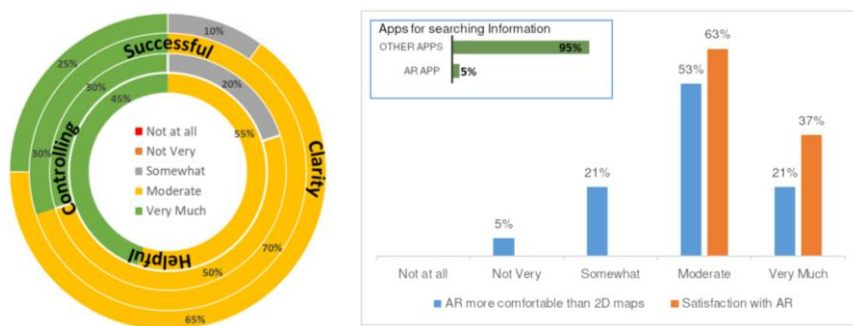


Fig. 4. (Left) Indirect evaluation of Satisfaction, (Right) Comfortability and Satisfaction of using AR compared to other 2D apps

The second evaluation of users satisfaction involved more direct questionnaires related to comfortability and satisfaction in compared to Map View. With the proposed AR application acquiring information and finding place around was lot easier and efficient for which almost every users were satisfied with majority of 63% and remaining 37% being very much satisfied. Furthermore, the bar chart in Fig. 4 shows that 74 % of the students were comfortable using the proposed AR UJI app with no difficulties in controlling the app, with 21% being somewhat comfortable about its controllability, compared to their usual 2D apps. The reason behind is the frequent crashing of the application due to low memory space. Better the technical specification of the smart phone smoother the performance of the application. Students found the app to be more entertaining, informative, and efficient for searching information in the vicinity, with one fourth participants willing to use the app for further searches and three fourth participants to use the app after slight updates and fixes. Every participants were enjoying and perceiving information through the use of the AR app which depicts that there has been lack of awareness about the true potential of AR apps.

DISCUSSION AND CONCLUSION

During the debriefing of the applications, participants expressed their problems faced during finding location and departments inside the university due to language problem and difficulty finding in google maps as they were referred with codes. Many stated that they had ended up being into another department while using 2D map service and almost felt lost during no internet connectivity. With the Augmented Reality application AR UJI, viewers are provided information on top of the real world. They affirmed that the application is far better and quick to know the information of the building with just a popup in front decreasing the search time and eliminating confusion. Also, in times of urgency, the ARUJI app proved to be more efficient than the 2D map, for locating information and services in the surroundings. Majority of the participants were totally satisfied with the applications and affirmed to use the applications with some minor update.

As with any empirical study, there are some limitations entangled with it. Foremost, the results are based on self-report study, as it involved participants to fill in questionnaires regarding their user experience of the ARUJI App. A Qualitative method with detailed interview and observation of the participants could have been more prolific and factual. Secondly, a convenience sampling technique was selected, as it was fast, inexpensive, and easier to recruit participants and proximity to the researcher. Thus subjected to limitations in generalization and inference, resulting to low external validity of the research. Thirdly, the research was conducted among students between 18 to 35 years age group (Millennials age group), as they are familiar with communications, media, and digital technologies.

In Conclusion, we have shown how augmented reality can help us in a smart city context. Thus, some studies related to AR we conducted, which lead us to explore new methods to support and offer better decisions tools for the citizens in a city context. Moreover, we demonstrate that users are open to use new technologies such as augmented reality in order to perform operations that usually were carried out by using a typical mapping mobile app such as Google or Apple Maps, engaging the user the entire time and making less aware of the surroundings. In a nutshell, AR

with smart mobiles has the potential to increase smartness in users, making them more compatible and eligible to live in smart cities.

REFERENCES

- Caudell, T. P. and Mizell, D. W. (1992) Augmented reality: an application of heads-up display technology to manual manufacturing processes, In: *Proceedings of the Twenty-Fifth Hawaii International Conference on System Sciences*, pp. 659–669.
- Chang, K. E., Chang, C. T., Hou, H. T., Sung, Y. T., Chao, H. L. and Lee, C. M. (2014) Development and behavioral pattern analysis of a mobile guide system with augmented reality for painting appreciation instruction in an art museum, *Computers and Education*, 71, pp. 185–197.
- Cheung, C. L., Wedlake, C., Moore, J., Pautler, S. E. and Peters, T. M. (2010) Fused video and ultrasound images for minimally invasive partial nephrectomy: A phantom study, In: *Lecture Notes in Computer Science (including subseries Lecture Notes in Artificial Intelligence and Lecture Notes in Bioinformatics)*, pp. 408–415.
- Dillman, D. A., Smyth, J. D. and Christian, L. M. (2014) *Internet, phone, mail, and mixed mode surveys: The tailored design method, BOOK*.
- Kim, K. H. and Wohn, K. Y. (2011) Effects on productivity and safety of map and augmented reality navigation paradigms, *IEICE Transactions on Information and Systems*, E94–D(5), pp. 1051–1061.
- Kourouthanassis, P. E., Boletsis, C. and Lekakos, G. (2013) Demystifying the design of mobile augmented reality applications, *Multimedia Tools and Applications*, 74(3), pp. 1045–1066.
- Lee, J.-D., Lee, H.-C., Hsieh, C.-H., Wu, C. and Lee, S. (2015) A Projection-based Medical Augmented Reality System, *Proceedings of the 8th International Symposium on Visual Information Communication and Interaction*, (3), pp. 164–165.
- Lee, J. Der, Huang, C. H., Lax, T. Y., Lee, S. T. and Wu, C. T. (2011) A medical augmented-reality system for image-guided surgery using marker-added ICP, *International Journal of Innovative Computing, Information and Control*, 7(11), pp. 6523–6539.
- Shamalina, S. (2017) Virtual and Augmented Reality Applications in Building Industry, In: Rassia, S. T. and Pardalos, P. M. (eds.), *Smart City Networks: Through the Internet of Things*. Springer International Publishing, Cham, pp. 11–24.
- Shang, L. W., Siang, T. G., Zakaria, M. H. Bin and Emran, M. H. (2017) Mobile augmented reality applications for heritage preservation in UNESCO world heritage sites through adopting the UTAUT model, In: *AIP Conference Proceedings*.
- Simpson, D. M. (2001) Virtual Reality and Urban Simulation in Planning: A Literature Review and Topical Bibliography, *CPL bibliography*, 15(3), pp. 359–376.
- Sisodia, A., Riser, A., Bayer, M. and McGuire, J. P. (2006) Advanced Helmet Mounted Display (AHMD) for simulator applications, In: Brown, R. W., Reese, C. E., Marasco, P. L., and Harding, T. H. (eds.), *International Society for Optics and Photonics*, p. 622400.
- Yovcheva, Z., Buhalis, D. and Gatzidis, C. (2013) Engineering Augmented Tourism Experiences, In: *Information and Communication Technologies in Tourism 2013*, pp. 24–35.

Zhao, H., Chen, H., Wang, J. and Zhang, R. (2016) Augmented Reality Game Development and Experience Based on Intelligent Mobile Phone, In.: Springer, Berlin, Heidelberg, pp. 38–47.

TRENDS IN COLLECTION OF TERRAIN INFORMATION IN THE CZECH MILITARY GEOGRAPHICAL SERVICE

Josef RADA

Department of Military Geography and Meteorology, Faculty of Military Technology,
University of Defence in Brno, Kounicova 65, Brno 662 10, Czech Republic

josef.rada@unob.cz

Abstract

A field of geo-data collection has never been studied from this kind of view. Authors own long-time experience in this branch brings a unique overview of the topic defining work constrains and opportunities in geo-information gathering from the territory of the Czech Republic. The army has always been a bearer of modern ideas and a leader in technology development. The study shows that many obstacles are in the way of smooth transformation to a new era. Solving these problems were main goals of the research. To keep up with high standards, military geographical service had to undergo a complex reform process, consisting of a reduction of personnel, upgrade of equipment and technologies and efficiency improve)ment of geographical production. To achieve this objective, forces were joined with the civilian national organization, the Czech geodetic and cadastral bureau. These two organizations can utilize their resources to create a common national vector database, thus, an activity abiding by the conditions of national GeoInfoStrategy. The modern trend of external data and information collection is represented by a current project of topographical survey in military training areas. Both military and civilian vector databases are checked inside of these areas for any change in one single work. This singular approach may unify national databases in the future. The mid-term projects signify the course of action in the upcoming geospatial support. The biggest emphasis is to be put in the preparation of future forms of military vector database and the foundations of next possible way of collecting data by changing the geodetic law itself to meet the requirements of the Czech army. Development of new military education and geospatial web services can also bring promising prospects. Results indicate that the contemporary shape of data collection and products publishing will have the utmost importance in the geospatial branch.

Keywords: military, geographical, support, data, collection, cooperation

INTRODUCTION

There has always been ongoing transformation in the area of technologies, approaches, products, software and personnel in the Czech state administration since the 1990s. The Armed forces of the Czech Republic and its specialized component, geographical service (Geos) are not exceptions in this. Changes that began with a revolutionary transition to digital technologies in the field of mapping and GIS (geographical information system) have never been discontinued. Over time, measures have been taken to balance productivity, accuracy and modern technologies for efficient geographical support of the army. One of the major means of achieving such a goal was to concentrate on a wider cooperation with the civilian sector and the development of

methods of terrain information gathering. Collection of data and information had eventually developed into extensive administrative work on creating and maintenance of contracts with governmental and civilian organizations. Progress has never stopped in any of these organizations, even from abroad. Today, the collaboration is based on exchange of complex databases or on provision of web geographical services. The common trend in the geographical service of ACR (the Army of the Czech Republic) and the state sector is to reconcile databases, reduce their duality and unequivocally set administrators for particular objects of terrain. In the geographical service of ACR, all current data collection procedures, as well as planned future military geographical products, are submitted to that objective. The Office of military geography and hydrometeorology (VGHMÚř), the key production element of Geos ACR, maintains the closest cooperation with Czech geodetic and cadastral office (ČÚZK). External collection of materials and development of production will be the essential elements for specialization in future public service. The aim of this work is to describe the current situation in the field of data collection terrain information in Geos ACR, indicate its possible development and present a proposal for improvement of the most sensitive parts.

MATERIALS AND METHODS

In order to determine the situation and level of progress in the field of data collection, it was necessary to study both latest historical facts and contemporary course of action. The author, as a member of department of data collection and editorials office, had a direct access to information, participated in countless interdepartmental meetings and conducted comparisons and analyses of available data from the Czech territory. The original intent was to extend this study of analysis of data from foreign territory; nonetheless, the results have exceedingly exceeded its former pre-planned extent, thus resulting in reducing this paper only in analysis of national data sources. A comparison of data sources abroad, their development and critical evaluation of existing methods using the international standards (NATO, OGC, ISO...) will be main core of second analytic report. The main goal of this study was to recapitulate 12 year work and collection of facts about this domain. The overall picture was completed with presentation of facts from available thematic articles and publications. The main methods used in the research were descriptive method, with its collection, arranging and classification of data and figures and their text evaluation. The other was comparative method, with ascertaining of differences between similar and researched objects, acquiring a notion of their geospatial relations and different characteristics. Information in databases and maps was compared in cartometric analysis with a purpose of processing of results with computer technology and save data in databases (Lauermann, Rybanský, 2002). Almost every data acquisition rested on terrain research, which means evaluation of acquired data. The main projects in recent years were “Analytic report of road data bank Ostrava” (J.Rada, M. Vejvoda 2008), project of data update of military training areas (VGHMÚř, 2017) and project of semi-automated data gathering form forest database ÚHÚL (VGHMÚř, 2017). All these methods and projects were comprised when creating this study resulting in unique overview in this field.

RESULTS

Each part of the research was classified into following chapters. This study covers main parts of the data collection branch, from analyses of recent historical phases and description of current situation to proposal of form of future path in data gathering.

Current situation in the domain of terrain information gathering

Nowadays, many approaches are encountered in the area of terrain information gathering. The predominant way is in direct (own) data collection. Areal or partial aerial imagery capturing is still the main source of information. Digital models of terrain are being improved by laser scanning. Data can be also gathered by direct taking of photos in the terrain or external collection of photos for a register of vertical obstacles. Access to all historical aerial imagery will be granted after scanning the whole archive in Dobruška. Geodetic measurement can be considered as one of the direct inputs of information, for example with attributes measured at airports or on vertical obstacles. Indirect collection of data rises in importance day by day. It is represented by optimizing resources by reduction of own activities only to objects of specific interest, e.g. Geos ACR would undertake only military objects, the road and motorway directorate only road network etc. Consequently, a focused collection will be in motion by requesting data from its original creators or administrators, e.g. other military units (military fords, buildings etc.), state or private companies (soil, attributes of river network, bridges, pipelines) or from partners abroad, adjacent states or NATO (North Atlantic Treaty Organization) (RETM – raster equivalents of topographic maps, vector datasets, aerial imagery etc.). This variant is already under way and will continue on being considerably endorsed, e.g. within the scope of GeoInfoStrategy. (Kubátová, 2015) On that account, various stances are taken into account to meet with the standards of that strategy.

Variability of information is a key part in the strategy. Paper maps and analogue materials (e.g. city plans) are still reliable sources, nonetheless, provided data from external companies have the biggest significance. Prospective problems with obsolescence of data can be sorted out by provision of web geographical services (wms, wfs etc.) based on up-to-date data sources via Internet. Such an approach cannot be utilised in VGHMÚř yet, due to technical limitations. Concentration on a particular area within gathering of materials is essential; either it's the territory of the Czech Republic or foreign territory. In view of the fact that military geographical products are sizeably oriented on adjacent foreign territory, gathering of information has to be adjusted to it. It is very demanding to collect relevant data and information about foreign territory. Since soldiers are not allowed to cross borders uninvited just to do topo survey, it is necessary to rely on external sources, albeit the data are often untrustworthy and obsolete. The last question in data collection resides in specification of a method of its utilization. Either information is inserted (edited) directly into vector database (applied in military database digital terrain model 1: 25 000 DTM 25) or the only information given is the identification number of an object and the rest of the attributes are obtainable in the original dataset. The Id approach facilitates updating. On the other hand, fulfilling of attributes enables faster comprehensive work with data without the necessity of studying and searching for original datasets. This military way of complex attributes

editing is currently untenable, therefore a compromise is being contemplated to partially make use of Ids and partially edit attributes. Basically, miscellaneous sources are capitalized, even more during last decade.

The latest updates of DTM 25 were significantly focused on relying on external data. So-called “second update” of DTM 25 was commenced in 2005. Most of the elements of the vector database were updated. VGHMÚř operated on the program ArcInfo with its own programmed basis. (AČR, 2008) No larger files were sendable via Internet because of the limited characteristics of the network itself. Exchange of data was solved by preparing a contract. Later, some companies used a possibility to share publicly most of their own data directly on the Internet, e.g. Povodí Labe A.S. Military data were provided contractually to civilian companies. Most of these were power industry companies (electric and gas distribution e.g. ČEZ) and others were Moravian oil mines, publishing company SHOCart and many more. Since 2005, military geographical products have limited distribution to authorities and companies included in national defence planning and crisis management. Regular private or partially state-owned companies were denied access to military geographical data. Reciprocally, their data were not at disposal for Geos ACR since then. According to the geodetic law, all private companies have to provide their geographical data to state institutions on demand. Even so, much of the information did not have to be shared. The reason is stipulated in the law: “provide results of geodetic activities”. So data provided were hollow geometric lines without any attributes, e.g. level of voltage. Military geographical production also faces limitations in two network systems in ACR, where all major systems are separated from the Internet, thus preventing direct use of external web services. Dependence on external data came with the new update of DTM 25 and the main reason is capacity restrictions.

The limitation of capacities has manifested itself over time and affected database updates. This and a request for updates of DTM 25 more often led to 2.5th interim update. The aim was to identify all the major objects of terrain and update them with the accelerated method. This was accomplished by softening the selective criteria and searching for changes just by comparing civilian and military databases, DTM 25 and ZABAGED (basic basis of geographical data) and eventually aerial imagery. The update took less than 2 years and greatly exceeded all expectations. However, some of the types of objects were not updated. A compensation for this depth is among other matters a part of current third update of DTM 25. It is primarily concerned with transitioning to a new software platform, ArcGIS, and at the same time returning to principles of the second update. Although long-winded now, this process, after its completion, may make future updates more efficient, thus, it might substitute the loss of work capacities.

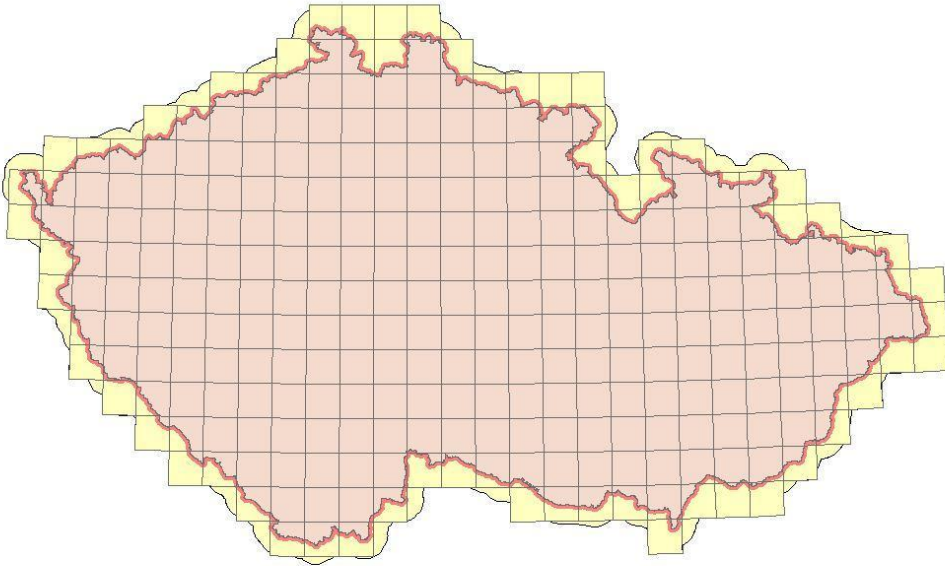


Fig. 1. Buffer zone exceeding standard coverage of topographic maps 1:25 000 highlights the area of extra vector database coverage, which is at least 10 km far from the national border.

Foreign data grows in importance. In connection with a complete update of the “vector buffer zone”, more time was invested into study of data sources abroad. Complete editing of data is very demanding on sources of information and their reliability. Foreign topographic maps and vector datasets of adjacent states or NATO were chosen as fundamental sources. The lack of precise and up-to-date data led to use of a publicly accessible and editable data source, OpenStreetMap. Utilization of open sources was officially allowed in NATO; nevertheless, these are to be taken only as support data, as only designated official NATO geographical products can be used. There are other international projects among recent foreign data collection on which Geos ACR participate. One can mention non-contact collecting of data, capturing satellite imagery or laser scanning. VGHMÚř participate in the creation and update of MGCP (Multinational Geospatial Co-production Program), global vector database administered by NATO nations and some other non-NATO nations. (Marša, 2013) Another useful project, TREx (TanDEM-X High Resolution Elevation Data Exchange Program) global elevation terrain model (Bělka, 2015) (DLR, 2017), is established on a basis of MGCP. Definitional library of images of objects in the world RWIL (Real World Image Library) (Tichý, 2017) can be also partially considered as data gathering. In summary, international projects and data increasingly complement the local production.

Collaboration of VGHMÚř and ZÚ

In VGHMÚř, the cooperation with civilian subjects is still active; however, contemporary strategic partner in many production aspects is ČÚZK. (Marša, 2013) Cooperation on a database level was established by writing a contract in 2008. The closer cooperation has arisen gradually and a beginning of dealings about coaction in terms of databases update is dated just from 2014.

ČÚZK has its own activity in data gathering. For this reason, other form of cooperation was settled. Not only in mutual provision of data, but as well support in sharing of information about third subjects. This way, ČÚZK obtained from VGHMÚř a metadata file about used external data, including all necessary attributes (e.g. contact telephone numbers, accuracy of data etc.). ČÚZK prepares some of the future data exchange contracts with regards to a possible use in Geos ACR. A favourable strategy could be a common attendance during negotiations with external civilian subjects, so that the demands would comply with the requirements of both institutions.

The development of ZABAGED in recent years pointed out a possible way, how to make more efficient and simplify update of own vector database. Working capacity and efficiency are key elements when dealing with this problem. ZABAGED is updated in more detailed way (the output is basic map 1:10 000, the output of DTM 25 is topographic map 1: 25 000) and other features are being added gradually. Some of these features were not dealt globally, for instance state institutions. Forest roads are one of the sensitive elements, since there are no capacities to their update across the national territory, neither in the military, nor in the civilian sector. Anyway, this is one of the top priorities for future direct connectivity of DTM 25 and ZABAGED, maintaining easily trends in mapping. Already existing joint projects could serve as an example. The most important projects are creating of aerial imagery of CR, processing of elevation digital model of relief (DMR), scanning of aerial imagery archive or laser scanning, which is after its complete realization in the phase of cyclical updates. The issue of collaboration can be raised not only by these projects, but as well by shifting it to the level of co-update of respective databases.

The basic active project is processing of aerial imagery into the form of orthophoto and joining each picture to create a seamless mosaic. Current period is set to 2 years cycle of update; a resolution of each pixel is 20 cm. VGHMÚř undertakes 1/3 of the Czech territory. Another important common activity is update and processing of DMR, which is further processed to create the fifth generation elevation model and the first generation model of surface. Digitalization of aerial imagery archive (placed in Dobruška) is a long-term project as well. (Břoušek, 2013) This project has its goal in transferring and preserving all historical imageries to a digital form in resolution 15 µm. At the end of 2017, 205 000 out of 750 00 photos were already scanned. The project runs for 6 years now and a complete database of historical aerial imageries (since 1936) will be at disposal after its finishing. The connection between VGHMÚř and ČÚZK, already steadily evolving, might attract more interesting publicly useful projects.

Project of detailed data update of military training areas

New ways of data update occur more often in Geos ACR lately. An in-depth topo survey and a data collection took place in the military training area Hradiště during summer 2017. It was the first survey of that kind, trial survey to test both the military and the civilian vector database with an objective of verifying and update objects in each database. ČÚZK has limited working options in military areas, thus the request was raised to simultaneously check specific layers of DTM 25 and ZABAGED. The civilian database, richer on objects and particularly a density of roads inside Hradiště led to an unprecedented situation in the field of topo survey.

A new type of topo survey was under way for four weeks in total in June and September 2017. The goal was to update DTM 25 in a maximum detail for the upcoming production of the military training area Hradiště map and at the same time verify objects of ZABAGED in the territory. To make the project viable, the most important thing was to prepare everything properly. Arrange a map project, datasets, instructions for every survey group, a plan for everyday departure of vehicles etc. The program was reconciled with representatives of the military training area mainly to avoid areas in time of shooting exercises. The territory was divided to 3x3 km squares by reason of pre-planned weapons training. Every single survey group was assigned particular area per day with corresponding features to scrutinize. Intensive exercises, along with the hilly terrain, were the biggest obstructions for a non-problematic data collection.

Beside a mountainous terrain and limitations in certain areas due to shooting exercises, other problems have occurred. The cell phone signal was one of them. Insufficient signal strength was reoccurring too often, so that coordinating difficulties could arise, mainly on borders between survey sectors. GPS had its signal coverage troubles as well, mainly in areas with dense foliage and during worsened climatic conditions. Used devices, GeoExplorer 2005 and 2008, had worked slowly when capturing data time to time. Cars equipped with off-road tyres are more useful and agile than regular ones in a difficult terrain and four wheels drive itself may not be enough. Any kind of precipitation significantly reduced passability of every cart track and forest track, mainly on slopes. The other substantial obstacle turned to be grass. An overgrown vegetation this time of the year caused problems when verifying existence of a track or hidden objects. Sometimes, not checkable tracks in June were identifiable in September because they were cleared since then.

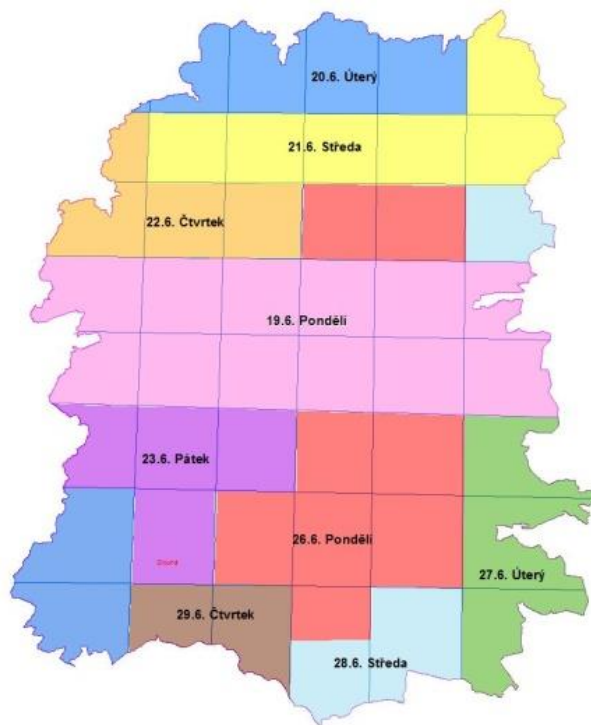


Fig. 2. A division of the military training area Hradiště to zones for the best possible assignment of tasks in more days and for multiple teams.

feature	quantity	verified/not	existing	not existing
forest/cart track	953	953 / 0	363	590
hard surface road	38	38 / 0	37	1
main road non-class	68	68 / 0	65	3
state road 3 rd class	1	1 / 0	1	0
stream	1	1 / 0	0	1
fence	2	2 / 0	2	0
power line	2	2 / 0	1	1
rock, bolder	81	19 / 62	13	6
total	1147	1085 / 62	483	602
%		94 % / 6 %	42,1 %	52,5 %

Fig. 3. A table of statistics of line objects verified during a topo survey in the military training area Hradiště.

Sizeably inaccurate or incorrect objects in forests were detected during objects verification of DTM 25 and ZABAGED. A larger number of tracks contained in the databases are passable with difficulties and sometimes they even do not exist. Time of the year was taken into account during an evaluation of communications. Many new objects were found, most of them were tracks and objects in some relation to them in closer vicinity. A performance of next topo surveys would be the most suitable in a month of May. This pilot project outlined the path of possible future collaboration of VGHMŮř and ČÚZK. Three remaining military training areas (Boletice, Březina and Libavá) will be successively updated from 2018 to 2020 on a ground plan of this project.

Future of data collection and production projects

A mid-term horizon will bring couple of essential adjustments of a production technology and data processing. One of the key projects today is a creation of a new form of a military vector database on the basis of ZABAGED. Other area of concern is establishing a backing in the law for easier collecting of data. A new form of web service is going to be created. It is a complex overview service which encompasses all own historical data, maps and databases of Geos ACR. Next generation of students – officers will have to be prepared for a closer cooperation with civilian sector for ensuring the bright future of Geos ACR in a personnel field.

DTM 25 on a basis of ZABAGED

An ever-increasing pressure on a harmonization of the national vector database has led to a commencing of a project of the military database on the basis of ZABAGED. To accomplish that, at least partially altered civilian database usable in ACR and NATO environments will be required. Furthermore, it is a determination of respective scope, e.g. similar as the collaboration on the aerial imagery capturing. A responsibility based on a territorial division may be one of the ways. The other approach could be in update only specific layers of interest, e.g. military objects and property used only for a future form of the military vector database. A strict orientation abroad is the third option. ZABAGED deals only with the Czech territory. On the other hand, military databases and topographic maps include a foreign territory at least 10 km far from the border.

This way, DTM 25's foreign data might be attached to ZABAGED to create a common database. (Marša, 2014)

A combination of all three aspects seems to be the most convenient option. Military topographs may contribute a lot with their experience to enhance future national vector database. They also have long-time experience in the field of update of foreign territory, partially thanks to cooperation in NATO. They possess, unlike civilian counterparts, almost unlimited access, possibility of movement, huge authority and knowledge of local conditions in the military training areas. The main intent of Geos ACR is to create a central register of all military objects, estates, training areas and other real estate. This database might be justified by keeping records of redundant figures and features, not only geographical character. ZABAGED could then extract all required information about military objects needed for national database.

Presently, intensive talks and a preparation for a transition to a new form of a vector database are already under way. A final date and the database's form have not been fixed yet. Third update of DTM 25 is going on at the moment with estimate of its finishing in 2022. The question is what is going to happen after that year. Whether there still is the same format of military database update or a new platform will be finally and completely endorsed. Whichever the eventual shape of national or military database will be, the intensive interdepartmental cooperation will continue on its flourishing.

Obligatory provision of data owned by private companies

A contemplated manner, how to replace a recent loss of a regular free data acquisition is to change the law. A fluent flow of external data into Geos ACR was interrupted by cutting civilian companies of access to military data and maps. Despite these restrictions, the geodetic law states a possibility of obtaining data:

§ 6 providing of results of geodetic activities: geodetic and cadastral authorities are obliged to provide on request of state administration documented results from their documents and information databases required for their activity, unless violating protection of rights according to special laws. (Government of the Czech Republic, 1994)

Thence, all results of geodetic activities, including administration of geographical information services, must be provided for the state administration. A limitation resides in a fact, that not all data can be considered as gathered by geodetic activities and a protection of rights can be an enormous barrier as well. Not mentioning possible financial compensations when forcing companies of issue expensive data. The information about voltage of power lines can serve as an example. And there is more information of that kind, e.g. a level of production, pressure of pipe lines or data of object owners. Though, these are vital information for the military database, which is more or less oriented on direct filling in of attributes of objects into geodatabase, not just by editing identification numbers of features. A possible solution would be in adjusting a wording of the geodetic law to include common statement about obligation of provision of geographical and other information systems to the Ministry of defence for a purpose of a defence planning.

Energy regulation office (ERÚ) has followed this path of a central collection of complex information in the branch of power industry. For completeness, the definition of activity and

province of ERÚ is quoted: One of the main scopes of activity of ERÚ is a supervision of energetics sector market. (ERÚ, 2017) According to (Government of the Czech Republic, 2000), licences are granted for a transfer of electricity or gas, a distribution of electricity or gas, storage of gas, a distribution of heat energy and activities as operator on the market. Within a licence granting, companies in power industry are obliged to regularly provide information and data about their companies, including GIS data to ERÚ. It collects all data by mutual contracts with individual subjects; nevertheless, none of these contracts allow access to obtained data for third parties. Since ERÚ stores every data of energetics sector, it would be useful to utilize it for the needs of Geos ACR. Data could be obtainable by mentioned adjusted geodetic law based on a limited (or restricted) distribution or an indirect update of databases (not copying of whole objects). Secret or other sensitive information would be used only in products with a higher classification level, e.g. level restricted. With this, a complete coverage of external data from all imaginable fields of activity of private, national or even international companies would be accessible.

Development of web geographical services

Today's web map services are considered as a completely ordinary thing so high demands are placed on them, both user and technical demands. A web application, *mapy.acr* is at disposal in ACR already for a long time. This application guarantees coverage of all military geographical data online, including making available a group of modules. Already existing modules or modules in the development are:

- Dělo (Cannon) – creating of local coordination report network for artillery fire;
- Ohrožené prostory (Endangered areas) – production of designs of endangered areas of gunfire under the regulation Děl-1-20 Ohrožené prostory;
- Zemětřesení (Earthquake) – display of seismic phenomena evaluated by the seismic station Polom;
- Geodetické body (Geodetic points) – display and search for geodetic points;
- Meteorological information – display and animation of meteorological info;
- KVV – administration of regional military commands;
- Hlášení změn (Report of changes) – report of changes in terrain and errors in geographical products;
- GEMIS – module in the development, register of all available up-to-date national and international or historical geographical products. (Kopecký, Stránský, 2013)

Key modules for data collection are “Endangered areas” and “Report of changes”. “Endangered areas” module is based on editing of information about range of fire of various guns and possibly about an extent of endangered territory in the military training areas. An extension of this module is planned to include all the sorts of thematic information, not just about endangered areas. Military personnel of a respective military training area will have a possibility to edit changes

inside the area directly via this service and afterwards these changes will be immediately updated in military databases and maps. This makes the update and data collection process much faster by partially transferring responsibility of some of the features to local admins.

The other helpful module is “Report of changes”. It enables users to report any type of update directly in a web map service. This module is considerably dependent on an activity and willingness of users to report errors; nonetheless, this option itself is very valuable for external information gathering. A great information asset will have future module “GEMIS”, which will allow a display of all available geo-related military products, mostly archival maps, including their metadata. Beside this military register of products, other register oriented only on civilian data and web services could exist. The most challenging part would be keeping this record up-to-date since in the civilian sector the changes are continuous. The complex central data register would sizeably facilitate a work on an update of geographical products and a data collect as well, thus, making web services extraordinary.

Prospects of military education in the field of data collection

The environment of ever changing needs of the army resulted in a fundamental change of requirements for the military research and professional activity of Geos ACR. The needs of a direct geographical support were significantly reduced in terms of performed tasks. This was induced by a reorganization of ACR, mainly by changes of certain weapon systems or their cancellation and also by external changes when using different technology for geodetical tasks, especially GNSS (Global Navigation Satellite System). This reflected in a change of university studies of new members of Geos ACR. Hourly dotation was reduced, mainly in geodetic related subjects, whilst dotation for cartography remained the same. At the same time, composition of other subjects and hours has substationally changed. Strengthening of a field of geoinformatics, a creation of geodatabases and a processing of analyses of geographical data was made. In this area of expertise, the practical part of the education was devoted to analyses of data sources and their utilisation, geospatial analyses and modelling of assigned tasks, a visualisation and a creation of map outputs. (Hubáček, Čapek, 2015) In spite of many changes in the military geography branch which had an impact on a profile and knowledges of students, the emphasis on the practical work has not changed. (Hubáček, Kovařík, 2015)

A requirement of change of the structure of teaching and more emphasized technical education of future officers came with a new university law. A study under new conditions will be commenced in September 2019. In connection with trends of streamlining of GIS administration in the state sector, implementation of a deeper teaching of external data sources used in the state administration and in civilian private companies will be advantageous. Due to a speeding up of a process of military units geographical support and demand of up-to-date data and services, at best in real time, a complete shortening of a products and data preparation will be required. Knowledge and utilisation of external databases will be a future priority for Geos ACR. This will furthermore transform its research and professional activity.

DISCUSSION

The results of this long-term project unequivocally set the priorities for contemporary and future development. Attempts for individual collection of geoinformation, data analyses and databases processing turned to be a dead end. Hardware and software environment has significantly changed during the research process, thus, considerably influenced overall result. Definite transition from local datasets to public web services and keeping up with this progress within the domain was the biggest challenge. The goals set by the initial intent were accomplished. In spite of number of limitations resulting particularly from capacity and security restrictions, clear target for future exploration has been set. Such results are especially bidirectionally available free geoinformation services and more extensive cooperation and sharing of projects, data and capacity means. The most significant result of this report is defining upcoming needs for services and data, for example military training areas vector database, common military and civilian national vector database or the web service containing all the necessary information about geo-related data sources in the Czech Republic.

CONCLUSION

The current trend in a collection and evaluation of external data resides in the collaboration with civilian sector in the unified attitude to this topic. Many common projects are under way. The cooperation deepens and evolves on an interdepartmental and international level and prepares a ground for more efficient approach in the field of geo-informatics. Future intents further outline the importance of broader cooperation in this area. Collection of data is needed to be comprehended in its whole range and complexity. It is not only about terrain survey, but also about gaining experience and participation on national and international projects. The main intent of this analysis is analysing the most important projects of Geos ACR which do have or might have a direct impact on a collection of external data and information and on analyses of these data and their subsequent processing. It will be necessary to focus all endeavours to this field for securing all existing and preparing products and over time this will have more significant role in creating of geographical products.

REFERENCES

200/1994 Sb., (1994) geodetic law, Government of the Czech Republic, Prague

458/2000 Sb. (2000) energetic law, Government of the Czech Republic, Prague

Army of the Czech Republic (2008) History of the Geographic Service of ACR: 1918-2008: Ministry of defence of the Czech Republic – Agency of military information and services, Praha.

BĚLKA, Luboš (2015) TREx – a New Multinational Project of the Elevation Data Production, *Vojenský geografický obzor*, 58/2, pp. 9–11.

BŘOUŠEK, Luděk (2013) Ten years of the Military Geographic and Hydrometeorologic Office, *Vojenský geografický obzor*, 56/2, p. 23–49.

DLR - TREx: http://www.dlr.de/dlr/en/desktopdefault.aspx/tabid-10081/151_read-19509/#/gallery/24516 (cit. 2017-12-03).

- ERÚ.cz, Province of ERÚ. <http://www.eru.cz/cs/o-uradu> (*cit. 2017-11-20*).
- HUBÁČEK, Martin; ČAPEK, Jaromír (2015) Practical Lessons as a Part of the University Education of the Military Geographers, *Vojenský geografický obzor*, 58/1, pp. 30–36.
- HUBÁČEK, Martin; KOVAŘÍK, Vladimír (2015) 23rd Central European Conference Of Central Europe Area in View of Current Geography, Brno, Czech Republic, 08-09 October, Central Europe area in view of current geography, University of defence, Brno pp.160-167.
- KOPECKÝ, R; STRÁNSKÝ J. (2013) Application „Mapy AČR“, *Vojenský geografický obzor*, 56/ 2, pp. 13–15.
- KUBÁTOVÁ, E. (2015) First step on the way of efficient utilisation of geospatial information throughout society, *ArcRevue*, 24/1, pp. 3–6.
- LAUERMANN, L.; RYBANSKÝ, M. (2002) *Military geography*, Praha: AVIS, p.12-15.
- MARŠA, J. (2014) Long term objectives of geographical support of the Ministry of defense resort and their realisation, *ArcRevue*, no. 4, pp. 4–7.
- MARŠA, J. (2013) Prospect of geographical support of the Ministry of defence resort for the period 2014 – 2018, *Vojenské rozhledy*, 54, no. 4, pp. 105–112.
- TICHÝ, B. (2017) Real World Image Library, *Vojenský geografický obzor*, 60, no. 1, pp.19–21.

THE SPECIFICS OF ACQUIRING EXPERTS OF GEOGRAPHIC AND METEOROLOGICAL SPECIALIZATIONS IN THE CZECH ARMY

Jaromir, CAPEK¹; Vaclav, TALHOFR²

¹Department of Military Geography and meteorology, Faculty of Military Technoloies, University of Defence in Brno, Kounicova 65, 66210, Brno, Czech Republic

jaromir.capek@unob.cz

²Department of Military Geography and meteorology, Faculty of Military Technoloies, University of Defence in Brno, Kounicova 65, 66210, Brno, Czech Republic

vaclav.talhofer@unob.cz

Abstract

The paper deals with the specific requirements for education for members of the Geographic and Hydrometeorological Service of the Czech Armed Forces. It describes the possibilities of acquiring experts from both civilian and military schools and the advantages and disadvantages of both options. As a solution to the problem, it provides the process of creating an "ideal" study program based on the analysis of employers' requirements. This is possible since the Armed Forces of the Czech Republic, specifically the Geographic and Hydrometeorological Service, are the only employers of graduated students. For this reason, the study programs can be "tailor made" with all the conditions for successful accreditation.

Keywords: study program, geographer, meteorologist, military expert, military geography and meteorology

INTRODUCTION

Military geographers and meteorologists have always been significant part of the military expertise, without their services (maps, weather forecasts etc.) we cannot imagine the functioning of the army.

In the history of war, there are many examples where the knowledge of the terrain and its proper use helped to achieve victory in the battles. One of the best-known examples is the Battle of Thermopylae (480 BC). The military alliance of the Greek city states managed to choose a narrow gulf for the battle where, despite the superior numbers of the Persian army, they had successfully defended themselves against the Persians. An example from the territory of the Czech Republic is the Battle of Sudoměřice (1420), where Jan Žižka used the terrain shapes to build on-site defence, which suited him well. In the Battle of Austerlitz (1805), in addition to his great tactical thinking, Napoleon used terrain and weather when he masked the movements of some of his troops (Hubacek 2016) by morning mist and terrain. Many other examples of land use in operations can be found in the literature about military geography (for example Collins 1998, Palka 2005). Despite the fact that examples of the history of using meteorological knowledge for military operations is not so common, we can find in the recent history that Jet Streams were used in the Second World War to accelerate aircraft (Riehl, H., M. A. Alaka, C. L. Jordan, and R. Renard, 1954).

Using the key characteristics of terrain to gain advantages over the opponent was in these examples rather a part of the commanders' genius mind and their understanding of the role of the terrain and the atmosphere in the combat activities, than their education in the fields of military geography and meteorology.

In the context of the Industrial Revolution during the 18th and 19th centuries and the connection with a modernization of weapons and the creation of larger armies, the first military institutions dealing with geography, mapping and the influence of terrain on military action have begun to emerge. These included, for example, the Military Survey founded in England in 1791, the Instituto Geographical Military, founded in Italy in 1818, the Militär-Geographisches Institut in Vienna, founded in 1839, the Géographique de l'Armée, founded in France in 1887, or the Instituto Geográfico Estadístico founded in Spain in 1870 (Dusatko, 2005).

After the establishment of Czechoslovakia in 1918, institutions of this type were established also in our country. Military Geographical Institute was established in Prague in 1919, where, besides the cartographic production and other development activities, military personnel were trained too (ARMY OF THE CZECH REPUBLIC 2008).

GEOGRAPHERS AND METEOROLOGISTS IN THE ARMY AND THEIR TASKS

Currently, coordinators and implementers of geographic and hydrometeorological support in the Ministry of Defence (MOD) of the Czech Republic are Geographic Service of the Czech Armed Forces (GeoSI) and Hydrometeorological Service of the Czech Armed Forces (HMSI). Both services deliver majority of their tasks within geospatial and hydrometeorological support using their own resources.

The basic long-term objectives of geospatial and hydrometeorological support in the Czech Armed Forces are according to Marša (2013) the following:

- Geospatial support
- Hydrometeorological support
- Printing service support
- Global Navigation Satellite Systems (GNSS) domain support
- Performance of State administration in the field of surveying and providing air meteorological services

These objectives can be broken down into the individual tasks that are in particular:

- processing and publishing a state mapping work destined particularly for the needs of state defence
- the creation and update of territorial information systems
- management and definition of the geodesic bases of the Czech Republic for the clear spatial assignment of geospatial information at the place and time with the required precision
- systematic data collection, evaluation and processing of information materials from the territory of the Czech Republic, as well as from areas of interest outside this territory
- direct geospatial support of MOD and units of Armed Forces

- providing distribution of geographic products
- guidance on GNSS
- processing the printing and reprographic requirements

Military geographers and meteorologists work in the Armed Forces of the Czech Republic in the different places and at the different levels. Most of them work in the Military Geographic and Hydrometeorology Office, which is dislocated in different places in the Czech Republic where military geographers and meteorologists work. Many geographers operate at strategic, operational and tactical command levels. Geographic and meteorological specialists are present also in specialized units (engineer, chemical, artillery ...) (TOPO 1-1, 2012, ZPRAV 1-2, 2016).

The system of personnel placement and creation of systematized positions, in line with the Law on Professional Soldiers (Law No 221/1999), foresees that newly graduated personnel will be working in basic positions for 2-3 years. However, from the beginning, they must be able to perform relatively independently the tasks described in the following text. The basic functions can be divided into the following four groups: surveyor, geoinformatic analyst, geoinformatic mapmaker, and forecaster. These can be characterized by the following main activities:

Surveyor

- Terrestrial and GNSS measurements
- Detailed geodetic mapping
- Coordinate transformation

Geoinformatic Analyst

- Network analysis
- Topological analysis
- Elevation analysis

Geoinformatic Mapmaker

- Data collection and editing
- Data storage management
- Map production

Forecaster

- Analysis of measured meteorological quantities
- Creating short-term forecasts
- Creating alerts for dangerous meteorological phenomena

HOW DO GEO/METEO EXPERTS COME TO THE ARMY?

From the previous enumeration of the main professional activities of specialists of military geographers it is obvious that it is necessary to obtain higher education in the given fields complemented by comparatively complex military education. However, there are two ways how a specialist can join the Geographic Service of the Czech Armed Forces or Hydrometeorological Service of the Czech Armed Forces:

- After graduating from a civilian college he or she is recruited to a specific military post
- He or she holds a university degree at a military college, i.e. the University of Defence in Brno

In the following text there are described pros and cons of both ways.

Civil studies

Civil universities offer many study branches, after which their graduates can be hired at GEOSI or HMSI. These fields can be divided into four areas:

- Geodesy and Cartography (for GEOSI)
- Geoinformatics (for GEOSI)
- Geography and Climatology (for GEOSI and HMSI)
- Meteorology (for HMSI)

The great advantage of civil studies is the relatively narrow focus of study and therefore studying the subject in detail. A graduate of the field of geodesy and cartography is directly ready to take on the basic function - surveyor. A graduate of the Faculty of Mathematics and Physics of the Charles University with a focus on atmospheric physics is prepared for the function of the synoptic.

The problem is that a civilian graduate must go through the recruitment process, which means fulfilling both health and physical tests. Then they must complete basic training, officer training and a specialized course for geographers and meteorologists. This means that the graduated person must spend about 1 year on the course before starting the work. During this period, he or she does not work in his or her expertise and he or she might lose some skills.

Another problem is that according to the military career requirements each military must, after serving a certain number of years, should be promoted which requires knowledge also from other areas, or military knowledge that may be inadequate for this group of experts.

Military studies

Preparation of military geographers and meteorologists has been for many years the domain of the University of Defence in Brno (UoD), or of its predecessor, the Military Academy, where the both professions were taught from the very beginning in 1951 (Hubacek & Kovarik, 2016).

Currently, meteorology and geography are studied in the joint study module of Military Geography and Meteorology as part of the field of study at Military Technology. Since the UoD is a state university which prepares graduated students for the MOD resort, it is possible to adapt the study programs to the current needs of the MOD and its departments, without suppressing the university level of study.

The graduate profile of the study is designed to meet with the requirements for geography and meteorology targeting competencies defined by GEOSI and HMSI, while at the same time meeting the general requirements for tertiary education in geodesy, cartography, geoinformatics and meteorology. In the following text there are commented the most important requirements.

The graduate knows:

- detailed geodetic reference systems and state map works binding on the territory of the Czech Republic, their parameters, principles of use, development and history
- detailed knowledge about general circulation of the atmosphere, distribution and circulation of water on Earth
- detailed information about satellite navigation systems, their technical parameters and the possibilities for their use for geodetic activities and navigation
- principles of the Earth's atmosphere dynamics, mathematical description of the field of flow and its time-space changes
- technology of creation of topographic, geographical and thematic maps, spatial databases creation technology, methods of their updating
- principles and methods of using digital data for analysis and modelling
- the professional knowledge of a person with a tertiary education degree in a master study program who is professionally qualified to surveying
- the professional knowledge of a graduate of a master study program of the meteorological direction that meets the professional requirements for the qualification requirements of the meteorological staff resulting from the Czech Republic membership in the World Meteorological Organization (WMO)
- expert knowledge of a person with a university degree in a master's degree study course aviation meteorologist - synoptic

The graduate is able:

- to manage and independently perform surveying activities in the needs of state defence
- to manage and independently provide aeronautical meteorological services in military aviation
- to manage and independently perform activities in the management of information systems in surveying designed for the needs of state defence
- to operate air meteorological facilities used in the provision of air meteorological services and perform their routine maintenance and operational metrological activities
- to manage the use and autonomous use of satellite navigation systems for the performance of surveying and navigation to manage the use and self-use of satellite navigation systems for the performance of surveying and navigation
- to perform geospatial and hydrometeorological support tasks in the field conditions
- to process military-geographic evaluations, aids, descriptions, and information at the areas of interest for all levels of command
- to conduct flight meteorological preparations for flight crews and air traffic control authorities
- to perform practically synoptic analyses of meteorological elements and phenomena
- to perform basic geospatial analyses, present geospatial data and analytical results
- to create a topographic, geographic and thematic map from available information.

It follows from the text above that the ideal solution is the creation of a tailor-made study program (module) - the only limiting factor of which is the requirements of the Higher Education Act (Act 111/1998).

"TAILOR-MADE" STUDY PROGRAM

After a thorough breakdown and analysis, it is possible to compile a study program of Military Geography and Meteorology with the following graduate profile (www.unob.cz):

Profile of Graduate:

The graduate gains a broad and deep theoretical basis with professional orientation on the knowledge of military applications of geodesy, cartography, geoinformatics, remote sensing, meteorology and climatology and their application in the field of military intelligence. In the wider context of the surveillance, graduates will be able to apply and design methods, procedures and resources necessary to solve a wide range of technical and organizational tasks related to the geographic and hydrometeorological security of the armed forces and the use of modern military technologies, both under normal conditions and critical situations of military and non-military nature. He or she is physically capable, able to communicate at work in good level of English and ready to work in a different cultural or diverse environment.

The subjects in the study program are oriented into these three areas:

- general background providing the student preparation, especially in the field of security studies education and preparing student for the role of a member in the Armed Forces of the Czech Republic (applied military technology, leadership, history, law, military and security issues, cyber security, command and control).
- the engineering base providing the student with the preparation of basic technical and engineering subjects (mathematics, physics, informatics).
- a profiling base providing students with a training course, especially in the field of earth sciences education and its links to security Studies (geodesy, cartography and geoinformatics, military geography and climatology, atmospheric physics, geographic and hydrometeorological security, synoptic and aviation meteorology, geospatial and meteorological support for intelligence)

The study program is implemented as combined in the field of education (Government Regulation No. 275/2016 Coll. 2016):

Security branches 30%

- Security threats of military and non-military nature
- Management of operations of military and non-military nature
- Crisis management
- Cyber security
- Applied Informatics for Security Corps

Earth Sciences 70%

- Geodesy
- Regional and political geography
- Cartography
- Geoinformatics
- Remote sensing and photogrammetry
- Meteorology and climatology.

In addition to accredited teaching, students of UoD are also trained in the development of military skills and competencies, especially in the following areas:

- Basic military preparation (shooting training, engineer training, chemical preparation, order preparation, topographical preparation, ...)
- Military staff preparation (tactical, personnel, logistics, ...)
- Physical training
- Language training

Graduates of this study, as opposed to civilian studies, have a smaller amount of teaching of highly specialized subjects, such as geodesy for civil engineering or numerical atmospheric models, but are ready to work professionally in such a complex organism as the armed forces.

CONCLUSION

The main objective was to show the specifics of training of specialists for Geographic Service and Hydrometeorological Service of the Czech Armed Forces. The main differences between civil educations are their possible broad professionalism, the potential rapid change of specialization, but also a relatively rapid shift to managerial positions. For these reasons, the best solution for employing new employees of GEOSI and HMSI members is to let them study at a military college that can prepare tailor-made study programs for them.

REFERENCES

- ARMY OF THE CZECH REPUBLIC. (2008). History of the Geographic Service of ACR: 1918- 2008. Ministerstvo obrany České republiky – Agentura vojenských informací a služeb. Praha. Czech Republic (in Czech)
- Collins, J. M. (1998). Military geography for professionals and the public. Brassey's, Washington, D.C.
- Dusatko, D. (2005). The development of geodesy and cartography in the background of historical events at a turn of the 18th and 19th century. *Vojenský geografický obzor*: No. 2, pp. 50–57. (in Czech)
- Government Regulation No 275/2016. (2016) Nařízení vlády o oblastech vzdělávání ve vysokém školství. Chamber of Deputies of the Parliament of the Czech Republic, Praha, Czech Republic (in Czech).
- Hubacek, M. and Kovarik, V. (2016) Landscape: A Friend or Foe?, In: *Central Europe Area in View of Current Geography, 8-9 October*. Masarykova univerzita, Brno, pp. 160-167.

- Lankeford, T. (1998). Aviation weather handbook. McGRAW – HILL, New York.
- Law No 221/1999. (1999). Zákon o vojácích z povolání, Chamber of Deputies of the Parliament of the Czech Republic, Praha, Czech Republic (in Czech).
- Law No 111/1998. (1998). Zákon o vysokých školách. Chamber of Deputies of the Parliament of the Czech Republic, Praha, Czech Republic (in Czech).
- Marsa, J. (2013). A Vision of Geospatial Support to Ministry of Defence 2014-2018. *Vojenské rozhledy*, No. 4, pp. 105–112. (in Czech)
- Palka, E. J. and Galgano, F. (2005). Military geography: from peace to war. McGraw Hill Custom Publishing, Boston
- Riehl, H., Alaka, M. A., Jordan, C. L. and Renard, R. J. (1954). The jet stream. *Meteor. Monogr.*, No. 7, Amer. Meteor. Soc., pp. 23-47
- TOPO 1-1. (2012). *Geographic support* in the Department of Defense. Ministerstvo obrany. Praha. Czech Republic (in Czech).
- Univerzity of Defence. <https://apl.unob.cz/AkrStudPrg/Pages/FreeArea/Default.aspx>, 1st. December 2017
- ZPRÁV 1-2. (2016). Hydrometeorological support. Ministerstvo obrany. Praha. Czech Republic (in Czech).

SAFETY SPATIAL ANALYSIS OF WILDLIFE ATTACKS IN CHITWAN, NEPAL

Aleš, RUDA¹; Jaromír, KOLEJKA²; Thakur, SILWAL³

¹Department of regional development and public administration, Faculty of regional development and international studies, Mendel university in Brno, třída gen. Píky 7, 613 00, Brno, Czech Republic

ruda@node.mendelu.cz

²Institute of Geonics, Drobného 28, 602 00, Brno, Czech Republic

jkolejka@centrum.cz

³Department of National Park and Wildlife Conservation, Institute of Forestry, Tribhuvan University, Pokhara Campus - 15, Hariyokharka, Pokhara, Nepal

tsilwal@iof.edu.np

Abstract

Population growth forces human community to expand into natural habitats of wild animals. Their effort to use natural sources often collide with wildlife attacks. These animals do not only protect their natural environment but in fact of losing the potential food sources they also penetrate in human settlements. Conflicts between humans and animals end with serious injuries or human casualties. The research was situated in the Chitwan National Park (CNP) in Nepal and the aim of this study was to investigate possible spatial (geographical) connections between attacks of all kinds of animals on humans in the CNP and its surroundings between 2003 and 2013. Data collected during this period did not prove any signs of spatial autocorrelation. Calculated magnitude per unit area using Kernel density together with purpose-defined land use groups were used to determine five risk zones of wildlife attacks. In conclusion, it was found that the riskiest areas are locations near the forest, covered by agricultural land and inhabited by humans.

Keywords: risk zonation, kernel density, safety analysis, Nepal

INTRODUCTION

The increase in human population leads to increasing pressure on space and natural resources, mainly represented by biomass, soil and water. Extensive pressures on natural resources, in particular, lead to the inclusion of ever larger areas in the economic activity of man and thus the accelerated reduction of areas of natural habitats. This process leads to efforts to protect the remaining segments of the natural environment from destruction. In particular, developing countries face a population explosion and destruction of the natural landscape during the dramatic expansion of human ecumenism. The well-known protected areas thus become the only shelters of many rare species of organisms, habitats and entire landscapes. Due to the often limited technical and organizational capabilities of human communities in the vicinity of protected areas, it has often been necessary to make a compromise on the relationship between the "protected nature area vs. local human community". Pre-agreed rules allow coexistence of the people and

nature. Firstly, the rules set out the conditions under which local people can enter protected areas and take their means away of subsistence. Secondly, the nature conservation institution (usually under the patronage of the state) undertakes to compensate local residents for damages caused by natural inhabitants of the protected area. Compliance failure with the established coexistence rules are caused both by the growing pressure of the human population on insufficient resources outside and inside the protected area, especially in the case of extensive pressures, and by the growth of populations of some protected biotype species that have been relatively safe in the protected area. In principle, it is an individual absence of respect for both parties, even in wildlife, of course, of being aware that their respect cannot be spoken. Specific coexistence rules exist especially in to the buffer zones of protected areas, where the rational cooperation of human community and nature conservation is particularly needed. Major problems have been, and probably are, the attacks of wildlife on humans. The situation is being solved by rural communities, nature conservation authorities and administrative authorities. Improving the impact of human activity is negatively reflected on wildlife and their habitats, often leading to frequent occurrences of wildlife outside the protected area. Interactions up to conflicts are often the result of continuing high dependence of local people on forests and other resources from the protected area, leading to the reduction of area of suitable natural habitats. The conflict between humans and wildlife is attributed to the loss, degradation and fragmentation of wildlife habitats through human activities such as logging, animal husbandry, agricultural expansion and development projects (Fernando et al., 2005). The result is contact and conflict with humans because wild animals try to meet their nutritional, ecological and behavioral needs. Damage on human interests may involve life losses, injuries, threats to economic security, reduced food security and livelihoods. This creates considerable antipathy in nature among people living on the periphery of protected areas and damages conservationist efforts (De Boer, Baquete, 1998; Nyhus et al., 2000). The attacks of wildlife on humans occur especially when:

- a) wild animals enter cultural landscapes (with settlements, crops and domestic animals),
- b) people enter natural habitats (walking, picking-up of forest fruits and materials, fishing).

Wild animals' attacks on humans depend on the geographical situation and distribution of different animal species. From 2008 to 2012, 135 cases of human casualties were reported in the Chitwan National Park (CNP) in Nepal (CNP, 2012a, Silwal et al., 2013b). Most researchs in the CNP were focused on tiger and its prey (Seidensticker, 1976; McDougal, 1977; Mishra, 1982; Tamang, 1982; Smith, 1984; Gurung et al., 2008, Bhattarai, Kindlmann, 2013). The Rhinoceros has also been the subject of many studies (Laurie, 1979; Dinerstein, Wemmer, 1991; Thapa et al., 2013). In recent years, the elephant has also become one of the research priorities (Pant, 2013). In the past, several studies have been conducted on socio-economic and political issues in the CNP (Sharma, 1991; Nepal, Weber, 1992; Budhathoki, 2004 and 2012; Silwal et al., 2013a and 2013b).

In case of animal attacks, we consider discrete point values bearing information about this event. Useful GIS analysis that enable the identification of event hotspots are Kernel Density and Getis-Ord G_i^* . The kernel is an estimator and it functions by generalizing or smoothing discrete point data into a continuous surface area (Silverman, 1986; Hart and Zandbergen, 2014). Getis-Ord G_i^*

is a spatial autocorrelation method that enables the recognition and understanding of hot and cold spots. According to Rosenshein (2010), Kernel Density and Getis-Ord G_i^* are two different geospatial analyses, in which Kernel Density performs calculation by considering arbitrary search radius and the cell size while Getis-Ord G_i^* considers the magnitude of each feature in the dataset in the context of its neighbours' values. Chainey (2010) compared G_i^* to other hotspot mapping techniques, including Kernel Density, for crime hotspot mapping. Based on the prediction accuracy index (PAI), G_i^* gave the best results in predicting the spatial extension of crime hotspots. Moreover, Getis-Ord G_i^* was the best mapping technique for capturing local clusters, and thus the identification of statistically significant hotspots. Getis-Ord G_i^* is also widely used in other disciplines essentially in health research, incident prevention and biodiversity distribution. Wubuli et al. (2015), used Geits-Ord statistic in detecting spatial clustering of pulmonary Tuberculosis (TB) incidence in Xinjiang, China.

The aim of this study is to investigate possible spatial (geographical) connections between attacks of all kinds of animals on humans in the CNP and its surroundings between 2003 and 2013. Fundamental wildlife attacks on humans have taken place in the collection of forest resources in forests and the movement of wildlife to the human landscape. The biggest challenge in protecting „big cats“ (tiger, leopard) is to eliminate conflict and killing each other. Predators' attack can never be ruled out but should be transferred to a boundary which can be accepted by humans (Jackson, 1999). The CNP has a large number of other endangered large animals such as elephant, rhinoceros, bear, deer, buffalo, etc. These animals also cause damages to local communities, their homes, crops and domestic animals. Cases registered in the park's office serve for compensation of victims and also lead to frequent local strikes aimed at alerting competent authorities to the increasing trend of damages and urgent need to solve this problem (CNP, 2012). One of the solutions may be the knowledge of types of locations, where the attacks are concentrated. The results of the input analysis are presented in the following text.

STUDY AREA

The following study was carried out on the territory of Chitwan National Park and its buffer zone in southern central Nepal (Fig. 1).

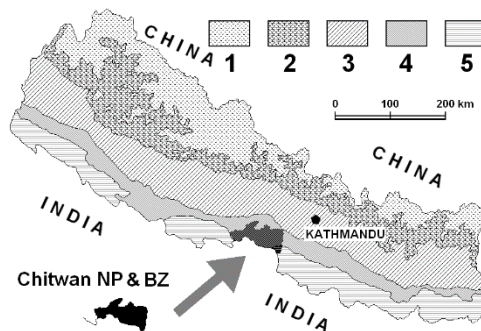


Fig. 1. Nepal: The location of Chitwan National Park and Buffer Zone with coverage of physiographic zones (Legend: 1. High Himalaya, 2. High Mountain, 3. Mid-Mountain, 4. Siwalik, 5. Terai)

The Park was founded in 1973 as the first protected area of Nepal. The Park protects the Terai lowland ecosystems and adjacent parts of the Siwalik Mountains with a total area of 932 km² on the territory of four administrative districts: Chitwan, Nawalparasi, Parsa and Makawanpur. This park crosses the border to the untouched natural area of the Valmiki Tiger Reserve in neighbouring India. On the north, foothills of Mahabharata Mts., the CNP is connected via the Brandabhar biocorridor which is the only remaining link between the mountains and the lowland that allows the migration of wild animals. This park is a part of an internationally recognized network of basic large-scale protected areas due to its ecological significance, it belongs to the Ramsar Wetland Site and it is on a list of the world's natural heritage registered by UNESCO. In its untouched environment (Fig. 2) and many endangered animals live, such as rhinoceros (*Rhinoceros unicornis*, Fig. 2), tiger (*Panthera tigris*), leopard (*Panthera pardus*), wild elephant (*Elephas maximus*), sloth bear (*Melursus ursinus*), wild boar (*Sus scrofa*), gaur bison (*Bos gaurus*), sambar deer (*Rusa unicolor*) and marsh crocodile (*Crocodylus palustris*). The diversity of birds and reptiles is high. Chitwan National Park generates a high amount of income, but every year it registers victims of human wildlife attacks. Human accidents occurred in CNP represent the majority in all protected areas in Nepal (Department of National park and wildlife conservation, 2010, Silwal et al., 2013b).

The Buffer Zone (BZ) of CNP covers an area of 750 km², covering 45 % of forests and 55 % of agricultural land adjacent to the park (Government of Nepal, 1996). The buffer zone is defined to meet local community requirements for forest products and was designed to reduce the park's pressure on local communities and vice versa. There are 0.25 million of inhabitants in BZ who hold more than 0.15 million of livestock, partly depending on forest resources (Chitwan National Park, 2014).



Fig. 2. Example of the typical natural environment within Chitwan NP (left) and young female rhinoceros grazing on the bank of the Rapti River (photo by J. Kolejka)

Grazing domestic animals in the forest, breaking branches for feeding, gathering firewood and other forest products are essential components of the daily living of local communities (Sharma, 1991). A large part of forests of BZ was handed over to communities as community forests (CF).

Regarding good management, CF has also become a suitable biotope sites outside the park and a good wildlife environment. On the other hand, however, they also increase the numbers of human victims (Budhathoki, 2003, Budhathoki, 2004). Although local residents have high ethnic diversity, the economy structure is similar to all ethnic groups except Bote and Darai who are more dependent on fishing (Sharma, 1991). Buffer zone of Chitwan national park also faces the highest number of conflicts each year, including human casualties in Nepal (Department of National Park and Wildlife Conservation, 2010).

DATA PROCESSING

This study relies on analysing point data in terms spatial statistics and spatial analysis for risk assessment of their spatial patterns using geostatistical techniques. At the beginning we examined appropriate spatial statistics parameters using ArcGIS spatial statistics tools. Regarding the extent of studied area represented by rectangle of 84 x 44 km following statistic tests were tested: Spatial autocorrelation using Moran's Index (Global Moran's I) and Hot Spot analysis.

Global Moran's I was used to measure spatial autocorrelation based on feature locations and feature values, it evaluates whether the pattern expressed is clustered, dispersed, or random. Global Moran's I Summary gave these results: Moran's I Index, p-value, z-score and variance. Because Global Moran's I represents an inferential statistic, the null hypothesis states that the attribute being analysed is randomly distributed among the features in our study area. The p-value is a probability that the observed spatial pattern was created by some random process. The lower the p-value is the higher is the probability for rejecting the null hypothesis. Typically, the p-value associated with a 95 percent confidence level is 0.05. According to given results the p-value is 0.29 which means that we cannot reject the null hypothesis and the distribution dealing with number of deadly animal attacks is random. For normal data distribution, z-scores are standard deviations and mostly are associated with p-values. Z-score between -1.96 and +1.96 indicates random distribution. This statement can be confirmed by given results where z-score is 1.05. Similarly, Moran's I index ($I = 0.09$) belonging to the interval -1 to +1 proves that the pattern does not appear to be significantly different than random. Given a set of weighted features, Hot Spot Analysis identifies statistically significant hot spots and cold spots using the Getis-Ord G_i^* statistic. The G_i^* statistic returned for each feature in the dataset is a z-score. For statistically significant positive z-scores, the larger the z-score is, the more intense the clustering of high values – hot spots. For statistically significant negative z-scores, the smaller the z-score is, the more intense the clustering of low values – cold spots. Given results revealed that only 5 percent of input points mostly localized in northern part of the study area were evaluated as significant hot spots. The rest did not prove statistically significant spatial clustering. Also incremental spatial autocorrelation did not indicate distances where spatial processes promoting clustering are most pronounced.

Subsequently, we worked with hypothetical postulate that animal attacks on humans are mostly located differently in present environment (e.g. accessible and rich in food land use categories). Available land use categories, provided in vector data format by the authority of the Chitwan

national park, were grouped into following environment categories considering their potential for different movement conditions and food access (Fig. 3):

environment	land use categories
a) unclear	forest land
b) mostly unclear	bush/shrub, scattered trees, nursery, orchard
c) natural open clear	barren land, grassland, sandy area
d) forage rich open clear	cultivated land, airports, built up areas
e) water	pond or lakes, waterbodies, river cutting/cliffs

Because previous geospatial analysis confirmed random data distribution and no cluster significance, application of Kernel Density tool followed. We used Kernel Density to calculate a magnitude-per-unit area from attacks using a kernel function to fit a smoothly tapered surface to each point, because suitable reclassification can generate significant zones showing higher probability of wildlife attacks (Fig. 4). The kernel density attacks raster layer was reclassified using the geometric interval algorithm (the frequency distribution is exponential, therefore geometric intervals are most appropriate) into 5 categories: very low, low risk, medium risk, high risk and very high risk. Kernel density estimation (KDE) is one of these techniques used to create a surface to indicate the intensity of the events or the phenomenon.

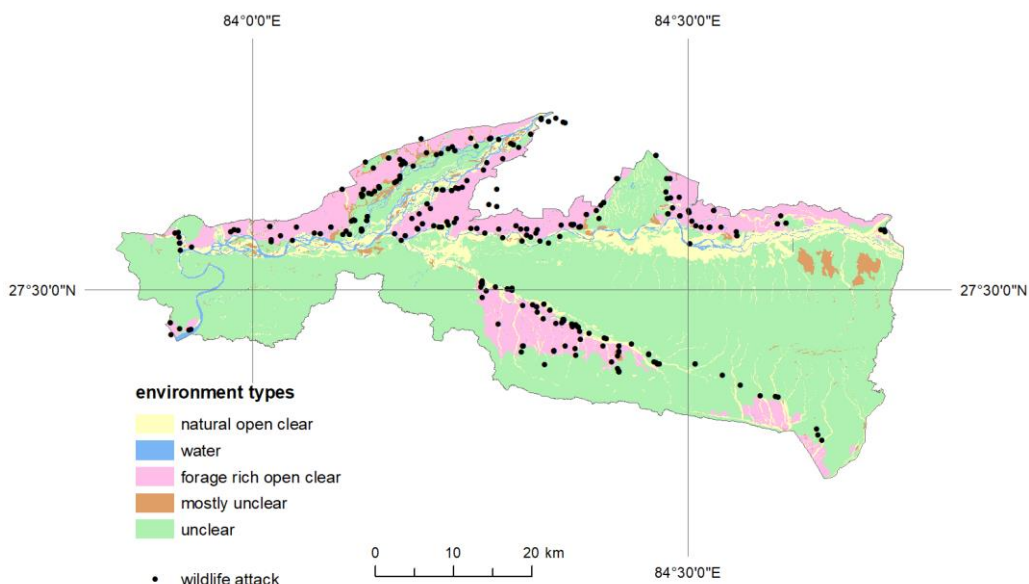


Fig. 3. Environment types of Chitwan NP and buffer zones

After Bailey and Gatrell (1995), assuming that $s_1 \dots s_n$ are locations of the events, then (s) , the intensity of the event can be estimated by

$$\hat{\lambda}_{\tau}(s) = \sum_i^n \frac{1}{\tau^2} k\left(\frac{(s - s_i)}{\tau}\right), \quad (1)$$

where τ is the bandwidth or the size of the kernel and k is the kernel function determining the shape of the kernel. The kernel function is a bivariate probability density function, which may take different forms (e.g. quartic kernel), different specifications of the function can provide equally reasonable results. However, the size of the kernel, or the bandwidth, may have more significant impact on the results. In general, using a smaller bandwidth will limit the density estimation to the local situation. The intensity estimated for locations will be limited to the events or density in the immediate neighbour if a relatively small bandwidth is used. Generating the intensity surface of a given event is quite useful for exploratory analysis, not just in event mapping. Often, the density surface identifies or exposes the so-called ‘hot spots’ when events are spatially clustered to a local area, or ‘cold spots’, where the events are much less frequent in the area (Gatrell, 2002).

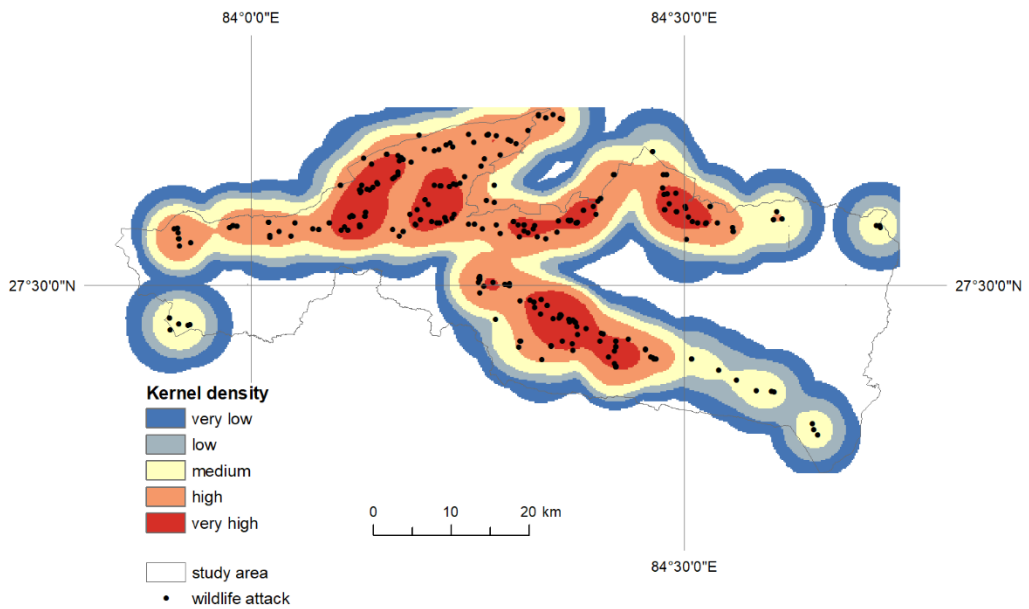


Fig. 4. Reclassified Kernel density results of wildlife attacks in Chitwan NP and buffer zones

RESULTS AND INTERPRETATION

Further statistical examining cleared up that only elephants attacked 50 % of their victims in unclear environment. Attacks of other animals (considering the range 51-95 %, where 5 % was considered as the usual statistical reserve) took place in different buffer zones around forests mostly in natural open clear environment and forage rich open clear (Table 1, Table 2). Forests were chosen as an input polygon for creating buffer zones because this land use category covers

more than 60 % of study area. These results were examined by chi-quadrat test where the null hypothesis states that different environment does not influence the number of attacks. According to given results the null hypothesis was rejected at the confidence level 0.05. The test proved that different environment influences the number of attacks. From this point of view, the riskiest environments are natural open clear environment (regarding the highest share of attacks up to 50 % and second highest share of attacks up to 95 % of victims) and forage rich open clear environment (highest share of attacks up to 95 % of victims).

Table 1. Attack environment – specific land use structure of wild-life attacks considering up to 95 % of victims attacked by each animal in buffer zones around forest.

			Specific land use structure buffer zone around forest (%)				
attackers	buffer zone around forests (in metres)	share of attacks in forests (%)	<i>unclear</i>	<i>mostly unclear</i>	<i>natural open clear</i>	<i>forage rich open clear</i>	<i>water</i>
tiger	1150	24.42	0	8.286	39.452	42.568	9.694
elephant	850	50	0	9.278	43.033	37.07	10.619
rhinoceros	2250	14.29	0	7.047	34.082	50.508	8.363
bear	900	23.08	0	9.089	42.321	38.148	10.442
leopard	1785	5.56	0	7.318	35.437	48.543	8.702
wild boar	1100	7.69	0	8.425	39.92	41.843	9.812

Table 2. Attack environment – specific land use structure of wild-life attacks considering up to 50 % of victims attacked by each animal in buffer zones around forest.

			Specific land use structure buffer zone around forest (%)				
attackers	buffer zone around forests (in metres)	share of attacks in forests (%)	<i>unclear</i>	<i>mostly unclear</i>	<i>natural open clear</i>	<i>forage rich open clear</i>	<i>water</i>
tiger	200	24.42	0	12.286	56.679	17.797	13.238
elephant	0	50	100	0	0	0	0
rhinoceros	380	14.29	0	11.469	51.987	23.932	12.612
bear	150	23.08	0	12.463	58.365	15.801	13.371
leopard	490	5.56	0	10.91	49.558	27.479	12.053
wild boar	470	7.69	0	11.02	49.985	26.838	12.157

Although cluster analysis did not show statistically significant clusters, the kernel function application allowed identification of core regions and distinguished areas with a lower risk of wildlife risk attack. Combining kernel density surface and statistically derived land use environment brought significant results generating final risk categories (Fig. 5). Points on the map are attack locations, colour zones represent intersection of kernel density layer (wildlife attacks on humans) with three purpose-defined land use groups (forests – the darkest areas under the risk zones, open – the lightest areas in ortophoto, and cultivated landscape) with regard to the degree of clarity for migrating animals and moving humans and the potential source of food. By spatial analysis of the spatial relationships of the three information layers (places of attacks), their spatial concentrations over land use types, it is possible to determine the most threatened areas of human wildlife attacks (of course, on the basis of previous recorded events). The majority of the attacks took place near the boundary of the forest, mostly up to 500 meters towards the cultivated landscape and less into the forest. If there are human farms in this area, the risk of wildlife attacks is relatively high. If the species of the attacking animal is taken into account, it is mainly wild boar, rhinoceros and probably leopard who seek the food on fields and near human settlements.

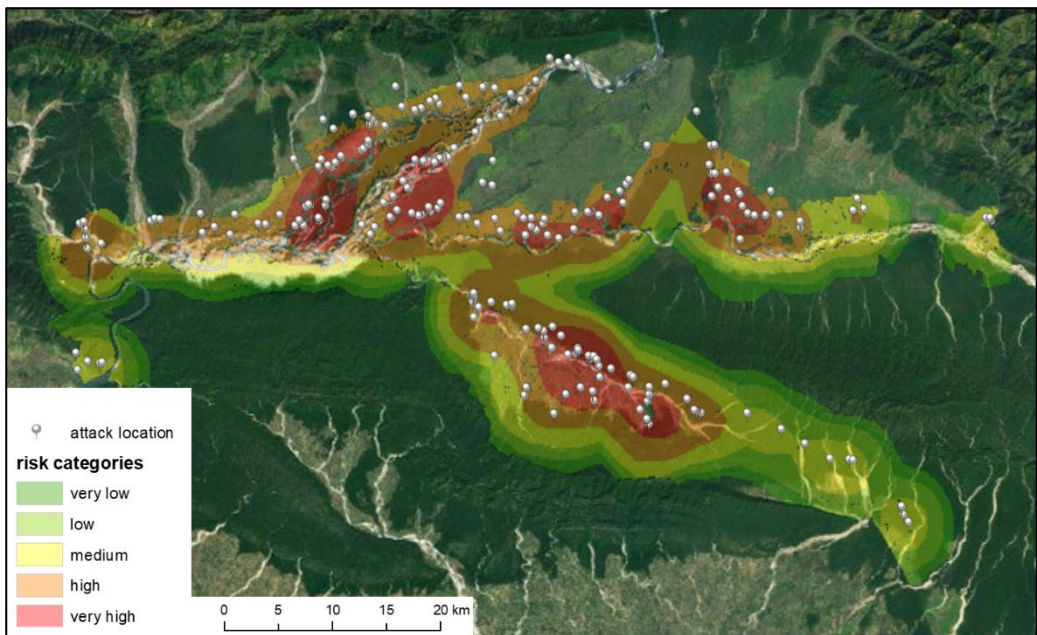


Fig. 5. Risk analysis of wildlife attacks in Chitwan National Park and buffer zone

On the other hand, bear and tiger do not follow them from the same reason. Areas of the highest risk of attacks can be described as locations:

- a) near the forest,
- b) covered by agricultural land,
- c) of inhabited areas
- d) with farm storage buildings.

Although this study includes only events from the period 2003-2013, it can be assumed that conflicts between humans and wild animals have started many years ago. The question is why humans settled down these high-risk areas. Another question follows. How to secure the current situation or at least improve the safety of residents of the riskiest localities?

CONCLUSION

In case of population explosions, increasing pressure on natural resources is inevitable. Obviously, the problem of wildlife attacks on humans has a very complex background.

The results of the analysis can provide an idea of the appropriate response to the dangers arising from the coexistence of the human community in the neighbourhood of the NP and wildlife:

- a) Move residential buildings as far as possible from the NP border, especially if it is represented by a forest.
- b) Separate economic objects from residential, because stored food and products (alcohol) are a wildlife decanter.
- c) Ensure the observation of open agricultural areas from secured watchtowers.

In the light of other general knowledge and experience, it is possible to create a sequence of tasks designed to address the results of the demonstrated analysis and to require state or regional administrations. A sequence of current proposals can be stated according to the degree of generality and urgency:

- 1) Reduce the population increase of the local population.
- 2) Intensify economic development.
- 3) Reduce the use of biomass in NP by humans to keep it more for wild animals which can reduced their motivation to leave the park for food.
- 4) Prevent animals' migration outside the park by technical means. The former primitive electric fence was easily overcoming by elephants (Fig. 6).
- 5) Concentrate the protection of residential and commercial buildings (Fig. 7).



Fig. 6. The present most sophisticated way of human community protection – electric fence along CNP borders (photo by J. Kolejka)



Fig. 7. Wooden house damaged by a wild elephant seeking rice wine (photo by J. Kolejka)

The results of the above-mentioned spatial analysis can be motivated by the recommendation that priority should be given to the risk of attacks in the riskiest areas. The risk, after stabilization of one site, can be moved to a less dangerous site by now, if the situation forces animals to leave the park as they do now. However, the risk may be moved to a hitherto less dangerous site after stabilizing one site if the situation forces the animals to abandon the park to the same extent as before (eg unregulated growth of the stock of high-risk game species). It is evident that the risk reduction can only be achieved by a comprehensive combination and selection from activities mentioned above, since the conflict with wildlife can never be completely ruled out.

REFERENCES

Bailey, T.C. and Gatrell, A.C. (1995) *Interactive Spatial Data Analysis*. Longman, London.

- Bhattarai, B. P. & Kindlmann, P. (2013) Effect of Human Disturbance on the Prey of Tiger in the Chitwan National Park- Implications for Park Management. *Journal of Environmental Management*, 131, pp. 343-350.
- Budhathoki, P. (2004) Linking Communities with Conservation in Developing Countries: Buffer Zone Management Initiatives in Nepal. *Oryx*, 38, pp. 334-341.
- Budhathoki, P. (2012) *Developing Conservation Governance Strategies: Holistic Management of Protected Areas in Nepal*. PhD Thesis, University of Greenwich, London.
- De Boer, W. F. & Baquete, D. S. (1998) Natural Resource Use, Crop Damage and Attitudes of Rural People in the Vicinity of the Maputo Elephant Reserve, Mozambique. *Environmental Conservation*, 25, pp. 208-218.
- Department of National Park and Wildlife Conservation (2010) *Annual Report (2009)*. Department of National Parks and Wildlife Conservation, Kathmandu.
- Department of National Parks and Wildlife Conservation (2012) Management plan for Xhitwan National Park and Buffer Zone (2012-2016). Department of National Parks and Wildlife Conservation, Kathmandu.
- Dinerstein, E. & Wemmer, C. M. (1991) Demography and Habitat Use by Greater One-horned Rhinoceros in Nepal. *Journal of Wildlife Management*, 55, pp. 401-411.
- Fernando, P., Wikramanayake, E., Weerakoon, D., Jayasinghe, L. K. A., Gunawardene, M. & Janaka., H. K. (2005) Perceptions and Patterns of Human-Elephant Conflict in Old and New Settlements in Sri Lanka: Insights for Mitigation and Management. *Biodiversity and Conservation*, 14, pp. 2465-2481.
- Gatrell, A.C. (2002) *Geographies of Health*. Blackwell Publishers.
- Government of Nepal (1996) *Buffer Zone Management Rules 2052*. Government of Nepal, Kathmandu.
- Gurung, B., Smitha, J. L. D., Mcdougall, C., Karki, J. B. & Barlow, A. (2008) Factors Associated with Human-Killing Tigers in Chitwan National Park, Nepal. ELSEVIER. *Journal of Biological Conservation*, 141, pp. 3069 –3078
- Hart, T.C. and Zandbergen, P.A. (2014) Kernel density estimation and hotspot mapping: Examining the influence of interpolation method, grid cell size, and bandwidth on crime forecasting. *Polic. An Int. J. Police Strateg. Manag*, 37, pp. 305–323.
- Chainey, S. (2010) *Advanced hotspot analysis: spatial significance mapping using Gi**. University College London, London.
- Chitwan National Park (2012) *Chitwan National Park: Annual Report - FY 2068/69 (2011/2012)*. Government of Nepal/Ministry of Forests and Soil Conservation/ Department of National Parks and Wildlife Conservation/Royal Chitwan National Park, Kasara.
- Chitwan National Park (2014) Annual Report - Fiscal Year 2070/71 (2013/2014). Government of Nepal/Ministry of Forests and Soil Conservation/ Department of National Parks and Wildlife Conservation/Royal Chitwan National Park, Kasara.
- Jackson, P. (1999) *Tigers in India in 1990s*. WWF Tiger Conservation Program. Three Years and Beyond, WWF TCP, New Delhi.
- Laurie, A. (1979) *The Economy and Behavior of the Greater One-horned Rhinoceros*. PhD Dissertation, University of Cambridge, Cambridge.

- McDougal, C. (1977) *The Face of the Tiger*. Rivington-Duetch, London.
- Mishra, H. R. (1982) Balancing Human Needs and Conservation in Nepal's Royal Chitwan National Park. *Ambio*, 11, pp. 246-257.
- Nepal, S. K. & Weber, K. E. (1992) *Struggle for Existence: Park-People Conflict in the Royal Chitwan National Park, Nepal*. Asian Institute of Technology, Bangkok.
- Nyhus, P. J. & Tilson, R. (2004) Characterizing Human Tiger Conflicts in Sumatra, Indonesia. *Oryx*, 38, pp. 68-74.
- Pant, G. (2013) Understanding the Nature and Extent of Human-Elephant Conflict in Central Nepal. A Research Report Submitted to The University of Queensland, Brisbane.
- Rosenshein, L. (2010) *Spatial Statistics*. Available at: <https://geonet.esri.com/thread/12214> (Accessed: January 4, 2018).
- Seidensticker, J. (1976) On the Ecological Separation Between Tigers and Leopards. *Biotropica*, 8, pp. 225-234.
- Sharma, U. R. (1991) *Park People Interaction in Chitwan National Park, Nepal*. A Dissertation Submitted to the Faculty of the Committee on Wildlife and Fisheries Science in Partial Fulfillment of the Requirements for the Degree of Doctor of Philosophy in the Graduate College, The University of Arizona, Tucson.
- Silverman B., (1986) Density estimation for statistics and data analysis, *Monograph on Statistics and Applied Probability*, 37, pp.1 –22.
- Silwal, T., Shrestha, B. P., Bhatta, B. P. & Devkota, B. P. (2013a) *Revenue Distribution Pattern and Park-People Conflict in Chitwan National Park, Nepal*. Banko Janakari. Department of Forest Research and Survey (DFRS), Ministry of Forests and Soil Conservation, Government of Nepal, Vol. 23 No. 1, Kathmandu.
- Silwal, T., Subedi, R., Poudel, B. S. & Lakhey, S. P (2013b) *Wildlife Damage and Adaptation Strategies. A Case Study in Chitwan National Park, Nepal*. A Research Report Submitted to IOF/ ComForM Project, University of Pokhara, Pokhara.
- Smith, J. L. T. (1984) *Dispersal, Communication and Conservation Strategies for the Tiger (Panthera tigris) in Royal Chitwan National Park, Nepal*. PhD Thesis, University of Minnesota, Minneapolis.
- Tamang, K. M. (1982) *The Status of the Tiger (Panthera tigris) and its Impacts on Principal Pray Populations in the Royal Chitwan National Park, Nepal*. PhD Thesis, Michigan State University, East Lansing.
- Thapa, K., Nepal, S., Thapa, G. & Bhatta, S. R. (2013) Past, Present and Future Conservation of the Greater One-Horned Rhinoceros *Rhinoceros unicornis* in Nepal. *Oryx*, 47, pp. 345–351.
- Wubuli, A., Xue, F., Jiang, D., Yao, X. Upur, H. and Wushouer, Q (2015) Socio-demographic predictors and distribution of pulmonary tuberculosis (TB) in Xinjiang, China: A spatial analysis, *PLoS One*, 10, pp. 1–22.

THE SELECTION OF EXPERIMENTAL AND CONTROL AREAS IN CRIME ANALYSIS – THE PROBLEM OF SPATIALLY AGGREGATED DATA.1

Adam, DĄBROWSKI¹; Piotr, MATCZAK²; Andrzej, WÓJTOWICZ³

¹Institute of Geoecology and Geoinformation, Faculty of Geographical and Geological Sciences, Adam Mickiewicz University in Poznań, Bogumiła Krygowskiego 12, 61-606, Poznań, Poland

adam.dabrowski@amu.edu.pl

²Institute of Sociology, Faculty of Social Sciences, Adam Mickiewicz University in Poznań, Augustyna Szamarzewskiego 89c, 60-568 Poznań, Poland

matczak@amu.edu.pl

³Faculty of Mathematics and Computer Science, Adam Mickiewicz University in Poznań, Umultowska 87, 61-614, Poznań, Poland

andre@amu.edu.pl

Abstract

The progress in surveillance technology has led to development of Closed-Circuit Television (CCTV) systems in cities around the world. Cameras are considered instrumental in crime reduction, yet existing research does not univocally answer the question whether installing them affects the number of crimes. The natural (quasi) experimental method applied usually to evaluate CCTV systems effectiveness faces difficulties with data quantity and quality. The former refers to the number of crimes allowing to infer conclusive results within the experimental procedure. The latter concerns available level of data aggregation on crimes. The lack of exact location of a crime incident in the form of a street address or geographic coordinates hinders the procedure of experimental and control areas selection. In this paper we propose a method to deal with data limitations within a quasi - experimental study on CCTV systems effectiveness in eight Polish cities. As the police data on crime incidents are geocoded into a neighbourhood or a street, we designed a method to overcome this drawback by applying measures of Euclidean similarity to time series and landscape metrics. The method enables to determine experimental (test) and control areas in the chosen cities, which are necessary to conduct the study on CCTV effectiveness based on the quasi-experimental design.

Keywords: crime analysis, urban landscape, GIS, landscape analysis, closed circuit television

INTRODUCTION

One of the vital issues of contemporary crime analysis that still remains unresolved is the question: does Closed-Circuit Television (CCTV) cameras influence the number of crime incidents (Brown, 1995; Squires, 1998; Lim, Kim, Eck and Kim, 2016)? Practitioners often emphasize the

¹ This paper was prepared within the MoWiz project, no. 2016/21/B/HS6/01158 financed by National Science Centre.

impact both in terms of ability to identify a criminal and as a prevention method that deters criminals (Gill and Spriggs, 2005; La Vigne, Lowry, Markman and Dwyer, 2011). Yet, a review of CCTV impact on crime reduction research by Lim et al. (2016) shows ambiguous findings. Although the effect is noticeable for vehicle crimes and car parks, it is usually not significant for city centers and for residential areas. However, the results are ambiguous, and a thorough look at particular studies reveals several methodological problems.

A quasi natural experiment method is often applied to assess the impact of an (Farrington, Gill, Waples and Argomaniz, 2007; Caplan, Kennedy and Petrossian, 2011). As a true randomized experiment, offering the most robust evaluative assessments is hardly feasible in practice, the quasi experimental design is the second best option. Relying on real life situations (not designed by an evaluator), this method tests the effect of an intervention (installation of a camera) considering two areas: the experimental (where the intervention occurs) and the control (without intervention). Having data on the numbers of crimes before the intervention and after, one can determine the effect. Nevertheless, the method faces difficulties. The main challenge lies in ensuring that both areas differ by the intervention only. If this condition is fulfilled, we can assume that the change is the effect of the intervention (Salkind, 2007). Thus, the selection of appropriate experimental and control areas is crucial (Farrington, Gill, Waples and Argomaniz, 2007). As the method depends on existing cameras implementation, the challenge is to identify areas with available data allowing for calculation the effect. The up-to-date research reveals various data deficiencies. They regard: (a) data on crime, which are necessary for determining the effect; and (b) data on the site characteristics, which is indispensable for ensuring that both areas are similar to the extent allowing to treat the areas as comparative (Cook, Campbell and Shadish, 2002).

Analyzing data on efficiency of cameras is problematic as geographic data available from the police are not precise enough. In this paper we propose a new method of selecting experimental and control areas based on time series and landscape analysis. This method was worked out for eight Polish cities. Suggested method can be used when crime incident records are aggregated to larger spatial units like streets or neighborhoods. The method is based on Euclidean similarity to time series and landscape metrics to select experimental and control areas, in coherence with the conditions suggested in the literature for performing the effectiveness analysis.

METHODOLOGICAL CHALLENGES IN EVALUATING EFFECTIVENESS OF CCTV VIA THE QUASI-EXPERIMENTAL METHOD

Most studies concerning the influence of CCTV camera installation or other interventions on crime rates, rely on quasi-experimental scheme (Welsh and Farrington, 2003). It requires choosing experimental and control areas to assess the impact of an intervention. Experimental areas are usually defined as the one cover by a camera, which is interpreted in a simplified way as a buffer of a given distance from the camera (Farrington, Gill, Waples and Argomaniz, 2007) or as a visibility area designated by the GIS tools (Piza, Caplan and Kennedy, 2014). In the case where cameras are placed densely and experimental areas overlap, they are combined into one area (La Vigne, Lowry, Markman and Dwyer, 2011). Experimental areas need to have at least one camera

installed. Moreover, some other conditions concerning designation of these areas are suggested. Welsh and Farrington (2003) proposed the following rules:

1. there should be at least 20 crime incidents before intervention (in our case: installation of a CCTV camera);
2. a control area should not be directly adjacent to the experimental area;
3. a mounted camera should be the main intervention taking place in a given experimental area;
4. there should be data concerning the number of crime incidents for at least one year before and one year after the occurrence of the intervention, in order to analyze the situation before and after the moment when the cameras were installed (Caplan, Kennedy and Petrossian, 2011).

Although the quasi-experimental method enables to analyze effects of a policy intervention, the necessary conditions of the method involve difficulties.

(a) Data on crime incidents both on experimental and control area are not always available (Welsh and Farrington, 2003).

(b) Even if data are available, the number of crime incidents is not always sufficient for robust statistical conclusions (Lim, Kim, Eck and Kim, 2016). For a particular experimental and control areas the number of actual crime incidents needs to be sufficient to draw any solid conclusions. As a pair of experimental/control areas must be as similar as possible, this condition is a limitation. A possible solution for this problem is to aggregate data spatially or temporally (e.g. by analyzing crime incidents in a larger area and/or through a longer period), or to aggregate different crime categories.

(c) The latter solution leads to another problem: the installation of a CCTV has various impact on different crime categories. Nevertheless, the decision must be made on the selection of crime categorization considered in a research. A careful crime categorization has to be worked out during the research. For instance, car robbery and car theft, which concern the same subject (cars) are treated as two different felonies. To detect CCTV impact Welsh and Farrington (2003) suggested to analyze crimes related to car theft and battering (street fights) only. They are relatively common crime types that occur due to a “window of opportunity” (Planells S., 2015).

(d) The crime rate itself is currently dropping in most of the European cities (Heidensohn and Farrell, 1993). This drop coincides with the CCTV technological progress in general. Therefore, it is difficult to separate from it the influence of CCTV cameras alone.

(e) Other difficulties include spatio-temporal autocorrelation of crime incidents (Wolfe and Mennis, 2012) and their spatial heterogeneity (Cattell, 2001). Supposing when police capture a bigger group of criminals operating on a specific site, influences the decrease of crime rate in this certain site regardless of placing a CCTV camera.

(f) The process of choosing proper control areas is a difficult matter. It is hardly possible to find an exact “twin” areas as similarity includes both criminal activity and other attributes of areas (Piza, Caplan and Kennedy, 2014; Boessen and Hipp, 2015).

(g) The level of spatial aggregation of crime incidents data can be a substantial issue. Current methods for selecting experimental and control areas base on buffers around cameras. Although they are sufficient if crime incidents are pinpointed to exact address or geographical coordinates, they cease to work if crimes are geocoded to bigger areas like streets or neighborhoods. Research conducted on aggregated crime data concerns the means of disaggregating them (Kennedy and Kennedy, 2004) or analyzing the relationship between crime and spatial characteristics such as unemployment (Raphael and Winter-Ebmer, 2001) or land use (Stucky and Ottensmann, 2009). Little research on the influence of an intervention on crime deterrence has been conducted for spatially aggregated crime data. One of the reasons for this situation may be the problem of proper selecting experimental and control areas for such data.

(h) In order to determine whether installation of a CCTV camera has a statistically significant effect on the number of crimes, an appropriate control area should be assigned to each experimental area (Farrington, 1997). Ideally, these areas should have similar socio-economic characteristics of residents (Farrington, Gill, Waples and Argomaniz, 2007), the same characteristics of landcover and landuse (La Vigne, Lowry, Markman and Dwyer, 2011) and similar traits of identified crimes in the period before installation of cameras (La Vigne, Lowry, Markman and Dwyer, 2011). If displacement (diffusion) effect is to be measured, then the first buffer around the installed camera is considered as an experimental area. The second concentric buffer is created around it – the area of diffusion of crimes, and then the third one represents the control area (Farrington, Gill, Waples and Argomaniz, 2007).

The conditions presented above can hardly be fulfilled ideally and some pragmatic choices are necessary. In next chapter we present a method which is designed for the study on the effectiveness of CCTV systems in eight Polish cities. Specifically, the city of Poznań is taken as an example. For the study the problem of spatially aggregated data posed the biggest problem.

DESCRIPTION OF THE DEVELOPED METHOD

Investigating the effectiveness and sustainability (durability of the effect) and effectiveness of CCTV systems in eight Polish cities were chosen, where data were available for ten years (2005-2015). The chosen cities had the most developed CCTV systems (more than 100 cameras) and the best availability of crime data within Poland. Relying on several cases increases the validity of results. The study follows the natural quasi-experiment methodology, which requires selection of experimental and control areas for each of the city. However, one of the main problems in crime analysis in Poland is the level of spatially aggregated crime data (Lisiecka, 2016). Most research concerning analysis of crime incidents relies on data comprising each reported crime incident located to exact place by geographic coordinates or (more often) to an exact address (Ceccato and Oberwittler, 2008; Boessen and Hipp, 2015; Lim, Kim, Eck and Kim, 2016). However, the lowest level of aggregation for crime incidents databases in Poland is the area of a street. The issue exists due to the internal procedures of the Polish Police. On the other hand, cameras

locations have usually exact addresses which gives an opportunity to define experimental areas as those streets on which CCTV cameras has been installed.

In order to resolve the issue of lack of exact crime data location a new method was developed. It was intended to ensure the selection of experimental and control areas, in accordance with the requirements of the method and with the guidelines of Welsh & Farrington (2003) concerning examining of CCTV systems efficiency. It aimed at overcoming the issues of spatially aggregated data.

The method of experimental areas selection is fairly easy, compared to the problem of finding appropriate control areas. Based on the literature review we adopted the following criteria:

1. the experimental area must have at least two cameras on 1 km of the street length; this criterion is to exclude the streets that were barely affected by the intervention;
2. the number of crime incidents preceding the intervention (installation of a camera) should be no less than 20 (Welsh and Farrington, 2003);
3. the total number of crime incidents should not be less than 100 in the ten years period taken for the analysis;
4. since crime incidents have been acquired for the time range of 2005-2015 we needed at least one year before and 2 years after the intervention in order to assess its impact; therefore, the next criterion was that only the streets on which the first camera was installed not earlier than in 2006 and not later than in 2013 were taken into consideration.

Concerning control areas, in order to find an appropriate one for each of pre-selected experimental area we have made the following assumptions.

First, each experimental area can have more than one control area. It is to decrease the influence of multiplicity of factors impacting unevenly crime rates across the whole study area (Cattell, 2001). For example, the distance from the city center may be a significant factor but only in a small radius which also may be connected with the number of pubs (Piza, Caplan and Kennedy, 2014). Also, different crime categories would not be affected the same way (Wolfe and Mennis, 2012). This means, that it is almost impossible to find ideal control area and it is difficult to assess how similar they are to their experimental area. Designating more than one control area gives us the opportunity to decrease the influence of uncontrolled factors on the examined effect and possible bias (Gill and Spriggs, 2005).

The second assumption concerned the crime rates themselves. A control area should have the similar number of crime incidents per kilometer of a street prior to the installation of CCTV cameras as compared to a corresponding experimental area. This fulfils the basic criterion of similarity for the control areas.

The third assumption is connected to the landscape similarity analysis (Alberti and Marzluff, 2004; Stewart and Neily, 2008). The landscape analysis is a method of modeling space and extracting knowledge from the patterns detectable in the landscape (Alberti, Marzluff, Shulenberger, Bradley, Ryan and Zumbrunnen, 2008). It allows to identify correlations of these

patterns with both processes and the functioning of a landscape system (Alberti, Marzluff, Shulenberger, Bradley, Ryan and Zumbrunnen, 2008). The research have shown, that criminal activity is also connected to the landscape variability (Wolfe and Mennis, 2012). The height or density of the buildings (Kuo and Sullivan, 2001), the abundance of green areas (Wolfe and Mennis, 2012) or the well known broken window theory (Gau, Corsaro and Brunson, 2014) are factors considered in the landscape analysis.

In its basic form, the landscape analysis uses diverse landscape metrics calculated on a raster landuse/landcover maps. Two commonly used datasets available from European Environmental Agency: Corine Land Cover and Urban Atlas are datasets that present low resolution, and aggregate data with insufficient details of the landscape diversity at the street level. They are not satisfactory for our study. Therefore we referred to a method developed by Dąbrowski (2016) to create a landcover map with ground resolution of 1 meter that presents the following classes of landcover: low buildings, medium height buildings, high buildings, constructions, dirt roads and places, paved roads and places, railroads, bridges, low vegetation (grass), medium vegetation (shrubbery), high vegetation (trees), arable land, anthropogenic land and water. This method uses GIS tools to transform an available vector topographic database (in scale 1:10 000) combined with LiDAR (Light Detection and Ranging) dataset to a high-resolution raster landcover map.

To calculate landscape metrics we also needed to define the areas for which those metrics will be calculated. For our study these were the basic spatial units, to which crime incidents were attributed. We defined them as a 40-meter buffer around the geometrical axis of each street. Next, using FRAGSTATS software (McGarigal, Cushman, Neel and Ene, 2012), we calculated the percentages of landscape covered by all the landcover classes.

Having both landcover dataset and defined areas to calculate metrics, we tested the assumption of the relationship between crime rates and landcover patterns by modeling the number of crime incidents on streets in the City of Poznań. We decided to use a metric called the percentage of landscape calculated for each landcover class (PLAND). Since the metrics were strongly cross correlated we calculated principle components for them. The results showed that more than 75% of the variance can be explained by the first three components (Tab.1).

Then, we used the components to model the number of crime incidents (Model 1) and their logarithm (Model 2). Both models showed that all variables (components) are highly significant, however the semi-logarithmic model explained more variance (Tab. 2).

Table 1. Variance explained by principle components calculated for the percentage of landscape covered by landcover classes.

	PC1	PC2	PC3	PC4	PC5	PC6	PC7
Standard deviation	13.37	12.52	8.02	7.14	6.35	3.98	3.02
Proportion of variance	0.34	0.30	0.12	0.10	0.08	0.03	0.02
Cumulative proportion	0.34	0.64	0.76	0.86	0.93	0.96	0.98

Table 2. The comparison of models estimating number of crime incidents at street level.

Significance codes:

*** – p -value < 0.001; ** – p -value < 0.01.

	Model 1		Model 2	
Function	Crime ~ PC1 + PC2 + PC3		log(Crime) ~ PC1 + PC2 + PC3	
	PC1	< 0.001 ***	< 0.001 ***	
Coefficient p -value	PC2	< 0.001 ***	< 0.001 ***	
	PC3	0.002 **	< 0.001 ***	
R^2		0.108	0.281	
p -value		< 0.001 ***	< 0.001 ***	

After testing the assumption of relationship between landscape diversity and crime rates, we used the PLAND metric to calculate the similarity (measured by Euclidean distance) between the experimental and the pre-selected control areas.

In short, basing on the above-mentioned assumptions we have selected the control areas using the following method.

1. First we aggregated quarterly crime incident data for each street and standardized the by dividing by the length of the street.
2. Second, to find control areas of similar crime rate patterns, we calculated the Euclidean distance for each experimental area, i.e.

$$d(p, q) = \sqrt{\sum_{i=1}^n (q_i - p_i)^2}.$$

The formula is calculated for the number of crime incidents per kilometer in each quarter prior to the intervention between the experimental area and every street that could become its control area. This allowed us to select 10 most similar (in terms of crime rates prior to the intervention) control areas. These streets, however, could have had similar time series due to sheer coincidence (which could happen especially for short time series like 1 year). Therefore, it had to be evaluated considering similarity of landscape as well.

3. Finally, we evaluated the similarity of the landscape between the experimental area and its pre-selected control areas. We used the same method, i.e. calculated the Euclidean distance, but this time regarded the landscape metrics.

APPLICATION OF THE METHOD TO A CASE STUDY

Our study was conducted for the city of Poznań. It is located in Western Poland and has about 556 000 inhabitants (Census 2011). The police dataset, including crime incidents, was acquired

for the period of 2005-2015. At this time 56 773 crime incidents have been reported in four categories, which were taken into consideration: a) battering (street fight); b) theft from a car; theft of a car and breaking into a car; c) damaging car; d) robbery.

Poznań has almost 2300 streets in Poznań, out of which the analyzed categories of crimes have been registered on 1798. Cameras were installed on 210 streets, but only 106 streets had cameras installed between 2006 and 2013 (this period includes one year prior and 2 years after the intervention). Only 24 streets from the selected ones had more than 100 crime incidents during the analyzed period and 22 of them had more than 20 crime incidents prior to intervention. After excluding from the analysis areas with less than 2 cameras per kilometer of the street, we reached 11 possible experimental areas.

In Poznań the interventions – installation of CCTV cameras – took place between 2010 and 2013. Therefore, to calculate the Euclidean distance between two time series, we aggregated quarterly the crime incidents and calculated the distance for all the data before 2010. Figure 1 shows the similarity between time series of the experimental area and one of its preselected control areas – Naramowicka street. Both streets are congested streets as they are the main access roads to the city center.

After selecting ten most similar streets in context of time series, we calculated the distance between the PLAND landscape metrics. Figure 2 presents how both streets look like on raster land-cover maps.

Overall distances of all 10 preselected control areas to corresponding experimental areas can be shown on a scree plot (Figure 3). Distances between time series of criminal events are on the vertical axis and distances between landscape metrics are on the horizontal axis. The smaller the values, the more similar control area to the experimental area. From this plot we can select the most similar streets: Naramowicka and Murawa.

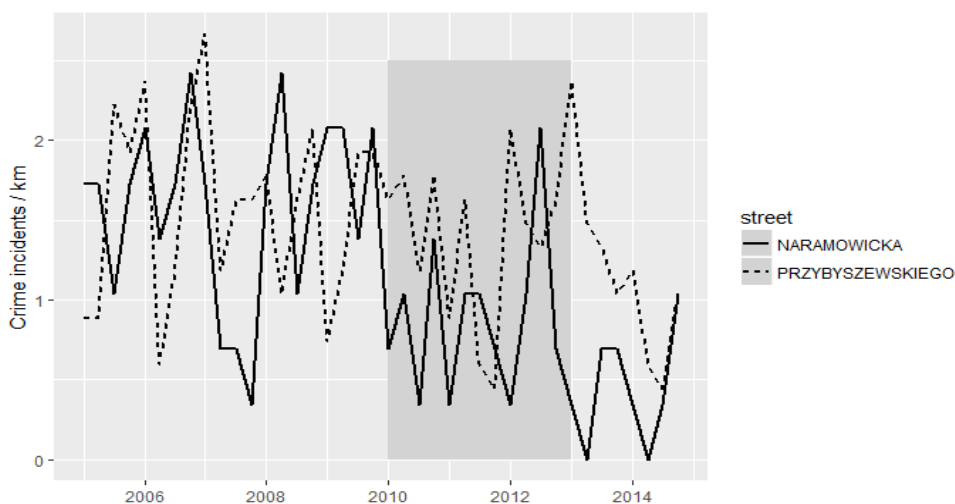


Fig. 1. Time series of crime incidents on Przybyszewskiego and Naramowicka streets.

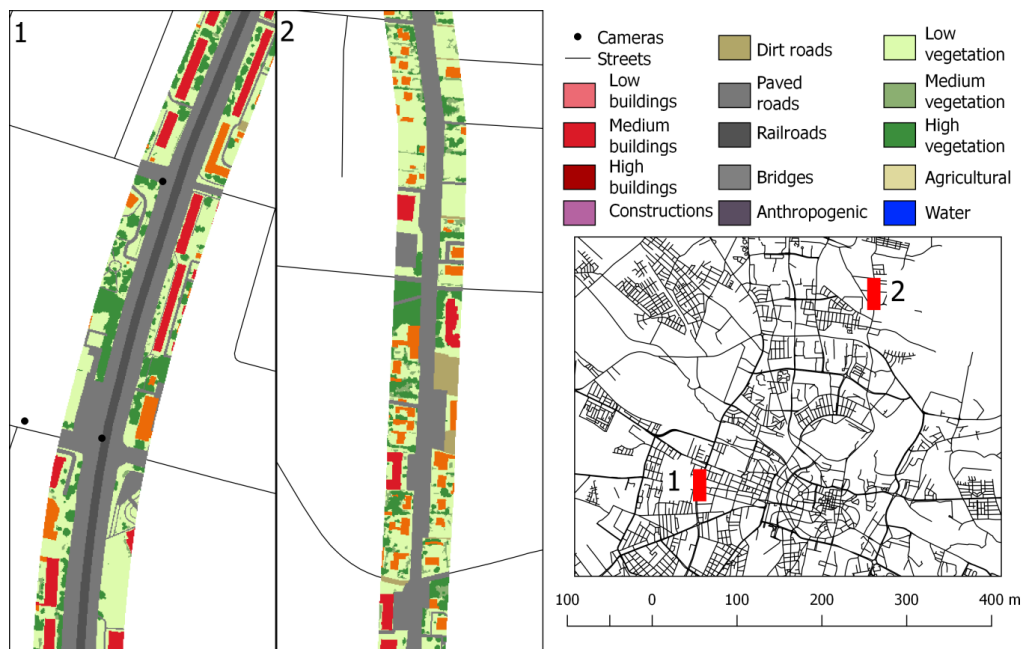


Fig. 2. On the left: parts of Przybyszewskiego (1) and Naramowicka (2) landscapes. On the right: streets location in Poznań.

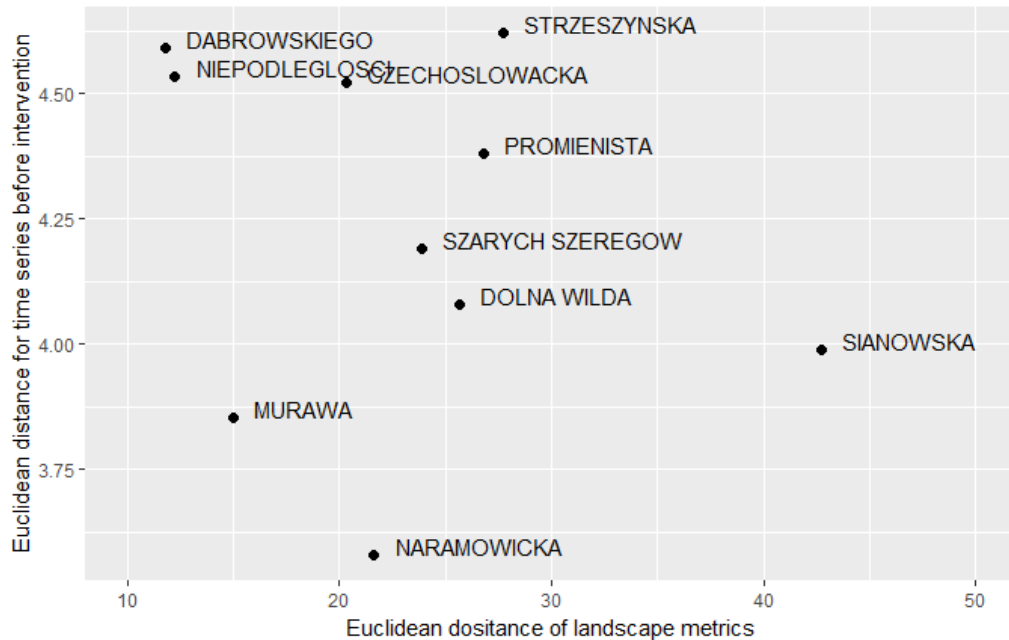


Fig. 3. The similarity of control areas to experimental area (Przybyszewskiego street).

DISCUSSION

The method presented in this paper overcomes the difficulty perform CCTV effectiveness analysis via the quasi experimental method in case of spatially aggregated crime incidents or data without exact locations. It applies for the similarity of crime occurrence time series prior to the intervention and the similarity of the landscape. Its advantage over the alternative selection methods, based on expert knowledge, is its reproducibility of experimental and control areas.

In this paper we used Euclidean distance as a similarity measure for time series proximity. For each pair of values, small differences are suppressed towards zero and large ones are penalized. Euclidean distance is a special case of L_p -norm distance (where $p = 2$). Further evaluation of our method should focus on selecting similarity measure. It should not be limited to checking different p (e.g. $p = 1$ equals to Manhattan distance) but it should carefully deliberate on the following question: which families of the similarity measures (or possibly their combinations) are suitable for the discussed problem? (Friedman, Hastie and Tibshirani, 2001; Aggarwal and Reddy, 2013).

More research is needed to analyze the relationship between landscape and crime incidents. It is possible, that other landscape metrics, such as the size of patches, or the Shannon diversity index, can explain more variance in crime incidents. Therefore, in comparison with the percentage of landscape that is covered by landcover classes, they may be better measures to assess the landscape similarity.

REFERENCES

- Aggarwal, C. C. and Reddy, C. K. (2013) *Data clustering: algorithms and applications*. CRC press, Boca Raton, FL.
- Alberti, M. and Marzluff, J. M. (2004) Ecological resilience in urban ecosystems: Linking urban patterns to human and ecological functions, *Urban Ecosystems*, 7(3), pp. 241–265. doi: 10.1023/B:UECO.0000044038.90173.c6.
- Alberti, M., Marzluff, J. M., Shulenberger, E., Bradley, G., Ryan, C. and Zumbrunnen, C. (2008) Integrating humans into ecology: Opportunities and challenges for studying urban ecosystems, *Urban Ecology: An International Perspective on the Interaction Between Humans and Nature*, 53(12), pp. 143–158. doi: 10.1007/978-0-387-73412-5_9.
- Boessen, A. and Hipp, J. R. (2015) Close-Ups and the Scale of Ecology: Land Uses and the Geography of Social Context and Crime, *Criminology*, 53(3), pp. 399–426. doi: 10.1111/1745-9125.12074.
- Brown, B. (1995) *CCTV in Town Centres: Three Case Studies, Crime Detection and Prevention Series*. Police Research Group, London.
- Caplan, J. M., Kennedy, L. W. and Petrossian, G. (2011) Police-monitored CCTV cameras in Newark, NJ: A quasi-experimental test of crime deterrence, *Journal of Experimental Criminology*, 7(3), pp. 255–274. doi: 10.1007/s11292-011-9125-9.
- Cattell, V. (2001) Poor people, poor places, and poor health: The mediating role of social networks and social capital, *Social Science and Medicine*, 52(10), pp. 1501–1516. doi: 10.1016/S0277-9536(00)00259-8.

- Ceccato, V. and Oberwittler, D. (2008) Comparing spatial patterns of robbery: Evidence from a Western and an Eastern European city, *Cities*, 25(4), pp. 185–196. doi: 10.1016/j.cities.2008.04.002.
- Cook, T. D., Campbell, D. T. and Shadish, W. (2002) *Experimental and quasi-experimental designs for generalized causal inference*. Houghton Mifflin Boston.
- Dąbrowski, A. (2016) Metodyka opracowywania szczegółowych map pokrycia terenu na podstawie istniejących źródeł danych przestrzennych [The methodology for creating high-resolution land cover data from the existing spatial data], *Problemy Ekologii Krajobrazu*.
- Farrington, D. P. (1997) Evaluating a community crime prevention program, *Evaluation*, 3(2), pp. 157–173. doi: 10.1177/135638909700300203.
- Farrington, D. P., Gill, M., Waples, S. J. and Argomaniz, J. (2007) The effects of closed-circuit television on crime: Meta-analysis of an English national quasi-experimental multi-site evaluation, *Journal of Experimental Criminology*, 3(1), pp. 21–38. doi: 10.1007/s11292-007-9024-2.
- Friedman, J., Hastie, T. and Tibshirani, R. (2001) *The elements of statistical learning*. Springer, New York, NY.
- Gau, J. M., Corsaro, N. and Brunson, R. K. (2014) Revisiting broken windows theory: A test of the mediation impact of social mechanisms on the disorder-fear relationship, *Journal of Criminal Justice*, 42(6), pp. 579–588. doi: 10.1016/j.jcrimjus.2014.10.002.
- Gill, M. and Spriggs, A. (2005) *Assessing the impact of CCTV*, Home Office Research, Development and Statistics Directorate. Available at: https://www.cctvusergroup.com/downloads/file/Martin_gill.pdf.
- Heidensohn, F. and Farrell, M. (1993) *Crime in Europe*. Routledge, London. doi: 10.4324/9780203423158.
- Kennedy, E. and Kennedy, L. W. (2004) Using dasymetric mapping for spatially aggregated crime data, *Journal of Quantitative Criminology*, 20(3), pp. 243–262. doi: 10.1023/B:JOQC.0000037733.74321.14.
- Kuo, F. E. and Sullivan, W. C. (2001) Environment and crime in the inner city does vegetation reduce crime?, *Environment and Behavior*, 33(3), pp. 343–367. doi: 10.1177/0013916501333002.
- Lim, H., Kim, C., Eck, J. E. and Kim, J. (2016) The crime-reduction effects of open-street CCTV in South Korea, *Security Journal*, 29(2), pp. 241–255. doi: 10.1057/sj.2013.10.
- Lisiecka, K. (2016) *GIS in the analysis of the diversity of space - time crime on the example of Ponań*, Arcana GIS. Available at: <http://www.arcanagis.pl/gis-w-analizach-zroznicowania-czasoprzestrzennego-przestepczosci-na-przykladzie-poznania/>.
- McGarigal, K., Cushman, S. A., Neel, M. C. and Ene, E. (2012) FRAGSTATS v4: Spatial Pattern Analysis Program for Categorical and Continuous Maps, *University of Massachusetts, Amherst, MA*. URL <http://www.umass.edu/landeco/research/fragstats/fragstats.html>, (2007). doi: citeulike-article-id:287784.
- Piza, E. L., Caplan, J. M. and Kennedy, L. W. (2014) Analyzing the Influence of Micro-Level Factors on CCTV Camera Effect, *Journal of Quantitative Criminology*, 30(2), pp. 237–264. doi: 10.1007/s10940-013-9202-5.

- Planells S., S. (2015) *Essays on the Economics of Crime: Determinants of Crime in an Urban Context, TDX (Tesis Doctorals en Xarxa)*. Universitat de Barcelona.
- Raphael, S. and Winter - Ebmer, R. (2001) Identifying the Effect of Unemployment on Crime, *The Journal of Law and Economics*, 44(1), pp. 259–283. doi: 10.1086/320275.
- Salkind, N. (2007) *Encyclopedia of Measurement and Statistics*. SAGE Publications, Inc, Thousand Oaks. doi: 10.4135/9781412952644.
- Squires, P. (1998) *Evaluation of the Ilford Town Centre CCTV System*. Brighton.
- Stewart, B. and Neily, P. (2008) *A Procedural Guide For Ecological Landscape Analysis*. Truro, NS. Available at: <https://novascotia.ca/natr/forestry/reports/Procedural-Guide-For-Ecological-Landscape-Analysis.pdf>.
- Stucky, T. D. and Ottensmann, J. R. (2009) Land use and violent crime, *Criminology*, 47(4), pp. 1223–1264. doi: 10.1111/j.1745-9125.2009.00174.x.
- La Vigne, N. G., Lowry, S. S., Markman, J. A. and Dwyer, A. M. (2011) *Evaluating the Use of Public Surveillance Cameras for Crime Control and Prevention*. Washington, DC. Available at: <https://www.urban.org/sites/default/files/publication/27546/412401-Evaluating-the-Use-of-Public-Surveillance-Cameras-for-Crime-Control-and-Prevention-A-Summary.PDF>.
- Welsh, B. C. and Farrington, D. P. (2003) Effects of closed-circuit television on crime, *Annals of the American Academy of Political and Social Science*, 587(1), pp. 110–135. doi: 10.1177/0002716202250802.
- Wolfe, M. K. and Mennis, J. (2012) Does vegetation encourage or suppress urban crime? Evidence from Philadelphia, PA, *Landscape and Urban Planning*, 108(2–4), pp. 112–122. doi: 10.1016/j.landurbplan.2012.08.006.

THREAT OF POLLUTION HOTSPOTS REWORKING IN RIVER SYSTEMS: EXAMPLE OF THE PLOUČNICE RIVER (CZECH REPUBLIC)

Jitka, ELZNICOVÁ¹; Tomáš, MATYS GRYGAR¹; Martin, SIKORA¹;
Jan, POPELKA¹; Michal, HOŠEK¹; Petr, NOVÁK¹

¹ Faculty of Environment, J.E. Purkyně University in Ústí nad Labem, Králova výšina 7,
40096 Ústí nad Labem, Czech Republic

*jitka.elznicova@ujep.cz; grygar@iic.cas.cz; sikoramartin26@gmail.com;
jan.popelka@ujep.cz; psitlapa@seznam.cz; petr.novak@ujep.cz*

Abstract

Mapping and evaluation of historically polluted fluvial sediments is an urgent topic as they may endanger quality of water and solids transported by rivers and thus impact biota including humans. The polluted sediment reworking may be triggered by floods and sometimes also by river engineering or revitalisation. A combination of diverse methods including geoinformatics allows pollution hotspots identification in floodplains and evaluation of their potential for their future reworking.

The Ploučnice River and its floodplain were polluted by local uranium mining (U-mining) in 1971–1989. This river has been studied since 2013 in aim to identify the relationship between the floodplain geomorphology and the spatial distribution of pollutants. Archive information on pollution history and past floods, old maps and aerial photographs, and older low-resolution gamma activity aerial survey were collected to understand the floodplain development and pollution heterogeneity. Afterwards, digital terrain model based on publically available LiDAR data (airborne laser scanning) was used to identify the sites of river channel shifts with GIS analysis. Finally a non-invasive geochemical mapping started, using portable X-ray fluorescence (XRF) and gamma spectrometers. The resulting datasets were processed by spatial statistical methods.

One of the main outputs of our study was the detailed analysis of pollution distribution in the floodplain. The results showed a relationship between deposition of polluted sediments and the past channel shifts. We found that an increased concentration of pollution occurred mainly in the cut-off meanders and lateral channel deposits from the period of mining, the latter being endangered by reworking (turning back to the river) in next decades.

Keywords: geomorphic analysis, portable analytical instruments, geostatistical interpolation, pollution distribution

INTRODUCTION

The rivers and their floodplains not only store historical pollution, but they also rework it and return it to the river transport. It is noteworthy that the first studies devoted to risks of reworking historically polluted fluvial sediments appeared in the domain of geomorphology (Miller, 1999; Ciszewski, 2001; Foulds et al., 2014). Also polluted floodplains in the Czech Republic represent environmental risk due to sediment reworking (Matys Grygar et al., 2014; Nováková et al., 2015).

Geographic information systems (GIS) offer very useful tools for study of spatiotemporal changes of rivers and provide perfect material for fluvial geomorphologic evaluation. GIS first used aerial photographs, then satellite images. Currently the main GIS tool for fluvial geomorphology is airborne scanning by LIDAR, which can produce very precise digital terrain models (Wohl, 2014).

Studies of polluted floodplains are facilitated by geophysical imaging and pollution mapping by portable analytical instruments, including in situ analyses (without any sample pre-treatment) (Matys Grygar et al., 2016; Faměra et al., 2018). Geophysical imaging, particularly methods acquiring electrical resistivity may save a lot of work associated with identification of sediment bodies within a floodplain, which is essential for floodplain studies (Houben, 2007; Notebaert et al., 2011). The performance of the resistivity imaging in floodplain studies has been demonstrated in Matys Grygar et al. (2013); Stacke et al.(2014); Matys Grygar et al., (2016); Faměra et al. (2018).

In the last decade portable analytical methods, in particular portable X-ray fluorescence (XRF), have achieved quality suitable for research in geology and monitoring in environmental sciences (Gałuszka et al., 2015). In environmental geochemistry portable XRF is mainly used for fast pollution survey and mapping (Hürkamp et al., 2009; Weindorf et al., 2012; Parsons et al., 2013; Brumbaugh et al., 2013). Portable gamma and XRF spectrometers also bring progress in detailed mapping of pollution by radionuclides (Kühn, 1996; Martin et al., 2015; Hošek, 2015; Slabá et al., 2015; Matys Grygar et al., 2016).

XRF offers a lot of advantages (Gałuszka et al., 2015): it has much lower operation costs, needs much less demanding sample preparation and it can even be used in situ in real time (each XRF "shot" lasts about 1 minute and results are immediately displayed). XRF can also serve for characterisation of sediment grain size, which is a factor essential for understanding floodplain sedimentary bodies (Notebaert et al., 2011; Matys Grygar et al., 2016). Most chemical elements (both polluting and lithogenic) are grain-size sensitive in chemically mature sediments. For example, aluminium to silicon (Al/Si) is considered "a surrogate" for grain size of fluvial sediments (Grygar et al., 2010; Bouchez et al., 2011; Bábek et al., 2015) because in mature sediments it increases with growing percentage of clay fraction (usually dominated by aluminosilicate clay minerals) at the expense of sand (usually dominated by quartz). Adversely, zirconium to rubidium (Zr/Rb) ratio in sediments is proportional to the content of coarser particles (Dypvik and Harris, 2001; Jones et al., 2012), because Zr is mainly in zircon (typical grain size about 0.1 mm) and Rb is mainly in finer particles of clay minerals (in mature sediments). XRF is suitable for analysis of both pollutants (risk elements) and lithogenic elements, including those of which determination by common methods like acid dissolution and ICP spectrometry is not possible, e.g., Si. In sediments concentrations of lithogenic elements are required for grain-size correction of the risk element concentrations to distinguish pollution from natural variability (Vijver et al., 2008; Grygar et al., 2010; Jiang et al., 2013; Matys Grygar et al., 2014; Guo et al., 2014; and Wang et al., 2015). The simplest grain-size correction is geochemical normalisation, e.g., expression of pollution extent as a ratio of risk element to lithogenic element such as Al, iron (Fe), Rb, titanium (Ti) (Matys Grygar and Popelka, 2016), which also corrects

for non-ideality of in situ XRF measurement (Löwemark et al., 2011). In situ XRF analysis for dense geochemical mapping opens new perspectives in analysis of polluted soils and sediments.

There are two ways how GIS approaches can contribute to the pollution mapping in floodplains: (1) geographic and geostatistic tools are essential for qualified imaging and interpretation of the results of floodplain mapping and (2) GIS systems considerably facilitates geomorphic interpretations by providing materials (maps, vectorised past channel positions, digital elevation models) for evaluation of floodplain past and future evolution. Hereafter questions of how GIS tools can help to understand the pollution hotspots were addressed, which have been empirically found in floodplains, and how GIS and geomorphic evaluation can help to predict the risk of remobilisation of pollutants from those hotspots. Using of these instruments has been demonstrated in this case study in study area "Martinova louka" (MS).

Study area

The Ploučnice River, a right bank tributary of the Labe (the Elbe) River, is 106 km long and drains 1194 km² of the Northern Bohemia, Czech Republic (Fig. 1). The source rocks in the catchment of the study areas are mainly Cretaceous sandstones, siltstones and marls; minor proportion of sediments is derived from isolated bodies of Cenozoic volcanics present mainly in form of individual hills with poor connection to the trunk river. Mean discharge is 2.30 m³/s in Mimoň, and 4.90 m³/s in Česká Lípa. In the upper reach downstream from Osečná, it has a gradient up to 33.8 ‰; while in the lower stream west of Žandov, it is approximately 7 ‰. In the middle part of the flow, where the uranium mining (U-mining) pollution was deposited, the slope decreases on average to about 0.8 ‰; in the section between Hradčany and Česká Lípa to 0.6 ‰ (Vitáček et al., online).

The Ploučnice River in the studied localities (Fig. 1) is actively meandering with valley gradient of only 0.6–1 ‰ and floodplain width of 100–200 m. The floodplain inundation is more or less annual; floods are currently caused mainly by summer local precipitation extremes. Frequent overbank flows precluded any intense agricultural use of the floodplain; crop fields in historical maps were located only in terraces above the active floodplain, while only meadows in the floodplain according to Stable Cadastre map (1843). The fluvial deposits have lithologies ranging from fine gravel to mud in channel, sand to silt in lateral sediment bodies (bars) and mud (silt and clay) in floodplain.

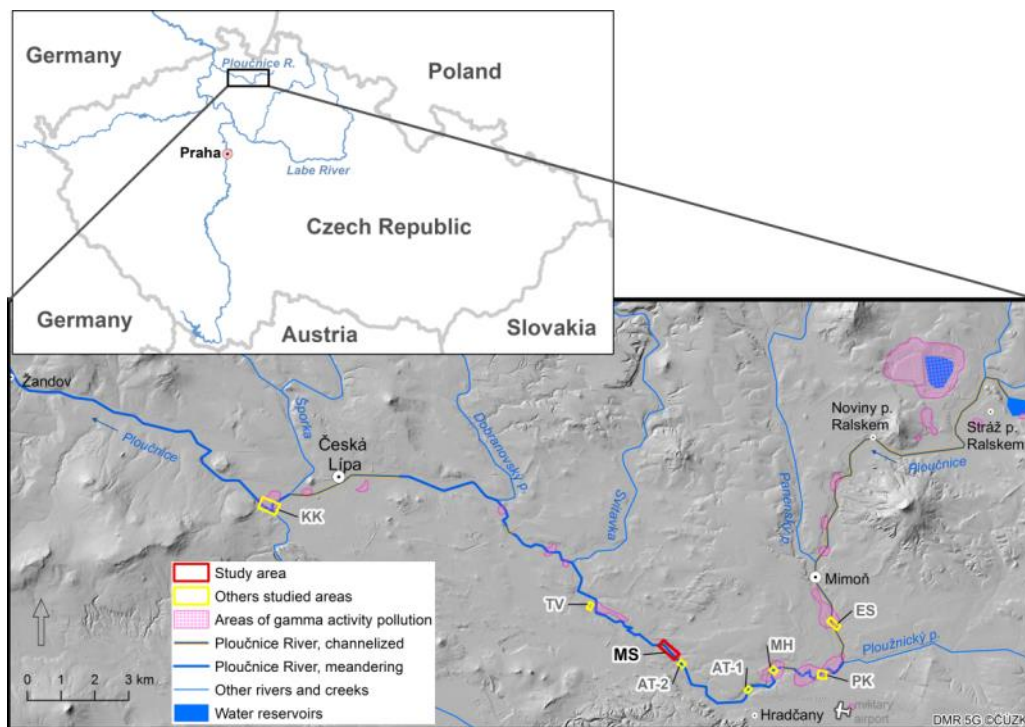


Fig. 1. Map of the study area (red colour) and previously studied areas (yellow colour)

Pollution history of Ploučnice River and its floodplain

Local industrial enterprises, regional metallurgy and coal combustion since the turn of 19th and 20th century (Novák et al., 2003) caused diffuse pollution of the waste areas of the Czech Republic (Matys Grygar et al., 2012; 2013) including the Ploučnice floodplain (Matys Grygar et al., 2014; Majerová et al., 2013). Local industries in the Panenský Creek, a right side tributary of the Ploučnice River, brought Pb and Zn pollution (Kühn, 1996; Hrdoušek, 2005). Considerable pollution of the Ploučnice River between towns of Stráž pod Ralskem and Česká Lípa has been caused by U-mining, which started at the turn of 1960s and 1970s; pollution of the Ploučnice River system followed nearly immediately (Kühn, 1997; Kafka, 2003; Slezák, 2000; Matys Grygar et al., 2014). The main pollutants from U-mining were radium (^{226}Ra), the main gamma emitting radionuclide in the polluted areas, uranium (U) and less dangerous free acids, nickel (Ni) and zinc (Zn) (Kühn, 1996; Kafka, 2003; Matys Grygar et al., 2014). In summer 1981 a local precipitation extreme caused flood exceeding 50-years river discharge (Q_{50}) in the middle river reach; it was the worst flood during the second half of the 20th century. Hanslík (2002) and Kühn (1997) stated that event to have caused transport of considerable amount of particulate radionuclides from the mining area to the Ploučnice River.

The primary pollution from the mining area was terminated in the second half of the 1980s when hydrodynamic barriers (series of drill cores controlling the underground move of fluids) stopped overflows of the solutions from the in situ leaching fields to the underground mines. Nearly

simultaneously with that a sewage disposal plant was built and run into operation. Soon after those measures the U-mining was dampened (Slezák, 2000; Kafka, 2003).

The results of airborne survey by gamma spectrometry at 250 m spatial grid (Gnojek et al., 2005) revealed several pollution hotspots in the Ploučnice River floodplain between Mimoň and Česká Lípa (Fig. 1). In the early 1990s, floodplain sediments were cored and analysed in one hotspot (Kühn, 1996) and ten years later Ploučnice channel sediments were analysed (Kolář, 2004; Hrdoušek, 2005), but the importance of fluvial processes in pollutant deposition and spread was not discussed in those early works. So far, a systematic study of the floodplain started in order to understand and interpret the pollutant distribution there and the reasons for the existence of contrasting gamma activity hotspots (Matys Grygar et al., 2014; 2016; Hošek, 2015).

MAPPING METHODS

Data processing

To understand the floodplain development and pollution heterogeneity, archive materials of the study area, information on pollution history, past floods and old maps and aerial photographs were collected (Fig. 2). Datasets for GIS analysis were purchased from the Czech Office for Surveying, Mapping and Cadastre (Imperial Obligatory Imprints of the Stable Cadastre, archive orthophoto from 1999 to recent orthophoto from 2015; ©ČÚZK), Geoinformatics Laboratory, J.E. Purkyně University (2nd Austrian Military Survey, 1836–1852; © UJEP), and Military Geographic and Hydrometeorology Office (aerial photos from 1938 till 1992; ©MO ČR). Aerial photos were orthorectified in Agisoft PhotoScan software.

The laser scanning dataset from 2010 (DMR 5G, © ČÚZK) was used to create a detailed digital elevation model; on its base a detailed geomorphologic analysis of the area was performed.

Data processing, analysis and visualisation were made in ArcGIS Desktop 10.4 with extension 3D Analyst. River channels were vectorised. The channel parameters (length, slope, and sinuosity) and changes of the Ploučnice River (straightening, lateral shifts, meander evolution, eventual cut-off) were analysed using spatial analysis.

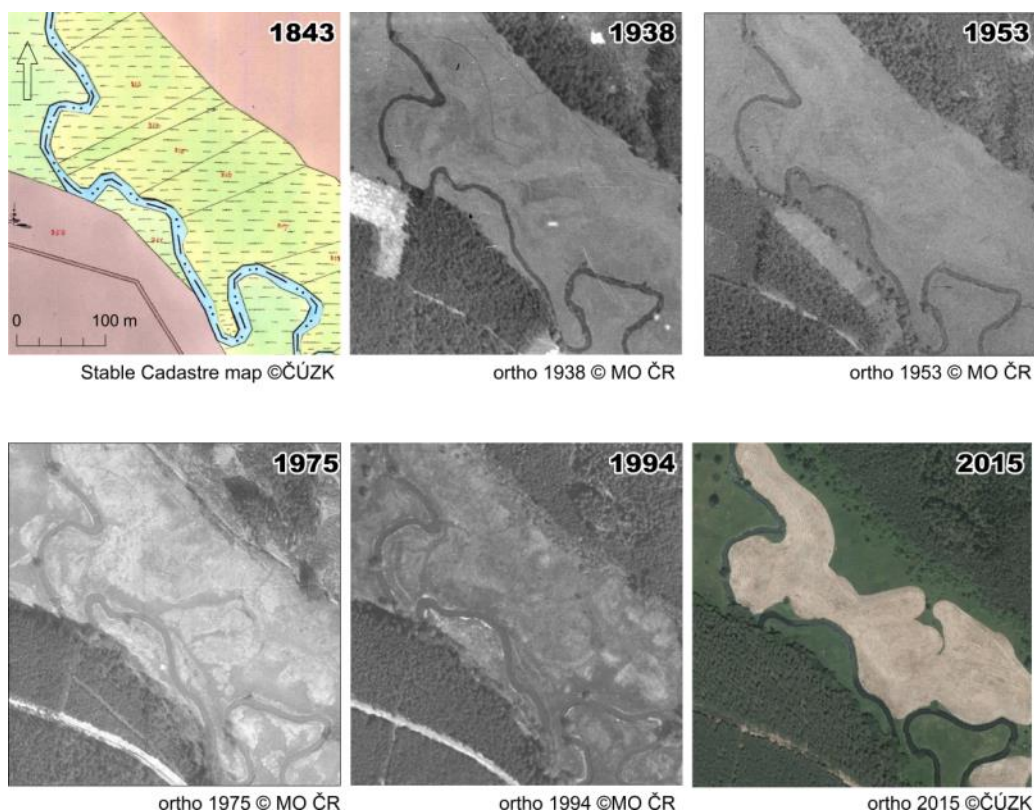


Fig. 2 Stable Cadastre map and archive orthophotos of study area

SAMPLING METHODS

Using the GIS analysis, the hotspots of river changes were identified and a non-invasive geophysical imaging was started there. Historical low-resolution map, based on aerial gamma spectrometry, which was performed with the handheld gamma spectrometer GT-30 (Georadis, Brno, Czech Republic) in 2005, was also used. Formal resolution of the interpolated gamma activity raster was about 25 m, but the distance between individual neighbouring measurement points was approx. 250 m.

The study area was scanned also by a drone from a height of 50 meters. The micro-UAV system SteadiDrone EI8HT with a Sigma 35 mm f/1.4 DG HSM Nikon lens and stabilization device (gimbal) was used.

Based on the resulting maps, the floodplain sediments were analysed by non-destructive in situ methods. The contamination of the floodplain was analysed mainly by two portable (handheld) instruments. The gamma-spectrometer DISA 400A or GT-30 were used for measuring the total surface gamma activity (main target nuclide was ^{226}Ra). Very effective was also the use of portable XRF Olympus Innov-X (DELTA Premium), which provides fast analysis of more than 30 elements, such as pollutants (Ba, Ni, Pb, U and Zn) and grain-size sensitive lithogenic elements (Al, Fe, Rb, Si, Zr). All instruments can be connected to GPS to obtain geographic coordinates.

Acquired data can be visualised in GIS (see Fig. 3). The drone mapping lasted about 2 hours, the gamma radiation mapping about 7 hours, and the XRF mapping about 25 hours.

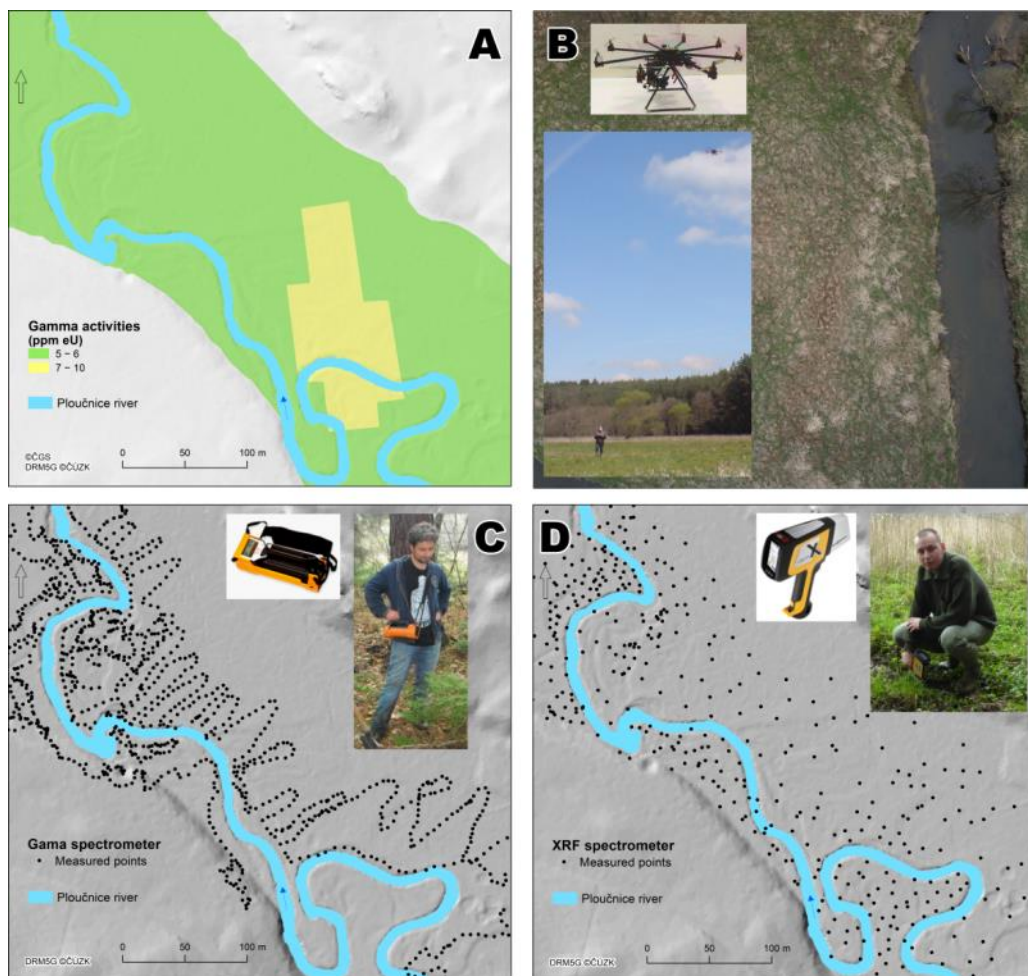
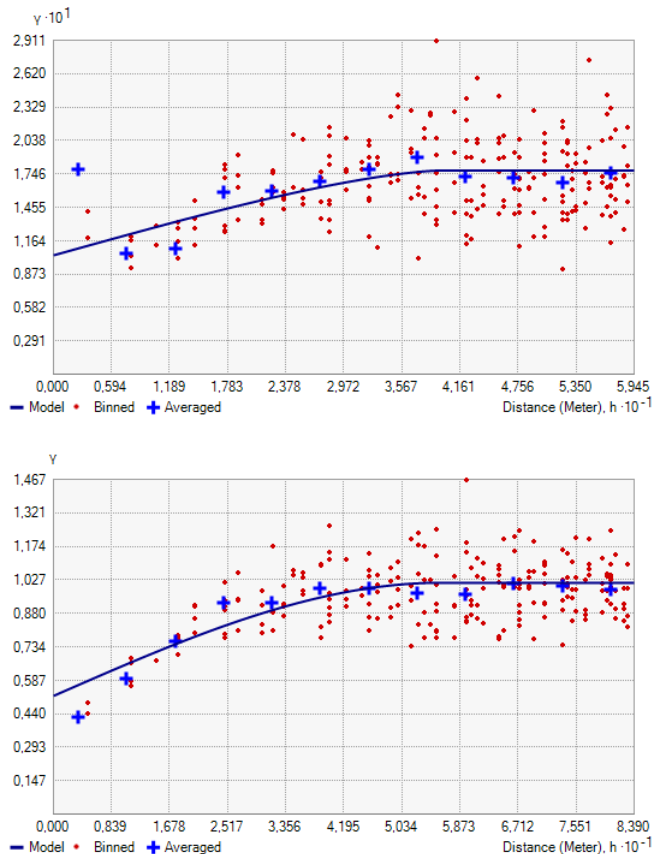


Fig. 3 Mapping instruments: low resolution gamma activity survey (A), drone and detail of high resolution image (B), gamma spectrometer and measuring points (C), XRF spectrometer and measuring points (D).

The geostatistical interpolation was performed to create statistically valid prediction of surface gamma activity, concentrations of Zn and U and relative ratios of selected elements. The data were transformed using normal score or logarithmic transformation at first and the surface in the data trend was removed with estimated constant value (see Table 1). In the next step the simple kriging method was applied along with optimal semivariogram function (see Fig. 4) chosen from a group of functions (stable, exponential, spherical, circular or J-Bessel), as the function provided the closest value of RMSPE to one (root mean square standardized prediction error; calculation based on Cross-Validation method). For detailed information about selected semivariogram functions and estimated parameters see Table 1. According to Oliver and Webster (2014) the minimum number of points in the interpolation neighbourhood was set to 7 and maximum to 25.

Table 1 Parameters of geostatistical interpolation (simple kriging)

XRF Value	Est. trend constant	Semivariogram function	Nugget	Partial Sill	Major Range	RMSPE
U	-6.306	Spherical	0.098	0.078	41.455	0.927
U/Fe	0.001	Circular	0.864	0.079	41.316	1.068
Zn	0.019	Spherical	0.519	0.496	55.936	1.035
Zn/Fe	0.011	Circular	0.761	0.238	27.933	1.004
Al/Si	0.303	J-Bessel	0.381	0.614	113.408	0.977
Zr/Rb	4.903	Circular	0.237	0.631	58.651	1.065

**Fig. 4.** Estimated optimal semivariogram function for U (above) and Zn (below).

RESULTS

River Dynamics and Engineering

The channel position of the Ploučnice River was analysed using GIS tools. To understand the floodplain development, old maps, aerial photographs and digital elevation model were used. The total channel length between Stráž pod Ralskem and Žandov (Fig. 1) decreased from 76.5 km (2nd Austrian Military Survey, 1836–1852) to 66 km (in 2011). Main changes of the river channel have been caused by channel straightening designed to prevent damages by floods and U-mining

pollution between Stráž pod Ralskem and Mimoň. Channel regulation was engineered also around Česká Lípa (Elznicová and Hrubešová, 2017). Due to the channel straightening, the sinuosity decreased from 2.56 to 2.22 and the gradient increased by 0.02‰.

Natural meandering in the middle reach of the river in the U-mining period took place in the territory between Mimoň and Česká Lípa towns. Lateral channel instability is an important feature of the middle river reach. The floodplain deposits of the Ploučnice are sandy to silty and the river channel has shown lateral shifts in the order of 10^0 to 10^1 m and several meander cut-offs during the U-mining period. The lateral shifts of the river channel have reworked sediments and thus continuously created novel sediment accommodation space. Overview of changes in the channel positions from aerial photos in study area is shown in Fig. 5.

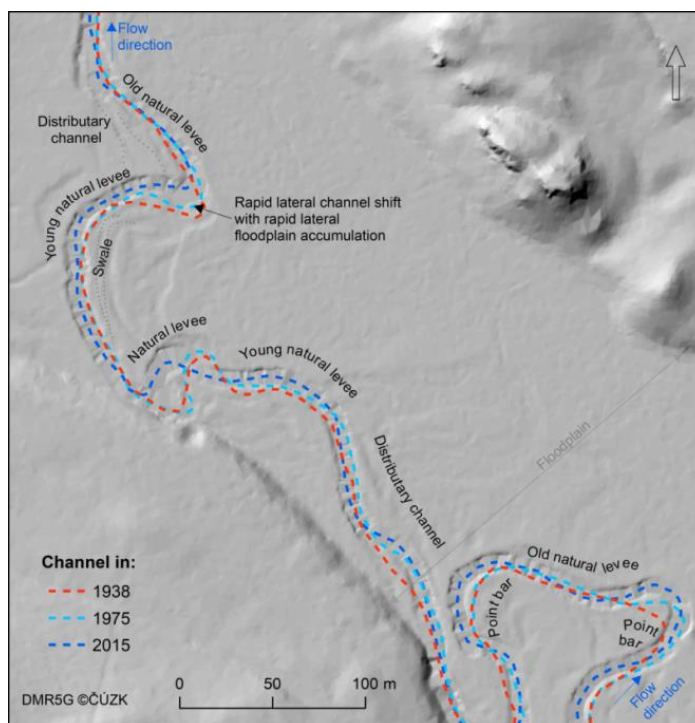


Fig. 5. Historical channel position and interpreting of geomorphologic features in study area.

Pollution mapping

This study area (Fig. 1) was the largest area, which we have subjected to high-resolution surface gamma activity and geochemical mapping yet. The area is more remote from the U-mining location than hotspot in Boreček studied previously (Kühn, 1996; Matys Grygar et al., 2014; 2016), as well as far from any river engineering. The study area seemed unpolluted or only very weakly polluted in low-resolution airborne gamma radiation survey (Fig. 3), however smaller but considerably polluted places were found here (Fig. 3, 6).

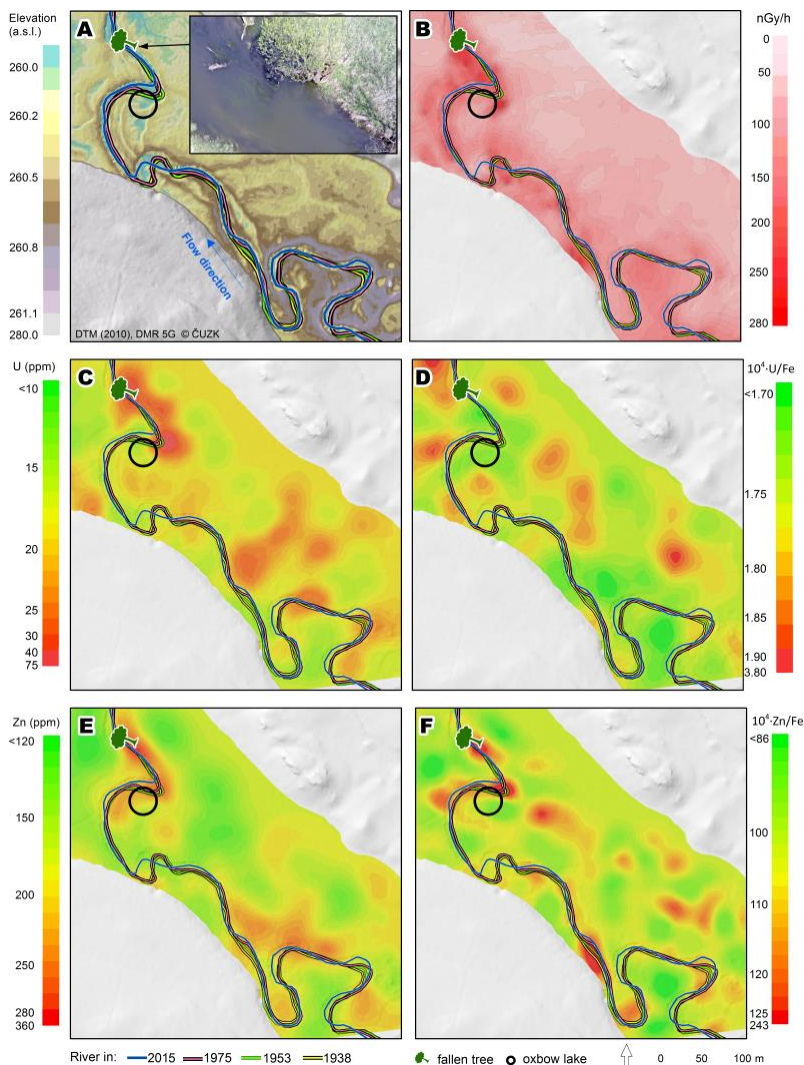


Fig. 6. Study area downstream from Hradčany. DTM and aerial photograph (panel A), the gamma activity map (panel B) and the XRF maps of U (panel C), U/Fe (panel D), Zn (panel E) and Zn/Fe (panel F). Historical channel positions are also shown. Inset in panel A shows aerial photograph of the tree remnant in the channel.

The main local pollution hotspot in the study area was revealed by both XRF and gamma radiation surveys in a place of the channel reorganisation during the U-mining period and in the nearby floodplain (Fig. 6 and 7, near the pictogram of a fallen tree and just upstream from that). Fast lateral channel shift resulted there according to historical aerial photographs in in-channel deposition between 1953 and 2008. There is still a small oxbow lake in that site (marked by circle in Fig. 6) and hence until now the surface topography clearly reveals the former channel shifts there. On a place very close downstream, remnants of a tree trunk base were found on the right bank, the trunk fragment in the channel and branches from the top of that tree crown on the left bank. The position of the fallen tree is marked in Fig. 6, in detail the tree remnants are shown in

UAV photograph in the inset in Fig. 6A. The trunk in the channel has inevitably become a hindrance to the water flow; it has therefore enhanced overbank flow and deposition of sediments in the proximal floodplain during floods. That main pollution hotspot is clearly discernible by elevated concentrations of Zn and U (Fig. 6C and 6E) as well as Zn/Fe (Fig. 6F). The polluted sediment there has larger mean grain size (lower Al/Si and higher Zr/Rb, see Fig. 7) and is situated in an elevated ridge along the channel obviously indicating that the hotspot is situated on top of natural levee.

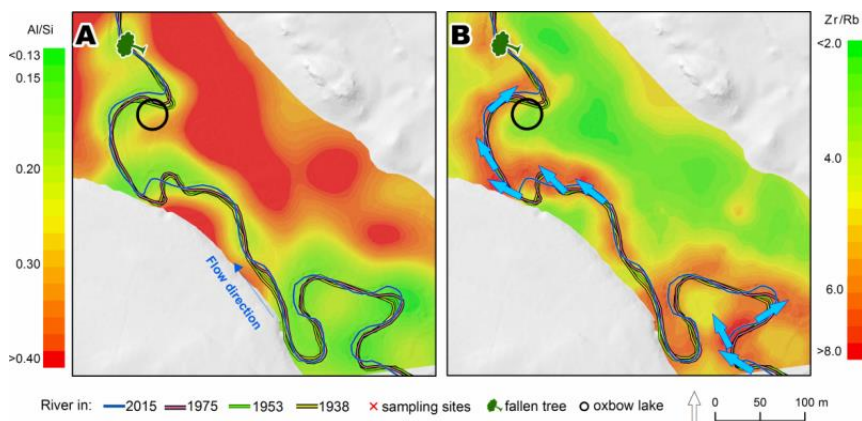


Fig. 7. Maps of Al/Si and Zr/Rb ratios. Blue arrows indicate enhanced transport paths of overbank clastics as extrapolation of flow directions; they point to areas with coarser overbank sediments, where GR and XRF mapping produced markedly different results.

In other sites of the study area the XRF and gamma activity mappings produced remarkably different images. Several gamma activity hotspots were found in the meander belt, i.e. tightly along the river channel in places of lateral recent channel shifts (Fig. 6B), where only medium surface concentrations of chemical pollutants (U, Zn) were found by XRF mapping (Fig. 6C to 6F). Only in one case the hotspot is visible in gamma activity map and Zn/Fe map (lower edge of panels in Fig. 6). Those hotspots are clearly coincident with point bars, i.e. in-channel deposits on places where the river channel has systematically (single-directionally) laterally shifted during the U-mining period (note changing historical position of river channel shown in Fig. 6 and 7). It allowed deposition in the channel belt as well as temporary preservation of those deposits. The reason of the discrepancy between gamma and XRF mapping is obvious: the deposition in bars is much faster (typically several centimetres per a year) than in the distal floodplain (typically several millimetres per a year) and hence the historical uranium pollution in the bars has been buried between 1990s and the present time by a too thick layer of less polluted (younger) sediments to reveal pollution by surface XRF analysis. The fact that the gamma activity hotspots along the river channel are really bars is also obvious from coarser sediments in the channel belt (low Al/Si and high Zr/Rb, Fig. 7). The blue arrows in Fig. 6 point to directions to which enhanced amount of coarser clastics could be expected to be currently exported at overbank flows based on the knowledge of fluvial deposition - in agreement with that coarser sediments (with larger Zr/Rb) are deposited there.

Lithogenic element-normalisation of the pollutant concentrations in XRF maps nearly levelled out variance in U concentrations in the study area: compare Fig. 6C and 6D and note much narrower variance in the corresponding colour scales. The reason is that the main driver of elevated surface U concentrations was mean sediment grain size: both U and Fe are elevated in finer sediments. On the contrary, even after normalisation, Zn pollution shows its maximum in the local pollution hotspots according to gamma activity mapping discussed above (Fig. 6E-F), although the normalisation also considerably decreased total variance of pollution extent. The reason of better correlation of surface Zn/Fe and gamma activity than surface U/Fe and gamma activity is currently unclear; obviously both surface Zn/Fe and gamma activity show the places in floodplains where pollutants were preferentially deposited.

DISCUSSION

The in situ analysis by handheld XRF is directly applicable in pollution mapping of floodplains (Fig. 6), although due to "native" water content the so far obtained results are only 45–70 % of the conventional total contents on the dry sample basis. Such effect of the water content is in line with previous observations (Argyrazi et al., 1997; Parsons et al., 2013; Weindorf et al., 2014). This inherent effect can be corrected by the used geochemical normalisation, i.e. expression of pollutant concentrations as relative ratios U/Fe and Zn/Fe. With in situ XRF it is also easy to perform lithological mapping of the floodplain surface (Fig. 7), which is essential to distinguish individual sediment facies, such as point bars, levee and flood deposits. Pollutant distribution in the study area (Fig. 6) has obviously been controlled by river channel dynamics: most of the gamma-activity hotspots coincide with recently formed point bars, i.e. lateral deposits along the inner (convex) banks of channel bends. In the Ploučnice River mostly coarser (sandy) sediments are deposited in point bars (high Zr/Rb ratio in Fig. 76B), but they always have finer (silty) laminas in their bodies and are usually covered by several decimetres thick layer of silty overbank fines with pollutants. Young (active) point bars have usually lower elevation than the floodplain floor (basin, distal floodplain level), in other words, they appear as curved, narrow depressions along the channel bends. They are covered by plant species typical for early stages of successions (species-poor plant assemblages, with no older shrubs and trees). The banks opposite to the point bars are usually steep due to ongoing lateral erosion. Representatives of point bars should certainly be included in the sampling and/or surface pollution mapping in floodplains.

Chemical pollutants in floodplains are usually associated with finer grain sizes in overbank fines. Contrarily to this expectation, channel sediments (including sandy deposits of bars) in the study area are more polluted than overbank fines (silty) in distal floodplain. One of the reasons is that in-channel deposits are formed under lower discharges when fluvially transported solids are not so intensively diluted by reworking less polluted (older) sediments. Although channel belt sediments could be expected to be only coarse, it is known that in the particular places both fine sediments and pollution can be deposited even directly in the channel (Ciszewski, 1998). Adversely, the deposits of extreme floods can be more diluted due to enhanced channel bank erosion (Navrátil et al., 2008; Bábek et al., 2011). Of course the previous statements are valid only if the precipitation extremes and resulting floods did not cause a pollution disaster such as a

failure of a settling pond or flush of temporary sinks of pollution in the catchment (Dhivert et al., 2015; this study). In such cases pollution is maximal in almost all kinds of the flood in deposits including overbank sediments far from the channel. Because the effects of large floods can be so contrasting and a priori unknown, in each novel pollution survey the sampling/mapping must include both channel belt (point bars and other possible deposits in proximal floodplain formed under lower discharges) and distal floodplain (deposits of extreme discharges during floods).

The characterisation of the pollution hotspots in the study area will be compared with those identified in the Ploučnice River floodplains in our previous works: summary in Table 2. Two major geomorphic prerequisites leading to pollution hotspots have been described:

1) abandoned meanders and laterally shifting channels, which have evolved (filled by sediment) during the pollution climax (1971-1989) can be found by GIS analysis, in particular using old maps and aerial photographs, and

2) other sediment traps in floodplain, such as meander scars (more ancient channels not depicted in old maps) and levees after channel shifts can be identified in DTM and by "sedimentary facies mapping", i.e. mapping sediment grain-size in the floodplain.

Table 2. Overview of polluted hotspots.

Study area	Hotspot position	Used methods	Reference
ES - South of Mimoň	Former depression in floodplain (meander scar?)	GIS, gamma, XRF, laboratory XRF, geostatistical analysis	Slabá (2015), Slabá et al. (2015)
PK - Boreček	Abandoned channel		Kühn (1996)
MH - Boreček	Former depression in floodplain (old, shallow flood channel)	GIS, XRF, gamma, ERT ² , DEMP ³ , OSL ⁴	Hošek (2015), Matys Grygar et al. (2016), Hošek et al. (submitted)
AT1 - Hradčany	Meander abandoned during U- mining	GIS, gamma, ERT ¹ , laboratory XRF	Tipanová (2016), Matys Grygar et al. (2016)
AT2 - West of Hradčany	Meander - started to cut off	GIS, ERT ¹ , laboratory XRF	Tipanová (2016), Matys Grygar et al. (2016)
MS - West of Hradčany	Channel bars and natural levees	GIS, gamma, XRF, drone mapping, geostatistical analysis	This paper , Sikora (2016)
TV - Veselí	Secondary river channel	GIS, gamma, XRF, laboratory XRF, geostatistical analysis	Váchová (2017)
KK - by Česká Lípa	Depression in floodplain (shallow flood channel)	GIS, gamma, DEMP ² , XRF	unpublished work (in progress)

² ERT - electric resistivity tomography

³ DEMP - dipole electromagnetic profiling

⁴ OSL - optically stimulated luminescence

All kinds of traps for polluted sediment represent lithological heterogeneities, which can also be visualised by geophysical imaging (Matys Grygar et al., 2016; Faměra et al., 2018). However, the tools reported in this paper are sufficient for identification and interpretation of pollution hotspots in the studied floodplains.

CONCLUSIONS

Our study demonstrated that very detailed, i.e. high-resolution analysis (mapping) of pollutant distribution in the floodplain can be achieved by portable analytical instruments. Afterwards it can be interpreted on the base of micro-geomorphology of the floodplain and fluvial deposition processes. GIS tools are essential for both mapping and interpretation. The gamma spectrometry can visualise pollution even if it has been buried by several decimetres thick younger and less polluted strata, while XRF analysis has a penetration depth less than 1 mm and can reveal only pollutants on the very surface of the analysed samples. Pollution mapping is very promising tool to analysis of polluted floodplains - it shows how unevenly the pollutants are distributed over the floodplain.

Most activity was found in places of recent channel shifts – in point bars and abandoned meanders. Increased activities/concentrations of pollutants were found also in old (fossil) natural levees. Due to chaotic lateral channel shifts in the current channel belt visualised by GIS tools we may predict that pollution hotspots in channel bars and levees will be reworked in the timescale of decades. Occasional meander development also observed in the Ploučnice River will rework the pollution in abandoned meanders in the target area within timescale of centuries.

ACKNOWLEDGMENT

The authors thank to P. Doškář (J. E. Purkyně University in Ústí nad Labem) for fieldwork including in situ XRF analysis and R. Barochová, Z. Hájková and P. Vorm (The Czech Academy of Sciences, Institute of Inorganic Chemistry, Řež) for laboratory processing sediment samples and their XRF analysis. P. Vorm also contributed by performing calibration of XRF by chemical analyses of Al and Si. Mapping work, entire fieldwork, verification of handheld XRF, evaluation and graphical presentation of experimental results and manuscript preparation were covered by Czech Science Foundation (project No. 15-00340S).

REFERENCES

- Argyrazi, A., Ramsey, M.H., & Potts, P.J. (1997) Evaluation of Portable X-ray Fluorescence Instrumentation for in situ Measurements of Lead on Contaminated Land, *Analyst*, 122, pp. 743-749.
- Bábek, O., Faměra, M., Hilscherová, K., Kalvoda, J., Dobrovolný, P., Sedláček, J. (2011) Geochemical traces of flood layers in the fluvial sedimentary archive; implications for contamination history analyses, *Catena* 87(2), pp. 281-290.

- Bábek, O., Matys Grygar, T., Faměra, M., Hron, K., Nováková, T., Sedláček, J. (2015) Geochemical background in polluted river sediments: how to separate the effects of sediment provenance and grain size with statistical rigour?, *Catena* 135, pp. 240-253.
- Bouchez, J., Gaillardet, J., France-Lanord, C., Maurice L., & Dutra-Maia, P. (2011) Grain size control of river suspended sediment geochemistry: Clues from Amazon River depth profiles, *Geochemistry Geophysics Geosystems* 12(3), pp. 1525-2027.
- Brumbaugh, W.G., Tillitt, D.E., May, T.W., Javzan, Ch., & Komov V. T. (2013) Environmental survey in the Tuul and Orkhon River basins of north-central Mongolia, 2010: metals and other elements in streambed sediment and floodplain soil, *Environmental Monitoring and Assessment* 185(11), pp. 8991–9008.
- Ciszewski, D. (1998) Channel processes as a factor controlling accumulation of heavy metals in river bottom sediments: Consequences for pollution monitoring (Upper Silesia, Poland), *Environmental Geology*, 36(1-2), pp. 45-54.
- Ciszewski, D. (2001) Flood-related changes in heavy metal concentrations within sediments of the Biała Przemsza River, *Geomorphology* 40, pp. 205–218
- Dhivert, E., Grosbois, C., Rodrigues, S., & Desmet, M. (2015) Influence of fluvial environments on sediment archiving processes and temporal pollutant dynamics (Upper Loire River, France), *Science of the Total Environment* 505, pp.121-136.
- Dypvik, H., & Harris, N.B. (2001) Geochemical facies analysis of fine-grained siliciclastics using Th/U, Zr/Rb and (Zr+Rb)/Sr ratios, *Chemical Geology* 181(1-4), pp.131-146.
- Elznicová, J., Hruběšová, D. (2017) Spatiotemporal changes of the Ploučnice River for the explanation of pollution distribution in the floodplain. In *17th International Multidisciplinary Scientific GeoConference SGEM 2017, Conference Proceedings*, 29 17(23), 29 June - 5 July, 2017, STEF92 Technology, Sofia, pp. 665-672.
- Faměra, M., Kotková, K., Tůmová, Š., Elznicová, J., Matys Grygar, T. (2018) Pollution distribution in floodplain structure visualised by electrical resistivity imaging in the floodplain of the Litavka River, the Czech Republic, *Catena* 165, pp. 157-172.
- Foulds, S. A., Brewer, P. A., Macklin, M. G., Haresign, W. ,Betson, R. E.,Rassner, S. M. E. (2014) Flood-related contamination in catchments affected by historical metal mining: an unexpected and emerging hazard of climate change, *Science of the Total Environment* 476, pp. 165-180.
- Gałaszka, A., Migaszewski, Z., Namieśnik, J. (2015) Moving your laboratories to the field - Advantages and limitations of the use of field portable instruments in environmental sample analysis, *Environmental Research* 140, pp. 593-603.
- Gnojek, I., Dědáček, K., Zabadal. S., Sedlák J. (2005) Letecké geofyzikální mapování radioaktivních zátěží Liberecka (*Aerial geophysical mapping of radioactive loads of the Liberec area*). Final report, Geofond Praha (the archive of the Czech Geological Survey).
- Grygar, T., Světlík, I., Lisá, L., Koptíková, L., Bajer, A., Wray, D.S., Ettler, V., Mihaljevič, M., Nováková, T., Koubová, M., Novák, J., Máčka, Z., Smetana, M. (2010) Geochemical tools for the stratigraphic correlation of floodplain deposits of the Morava River in Strážnické Pomoraví, Czech Republic from the last millennium, *Catena* 80(2), pp. 106–121.
- Guo, Y.-Q., Huang, C.-C., Pang, J.L., Zha, X.-C., Li, X.P., Zhang Y.Z. (2014) Concentration of heavy metals in the modern flood slackwater deposits along the upper Hanjiang River valley, China, *Catena* 116, pp. 123-131.

- Hanslík, E. (2002). Vliv těžby uranových rud na vývoj kontaminace hydrosféry Ploučnice v období 1966-2000 (*Impact of uranium ore mining on course of pollution of Ploučnice hydrosphere in period of 1966-2000*). Výzkumný ústav vodohospodářský T.G. Masaryka, Prague.
- Hošek, M. (2015). Kontaminace nivy Ploučnice těžkými kovy ve vztahu k její architektuře (*Pollution of Ploučnice floodplain by heavy metals in relation to its architecture*), Diploma Thesis, Faculty of Science, Charles University, Prague.
- Hošek, M., Matys Grygar, T., Elznicová, J., Faměra, M., Popelka, J., Matkovič, J., Kiss, T. (submitted, January 2018) Geochemical mapping in polluted floodplains using in situ X-ray fluorescence analysis, geophysical imaging, and statistics: surprising complexity of floodplain pollution hotspot, *Catena*.
- Houben, P. (2007) Geomorphological facies reconstruction of Late Quaternary alluvia by the application of fluvial architecture concepts, *Geomorphology* 86(1–2), pp. 94–114.
- Hrdoušek, F. (2005) Těžké kovy v sedimentech Panenského potoka a středního toku Ploučnice (*Heavy metals in sediments of Panenský Creek and middle reach of Ploučnice*). Diploma Thesis, Faculty of Science, Charles University, Prague.
- Hürkamp, K., Raab, T., Voelkel, J. (2009) Two and three-dimensional quantification of lead contamination in alluvial soils of a historic mining area using field portable X-ray fluorescence (FPXRF) analysis, *Geomorphology* 110(1-2), pp. 28-36.
- Jiang, J.-B., Wang, J., Liu, S.-Q., Lin, C.-Y., He, M.-C., & Li, X.-T. (2013) Background, baseline, normalization, and contamination of heavy metals in the Liao River Watershed sediments of China, *Journal of Asian Earth Sciences* 73, pp. 87-94.
- Jones, A.F., Macklin, M.G., Brewer, P.A. (2012). A geochemical record of flooding on the upper River Severn, UK, during the last 3750 years, *Geomorphology* 179, pp. 89-105.
- Kafka J. (2003). Rudné a uranové hornictví České republiky (*Ore and Uranium Mining in the Czech Republic*). DIAMO, Czech Republic.
- Kolář, J.(2004). Distribuce vybraných těžkých kovů v sedimentech horního toku Ploučnice (*Distribution of Selected Heavy Metals in Sediments of Upper Reach of Ploučnice*). Diploma Thesis. Faculty of Science, Charles University, Prague.
- Kühn P. (1997) Radioaktivní znečištění údolní nivy Ploučnice v bývalém VVP Ralsko (*Radioactive pollution of the floodplain of the Ploučnice in former military area Ralsko*). Bezděz 5, Okresní vlastivědné museum Česká Lípa, Czech Republic.
- Kühn, J. (1996) Distribuce uranu a vybraných těžkých kovů v sedimentech údolní nivy Ploučnice (*Distribution of uranium and selected heavy metals in sediments of the floodplain of the Ploučnice River*). Doctoral Thesis, Faculty of Science, Charles University, Prague.
- Löwemark, L., Chen, H.-F., Yang, T.-N., Kylander, M., Yu, E.-F., Hsu, Y.-W., Lee, T.-Q., Song, S.-R., Jarvis, S. (2011) Normalizing XRF-scanner data: A cautionary note on the interpretation of high-resolution records from organic-rich lakes, *Journal of Asian Earth Sciences* 40 (6), pp. 1250-1256.
- Majerová, L., Matys Grygar, T., Elznicová, J., Strnad, L. (2013) The Differentiation between Point and Diffuse Industrial Pollution of the Floodplain of the Ploučnice River, Czech Republic, *Water, Air, and Soil Pollution* 224 (9), pp. 1688.

- Martin, P.G., Payton, O.D., Fordoulis, J.S., Richards, D.A., Scott, T.B. (2015) The use of unmanned aerial systems for the mapping of legacy uranium mines, *Journal of Environmental Radioactivity* 143, pp. 135-140.
- Matys Grygar, T., Sedláček, J., Bábek, O., Nováková, T., Strnad, L., Mihaljevič, M. (2012) Regional contamination of Moravia (south-eastern Czech Republic): temporal shift of Pb and Zn loading in fluvial sediments, *Water Air Soil Pollut.* 223 (2), pp. 739–753.
- Matys Grygar, T., Nováková, T., Bábek, O., Elznicová, J., Vadinová, N. (2013) Robust assessment of moderate heavy metal contamination levels in floodplain sediments: A case study on the Jizera River, Czech Republic, *Science of the Total Environment* 452, pp. 233-245.
- Matys Grygar, T., Elznicová, J., Bábek, O., Hošek, M., Engel, Z., Kiss, T. (2014) Obtaining isochrones from pollution signals in a fluvial sediment record: A case study in a uranium-polluted floodplain of the Ploučnice River, Czech Republic, *Applied Geochemistry* 48, pp. 1-15.
- Matys Grygar, T., Elznicová, J., Tůmová, Š., Faměra, M., Balogh, M., Kiss, T. (2016) Floodplain architecture of an actively meandering river (the Ploučnice River, the Czech Republic) as revealed by the distribution of pollution and electrical resistivity tomography, *Geomorphology* 254, pp. 41-56.
- Matys Grygar, T., Popelka, J. (2016) Revisiting geochemical methods of distinguishing natural concentrations and pollution by risk elements in fluvial sediments, *Journal of Geochemical Exploration* 170, pp. 39-57.
- Miller, J., Barr, R., Grow, D., Lechler, P., Richardson, D., Waltman, K., Warwick, J. (1999) Effects of the 1997 flood on the transport and storage of sediment and mercury within the Carson River valley, west-central Nevada, *Journal of Geology* 107(3), pp. 313-327.
- Navrátil, T., Rohovec, J., Žák, K. (2008) Floodplain sediments of the 2002 catastrophic flood at the Vltava (Moldau) River and its tributaries: mineralogy, chemical composition, and post-sedimentary evolution, *Environmental Geology* 56(2), 399-412.
- Notebaert, B., Houbrechts, G., Verstraeten, G., Broothaerts, N., Haecx, J., Reynders, M., Govers, G., Petit, F., Poesen, J. (2011) Fluvial architecture of Belgian river systems in contrasting environments: implications for reconstructing the sedimentation history, *Netherlands Journal of Geosciences — Geologie en Mijnbouw* 90 (1), pp. 31–50.
- Novák, M., Emmanuel, S., Vile, M.A., Erel, Y., Véron, A., Pačes, T., Wieder, R.K., Vaněček, M., Štěpánová, M., Břízová, E., Hovorka J. (2003) Origin of lead in eight Central European peat bogs determined from isotope ratios, strengths, and operation times of regional pollution sources, *Environmental Science and Technology* 37(3), pp. 437-445.
- Nováková, T., Kotková, K., Elznicová, J., Strnad, L., Engel, Z., Matys Grygar, T. (2015) Pollutant dispersal and stability in a severely polluted floodplain: A case study in the Litavka River, Czech Republic, *Journal of Geochemical Exploration* 156, pp. 131-144.
- Oliver, M. A., Webster R. (2014) A tutorial guide to geostatistics: Computing and modelling variograms and kriging, *CATENA* 113, pp. 56-69.
- Parsons, C., Grabulosa, E.M., Pili, E., Floor, G.H., Roman-Ross, G., Charlet, L. (2013) Quantification of trace arsenic in soils by field-portable X-ray fluorescence spectrometry: Considerations for sample preparation and measurement conditions, *Journal of Hazardous Materials* 262, pp. 1213-1222.

- Sikora, M. (2016) Zhodnocení vývoje radioaktivního znečištění toku a údolní nivy Ploučnice (*The evaluation of radioactive contamination of the Ploučnice River and floodplain*). Diploma Thesis, J.E. Purkyně University in Ústí nad Labem.
- Slabá, E. (2015) Posouzení navržených revitalizačních opatření řeky Ploučnice u Mimoň z hlediska remobilizace historické kontaminace (*Evaluation of proposed revitalization of the river Ploučnice close to Mimoň in terms of remobilization of historical contamination*). Diploma Thesis, J.E. Purkyně University in Ústí nad Labem.
- Slabá, E., Matys Grygar, T., Elznicová J. (2015) Posouzení navržených revitalizačních opatření řeky Ploučnice u Mimoň z hlediska remobilizace historické kontaminace. (Evaluation of proposed revitalization of the river Ploučnice close to Mimoň in terms of remobilization of historical contamination) In *Sborník konference Krajinné inženýrství 2015. Provoz a údržba staveb krajinného inženýrství, September 2015*. Česká společnost krajinných inženýrů, Praha, pp. 105-120.
- Slezák, J. (2000). Historie těžby uranu v oblasti Stráže pod Ralskem v severočeské křídě a hydrogeologie (History of uranium production in the area of Stráž pod Ralskem (the North Bohemian Cretaceous basin) and hydrogeology), *Sborník geologických věd; Hydrologie, inženýrská geologie* 21, pp. 5-36.
- Stacke, V., Pánek, T., Sedláček, J. (2014) Late Holocene evolution of the Bečva River floodplain (Outer Western Carpathians, Czech Republic). *Geomorphology* 206, pp. 440–451.
- Tipanová, A. (2016) Transport polutantů z těžby a zpracování uranu říčním systémem Ploučnice (*Transport of pollutants from mining and processing of uranium in river system Ploučnice*) Diploma Thesis, Faculty of Science, Palacký University, Department of Geology, Olomouc, 75 p.
- Váchová, T. (2017) Využití geostatistických metod při mapování znečištění v nivě řeky Ploučnice (*Application of Geostatistical Methods for Mapping Pollution in the River Floodplain Ploučnice*), Diploma Thesis, J.E. Purkyně University in Ústí nad Labem, 81 p.
- Vijver, M.G., Spijker, J., Vink, J.P.M., Posthuma, L. (2008) Determining metal origins and availability in fluvial deposits by analysis of geochemical baselines and solid-solution partitioning measurements and modelling, *Environmental Pollution* 156 (3), pp. 832-839.
- Vitáček Z., Knauerová M., Kühn P. (2018) Řeka Ploučnice a příroda v okolí (*Ploučnice River and nature around*). Mikroregion Podralsko. Available at: <http://www.podralsko.info/zelena-cyklomagistrala-ploucnice/informace-o-rece-ploucnice/> (Accessed 7 February 2018).
- Wang, J., Liu, G.-J., Lu, L.-L., Zhang, J.-M., Liu, & H.-Q. (2015) Geochemical normalization and assessment of heavy metals (Cu, Pb, Zn, and Ni) in sediments from the Huaihe River, Anhui, China, *Catena* 129, pp. 30-38.
- Weindorf, D.C., Zhu, Y., Chakraborty, S., Bakr, N., Huang, B. (2012) Use of portable X-ray fluorescence spectrometry for environmental quality assessment of peri-urban agriculture, *Environmental Monitoring and Assessment* 184, pp. 217–227.
- Weindorf, D.C., Bakr, N., Zhu, Y., Mcwhirt, A., Ping, C.L., Michaelson, G., Nelson, C., Shook, K., Nuss, S. (2014) Influence of Ice on Soil Elemental Characterization via Portable X-Ray Fluorescence Spectrometry, *Pedosphere* 24(1), pp. 1-12.
- Wohl, E. (2014) Time and the rivers flowing: Fluvial geomorphology since 1960, *Geomorphology* 216, pp. 263-282

NATURAL DISASTER VULNERABILITY, MANAGEMENT AND THE ROLES OF LAND USE/LAND COVER: AN ASSESSMENT OF LANDSLIDES USING GIS IN JOS, NIGERIA

Chukwudi NWAOGU^{1*}, Shitta HABU², Onyedikachi OKEKE³, Vilém PECHANEC¹,
Tomaš POHANKA¹, Olutoyin FASHAE⁴

¹ Department of Geoinformatics, Palacký University Olomouc, 771 46 Olomouc, Czech Republic.

² Department of Geography, University of Abuja, P.M.B. 117 FCT-Abuja, Nigeria.

³ Sambus Geospatial Limited, Abuja, Nigeria.

⁴ Department of Geography, University of Ibadan, 200284 Ibadan, Oyo, Nigeria

cnwaogu@gmail.com

Abstract

Landslide has become a threat to properties and live in Jos South, causing about \$100 million damages and annual death and extinction of many fauna and flora. In an area subjected to rising population, increased mining activities, lateristic hilly soil slope, intensified climatic storms, the incidence and cost of landslide, and socioeconomic risks are inevitable. This paper aimed at identifying the landslide vulnerability and key causal factors using Remote sensing and GIS. We hypothesized that although bio-geophysical factors affect the landscape, the anthropogenic factors had substantial effects on the landuse-landcover (LULC) which became significant in the Jos South landslide occurrences. Data were collected, processed and analyzed on the associated variables using remote sensing devices, ArcGIS 10.1 and ENVI 4.7. Five landslide vulnerabilities (severely high, high, moderate, low and very low), and the vulnerability areas were identified. Moderate areas ranked highest with 234.85km² (46%) of the study area, low susceptibility had 175.5 km² (34.4%), very low susceptibility was 79.9 km² (15.7%) while, high and severely high were below 4% in area. Drainage, LULC, and soil were the main landslide causative factors. The applications of geoinformatics have proved to be exceptionally effective in analyzing, monitoring and managing landslide in the area.

Keywords: GIS, shallow landslide, land use-cover, mining, drainage, lithology-slope types

INTRODUCTION

Landslide is a geological phenomenon, which occurs due to changes in slope movements especially, when the down slope weight (driving force) exceeds the soil strength (resisting force). Landslides are very prominent where slope stability has been compromised and can be stimulated by severe rainfall, erosion, volcanic activity, earthquakes, saturation of slope with water, LULC changes, groundwater modification, environmental disturbance, and slope terrain alteration by human activities, or any combination of these factors. In arithmetic term, landslide can be represented as the probability of spatial occurrence of slope failures, given a set of geoenvironmental conditions (Guzzetti et al.,1999). Landslide susceptibility (LS) maps are important delineators of areas with different potentials for future landslide movement. According

to Carrara et al., (1995), the LS maps could be simple estimation of landslide-prone geological units developed from geological maps, or they could be complex computer generated mathematical models linking several factors that influence slope stability. Contemporarily, Remote sensing and GIS technologies are being used to monitor and map landscape structures, identify spatio-temporal changes, and the causal factors (Luzi et al., 1999). There have been numerous methods to analyze the vulnerability of slope movements using geoinformatics (Akpan et al., 2015; Igwe, 2015a; Rasyid et al., 2016) with majority focusing on the comparison between the determining factors and the territorial distribution of the movement observed. Although, these new technologies and their applications are still lacking in the developed countries (Akpan et al., 2015; Igwe, 2015b). In Nigeria for example, recent researches on landslide susceptibility revealed that limited studies with application of GIS are performed in the region (Igwe, 2013, 2015a, 2015b; Akpan et al., 2015).

Environmental indicators showed that Jos South is rapidly becoming high vulnerable to slope failures, rock falls and landslide due to anthropogenic activities including Tin mining, rock blasting, and farming (Habu, 2014). The problem is compounded due to dearth of research which applied land use modelling technology such as GIS in landslide vulnerability assessment in the study area. On this background, the study aimed at using the potentials of remote sensing and GIS to analyze landslide susceptibility areas and to give sustainable management measures in Jos south. It is hypothesized that although bio-geophysical factors affect the landscape, the anthropogenic factors had substantial effects on the LULC which was consequently significant in the Jos South landslide occurrences. In this context, the study attempted to address the following questions: (i) what are the main causes of the landslide? (ii) where are the most vulnerability areas? (iii) does seasonality play any role in the landslide occurrences? (iv) how can the risks be mitigated or adapted?

MATERIALS AND METHODS

Study area

The Jos in Plateau state is located in the north-central part of Nigeria. Jos South lies between latitudes 8° 30' N and 10° 30' N and longitude 8° 20' E and 9° 30' E (Fig. 1), with a population of 306,716 from the last population census (NPC, 2006). Geologically, Jos South is dominated by younger granites which were intruded into older granite rocks. Due to its high altitude (1100 m -1500 m), the area has cool climatic condition with annual temperature ranging from 18 °C – 22 °C, and annual rainfall ranging from 1000 mm to 2500 mm (Olowolafe, 2003). Lateritic soils of granitic and basaltic formation occupy extensive areas of land (Olowolafe, 2003). The original woodland vegetation has been significantly reduced for mining, settlement and agricultural purposes.

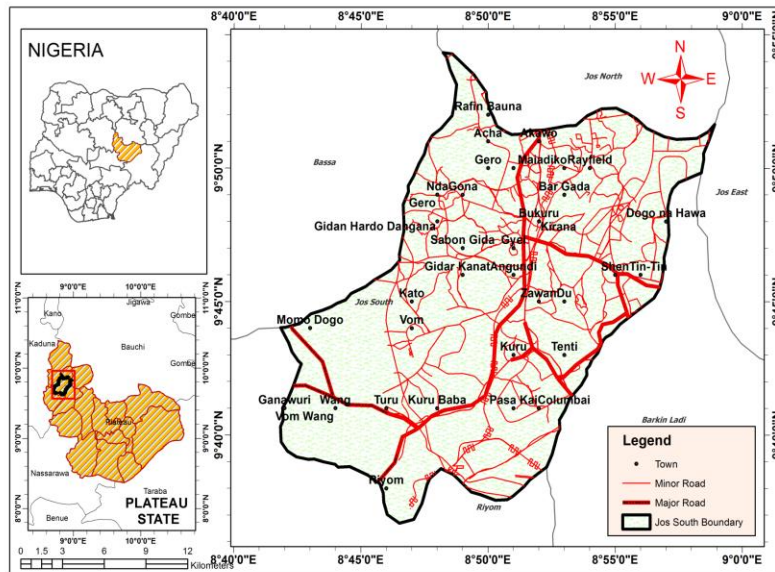


Fig. 1. Jos south in Plateau State, Northern Nigeria - the study area

Data collection and analyses

The adopted methodology for the study is shown in Fig. 2. All the physical and anthropogenic data associated with the landslides were collected via Landsat, SPOT images, Ikonos and Quickbird, GPS points, aerial photos, topographic maps, Shuttle Radar Topography Mission (SRTM). The field surveys were performed by walking round the landslide areas throughout the months in 2015 with at least twice visit each month. A total of 34 days was used for the fieldwork. Spatial and attribute data were collected on drainage, land use and land cover, soil, geology, Lineament, geomorphology, slope, population and human activities. The field samplings were scheduled in 2nd week and last week of every month from November to May while, June to October had 4 times observations each (that is a visit per week) because these months are the seasons with extreme rainfall. For the image classification, the FAO land cover classification system together with the field information was used, and the LULC types were generated (Table 1). Watershed, stream order, and other drainage morphometric analyses were generated from the drainage map while LULC and its class statistics were generated from the classified image. The data were processed and analysed using ArcGIS version 10.1, ENVI version 4.7, and Surfer 10 tools. Geostatistical analyses such as Kriging, inverse distance weight, and 3D-surface analysis tools in ArcGIS were used to generate the TIN and slope from contour which helped to generate the DEM. ArcGIS built-in MCE module (Weighted Overlay) was used to estimate the landslide vulnerability factors while, Analytical Hierarchy Process (AHP) was used for validation.

RESULTS AND DISCUSSION

LULC types were classified, and their areas and percentages in relation to the entire study landmass were; bare surface (5.6 km²; 1.1%), built-up area (56.3km²; 11%), mining site (30.7

km²; 6%), rock outcrop (393.6 km²; 77.2%), vegetation (17.7 km²; 3.5%), and water (5.8 km²; 1.2%) (**Table 1**). This result showed the importance of LULC and its changes in landslides occurrence. For example, less than 4% land still have vegetation cover with large areas exposed by mining. Therefore, these human activities caused LULC changes, degradation of the lithology and consequently landslides. Some authors have reported significant increase in landslide incidents with land use changes (Wasowski et al., 2010).

Transportation, settlement, and other infrastructural development also promoted landslides. The result indicated that decrease in vegetation caused by anthropogenic activities contributed to about 42% of landslides occurrence (**Table 2**). This finding was consistent with previous studies in Nigeria and in many other developing countries where, major motor-highways, built-up area, urban development, and agricultural activities led to decline in vegetation and have been identified as contributing factors to landslides (Akpan, 2015; Igwe, 2015b; Knapen et al., 2006).

Table 1. Classified Land use-land cover types and overall classification accuracy.

S/N	Classes	Description	Area (Km ²)	%
1	Bare surface	Open land and non-vegetated land.	5.6	1.1
2	Built-up area	Residential, Commercial, Industrial, Government facilities and settlement.	56.3	11
3	Mining site	Areas for the exploitation of the natural/mineral resources such as tin, coal, gravels, and others.	30.7	6.1
4	Rock outcrop	Type of vegetation found on rocky areas or the part of a rock formation that is exposed on the surface of the ground.	393.6	77.2
5	Vegetation	Evergreen forest and mixed forests with higher density of trees.	17.7	3.5
6	Waterbody	Areas cover by open water such as river, ponds, Lagoons, dam and water-logged area	5.8	1.1
<i>Image classification accuracy</i>				
Overall Accuracy (%)				90.5
Kappa Coefficient (K)				0.79

However, landslides are natural disasters, but they can be intensified by population growth because increase in Nigerian population between 1955-2015 elevated demand for land resources which in turn mounted severe pressure on the land which consequently reduced the stability of the slopes (Knapen et al., 2006). In Uttarakhand, one of the dense populated area in India, Panikkar and Subramaniyan (1997) revealed that population growth accelerated deforestation and urbanization which in turn exacerbated landslides. Mining sites covered an of 1.02km² representing 4.73% of the landslide susceptible area with a weight of 6 represented severely high instability area (Table 2).

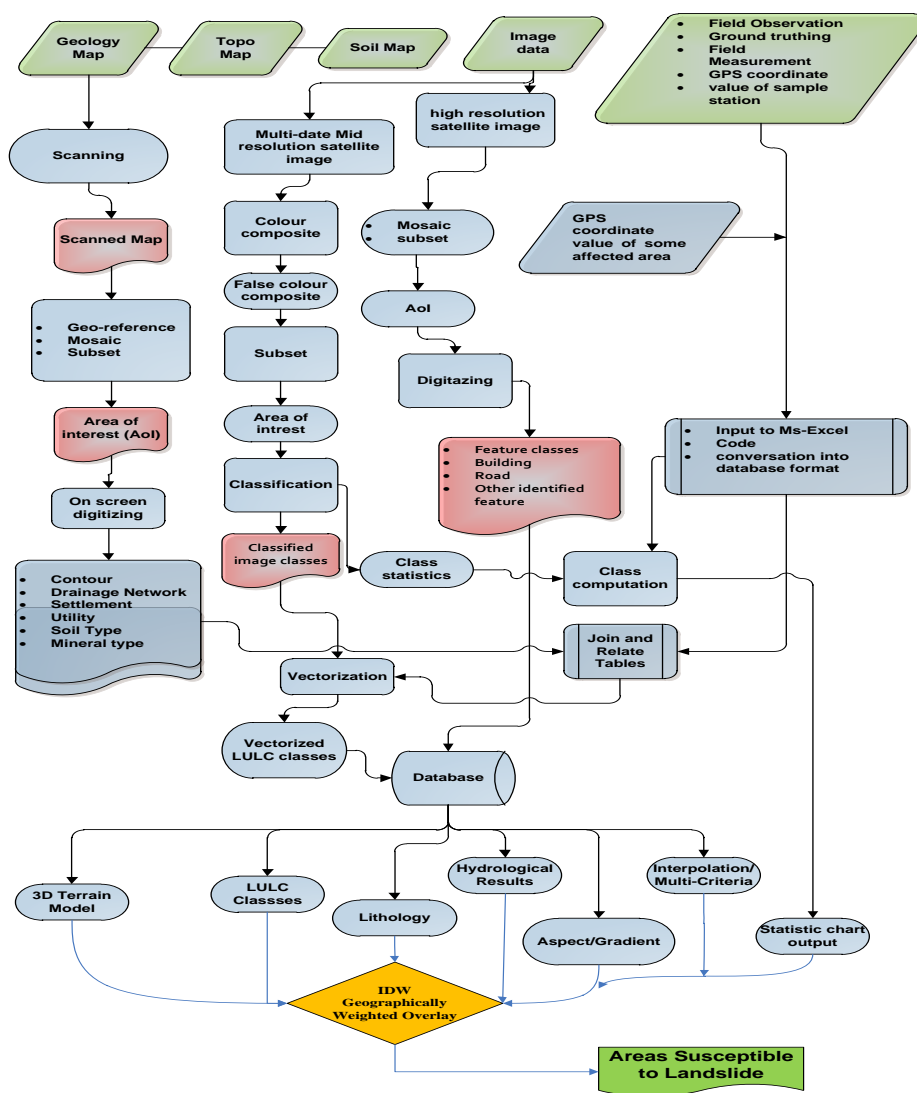


Fig. 2. Schematic flow diagram of the study methodology

Shallow landslides were common in our study area because the Acrisol mining soil which dominated this region has high instability to landslides due to mining activities which influenced the rate of water movement in the soils and the capacity of the soil to hold water (Sidle et. al., 1985). This was compounded by the prevailing high annual mean rainfall (> 2000mm) (Table 2).

Rock outcrop is highly unstable to landslides, and had about 43% of the areas covered by landslides. Unpropitiously, larger part of the study area has granitic bedrock and ought to be resistance to mass-flow, but environmental and human-induced weathering have modified the mechanical, mineralogical and hydrologic attributes of the regolith, and weakened the bedrocks

leading to slope instability (Igwe, 2013). The areas with high vulnerability to landslides had stream and rivers of average length 3.05 km and above and with high density (Fig. 3a). This finding correlated with the results by other others on this concept (Hasegawa et al. 2013) who reported that terrain having higher drainage density and thin soil layer was comparatively more vulnerable to shallow seated landslide. Mining and mined sites, rock outcrop, and built-up areas were the LULC classes that have the highest influence on the landslide (Table 2, and Fig.3b).

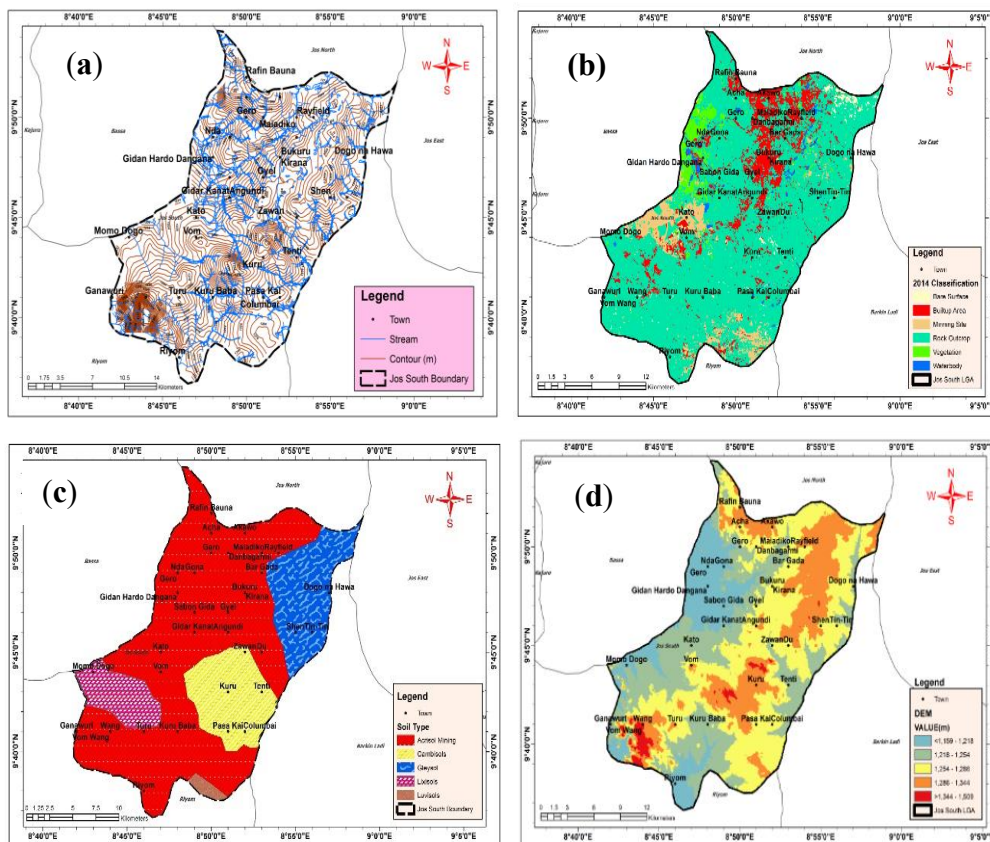


Fig. 3. Jos south showing (a) drainage and contour (b) land use-land cover classification (c) the dominant soil types (d) digital elevation model (DEM).

Soil types found in the study area included, Gleysol, Lixisol, Luvisol, Cambisols and Acrisol mining see (Table 2, and Fig. 3c). Acrisol mining covered about 80% of the area, and was formed from strongly weathered acidic soil with low base saturation and high susceptibility to landslide. The overall result revealed that less than 0.1% of the area had severe landslide, while moderate landslide type covered about 235 km² of the landslide area (Table 3). However, none of the towns was found in the severely high landslide area though some areas have high tendency for landslide susceptibility (Table 4).

Table 2. Summary of overall results of the analyses on landslides and causative factors

S/N (Code)	Class/Type/% Raise	Landslides area (km ²)	%	Weight	Instability
<i>Overlay/integration results of the landslide layer and LULC layer</i>					
Class					
1	Bare surface	0.07	0.32	2	Low
2	Built-up area	1.92	8.91	5	Very high
3	Mining site	1.03	4.75	6	Severely high
4	Rock outcrop	9.34	43.36	4	High
5	Vegetation	8.99	41.73	1	Very low
6	Waterbody	0.21	0.93	3	Moderate
	TOTAL	21.56	100		
<i>Integration of landslide layer and geology layer</i>					
Type					
BB	Basalts, Trachyte & Rhyolite	0.65	3.02	3	Moderate
OGH	Hornblende gneiss	7.7	35.7	2	Low
JYG	Granite	13.21	61.28	1	Very low
	TOTAL	21.56	100		
<i>Integration of landslide layer and soil layer</i>					
Type					
ACf	Acrisol mining	20.71	96.1	5	Very high
CMo	Cambisols	0.85	3.9	4	High
	TOTAL	21.56	100		
<i>Integration of landslide layer and mean rainfall layer</i>					
Average annual rainfall (mm)					
1	500	6.94	32.19	1	Very low
2	1000	5.2	24.12	2	Low
3	1500	5.15	23.89	3	Moderate
4	2000	3.14	14.56	4	High
5	2500	1.13	5.24	5	Very high
	TOTAL	21.56	100		
<i>Integration of landslide layer and Slope layer</i>					
Percentage Raise					
1	4	1.33	6.11	1	Very High
2	6	5.2	23.89	2	High
3	13	3.14	14.43	3	Moderate
4	25	5.15	23.68	4	Low
5	52	6.74	31.89	5	Very Low
	TOTAL	100	21.56	100	

Table 3. Overall statistics of the landslides susceptibility areas (in km²)

S/N	Ranking	area(km ²)	%	Mean/SD	Range(km ²)
1	Severely high	0.31	0.06	0.10±0.01	0.01 - 0.1
2	High	19.79	3.88	0.13±0.75	0.01 - 7.31
3	Moderate	234.85	46.01	1.13±15.71	0.01 - 226.6
4	Low	175.51	34.39	0.63±4.69	0.01 - 50.68
5	Very low	79.94	15.66	0.97±5.01	0.01 - 36.53
	TOTAL	510.4	100		

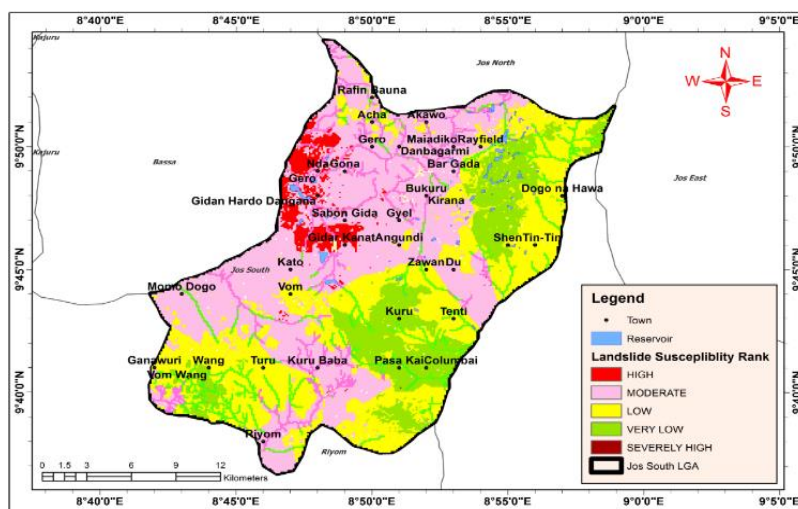


Fig. 4. Overall/Final Result of Jos South landslide susceptibility

Table 4. Landslides vulnerability in relation to settlements

S/N	Ranking	Most vulnerable areas
1	Severely high	None
2	High	Gidar Kanat, Sabon Gida, Gidan Hardo Dangana, Gona, Nda, and Gero.
3	Moderate	Acha, Akawo, Angundi, Bar Gada ,Bukuru, Danbagarmi , Du , Gero, Gona, Gyel, Kato, Kirana, Kuru Baba, Maiadiko, Momo Dogo, Rafin Bauna, Rayfield, Riyom, Sabon Gida Riyom, and Sabon Gida.
4	Low	Dogo na Hawa,Ganawuri,Shen,Tenti,Tin-Tin,Turu, and Zawan.
5	Very low	Columbai, Kuru, Pasa Kai, Vom Wang, and Wang.

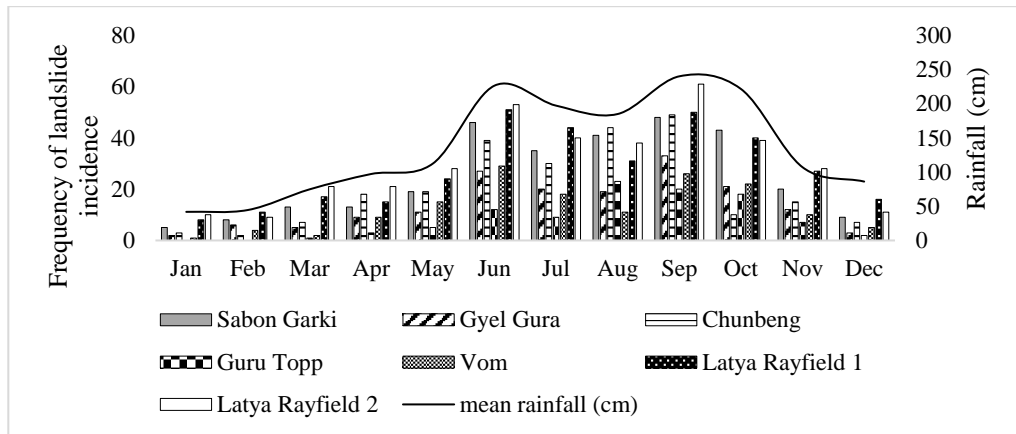


Fig. 5. Seasonality in landslides occurrence and mean rainfall in the most vulnerable sites in Jos South from 1955 to 2015.

High and moderate landslide areas recorded the highest number of settlements (**Fig. 4**). The results further revealed that high and severely high landslide susceptible areas tend to be found in places between 500-1200 meters above sea level (**Fig. 3d**), instead of the very highest steep areas. For example, areas raised with less than 15% showed more instability than areas raised by 20% and above (**Table 2**). This indicated that gentle slopes have significant effect on the landslide susceptibility than the steep slopes hence, slope factor had the lowest weight % among the factors contributing to landslide in the area. The indication that the gentle slopes were more vulnerable to landslide occurrences in our study could be attributed to other factors such as the presence of the valley, and water saturated soil within the gentle slope zone (Pathak, 2016). Shallow landslide at the lower base of the steep highlands have been reported by several authors (Hsu, 2016; Pathak, 2016; Akpan et al., 2015). In southern Nigeria, at the Obot Ekpo Landslide site, Akpan et al. (2015), also reported shallow landslides, and related the water saturation of the underlying rocks due to extremely frequent heavy rainfall as the main cause. However, our finding was inconsistent with some other studies where steeper slopes tend to be more responsible to landslide incidents (Wang et al. 2015).

The long-term spatio-temporal variations in landslide was observed to be substantially related to the monthly rainfall as shown in the most vulnerable sites in our study (**Fig. 5**). Higher incidents of landslide were recorded between June to October as compared with other months. This could be explained by the tropical torrential rainfall between June and October (Harp et al., 2004).

CONCLUSION

The result from this study is uniquely important because contrary to many findings that landslides are most common in steep slopes, our finding showed the gentle slopes to be most vulnerable to mass wasting referred as shallow landslides. The causal factors identified in order of their percentage weight were drainage, land use and land cover, soil, geology, lineament density, geomorphology, and slope. Acrisol mining soil, extreme rainfall, and increased human population with their rapid activities especially, intensive open-cast Tin mining and farming contributed

substantially to the landslide. The tools of geoinformatics have proved very efficient with satisfactory result in the assessment of the landslide and its vulnerability areas. Similar studies should be further applied in the S.E. Nigeria where severe gully erosions and landslides have recently become major environmental threats. However, afforestation might reduce excess soil moisture yet, proper family and land use planning could be more sustainable by decongesting the area and reducing the high human pressure on the land resources.

REFERENCES

- Akpan A E, Ilori O A, Essien N U. (2015) Geophysical investigation of Obot Ekpo Landslide site, Cross River State, Nigeria. *Journal of African Earth Sciences*, 109:154–167.
- Habu S N. (2015) Application of Remote sensing and GIS techniques for geospatial detection of areas susceptible to landslides in Jos South LGA, Plateau State, Northern Nigeria. Unpublished MSc. Thesis. University of Abuja, Nigeria. pp. 36.
- Harp E L, Reid M E, McKenna J P. (2009) Mapping of hazard from rainfall-triggered landslides in developing countries: Examples from Honduras and Micronesia. *Engineering Geology*, 104: 295–311.
- Hasegawa S., Nonomura A., Nakai S., Dahal R. K. (2013) Drainage Density as Rainfall Induced Landslides Susceptibility Index in Small Catchment Area. *Int. J. Lslid. Env*, 1(1), 27-28.
- Hsu C, Tsao T, Huang C. (2016) Using Remote Sensing Techniques to Identify the Landslide Hazard Prone Sections along the South Link Railway in Taiwan. *Procedia Engineering*, 143: 708–716.
- Igwe O. (2015a) The study of the factors controlling rainfall-induced landslides at a failure-prone catchment area in Enugu, Southeastern Nigeria using remote sensing data. *Landslides*, 12:1023–1033.
- Igwe O. (2015b) The geotechnical characteristics of landslides on the sedimentary and metamorphic terrains of South-East Nigeria, West Africa. *Geoenvironmental Disasters*, 1: 1-14.
- Igwe O. (2013) ICL/IPL activities in West Africa: landslide risk assessment and hazard mapping approach. *Landslides*, 10:515–521.
- Knapen A, Kitutu M G, Poesen J. (2006) Landslides in a densely populated county at the foot-slopes of Mount Elgon (Uganda): characteristics and causal factors. *Geomorphology*, 73: 149–165.
- Luzi L, Pergalani F, 1999. Slope instability in static and dynamic conditions for urban planning: the "Oltre Po Pavese" case history (Regione Lombardia – Italy). *Natural hazards*, 20: 57-82.
- NPC. (2006) National Population Commission. 2006 Census Report. Abuja-Nigeria.
- Olowolafe E A. (2004) Assessment of soil fertility indicators using soil survey data on the Jos Plateau, Nigeria. *Journal of Environmental Sciences*, 8: 54-61.
- Panikkar S, Subramaniyan V. (1997) Landslide hazard analysis of the area around Dehra Dun and Mussoorie, Uttar Pradesh. *Current Science*, 73:1117–1123.
- Pathak D. (2016) Knowledge based landslide susceptibility mapping in the Himalayas. *Geoenvironmental Disasters*, 3:8-11.

- Rasyid A R, Bhandary N P, Yatabe R. (2016) Performance of frequency ratio and logistic regression model in creating GIS based landslides susceptibility map at Lompobattang Mountain, Indonesia. *Geoenvironmental Disasters*, 3:19.
- Sidle RC, Pearce AJ, O'Loughlin CL. (1985) Hillslope stability and land use. American geophysical union, Washington DC, USA, 125 pp.
- Wang, Z.Y., Lee, J.H.W., Melching, C.S. (2015) Debris flows and landslides. In: *River dynamics and integrated river management*. Springer, Berlin, pp. 193-264.
- Wasowski J, Lamanna C, Casarano D. (2010) Influence of land use change and precipitation patterns on landslide activity in the Daunia Apennines, Italy. *Quarterly Journal of Engineering Geology & Hydrogeology*, 43: 387–401.

AIR POLLUTION DISPERSION MODELLING USING SPATIAL ANALYSES

Jan BITTA^{1,2}, Irena PAVLÍKOVÁ^{1,2}, Vladislav SVOZILÍK^{2,3,4}, Petr JANČÍK^{1,2,3}

¹Department of Environmental Protection in Industry, Faculty of Metallurgy and Material Engineering, VSB - Technical University of Ostrava, 17.listopadu 15/2172, 708 33, Czech Republic

Kat616@vsb.cz

²Institute of Environmental Technology (IET), VSB - Technical University of Ostrava, 17.listopadu 15/2172, 708 33, Czech Republic

³Joint Institute for Nuclear Research (JINR), Joliot-Curie 6, 141980 Dubna, Moscow region, Russia

svozilik@jinr.ru

⁴Institute of Geoinformatics, Faculty of Mining and Geology, VSB - Technical University of Ostrava, 17.listopadu 15/2172, 708 33, Czech Republic

Abstract

The air pollution dispersion modelling via spatial analyses (Land Use Regression – LUR) is an alternative approach to the air quality assessment to the standard air pollution dispersion modelling techniques. Its advantages are mainly much simpler mathematical apparatus, quicker and simpler calculations and a possibility to incorporate other factors affecting pollutant's concentration.

The goal of the study was to model the PM₁₀ particles dispersion modelling via spatial analyses in Czech-Polish border area of Upper Silesian industrial agglomeration and compare results with results of the standard Gaussian dispersion model SYMOS'97.. Results show that standard Gaussian model with the same data as the LUR model gives better results (determination coefficient 71% for Gaussian model to 48% for LUR model). When factors of the land cover and were included into the LUR model, the LUR model results were significantly improved (65% determination coefficient) to the level comparable with Gaussian model.

Keywords: Pollution dispersion; PM₁₀; air quality; Land Use Regression; Symos'97

INTRODUCTION

Particulate pollution

The PM (Particulate matter) is called a mixture of solid or liquid both organic and anorganic substances in the air. It mainly consists of sulfates, nitrates, ammoniac, salts soot, mineral particles, metals, bacteria, pollens and water. Particles of diameter smaller than 10 µm (PM₁₀) have severe health effects because they may get into lungs or even join the blood stream (US EPA, 2017), (WHO, 2017), (Obroučka 2003).

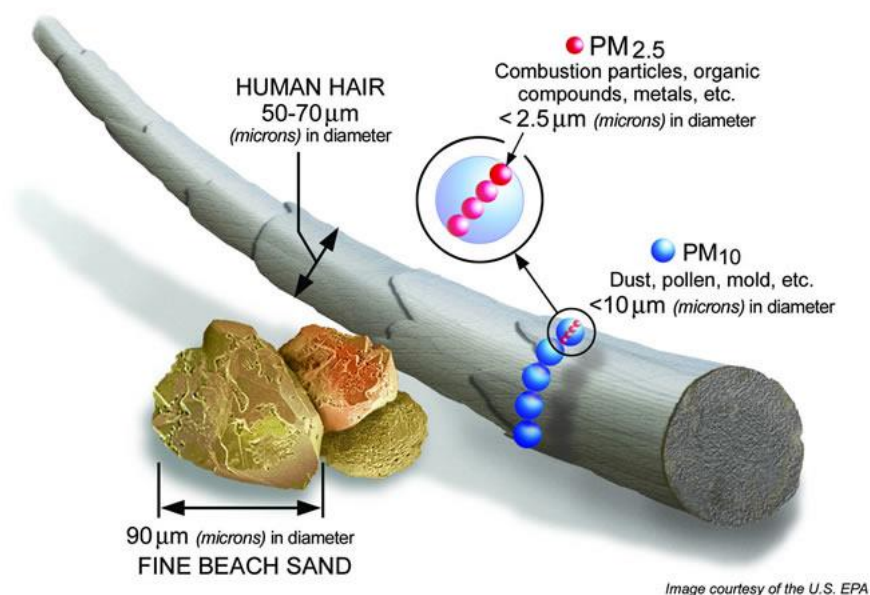


Fig. 1. Illustration of PM₁₀ and PM_{2.5} size, (US EPA, 2017)

Natural PM₁₀ sources are forest fires, dust storms, volcanic processes, erosion or sea water (Aus DEE, 2017), (IRZ, 2017). Large part of PM₁₀ has anthropogenic origin (Zajusz-Zubek, 2015). It consists of combustion processes (thermal power plants, heating, internal combustion engines), industrial processes like coking, blast furnaces, steelworks, sinter plants, cement production or mineral extraction, dust resuspension from roads and agriculture (soil erosion) (Obroučka 2003), (Pavlíková, 2013), (Grynkiewicz-Bylina, 2005), (Francova, 2016).

Recent research indicates non-existence of a minimal threshold concentration value for human health effects (Aus DEE, 2017). Factors influencing health effects are particles' size and geometry, their chemical composition, physical properties, concentration and time of exposure. Particles greater than 10 μm are caught by ciliated epithelium of upper respiratory tract and have low health impact. Particles smaller than 10 μm cumulate in bronchi and lungs and cause health issues. Particles smaller than 1 μm possess the biggest health threat because they may get into alveoli and frequently contain adsorbed carcinogenic substances.

The PM₁₀ inhalation damages mainly heart and lungs and is a cause of premature death of people with heart or lung disease, cancer, fibrosis, allergic reactions, asthma, lung insufficiency, heart attacks, respiratory tract irritation and cough (US EPA, 2017), (WHO, 2017), (Obroučka 2003), (Aus DEE, 2017), (IRZ, 2017).

There are two legal pollution limits for PM₁₀. The 24-hour average limit is 50 μg/m³ which can be exceeded no more than 35 times per year. The annual average concentration limit is set as 40 μg/m³ (Law 201, 2012), (Law 330, 2012).

Land Use Regression modelling

The Land Use Regression (LUR) modelling is an empirical modelling approach which is based on multivariate linear regression. It combines pollution monitoring data with spatial variables describing vicinity of monitoring sites which are typically obtained via spatial analyses in Geographic Information Systems (GIS). The result of the analyses is the linear model

$$[\text{Pollution}] = [\text{Coef}_1] * [\text{Factor}_1] + [\text{Coef}_2] * [\text{Factor}_2] + \dots + [\text{Coef}_n] * [\text{Factor}_n]$$

where [Factor_*] are selected spatial factors and [Coef_*] are regression coefficients obtained from the linear regression analysis at the pollution monitoring sites. The empirical model can be then used to estimate spatial distribution of the PM₁₀ pollution in the area of interest.

The LUR model was first used for the air pollution monitoring in the SAVIAH (Small Area Variations in Air quality and Health) project. This approach was used to study NO_x concentrations in three European cities – Amsterdam, Huddersfield and Prague. The successful application of the LUR in the SAVIAH project model spurred its usage in further studies in European countries and in the rest of the world (Hoek, 2008), (Li, 2012), (Kryza, 2011)

Gaussian dispersion modelling

Gaussian dispersion models assume an emission transport from continuous pollution sources in homogenous wind field without spatial limits. The transport itself is in the model provided by the convection by wind and via turbulence diffusion which is described statistically by Gaussian distribution. Spatial limitations, mainly the terrain, are included into model by correction coefficients. Gaussian dispersion models are commonly used for long term (f.e. annual) average concentrations modelling. The dispersion is calculated for a set of standard meteorological conditions and summed, weighted by probability of occurrence of such conditions. The most commonly used Gaussian dispersion models are CALINE3 (Benson, 1979) and ADMS-Urban (ADMS, 2017).

The SYMOS'97 model (Symos, 1998) is a reference pollution dispersion model in the Czech Republic. It is a Gaussian model which calculates pollution dispersion of both gaseous and particulate pollutants from point, linear and area pollution sources. The model takes into account both dry and wet deposition as well as chemical reactions during transport.

DATA SOURCES

The study area was selected to match the area of the Air Silesia project (Air Silesia, 2013). All air pollution source and monitoring data used in the study were purchased from published results of the Air Silesia project and are relevant to the year 2010.

The Air Silesia project was focused on collecting the air pollution data and assessment of the air quality in the border region of the Upper Silesian industrial region. The following Fig. 2 shows the study area and the annual mean PM₁₀ concentrations [$\mu\text{g}/\text{m}^3$] at the pollution monitoring stations

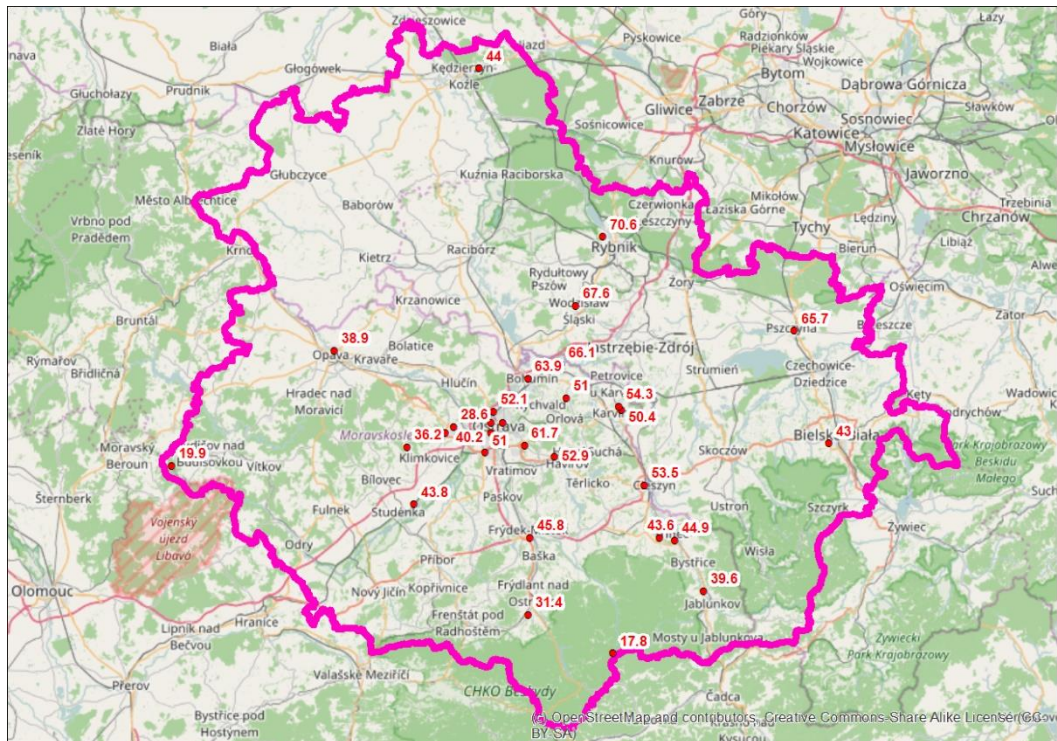


Fig. 2. The study area and pollution monitoring stations with annual average of PM₁₀

There are 2.5 million inhabitants in the study area which is one of the most air polluted regions of the EU (Fig. 3). The most severe pollutants in the region are particulates, polyaromatic hydrocarbons (PAH) and heavy metals (As, Cd, Hg). High level of pollution concentrations are determined by the combination of several key factors – high population density, presence of heavy industries (coal mining and processing, iron and steel production, heavy chemistry), coal energetics (utility and industrial scale to domestic use scale) and unfavorable basin-like terrain configuration.

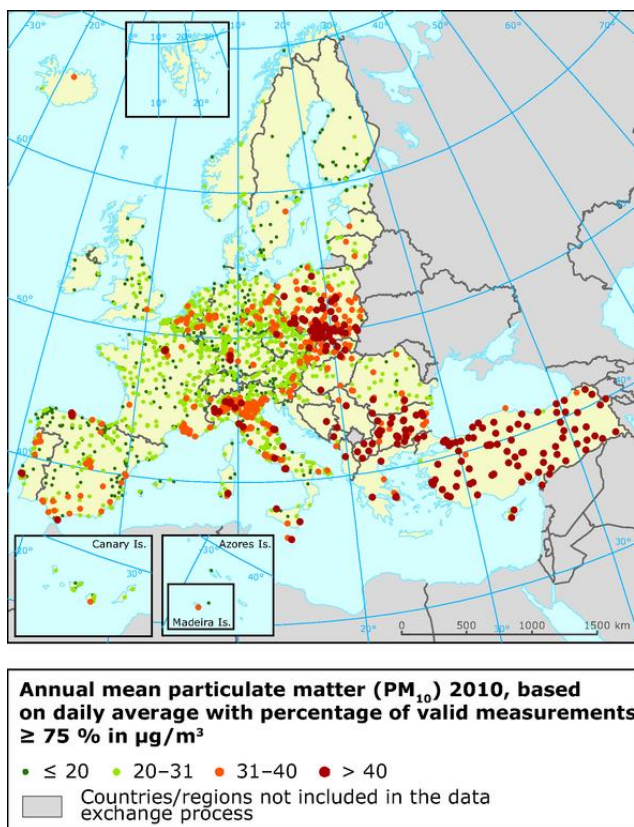


Fig. 3. Annual mean PM₁₀ concentrations in 2010, (EEA, 2013)

Air pollution data

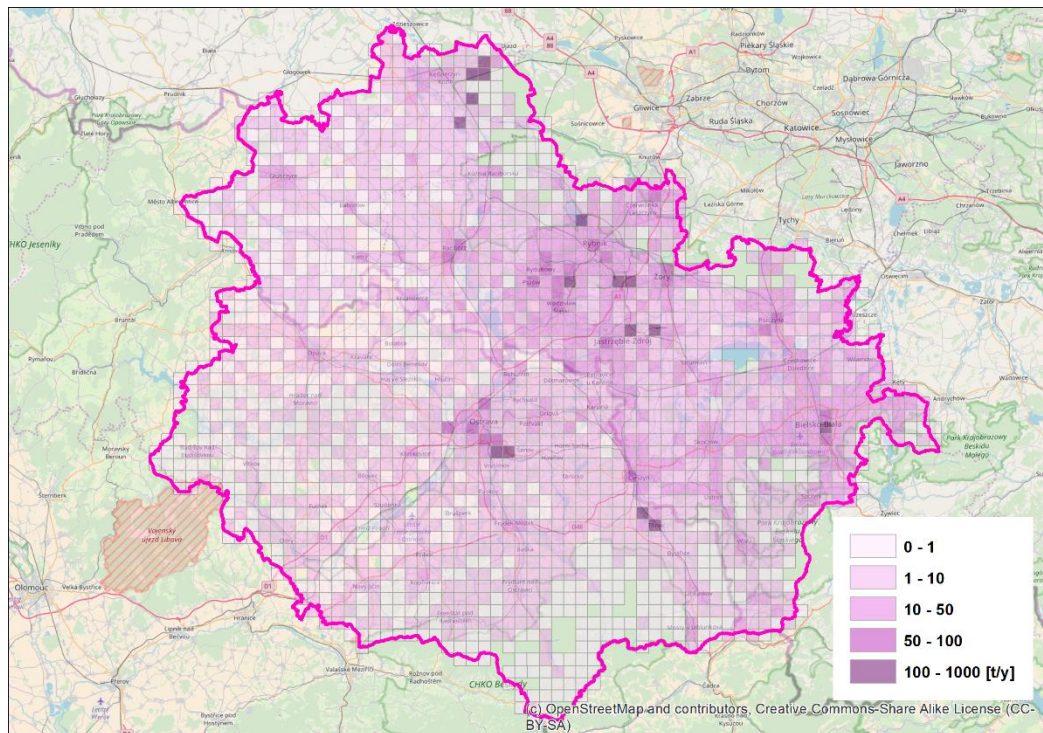
The air pollution data – yearly averages of PM₁₀ concentrations, were obtained from the yearbooks (CHMI, 2011) of the Czech Hydrometeorological Institute and the Voivodship Inspectorate of the Environmental Protection of Silesian Voivodship (WIOS, 2013) There have been 27 air pollution monitoring stations in the study area measuring the PM₁₀ concentrations (Fig. 2).

Pollution source data

The pollution source data were obtained from the pollution source database provided by the Air Silesia project. The data have been divided by the land of origin (Czech-Polish) and by the kind of the pollution source (industrial, domestic heating, car traffic). Brief statistics of emissions are presented in following Tab.1 and emission squares (Fig. 4)

Table 1. The PM₁₀ pollution sources in the study area, (Air Silesia, 2013)

Country	Pollution sources	No. of sources	Emissions [t/y]
Czechia	Industrial	2025	2315
	Domestic heating	21824	1589
	Car traffic	56057	961
Poland	Industrial	1598	13400
	Domestic heating	33301	8610
	Car traffic	55745	911

**Fig. 4.** The PM₁₀ distribution in the study area, Basemap:OpenStreetMap

Land Use data

The land use data were obtained from the CORINE Land Cover dataset (EEA, 2015) as vector datasets. There were four kinds of land cover selected for the analysis – built-up areas, forested areas, areas with grass cover and open soil-agricultural areas.

METHODOLOGIES AND RESULTS

There were two basic groups of factors considered in the study – factors of pollution sources and factors of land cover. Each factor (except distance to the nearest major road) was calculated in the similar fashion. There was a buffer of the selected perimeter created around each of pollution monitoring stations. The factor was then calculated as a sum, percentage or length-weighted average of the vector data cut by the buffer. Factors were calculated uniformly (U) or they were calculated as a weighted average based on wind direction probability (W). The area of modelling was split into 14 areas according to the terrain configuration. Meteorological condition in each area were represented by its own dataset (Fig. 5). In that case, buffer zones were split into 8 slices representing 8 wind directions. Factors were calculated for each slice area and final weighted factors were calculated as a weighted average of those factors where weights were probability of wind blowing from corresponding direction.

Table 2. Factors of pollution sources, factors of land cover

Factor	Identifier	Distances	Weighing	Unit
Emissions from industrial sources	IS	100,200,500,1000,2000	U,W	t/y
Length of roads	LR	100,200,500,1000,2000	U,W	m
Average traffic intensity weighted by length of road sections	TI	100,200,500,1000,2000	U,W	car/day
Emissions from domestic heating	DH	100,200,500,1000,2000	U,W	t/y
Distance to the nearest road	NR			
Grass covered land	GCL	100,200,500,1000,2000	U,W	% of area
Forested land	FL	100,200,500,1000,2000	U,W	% of area
Built-up land	BL	100,200,500,1000,2000	U,W	% of area
Open soil	OSL	100,200,500,1000,2000	U,W	% of area

For the purpose of the study, all factors were encoded. For example, the [FL_500_W] code means the factor of forested land cover counted for the buffer distance 500m and weighted by the wind direction probability distribution.

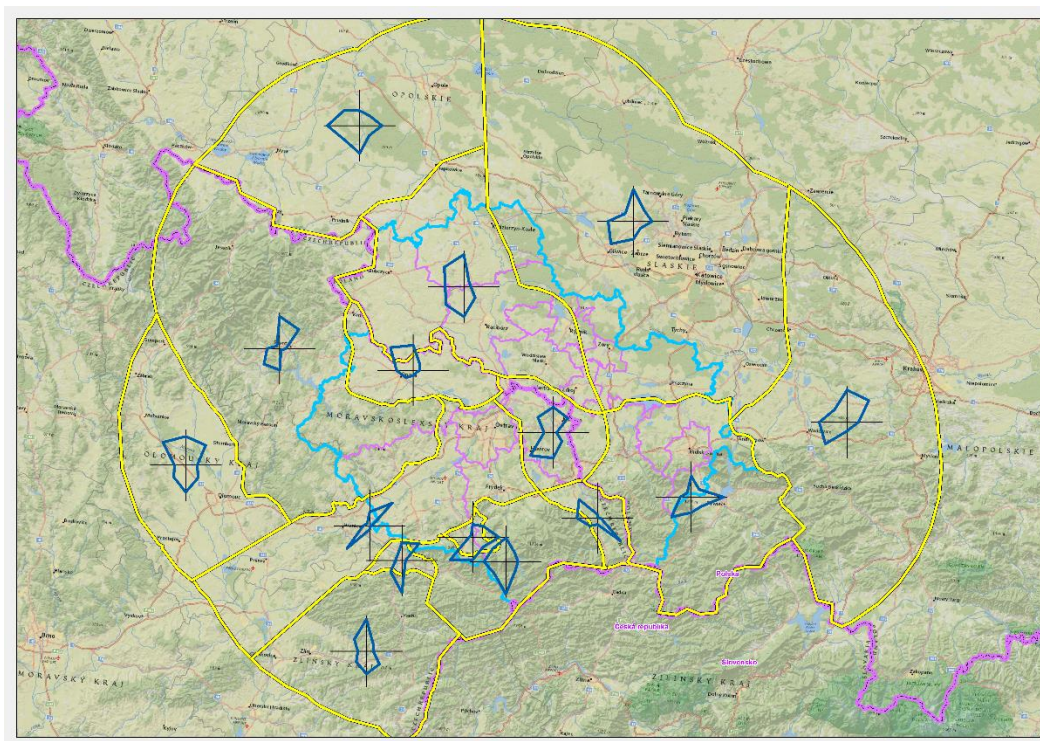


Fig. 5. Wind direction probability distribution, (Air Silesia, 2013)

Regression analyses were performed in the Statgraphics software. The regression models were constructed for combinations of industrial sources ([IS_*_*]), traffic intensity ([TI_*_*]), domestic heating ([DH_*_*]) and nearest road ([NR]). Regressions consisted of two steps, statistical significance/insignificance of each factor was evaluated and regression coefficients were calculated with statistically significant factors.

The best statistical analysis result was a regression model:

$$[\text{PM}_{10} \text{ concentration}] = 30.8507 + 0.00789643 * [\text{IS}_{2000_W}] + 0.000583609 * [\text{TI}_{2000_W}] + 0.214567 * [\text{DH}_{2000_W}] + 0.01368 * [\text{NR}]$$

The R^2 of the model is 48% and mean quadratic error of the model was $10.59 \mu\text{g}/\text{m}^3$.

When factors of the land cover were taken into account, the resulting best linear model was constructed as

$$[\text{PM}_{10} \text{ concentration}] = 46.3802 + 0.00113242 * [\text{IS}_{2000_W}] + 0.203484 * [\text{DH}_{2000_W}] - 0.299948 * [\text{FL}_{1000_W}]$$

The R^2 of the model is 65% and mean quadratic error of the model was $8.34 \mu\text{g}/\text{m}^3$.

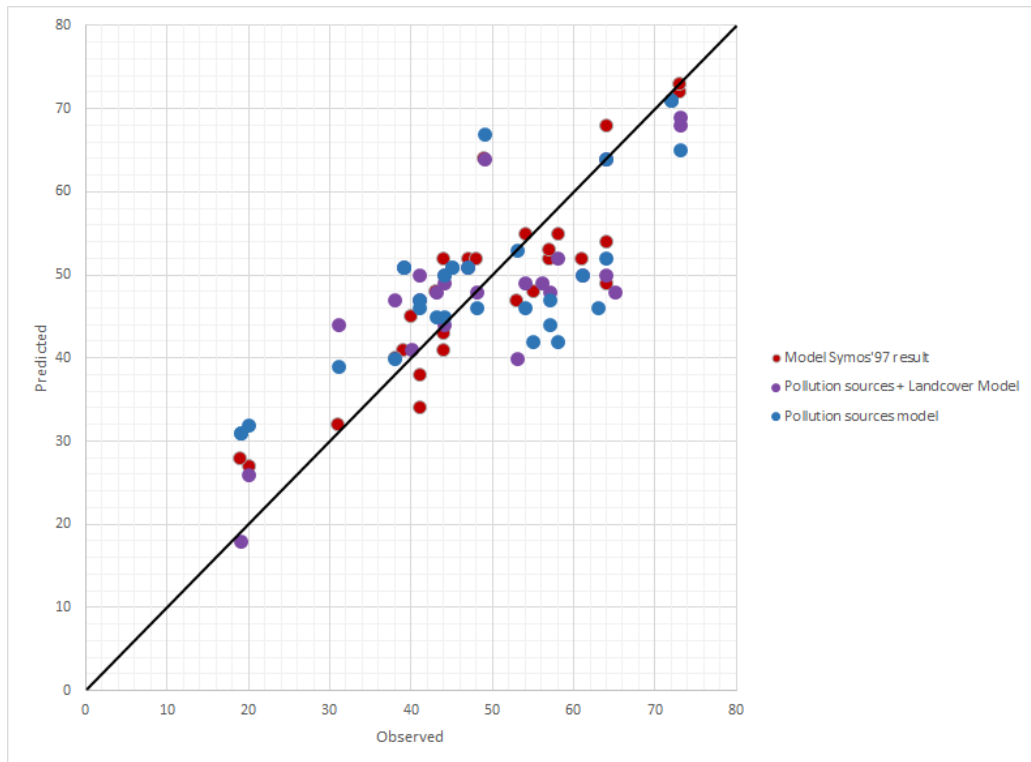


Fig. 6. Observed to predicted comparison of results

The results of the SYMOS'97 model were statistically evaluated with the measurements at monitoring sites. The R^2 of the model is 71% and mean quadratic error of the model was $7.44 \mu\text{g}/\text{m}^3$.

DISCUSSION

The LUR model gives with the similar input data much worse results than Gaussian dispersion model (R^2 48% x 71%). The LUR model was providing good estimates of the air pollution when the pollution monitoring station was positioned within the urban environment in the vicinity of air pollution sources. On the other hand, predictions at rural and natural sites were inaccurate because the model, as constructed, is not able to take into account the long distance pollution transport. The LUR model also did not take into account other parameters of pollution sources used in Gaussian models, mainly source height, exhaust gas speed and temperature, speed and fluency of the traffic stream, etc. The pollution dispersion is also in Gaussian models more accurately described in the form of non-linear dispersion formulas.

The LUR model with added land cover factors gives better predictions of PM₁₀ concentrations (R^2 65%) which are comparable but still worse than a Gaussian model. The addition of land cover factors greatly improved the quality of forecasts in natural and rural monitoring sites. The Gaussian model provided better results in industrial and urban-background monitoring sites while the LUR model with land cover factors outperformed it slightly at the rural and natural monitoring sites. The LUR model was also able to explain the reason of significant PM₁₀ concentration underestimation by Gaussian model at three monitoring sites (Opava-Kateřinky, Věřňovice, Studénka). The LUR model showed that all three sites which are positioned close to the edge of intravilans are heavily influenced by the nearby agricultural activities and/or wind-caused reemissions and erosion represented in the LUR model by the Open soil factor.

CONCLUSION

The LUR modelling is an alternative approach to the standard dispersion models. The biggest advantages of the LUR approach are relative simplicity of calculation compared with time and computational power demanding dispersion modelling and ability to incorporate factors not included in dispersion modelling. Although their results in the study did not match the quality of the Gaussian model the LUR approach should not be dismissed because they may incorporate phenomena which are usually omitted by standard dispersion models. So, it should be considered to look for some kind of a hybrid approach which would be able to combine better air pollution dispersion characterization of Gaussian models and ability to incorporate other factors to LUR models to provide more accurate modelling results.

ACKNOWLEDGEMENT

Access to computing and storage facilities owned by parties and projects contributing to the National Grid Infrastructure MetaCentrum, provided under the programme "Projects of Large Research, Development, and Innovations Infrastructures" (CESNET LM2015042), is greatly appreciated.

This work was financially supported by the Ministry of Education, Youth and Sports of the Czech Republic in the "National Feasibility Program I", project LO1208 "Theoretical Aspects of Energetic Treatment of Waste and Environment Protection against Negative Impacts".

This research was supported in part through computational heterogenous cluster „HybriLIT“ provided by The Laboratory of Information Technologies, Joint Institute for Nuclear Research in Dubna, Moscow region, Russia

REFERENCES

ADMS (2017) Cambridge Environmental Research Consultants, <http://www.cerc.co.uk/environmental-software/ADMS-Urban-model.html>, ADMS-Urban model, [2017-01-12]

Air Silesia (2013) http://www.air-silesia.eu/cz/a1170/V_stupy.html, Air Silesia - výstupy, [2017-01-12].

- Aus DEE (2017) Australian Government: Department of the Environment and Energy, <http://www.npi.gov.au/resource/particulate-matter-pm10-and-pm25>, Particulate matter (PM10 and PM2.5), [2017-01-12].
- Benson P. (1979) CALINE3 - A Versatile Dispersion Model for Predicting Air Pollutant Levels Near Highways and Arterial Streets, US EPA, Washington D.C.
- Bubník, J., et al. (1998) SYMOS '97 - Systém modelování stacionárních zdrojů., Praha, Český hydrometeorologický ústav, ISBN: 80-85813-55-6.
- ČHMÚ (2011) http://portal.chmi.cz/files/portal/docs/uoco/isko/tab_roc/2010_enh/cze/index_CZ.html, Znečištění ovzduší a atmosférická depozice v datech, Česká republika 2010, [2017-01-12].
- European Environment Agency (2013) <http://www.eea.europa.eu/data-and-maps/figures/annual-mean-particulate-matter-pm10>, Annual mean particulate matter (PM10) 2010, based on daily average with percentage of valid measurements $\geq 75\%$ in $\mu\text{g}/\text{m}^3$, [2017-01-12].
- European Environment Agency (2015) <http://www.eea.europa.eu/publications/COR0-landcover>, CORINE Land Cover, [2017-01-12].
- Francova, A., et al. (2016) Evaluating the suitability of different environmental samples for tracing atmospheric pollution in industrial areas, Environmental Pollution, Volume 220, p. 286-297.
- Gryniewicz-Bylina B., Rakwicz B., Pastuszka J.S. (2005) Assessment of Exposure to Traffic-Related Aerosol and to Particle-Associated PAHs in Gliwice, Poland. Polish Journal of Environmental Studies. Volume 14, p. 117-123.
- Hoek G., et al. (2008) A review of land – use regression models to assess spatial variation of outdoor air pollution, Atmospheric Environment, Volume 42, p.7561 – 7578.
- Integrovaný registr znečišťování (2017) <http://www.irz.cz/node/85>, Poléťavý prach (PM10), [2017-01-12].
- Kryza M., Szymanowski M., Dore A. J., Werner M. (2011) Application of a land – use regression model for calculation of the spatial pattern of annual NOx air concentrations at national scale: a case study for Poland, Procedia Environmental Sciences, Volume 7, p. 98 – 103.
- Law 201 (2012) Zákon č. 201/2012 Sb., o ochraně ovzduší. In: Sbíрка zákonů. 2. 5. 2012, <https://portal.gov.cz/app/zakony/zakonPar.jsp?idBiblio=77678&nr=201~2F2012&rpp=15#local-content>
- Law 330 (2012) Vyhláška č. 330/2012 Sb. o způsobu posuzování a vyhodnocení úrovně znečištění, rozsahu informování veřejnosti o úrovni znečištění a při smogových situacích. In: Sbíрка zákonů. 8. 10. 2012, <https://portal.gov.cz/app/zakony/zakonPar.jsp?idBiblio=78340&nr=330~2F2012&rpp=15#local-content>
- Li L., Wu J., Wilhelm M., Ritz B. (2012) Use of generalized additive models and cokriging of spatial residuals to improve land – use regression estimates of nitrogen oxides in Southern California, Atmospheric Environment, Volume 55, p. 220 – 228.
- Obroučka K. (2003) Ochrana ovzduší I.: Látky znečišťující ovzduší, VŠB-TU Ostrava, Ostrava.
- Pavlíková I., Jančík P. (2013) Metallurgical source-contribution analysis of pm10 annual average concentration: A dispersion modeling approach in Moravian-Silesian region, Metallurgija. Volume 52, p. 497-500. ISSN 0543-5846.

- US EPA (2017) United States Environmental Protection Agency, <https://www.epa.gov/pm-pollution/particulate-matter-pm-basics>, Particulate matter (PM) Basics, [2017-01-12].
- WHO (2017) World Health Organisation, <http://www.who.int/mediacentre/factsheets/fs313/en/>, Ambient (outdoor) air quality and health, [2017-01-12].
- WIOŚ Katowice (2013) <http://www.katowice.pios.gov.pl/index.php?tekst=monitoring/informacje/stan2010/i>, Informacje o stanie środowiska w województwie śląskim w 2010 roku, [2017-01-12].
- Zajusz-Zubek E., Mainka A., Korban Z., Pastuszka J.S. (2015) Evaluation of highly mobile fraction of trace elements in PM10 collected in Upper Silesia (Poland): Preliminary results, Atmospheric Pollution Research, Volume 6, p. 961-968. ISSN: 1309-1042.

IDENTIFICATION OF R PACKAGES FOR SPATIAL DATA HANDLING AND ANALYSES

Jan, CAHA¹

¹Department of Regional Development and Public Administration, Mendel University in Brno, Zemědělská 1, 613 00, Brno, Czech Republic

jan.caha@mendelu.cz

Abstract

R is becoming one of the most used programming languages for data analysis. One of the main reasons for this is probably a wide range of packages that extend R's functionality. Packages are usually focused on specific topics or domains of data processing e.g. time series analyses or spatial data modelling and processing. As of December 2017 there were 12 009 packages available from the R's online resource. For users it is becoming rather complicated to find packages relevant to their topic or domain. In this paper we analysed the text description of packages and their dependence on other packages to identify packages that are focused on spatial data modelling and analyses. The result of this analysis is the identification of 895 packages which are not listed under Spatial or SpatioTemporal CRAN Views.

Keywords: R, CRAN, package, spatial, GIS, text analysis, dependency analysis

INTRODUCTION

The topic of safety and security management in the field of GIScience covers a wide range of topics that spans from crime data analyses (Horák *et al.* 2017, Wang 2012), epidemiology (Marek and Pászto 2017), analyses of dangerous segments of transport lines (Bíl *et al.* 2017, Ivan and Tesla 2015) to topics such as flood forecasts (Rapant and Kolejka 2018) or landslide susceptibility mapping (Karell *et al.* 2017, Marjanović *et al.* 2015). As mentioned by Brunsdon and Comber (2015), standard GIS software can not represent state of the art tool when it comes to complex modelling and analysing tasks. The main reason is that the state of the art approaches often utilize innovative mathematical or statistical approaches towards the data that usually are not implemented within GIS. Because of this issue a significant part of research within GIScience is done in non-GIS software that allows easier implementation and utilization of new methods as well as more suitable sharing and reproducibility of research (Gil *et al.* 2016). Two programming languages play an important role in this approach towards GIScience – R and Python. For both of them, there is a considerable number of packages (extensions) that introduce state of the art methods and approaches for spatial data analyses with new ones emerging almost daily. The rising number of these extensions brings with it an important issue for both users and researchers: how to find relevant packages for a specific task or analysis? In this paper the packages for R are studied to identify those that are focused on processing of spatial data.

R is a statistical computing language heavily influenced by languages S and Scheme (Ihaka and Gentleman 1996), developed as an open source software and distributed under GPL-2 and GPL-3 licences. The development of the language has begun in 1993 and it was publicly presented in 1996 (Ihaka and Gentleman 1996). One of the reasons why R is popular (especially amongst

researchers) is probably a wide variety of packages (Wickham 2015). A package is a fundamental unit of shareable code that bundles together functions, in form of R code, documentation of functions, software tests and possibly also data (Wickham 2015). The concepts of packages allows R to be easily expandable with new tools, methods and datasets. If the package fulfils rules listed in *CRAN Repository Policy* (<https://cran.r-project.org/web/packages/policies.html>) it can be published on *Comprehensive R Archive Network* (CRAN). CRAN (<https://cran.r-project.org/>) is an online repository of packages from which a package can be installed in R using one simple command. Even though, that it is not necessary for package to be available on CRAN, it can be also installed from a file or from an online code repository (e.g. GitHub), it is usually desirable to publish the package on CRAN as it serves as a well known source and it also guarantees certain quality of the package (existence of the documentation, portability of the code, verification of package licence etc.). One of the requirements to publish a package on CRAN is that the package has to be licensed under one of the open source licences. This significantly supports open and reproducible research (Gandrud 2014).

One of the first attempts to statistically analyse spatial datasets in R were performed by Bivand (2000). The main reason for utilization of R for spatial data processing is the connection to advanced statistical methods and tools that are usually not available in GIS. In 2003 (Bivand 2003) presented overview of R packages focuses on spatial statistics applications and divided them into four categories: point patterns, geostatistics, lattice/area data and others. Altogether these included 21 packages, with 17 of them being available on CRAN. The packages in the category *other* focused mostly on mapping functions and GIS interfaces. However, at that time there was no universal set of classes and functions for representation of spatial data types in the geoinformatics sense (Pebesma and Bivand 2005). Such set of classes was introduced in 2005 by the `sp` package which allows coherent representation of both vector (points, lines, polygons) and raster spatial data in R (Pebesma and Bivand 2005). The `sp` package quickly became de facto a standard for handling spatial data within R environment with many other packages directly depending on it (Bivand *et al.* 2008, Brunsdon and Comber 2015). As an example of dependent package the `raster` package can be presented (Hijmans 2017). The `raster` package depends on `sp` and adds further functionality for working with raster datasets in R. Recently new package `sf` was introduced (Pebesma 2017b) which implements simple features standard (ISO 19125-1:2004) for representation of spatial objects. This package aims to cover some implementation gaps in the `sp` package and it should in long term to succeed the `sp` package (Pebesma 2017b).

One of the issues with R packages is their quickly growing number. In January 2015 Wickham (2015) reported 6 000 packages on CRAN. In the end of December 2017, time of writing of this paper, the number of packages on CRAN just exceeded 12 000. This presents a new challenge for users, to find a functionality they need. CRAN provides so called Task Views (<https://cran.rstudio.com/web/views/>) which list packages based on specific categories of topics (e.g. Econometrics, Machine Learning & Statistical Learning, Analysis of Spatial Data etc.). However, only a small portion of packages, that focus the given topic, is listed in these Task Views. Unless package's author contacts Task View maintainer and suggests addition of the package to the Task View or the package is really significant and important within the field it is quite unlikely for the package to appear in the Task View.

In this paper we want to overview all the packages that are available on CRAN and identify those that may be relevant for handling and analysing spatial data. In order to archive this goal the Description of packages, which is a text representation that should summarize functionality of the package, and their dependence on other packages will be studied. The main question behind this research can be summarized as: How many packages related to spatial data handling and analysing are available on CRAN and how is it possible to identify them?

DATA

Two types of data are used in this study. First type of data is obtained directly from CRAN web-site and the second type is mediated by *METACRAN* website (<https://r-pkg.org/>). According to its description *METACRAN* is a collection of small services built around the CRAN repository of R packages. *METACRAN* provides list of all packages on CRAN and their download statistics from RStudio mirror. Several R packages are also associated with the *METACRAN* website. For the purpose of this work the relevant package is `cran_db` (Csardi 2017) which allows obtaining metadata (including description) for individual packages.

The list of packages and the metadata for packages were collected on 29. 12. 2017 during the time when submission were suspend due to vacation and server maintenance (the period lasted 22. 12. 2017 3. 1. 2018).

For the purpose of this study three metadata columns are important. Description is a text field which describes the content of the package, other important columns are *Depends* and *Imports* which provide information about other packages that user needs to be able to use specific package. Historically, *Depends* was the only way to link content of another package, from which usually a functionality is needed. The more modern and preferable way to include content of another package currently is to use *Import* (Wickham 2015). The details are provided by Wickham (2015) and for the purpose of our study we can consider both methods as equal because both fields mean that the packages listed in them are necessary to run the main package. These metadata fields can contain from 0 to n packages. The example listing only the important fields from the metadata for package `sf` looks like this:

```
sf
Description: Support for simple features, a standardized way to encode
spatial vector data. Binds to GDAL for reading and writing data, to
GEOS for geometrical operations, and to Proj.4 for projection
conversions and datum transformations.
Imports: utils (*), stats (*), tools (*), graphics (*), grDevices (*),
grid (*), Rcpp (*), DBI (>= 0.5), units (>= 0.4-6), classInt (*),
magrittr (*)
Depends: R (>= 3.3.0), methods (*)
```

The value inside brackets specifies if certain version of package is required. E.g. `units (>=0.4-6)` means that package `units` with version higher 0.4-6 is required to run `sf` package. If no specific version is provided, e.g. `grDevices (*)`, then no specific version is required.

Besides data obtained with the use of `cran_db` package several pieces of information were directly scrapped from CRAN website with the use of `rvest` package (Wickham 2016). Web scrapping

is a technique which programmatically access webpages, finds specific elements in these webpages, transforms them if necessary and stores them in form of structured dataset (Boeing and Waddell 2017). The information that was scrapped from website were lists of packages that belong individual CRAN Views. Even though, that Spatial (Bivand 2017) and SpatioTemporal (Pebesma 2017a) CRAN Views are the main interest for this research, for the upcoming text analysis it is necessary to know also packages in other CRAN Views.

The dataset contains 12 009 packages. Using the `crandb` package (Csardi 2017) the meta-data for each package were obtained. The metadata for each package were gained in form of a named and nested list. While these lists have the same general structure for all packages they can vary quite significantly internally. Several fields of the metadata have to be present, for example *Title*, *Description*, *Version*, *Maintainer* and *Licence*, while other fields, like for example *Author*, *Depends*, *Imports* and *Suggests*, either do not have to be present or can have various length.

The metadata of packages were simplified in such way that a data frame containing name of package, its description and list of packages that the package either depended upon or imported was created. The information about package membership to CRAN View was also included. Since every package can be belong to more than one View the information was simplified. Every package is connected only with one View, the first view under which it is listed is used if the package belong to more than one View. The exception of this rule are packages listed under either Spatial or SpatioTemporal View which are always listed under one common View which was marked as SpatialView as those are the main focus of this research. This divides packages into 35 categories, 33 representing individual CRAN Views, one named SpatialViews that combines Spatial and SpatioTemporal CRAN Views and a category *Not listed* that summarizes packages that do not belong into any CRAN View.

ANALYSIS OF SPATIAL PACKAGES

There are two possible approaches towards identification of packages that are likely to work with spatial data in some way. The first is to carry out a text analysis of package description in order to find out if there are words specific to the field of geoinformatics. This, however, requires compilation of list of domain specific words that can be later searched for. The second possible approach is to identify packages that depend on other spatial packages. For this approach we have identify packages most commonly used as dependencies in SpatialViews.

The first step for both approaches is obtaining list of packages that belong to either Spatial (Bivand 2017) or SpatioTemporal (Pebesma 2017a) CRAN View. Altogether these two views contain 223 unique packages. The packages in spatial views represent roughly 1.857% of all packages. This set of packages will be used to estimate domain specific words and important imported packages for the topic of spatial data handling.

Text analysis of package descriptions

The text analysis of packages descriptions is performed using `tidytext` package (Silge and Robinson 2016, Silge and Robinson 2017) and `tm` package (Feinerer *et al.* 2008, Feinerer and Hornik 2017).

The preprocessing stage for the text analysis consists of several steps. From the description of packages numbers, punctuation and stop words are removed. Stop words are, according to Silge and Robinson (2017), extremely common words that are not useful for text analysis (e.g. the, a, of, to). Then the text is converted into lower case and word stems are determined. The process is called stemming and is common in text mining research (Feinerer *et al.* 2008). `tm` package uses Porter's stemming algorithm (Feinerer and Hornik 2017). Stemming allows interception of word in various forms, for example both words `spatial` and `spatially` have the same stem `spatial` using Porter's algorithm. This helps with compaction of text into more manageable form. With words stems the number of individual stems occurrence can be calculated, however, since we want to identify words typical for `SpatialViews` the individual occurrence of words need to be calculated with respect to the CRAN Views. Ten most frequent words are summarized in Tab. 1. The tables shows than one of the most common word stems through the different CRAN Views is `model` as it is present 4 times in the 10 most frequent words.

Table 1. Ten most frequent word stems in package descriptions with respect to CRAN View.

CRAN View	Word stem	count
Distributions	distribut	287
Survival	model	244
SpatialViews	data	197
ExperimentalDesign	design	191
Psychometrics	model	188
Bayesian	model	174
SpatialViews	model	172
TimeSeries	time	172
TimeSeries	seri	170
Distributions	function	169

At this point we need to identify words that are more important for `SpatialViews` than for other corpora. In this case corpus is a set of package descriptions that belong to one of 35 categories described previously. According to (Silge and Robinson 2017), the specific words for given corpus in comparison to other corpora can be indentified using TF-IDF (term frequency – inverse document frequency). TF-IDF is calculated as:

$$TF-IDF = \frac{n_{term}}{n_{all\ terms}} \times \ln \left(\frac{n_{documents}}{n_{documents\ containing\ term}} \right) \quad (1)$$

where n is number of occurrences for specific term. TF is the first fraction in the equation and is calculated with respect to occurrence of specific word in the corpus of CRAN View, while IDF is the second fraction that specifies how common the term is within all corpora. For words that

occur in every corpora the value of TF-IDF is equal to 0 which indicates that the word is rather common and not very specific for one corpus. Tab. 2 shows ten most specific word stems in package descriptions.

Table 2. Ten most specific stems in package descriptions with respect to CRAN View sorted by TF-IDF

CRAN View	Word stem	count	TF	IDF	TF-IDF
MetaAnalysis	metaanalysi	81	0.0229	1.9459	0.0446
Pharmacokinetics	pharmacokinet	12	0.0225	1.9459	0.0437
gR	grbase	10	0.0116	3.5553	0.0411
Phylogenetics	phylogenet	52	0.0208	1.9459	0.0405
Pharmacokinetics	linearup	6	0.0112	3.5553	0.0399
Pharmacokinetics	winnonlinr	6	0.0112	3.5553	0.0399
Pharmacokinetics	dose	9	0.0169	2.1691	0.0366
ExtremeValue	threshold	9	0.0429	0.8473	0.0363
Pharmacokinetics	noncompartment	5	0.0094	3.5553	0.0333
Genetics	haplotyp	10	0.0135	2.4567	0.0332

From the list of word stems ranked by TF-IDF the stems specific for the SpatialViews can be filtered. Fifty stems with highest values of TF-IDF are selected as candidate domain stems for GIScience. These are manually evaluated for occurrence of word stems that are not domain specific. Nineteen of the fifty stems were selected as not being domain specific: *anim, fleme, car, pattern, irregular, interpol, geometri, potter, mat, ss, mont, patterns, acoust, autoregress, heap, tessell, epidem, carlo, air*. The remaining words stems are considered as domain specific for field of geoinformatics: *spatial, spatiotemporal, movement, geograph, raster, geostatist, map, geojson, grass, netcdf, gdal, krige, variogram, geospati, ncdf, sp, arcg, qgis, gis, spacetim, gw, shapefil, cartograph, moran, saga, spde, polygon, grid, track, gps, coordin, areal, proj*. The list of domain specific stems will later be used to identify packages that contain any of these stems in their description.

Analysis of package dependence

The packages that are likely to work with spatial data can also be identified by dependence on most important spatial packages (e.g. *sp, raster, rgdal*). As mentioned previously, we will use fields *Depends* and *Imports* from package metadata to identify dependencies of each package because for our purpose these fields can be considered as equal. While it would be possible to specify important packages that work with spatial data manually based on expert opinion but the goal is to propose at least a semi-automatic method based on objective criteria.

The analysis of package dependence can be done in the same way as text analysis of package descriptions. If every package that is listed in *Depends* or *Imports* field is treated as word (or word stem), then the corpus for the CRAN View is a list of all imported packages. From this data the TF-IDF of dependency packages is calculated. Ten packages that are most often used as dependencies are listed in Tab. 3.

Table 3. Ten packages that are used as dependence with respect to CRAN Views.

CRAN View	Package	count	TF	IDF	TF-IDF
Phylogenetics	ape	63	0.1422	1.7636	0.2508
DifferentialEquations	deSolve	14	0.1239	1.1575	0.1434
ExtremeValue	ismev	2	0.0500	2.8622	0.1431
NaturalLanguageProcessing	tm	13	0.0510	2.4567	0.1252
NaturalLanguageProcessing	NLP	11	0.0431	2.4567	0.1060
WebTechnologies	httr	73	0.0979	1.0704	0.1047
FunctionalData	fda	15	0.0647	1.6094	0.1041
MetaAnalysis	metafor	14	0.0401	2.4567	0.0986
MedicalImaging	oro.nifti	6	0.0429	2.1691	0.0930
ExtremeValue	revdbayes	1	0.0250	3.5553	0.0889

In the same way that fifty candidate words were selected thirty package that act as dependency for packages in SpatialViews with highest TF-IDF are selected as important spatial dependencies. The resulting list is manually evaluated for packages that are not focused on spatial data handling. Seven of the thirty packages can not be considered as focused on spatial data: `classInt`, `jsonlite`, `zoo`, `ade4`, `foreign`, `spam`, `CircStats`. Even though, that these packages are used as dependencies more often amongst spatial packages than in other CRAN Views they do not have to be used exclusively for handling of spatial data. The remaining 21 packages are considered as important spatial dependencies that indicate that the focus of package that list any of these package in either imports or depends field will be on spatial data. The list consists of these packages: `sp`, `raster`, `rgdal`, `rgeos`, `maptools`, `spatstat`, `spdep`, `splancs`, `geosphere`, `gstat`, `fields`, `maps`, `spacetime`, `RandomFields`, `SpatialTools`, `adehabitatMA`, `gdistance`, `ncdf4`, `sf`, `shapefiles`, `spatstat.utils`, `deldir`, `leaflet`.

RESULTS

Using the domain words and important spatial packages identified in previous section the packages that contain the selected word stems and/or depend on main spatial packages are selected. From the list of 11 786 packages, that are not listed under either of CRAN Views focused on spatial data, 602 are selected based on based on dependency on at least one of important spatial packages. 497 packages are selected based presence of domain specific word stem in the package description. Both criteria fulfils 204 packages from which 104 are listed in other CRAN Views besides the spatial views.

Examples of three randomly selected packages that were identified based on analysis of description are listed below.

`macleish`

Description: Download data from the Ada and Archibald MacLeish Field Station in Whately, MA. The Ada and Archibald MacLeish Field Station is a 260-acre patchwork of forest and farmland located in West Whately, MA that provides opportunities for faculty and students to pursue

environmental research, outdoor education, and low-impact recreation (see <http://www.smith.edu/ceeds/macleish.php> for more information). This package contains weather data over several years, and spatial data on various man-made and natural structures.

CensSpatial

Description: Fits linear regression models for censored spatial data. Provides different estimation methods as the SAEM (Stochastic Approximation of Expectation Maximization) algorithm and seminaive that uses Kriging prediction to estimate the response at censored locations and predict new values at unknown locations. Also offers graphical tools for assessing the fitted model.

htdp

Description: Provides bindings to the National Geodetic Survey (NGS) Horizontal Time Dependent Positioning (HTDP) utility, v3.2.5, written by Richard Snay, Chris Pearson, and Jarir Saleh of NGS. HTDP is a utility that allows users to transform positional coordinates across time and between spatial reference frames. See <https://www.ngs.noaa.gov/TOOLS/Htdp/Htdp.shtml> for more information.

Example of three packages that were found based on their dependency.

prevR

Depends: R (>= 2.10), sp (*), rgdal (>= 0.7-4), ggplot2 (*), directlabels (*), Imports: GenKern (*), fields (*), gstat (*), foreign (*), maptools (*), methods (*),

TIMP

Depends: R (>= 2.10.0), methods (*), fields (>= 4.1)
Imports: deSolve (*), nls (>= 1.1), colorspace (*), splines (*), minpack.lm (>= 1.1-1), gclus (*), gplots(*), grDevices (*), graphics (*), stats (*), utils (*),

vegclust

Depends: R (>= 3.4.1), vegan (*) Imports: sp (*), Rcpp (>= 0.12.12)

From the six packages listed here as examples prevR is listed in OfficialStatistics and TIMP in ChemPhys CRAN View.

DISCUSSION

The presented approach can be utilized to identify packages with different focus than spatial data and operations. Using different CRAN View as source for text and package dependence analysis can be used to identify packages with focus on specific topic. Domain specific words, or more precisely their stems, do not have to be obtained from package descriptions. The source of such words can be other text corpus that would allow identification of words specific to certain topic which would allow search for topics that do not have their dedicated CRAN View.

The presented approach may suffer from two classic types of inaccuracies. First cases are packages that might be identified as having relation to spatial data handling because of occurrence of domain specific word that is used in different context. The context can influence the meaning of the word in such way that the word is no longer domain specific for the field of geoinformatics. An example can be word *map* that is identified as domain specific by text analysis, however, the word has specific meaning, related to functional programming, in package `purrr` (Henry and Wickham 2017) and it is quite possible that there are packages related to the `purrr` package that use the word in non-geoinformatics meaning. On the other hand, there are packages that can be and were used to process spatial data that do not contain any domain specific word nor do they depend on important spatial packages. Such packages could not be identified in this study. An example of such package can be for example `fuzzyAHP` (Caha 2017), the package calculates fuzzy AHP and was used even for spatial data (Caha and Burian 2017).

While the approach based on text analysis of package description is rather general and can be used for almost any field or topic the approach based on analysis of package dependence is useful only for topics where some specific set of prominent packages can be identified. For some fields this might pose a problem as set of prominent packages related to the field or topic might not exist. Fortunately, this was not the case with geoinformatics.

CONCLUSIONS

The presented approach showed how package metadata available from CRAN can be used to identify packages with focus on a defined topic. Two approaches towards the issue were proposed. One approach is based on text analysis of package description to identify presence of domain specific words. The second approach is based on analysis of package dependence on other packages that are in some way prominent for a given domain.

The complete analysis was performed in R with focus on reproducibility, so that the analysis can be repeated after a period of time, when the number of packages on CRAN changes, or it can be modified to focus on another domain than geoinformatics.

All packages available on CRAN to the date 31. 12. 2017 were analysed. From the set of 11 786 packages that were not listed under Spatial or SpatioTemporal CRAN view 497 was identified as having focus on spatial data handling by the text analysis, 602 of packages was identified by their dependency on prominent spatial package. Intersection of these two classes is set of 204 packages that were identified by both approaches.

The presented approach and results can be used by users of R for better navigation amongst ever increasing number of packages that are available on CRAN.

ACKNOWLEDGEMENT

This work was supported by the Czech Science Foundation (No. 16-13231S).

APPENDIX

The code for analysis is available from: <https://github.com/JanCaha/GIS-Ostrava-2018> with documentation at: <https://jancaha.github.io/GIS-Ostrava-2018/>.

REFERENCES

- Bivand, R. (2017a) ClassInt: Choose univariate class intervals. Available at: <https://CRAN.R-project.org/package=classInt>.
- Bivand, R. (2017b) CRAN task view: Analysis of spatial data. Available at: <https://CRAN.R-project.org/view=Spatial>.
- Bivand, R. S. (2000) Using the R statistical data analysis language on GRASS 5.0 GIS database files, *Computers and Geosciences*, 26(9-10), pp. 1043–1052. doi: 10.1016/S0098-3004(00)00057-1.
- Bivand, R. S. (2003) Approaches to Classes for Spatial Data in R, In: Hornik, K., Leisch, F., and Zeileis, A. (eds.), *Proceedings of the 3rd international workshop on distributed statistical computing (dsc 2003)*, March 20-22, vienna, austria. Vienna, Austria.
- Bivand, R., Pebesma, E. and Gómez-Rubio, V. (2008) *Applied spatial data analysis with R*. Use R! Springer, p. 378. doi: 10.1007/978-0-387-78171-6.
- Bíl, M., Andrášik, R., Nezval, V. and Bílová, M. (2017) Identifying locations along railway networks with the highest tree fall hazard, *Applied Geography*, 87, pp. 45–53.
- Boeing, G. and Waddell, P. (2017) New Insights into Rental Housing Markets across the United States: Web Scraping and Analyzing Craigslist Rental Listings, *Journal of Planning Education and Research*, 37(4), pp. 457–476. doi: 10.1177/0739456X16664789.
- Brunsdon, C. and Comber, L. (2015) *An Introduction to R for Spatial Analysis & Mapping*. Sage Publications Ltd, London.
- Caha, J. (2017) Examples of FuzzyAHP package application (ver. 0.9.0). Available at: <https://cran.r-project.org/web/packages/FuzzyAHP/vignettes/examples.html>.
- Caha, J. and Burian, J. (2017) Comparison of Fuzzy AHP Algorithms for Land Suitability Assessment, In: Ivan, I., Horák, J., and Inspektor, T. (eds.), *Dynamics in giscience. GIS ostrava 2017. Lecture notes in geoinformation and cartography*. Springer, Cham, pp. 31–46. doi:10.1007/978-3-319-61297-3_3.
- Csardi, G. (2015) Cranlogs: Download logs from the 'rstudio' 'cran' mirror. Available at: <https://CRAN.R-project.org/package=cranlogs>.
- Csardi, G. (2017) Crandb: Query the unofficial cran metadata database. Available at: <https://github.com/metacran/crandb>.
- Feinerer, I. and Hornik, K. (2017) Tm: Text mining package. Available at: <https://CRAN.R-project.org/package=tm>.
- Feinerer, I., Hornik, K. and Meyer, D. (2008) Text mining infrastructure in r, *Journal of Statistical Software*, 25(5), pp. 1–54. Available at: <http://www.jstatsoft.org/v25/i05/>.
- Gandrud, C. (2014) *Reproducible Research with R and RStudio*. CRC Press, Boca Raton.
- Gil, Y., David, C. H., Demir, I., Essawy, B. T., Fulweiler, R. W., Goodall, J. L., Karlstrom, L., Lee, H., Mills, H. J., Oh, J.-H., Pierce, S. A., Pope, A., Tzeng, M. W., Villamizar, S. R. and Yu, X. (2016) *Toward the Geoscience Paper of the Future: Best practices for documenting*

- and sharing research from data to software to provenance. (10), pp. 388–415.
doi: 10.1002/2015EA000136.
- Henry, L. and Wickham, H. (2017) Purrr: Functional programming tools. Available at: <https://CRAN.R-project.org/package=purrr>.
- Hijmans, R. J. (2017) Raster: Geographic data analysis and modeling. Available at: <https://CRAN.R-project.org/package=raster>.
- Horák, J., Ivan, I., Inspektor, T. and Tesla, J. (2017) Sparse Big Data Problem. A Case Study of Czech Graffiti Crimes, In: Ivan, I., Singleton, A., Horák, J., and Inspektor, T. (eds.), The rise of big spatial data. Springer International Publishing, Cham, pp. 85–106.
doi: 10.1007/978-3-319-45123-7_7.
- Ihaka, R. and Gentleman, R. (1996) R: A Language for Data Analysis and Graphics, *Journal of Computational and Graphical Statistics*, 5(3), pp. 299–314.
doi: 10.1080/10618600.1996.10474713.
- Ivan, I. and Tesla, J. (2015) Road and Intersection Accidents: Localization of Black Spots in Ostrava, *GEOGRAFICKÝ ČASOPIS*, 67, pp. 323–340.
- Karell, L., Muňko, M. and Ďuračiová, R. (2017) Applicability of Support Vector Machines in Landslide Susceptibility Mapping, In: Ivan, I., Singleton, A., Horák, J., and Inspektor, T. (eds.), The rise of big spatial data. Springer International Publishing, Cham, pp. 373–386.
doi:10.1007/978-3-319-45123-7_27.
- Marek, L. and Pászto, V. (2017) Spatio-temporal outbreaks of campylobacteriosis and the role of fresh-milk vending machines in the Czech Republic: A methodological study, *Geospatial Health*, 12(2), pp. 264–273. doi: 10.4081/gh.2017.572.
- Marjanović, M., Caha, J. and Miřijovský, J. (2015) Proposition of a Landslide Monitoring System in Czech Carpathians, In: Lollino, G., Giordan, D., Crosta, G. B., Corominas, J., Az-zam, R., Wasowski, J., and Sciarra, N. (eds.), *Engineering geology for society and territory - volume 2 se - 14*. Springer International Publishing, pp. 139–142. doi: 10.1007/978-3-319-09057-3_14.
- Pebesma, E. (2017a) CRAN task view: Handling and analyzing spatio-temporal data. Available at: <https://CRAN.R-project.org/view=SpatioTemporal>.
- Pebesma, E. (2017b) Sf: Simple features for r. Available at: <https://CRAN.R-project.org/package=sf>.
- Pebesma, E. and Bivand, R. (2005) Classes and methods for spatial data in R, *R-NEWS*, 5(2), pp. 9–13.
- Rapant, P. and Kolečka, J. (2018) Dynamical Flash Flood Risk Forecast, In: Ivan, I., Horák, J., and Inspektor, T. (eds.), *Dynamics in giscience*. Springer International Publishing, Cham, pp. 373–381. doi: 10.1007/978-3-319-61297-3_27.
- RStudio Team (2016) RStudio: Integrated development environment for r. RStudio, Inc., Boston, MA. Available at: <http://www.rstudio.com/>.
- Silge, J. and Robinson, D. (2016) Tidytext: Text mining and analysis using tidy data principles in r, *JOSS*, 1(3). doi: 10.21105/joss.00037.
- Silge, J. and Robinson, D. (2017) *Text Mining with R - A Tidy Approach*. O'Reilly Media, p. 184. Available at: <http://tidytextmining.com/index.html>.

Wang, F. (2012) Why police and policing need GIS: an overview, *Annals of GIS*, 18(3), pp. 159–171. doi: 10.1080/19475683.2012.691900.

Wickham, H. (2015) *R Packages*. O'Reilly Media, Inc., Sebastopol.

Wickham, H. (2016) Rvest: Easily harvest (scrape) web pages. Available at: <https://CRAN.R-project.org/package=rvest>.

IDENTIFICATION OF ACTIVE SLOPE MOTION IN CZECH ENVIRONMENT USING SENTINEL-1 INTERFEROMETRY

Milan, LAZECKY

¹IT4Innovations, VSB-TU Ostrava, 17. listopadu 15, 708 33 Ostrava-Poruba, Czech Republic

milan.lazecky@vsb.cz

Abstract

This article shows an experimental approach of using an automatized solution for identification of activity of slow landslides using Sentinel-1 interferometry over a landslide-active area nearby Sance dam and Sokolov. The successful identification of active landslides can lead to a progressive inventory of currently active landslides over Czech Republic that is one of GIS layers used by risk management decision makers especially in emergency situations connected to consequences of intense rains.

The challenge is mainly in identification of subtle motion at slopes that are covered by dense vegetation and forests causing a total loss of signal due to continuous movements and growth of tree leaves. The results show a possibility to identify a landslide activity in such areas on a relatively low confidence level. The article picks out several points to be considered and evaluated before offering the active landslides map based on Sentinel-1 interferometry as a trustworthy service.

Keywords: SAR interferometry, Sentinel-1, landslide, risk management, Floreon+

INTRODUCTION

Czech risk managers deal with various geospatial layers as sources of valuable information helping to assist decision making in cases of emergency. Floreon+ is a GIS system being developed to support Czech emergency operators by experimental services, such as a prediction of flood events and flooded areas (Podhoranyi et al., 2017). In case of floods, operators maintain multicriterial geospatial analyses. One of critical information is a presence of landslide-prone hill slopes. Currently a database of active or non-active landslides exists in the form of a geospatial layer and is maintained by Czech Geological Survey (ČGS). The updates of this layer are prepared ad-hoc, landslide mapping missions are performed sparsely and are economically and time exhausting.

Satellites with a Synthetic Aperture Radar (SAR) onboard allow identification of a slope motion in a high sensitivity beginning in a millimetric range. Methods based on interferometric combination of SAR images (InSAR) are used for this purposes. They are recognized for a capability of landslide inventory mapping by providing information about the state of activity of slow landslides (Scaioni et al., 2014).

A systematic approach to landslide identification is possible in case of proper SAR data availability. European Earth Observation programme Copernicus contains several missions

including a constellation of two SAR satellites called Sentinel-1. Copernicus satellites provide an open and free access to the imagery. Sentinel-1 data over Czech Republic are acquired in periodicity of 12 days since October 2014 and 6 days since October 2016. Data are of a moderate ground spatial resolution (around 4x20 m) and the SAR carrier frequency allows a moderate effectivity of identification of a motion of sparsely vegetated slopes.

Several investigations have proven a potential of Sentinel-1 InSAR-based landslide mapping with the intention to include confident results in national landslide inventories (Barra et al., 2017; Lazecký et al., 2016). Conditions of Czech slopes are challenging the Sentinel-1 InSAR potential, yet the target of this work is to prepare a methodology for establishment of an experimental GIS layer of identified slope activity to converge with currently existing landslide inventory map of Czech Republic to be accessible through Floreon+ system for risk management decision makers. An automatic system for Sentinel-1 processing established at IT4Innovations (IT4S1), the national supercomputing center, should handle algorithms and perform experiments and updates of such layer (Lazecky, 2017).

METHODOLOGY AND CONSTRAINS

Interferometric combination of two SAR images yields an interferogram image containing information about temporal phase change of the sent and reflected microwave. There are several sources of this radar phase contribution limiting the confidence of the identification of terrain displacements (being only one of the contributions). In order to increase this confidence of results, multitemporal InSAR techniques (using multiple SAR images) established possibilities of filtering of atmosphere delay contribution and applying special time series investigation algorithms for evaluation of terrain displacements for stably reflecting points – Permanent Scatterers Interferometry (PSI) (Ferretti et al., 2001). This technique leads to accurate and confident time series of displacements over objects with no or subtle influence of variable scatterers such as vegetation. In order to monitor natural areas, a technique of Small Baselines Interferometry (SBI) has been introduced (Berardino et al., 2002) based on interferometric combination of temporally close SAR images. This approach expects a relatively high coherence of the signal in natural areas that would be lost in case of combination of images taken in a long time difference.

Further experience showed other constrains – vegetation growth still introduces a phase contribution considered as noise, average rate of displacements is often overestimated due to the short temporal combinations, very slow motion is particularly less identifiable etc. A technique combining both PSI and SBI images has been introduced as an open-source set of algorithms known as STAMPS (Hooper, 2008). While other techniques are further being developed, this work is based on the current version of STAMPS algorithms, anyway used at works in national scales for monitoring of geodynamics (Li et al., 2016). While STAMPS offers combination of both PSI and SBI algorithms, they were applied separately in this work, for comparison purposes.

The current processing workflow at IT4S1 deals with InSAR-enabled Sentinel-1 images over the Czech Republic. Once an area of interest is specified, the system performs a basic PSI and SBI processing using all available images. Since SAR images are available from two geometries –

depending on the descending and ascending pass of the Sentinel-1 orbit, the slopes are observed from two different line of sight (LOS) angles and results from both passes should yield a complementary information. Also due to a large wide swath of Sentinel-1 images (around 250 km in W-E direction), all areas in Czech Republic are observed from each pass in track overlaps and therefore processing of images within each track can give a self-verifying results. An example of a processing experiment is shown in the further section.

APPLICATION TO SANCE DAM AREA

An area around Sance dam in Beskydy mountains is a typical example of a landslide zone affected by hydrological changes due to increased pressure of water in the reservoir. While most of the slopes are considered already inactive, at least one (in perimeter of over 600 m) is known for a continuous landslide activity (see Fig. 1). The slopes are covered by dense mixed or coniferous forests disallowing identification of displacements using Sentinel-1 InSAR during most of the year. While some landslide-based artefacts can be interpreted by chance manually investigating the whole set of available data (there are 4 tracks of Sentinel-1 available with over 100 images per track), this work is trying to prove possibility of landslide identification using an autonomous way, especially by processing pixels that keep signal coherent, i.e. with a limited influence of vegetation.

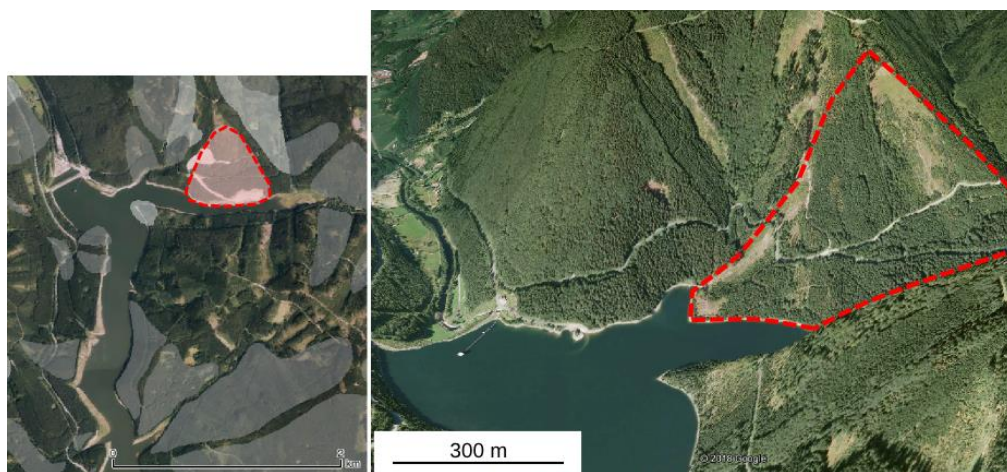


Fig. 1. Area of interest – Sance dam surroundings. Left: top-view orthophotomap, Right: closer view at active landslide (marked red).

Both PSI and SBI techniques were applied. Using PSI method, only a sparse set of points has been evaluated due to lack of stably reflecting objects in the area – see Fig. 2. More points could be evaluated by SBI technique using only short-term interferograms that were spatially filtered. The set of interferograms in this case has been optimized by using more connections in case of springtime (March-May) and autumn-time (October-November) images. In order to achieve larger selection of points, the SBI processing parameters were set for a higher tolerance. Thus the dataset contains more noise due to presence of less confident points.

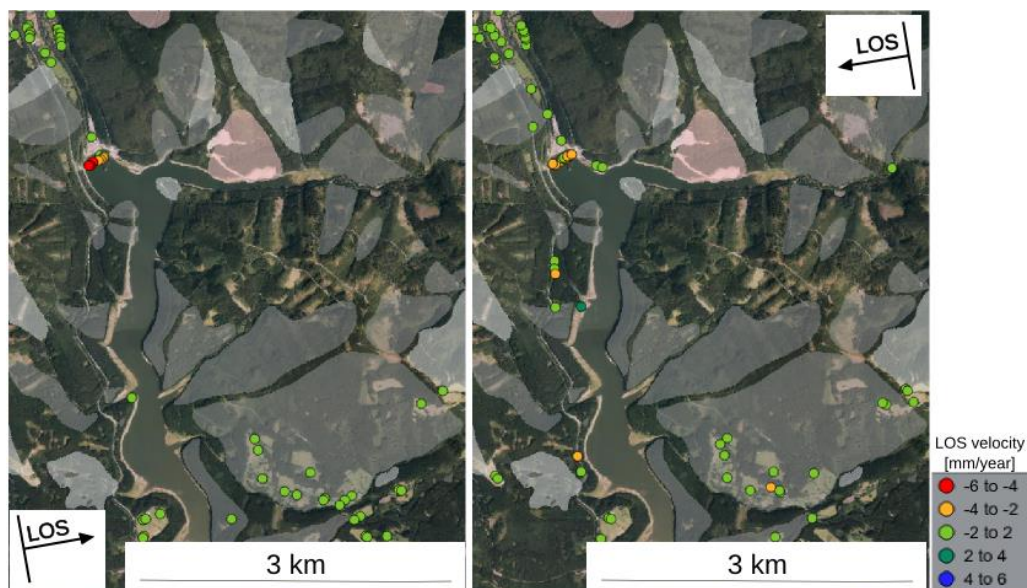


Fig. 2. Results of PSI processing of ascending Sentinel-1 data (left) and descending data (right). The map background contains ČGS-based landslide inventory map: grey marks inactive landslides.

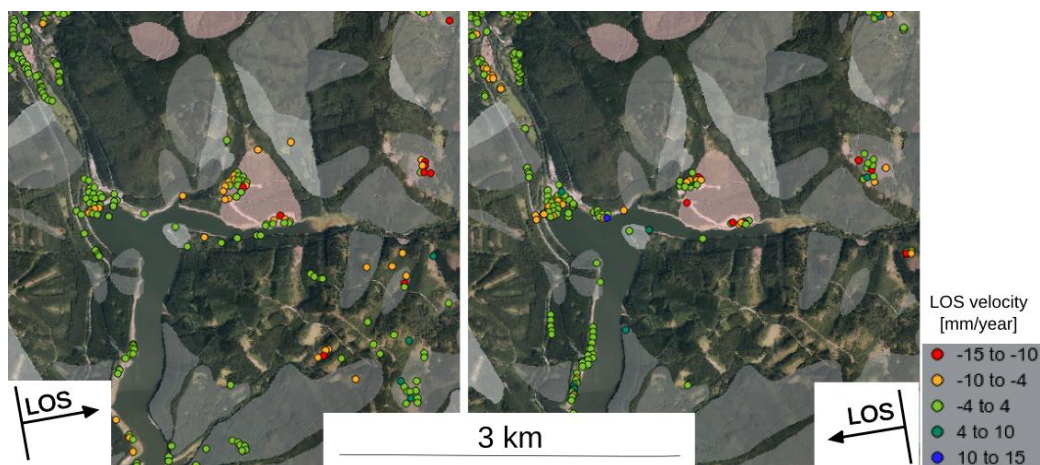


Fig. 3. Results of SBI processing of ascending Sentinel-1 data (left) and descending data (right).

APPLICATION TO SOKOLOV AREA

As a second testing area, surroundings of Sokolov city were selected for an automatic analysis. This area is known for surface mining of brown coal. As input to the IT4S1 automatized system, coordinates of Sokolov city center were given with radius 6 km. The processing of over 100 images per two ascending and descending orbital tracks has been run on two computing nodes in parallel and finished within 15 minutes (approx. 3 minutes for PSI processing and 12 for SBI). Resulting data were filtered (only points with temporal coherence >0.75 were selected) and due to their large number per km^2 , their values of an average velocity of point displacements were

aggregated into hexagonal cells of approx. 100x100 m area (using Quantum GIS toolbox MMQGIS). Similarly to the previous study, following figures show results using PSI (Fig. 4) and SBI (Fig. 5) techniques demonstrating possibility to identify displacements in areas not covered by permanent vegetation. Colour scale was unified for comparison purposes. It can be observed that points of a higher rate of displacements (over a cm/year) were not properly interpreted using PSI technique. Both datasets show similar pattern of slope motion, including uplift around Medard lake on the W and slope displacements of over 5 cm/year at the surface mine on the N.

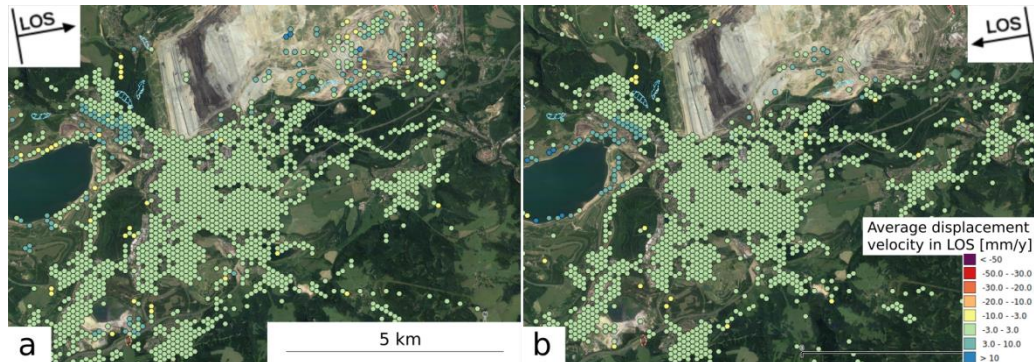


Fig. 4. Results of PSI processing of ascending Sentinel-1 data from orbital track 44 (a) and descending data from orbital track 168 (b) over Sokolov area.

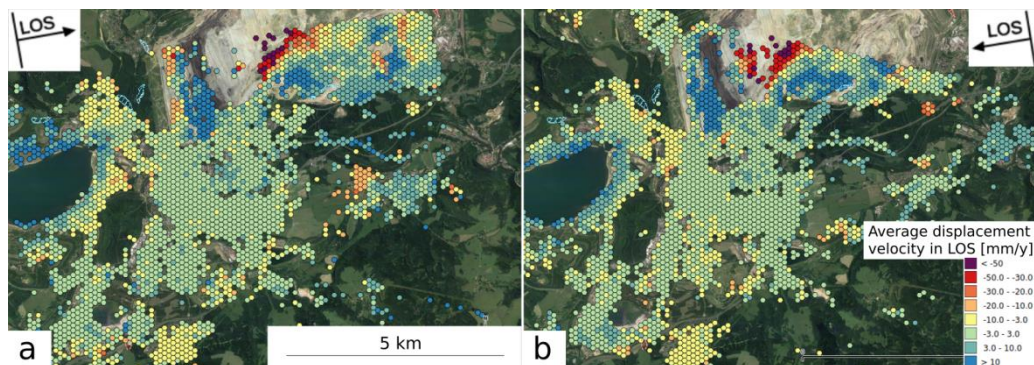


Fig. 5. Results of SBI processing of ascending Sentinel-1 data from orbital track 44 (a) and descending data from orbital track 168 (b) over Sokolov area.

DISCUSSION AND CONCLUSIONS

Due to a constant presence of vegetation cover in the majority of Czech slopes, the identification of slow landslide displacements using the SAR satellite with a moderate-size C-band wavelength as Sentinel-1 is fairly experimental. The approach of using SBI method with increased number of interferogram connections at times with a low vegetation activity seems to help increasing the number of evaluable points, however decreases their quality, lowering accuracy and confidence of the results. Yet, the activity of a given slope in Ostravice area has been detected.

There are various attempts possible to improve the situation and allow to prepare a confident map of active landslides. First of all, data from a long wavelength (L-band) SAR satellite such as ALOS-2 can be used for InSAR processing since the longer wavelengths should penetrate the vegetation cover better than C-band waves. Second, a different set of algorithms may yield different outcomes, for example when using only spring/autumn-time dataset. However, it appears that observed slope failures are proceeding too slowly to be captured within the short period of few vegetation-free months.

The application of SBI technique identified moving points in areas considered non-active by ČGS (see Fig. 3). This identified motion is to be consulted with ČGS before proceeding into monitoring in larger scales and optimizing the methodology to cover the whole Czech Republic.

ACKNOWLEDGMENTS

This work was supported by The Ministry of Education, Youth and Sports from the National Programme of Sustainability (NPU II) project „IT4Innovations excellence in science - LQ1602“ and from the Large Infrastructures for Research, Experimental Development and Innovations project „IT4Innovations National Supercomputing Center – LM2015070“. Access to computing and storage facilities owned by parties and projects contributing to the National Grid Infrastructure MetaCentrum, provided under the programme "Projects of Large Infrastructure for Research, Development, and Innovations" (LM2010005), is greatly appreciated.

REFERENCES

- Barra A., Monserrat, O., Crosetto, M., Cuevas-Gonzalez, M., Devanthery, N., Luzi, G., Crippa, B. (2017) Sentinel-1 Data Analysis for Landslide Detection and Mapping: First Experiences in Italy and Spain, *Advancing Culture of Living with Landslides*, WLF 2017, Springer, Cham, DOI: 10.1007/978-3-319-53487-9_23.
- Berardino, P.; Fornaro, G.; Lanari, R.; Sansosti, E. A new algorithm for surface deformation monitoring based on small baseline differential SAR interferograms. *IEEE Geosci. Remote Sens.* 2002, 40, 2375–2383.
- Ferretti, A.; Prati, C.; Rocca, F. (2001) Permanent Scatterers in SAR interferometry. *IEEE Geosci. Remote Sens.*, 39, pp. 8–20.
- Hooper, A. (2008) A multi-temporal InSAR method incorporating both persistent scatterer and small baseline approaches, *Geophysical Research Letters*, 35, DOI: 10.1029/2008GL034654
- Lazecky, M., Canaslan Comut, F., Nikolaeva, E., Bakon, M., Papco, J., Ruiz-Armenteros, A. M., Qin, Y., Sousa, J. J. M., Ondrejka, P. (2016) Potential of Sentinel-1A for nation-wide routine updates of active landslide maps, *Int. Arch. Photogramm. Remote Sens. Spatial Inf. Sci.*, XLI-B7, pp. 775-781, DOI: 10.5194/isprs-archives-XLI-B7-775-2016, 2016.
- Lazecky, M. (2017) System for Automatized Sentinel-1 Interferometric Monitoring, *Proc. of ESA Big Data in Space 2017*, Toulouse, 28-30 Nov 2017, 4 pp., DOI: 10.2760/383579.
- Li, Z., Wright, T., Hooper, A., Crippa, P., Gonzalez, P., Walters, R., Elliott, J., Ebmeier, S., Hutton, E., Parsons, B. (2016) Towards InSAR everywhere, all the time, with Sentinel-1, in:

International Archives of the Photogrammetry, Remote Sensing and Spatial Information Sciences - ISPRS Archives, pp. 763–766, DOI:10.5194/isprsarchives-XLI-B4-763-2016.

Podhoranyi, M., Veteska, P., Szturcova, D., Vojacek, L., Portero, A. (2017) A web-based modeling and monitoring system based on coupling environmental models and hydrological-related data, *Journal of Communications*, 12 (6), pp. 340-346, DOI: 10.12720/jcm.12.6.340-346.

Scaioni, M., Longoni, L., Melillo, V., Papini, M. (2014) Remote Sensing for Landslide Investigations: An Overview of Recent Achievements and Perspectives, *Remote Sensing*, 6, pp.(1–x):53.

FLOREON+: INTEGRATION OF DIFFERENT THEMATIC AREAS

Václav, SVATOŇ¹; Patrik, VETEŠKA¹; Jan, KŘENEK¹; Jiří, HANZELKA¹; Petr, BERGLOWIEC¹; Jan, MARTINOVIČ¹; Michal, KRUMNIKL¹; Vít, VONDRÁK¹

¹ IT4Innovations, VŠB - Technical University of Ostrava, 17. listopadu 15/2172, 708 33 Ostrava-Poruba, Czech Republic

{*vaclav.svaton, patrik.veteska, jan.krenek, jiri.hanzelka, petr.berglowiec, jan.martinovic, michal.krumnikl, vit.vondrak*}@vsb.cz

Abstract

The main goal of this article is to present an overview of the different thematic domains integrated in the Floreon+ system. Previously being just an online flood monitoring and prediction system, Floreon+ was primarily developed for the Moravian-Silesian region in the Czech Republic; however, the system is now also providing real-time data and simulations from the areas of traffic monitoring and modelling, toxic pollution and population mobility. The main focus of the Floreon+ system is to provide comprehensive information about the current or future situations with the interactions between different thematic domains, therefore providing additional information for the decision making process of the crisis staff.

Keywords: Floreon+, decision support system, hydrological modelling, traffic monitoring, cloud pollution, mobility, domain interaction

INTRODUCTION

In the case of major emergencies and crisis situations, the security community in general, and especially the part that is assigned to the operational centers of the integrated rescue system and crisis staff members at all levels of hierarchy, are exposed to massive workload of more or less valid information from affected areas.

The overall picture of the situation is composed based on the information from the intervention commanders, representatives of the affected municipalities, and citizens. More recently, this information has been passed on to the operational centers or to the crisis staff orally, by telephone, radio, or fax. Now smart phones capable of conveying photos, video, GPS coordinates, etc. can play a key role in providing information about the situation on the scene of the event. The follow-up information is provided to the contact staff of these centers through social networks, the media community, territory data (smart city projects, smart region) and, in the near future, via IoT (Internet of Things) data.

Both the operational center and crisis management staff are then expected to properly evaluate all of this information and data, connect and quickly decide on the best solution that will lead to as little loss of life, health, and property as possible. The fact is that the tools which are currently available within most operational centers of Integrated Rescue Services in the workplace of crisis staff are more or less self-serving and often require a considerable routine ability.

A major problem is the situation where a number of extraordinary events occur simultaneously in the same affected area (e.g. flood, toxic cloud pollution, disruption in some parts of the transportation system, etc.). In this case, it is virtually impossible to model both the current situation and its expected development scenarios as correctly and quickly as possible as well as promptly propose partial steps to eliminate the consequences.

Floreon+ is a decision support system, which integrates a number of different thematic areas and tools to quickly analyze the possible impacts of emergencies, crisis situations, and interactions between them in the affected area. This system offers additional information for the decision making process of the crisis staff during the crisis situations.

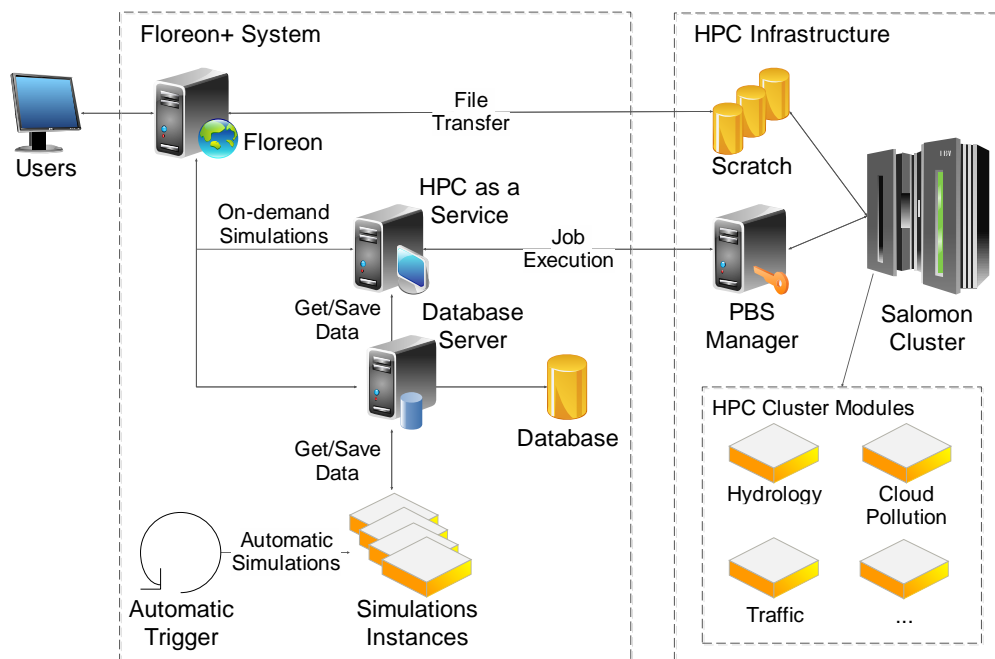


Fig. 1. Floreon+ system architecture overview

FLOREON+ SYSTEM ARCHITECTURE

The architecture of the Floreon+ system consists of a number of interconnected parts and modules (see Figure 1). The system's application logic is represented by a web server that hosts the web graphical user interface of the system, a database server used to access the relation database, and a number of support applications or services used mainly for monitoring, security, and data management purposes.

This architecture integrates our in-house developed application framework for cluster remote execution called HPC as a Service Middleware (Svatoň, 2017). Via this middleware, the Floreon+ system is able to utilize the HPC infrastructure within IT4Innovations National Supercomputing Center (the Anselm and Salomon HPC clusters). Therefore, the users of the Floreon+ system are

able to execute computationally demanding applications or simulations in an HPC environment through a web GUI without the necessity of a direct cluster access.

Dynamic Data Processing

The Floreon+ system can be roughly divided into two main parts in terms of dynamic data processing. The first system's part deals with automatic simulation execution, while the second part consists of on-demand user-initiated simulations designed specifically for HPC cluster execution.

Automatic Simulations

Automatic data processing includes processes and simulations that are being executed automatically in a predefined time intervals and subsequently visualized directly in the web interface of the system.

The simulations consist mainly of hydrologic modelling. Measured hydrological data provided by the Povodi Odry state enterprise in the 10-minute interval. The system computes hydrographs and inundations from these measured values at hourly intervals (Kubiček, 2008) and makes these results available to users via web user interface.

Automatic processes are further responsible for the automatic update of the current traffic load of road segments (FCD – floating car data), traffic information about accidents, road closures (ITIS - Integrated Traffic Information System), camera snapshots for a set of crossroads provided by OVANET and mobility of population calculated from the mobile operators' data.

On-demand Simulations

Apart from the automatic simulations, the system allows users to initiate custom on-demand simulation with the user-defined parameters in the form of What-If analysis. Due to these parameters, the on-demand simulations can be much more computationally demanding than the predefined automatic simulations, and thus they are natively executed within an HPC environment. Therefore, these on-demand simulations (What-If analysis) are implemented as HPC modules and prepared to be executed on one of the supercomputers.

The system currently offers three types of What-If analysis: hydrological simulation, cloud pollution modelling, and traffic modelling. Hydrological simulation calculates the water flow and inundation based on the user-defined precipitations for a selected set of measuring stations, river basin, schematization, and rainfall-runoff model. Cloud pollution modelling simulates the spread of hazardous substances through the air and traffic modelling is able to visualize the changes in the traffic flow during some unexpected situations.

Stored Events

Floreon+ system contains so-called stored events data model. This model enables the system to detect some relevant/crisis situations that may occur and archive the data for later analysis or to visualize these events automatically in a web interface. The example of such hydrological event

is for example the exceedance of level of flood activity (SPA) for one of the measuring stations. This model is applicable also for other thematic domains (traffic modelling, cloud pollution modelling, etc.) and for the both automatic and on-demand simulations as well.

THEMATIC DOMAINS

The Floreon+ system currently integrates data, models, and simulations from the four main thematic domains: hydrological modelling, cloud pollution modelling, traffic modelling, and mobility of population.

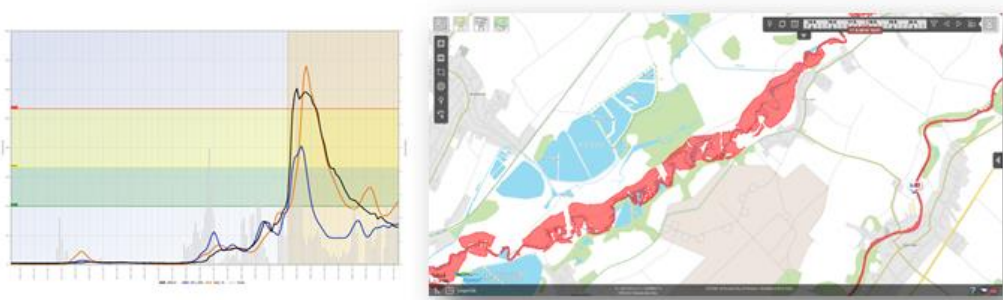


Fig. 2. Hydrograph and flooding

Hydrologic Modelling

The hydrological analysis is a very powerful tool for simulation of river floods and river inundations depending on the selected precipitations in a critical situation. Hydrological simulation available in the Floreon+ system may be computed for each of the main four basins in the Moravian-Silesian region (Opava, Odra, Olše, Ostravice).

Hydrological modelling in the Floreon+ system consists of several steps. The first part consists of real measured values from measuring stations together with the predicted rainfall-runoff values. These data are retrieved and updated every 10 minutes from Povodi Odry and the predicted precipitation values are computed from the Medard predictive model (Medard, 2016), provided by third parties. The data is processed and then stored permanently in the system's database.

Based on these data, hydrographs with the real rainfall-runoff values and the predicted flow will be computed. The system currently uses HEC-HMS (CPD-74A, 2010) and Math1D (internal model developed in cooperation with the Department of Applied Mathematics at VSB) (Kubíček, 2008) hydrological rainfall-runoff models to compute the hydrographs. The hydrographs are then used as the input for the hydrodynamic models to compute inundations. The hydrodynamic model 1D HEC-RAS (CPD-68, 2010) is used for computing the inundations.

The results obtained in the form of hydrographs and flood lakes are visualized directly in the map interface of the Floreon+ web GUI. The hydrographs can be viewed in the detailed view of a particular measuring station. Inundations are visualized by the map layer that highlights the areas which are in the critical zone with the risk of real flooding in red color (see Figure 2).

The above-described process is fully automatic, therefore always showing actual hydrologic situation for the Moravian-Silesian region. In case of the on-demand hydrological simulations the user fills in the starting time of the simulation, simulation's duration, and precipitations for selected precipitation stations. This type of simulation also allows the user to edit the default parameters of sub-basins and channels (Halmo, 2006).

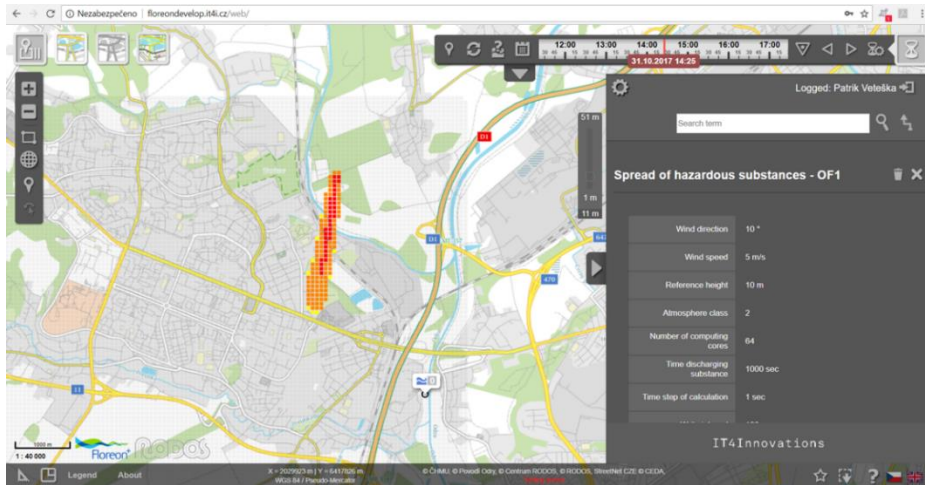


Fig. 3. Cloud pollution modelling

Cloud Pollution Modelling

Another type of thematic domain implemented in the Floreon+ system is cloud pollution modelling. This type of analysis is only available as a user-defined What-If analysis. Using this analysis, the user can simulate the spread of a dangerous substance in the air. This simulation is utilizing the OpenFoam solver to compute the diffusion of a specified substance into the environment (Ronovský, 2017).

Users must fill in the submission form with a set of input parameters such as the area of interest (AOI) for the pollution simulation, epicenter for substance discharge, wind direction, wind speed, reference height, atmosphere class, and diffusion coefficient. AOE is used to query Geoserver instance so that the 3D model of a selected area could be generated. This 3D model together with the user-defined parameters is used as an input for the OpenFoam solver.

The result of the solver is calculated for a 3D model that describes the spread of the defined substance into the environment. The Floreon+ system currently does not support 3D visualization. Therefore, the result is visualized in 2D for the vertical cuts (in meters) and the time selected on the timeline of the map interface (see Figure 3). Changes to the distribution of a dangerous substance are visualized simply by changing the time on the timeline and by selecting the level of vertical cuts.

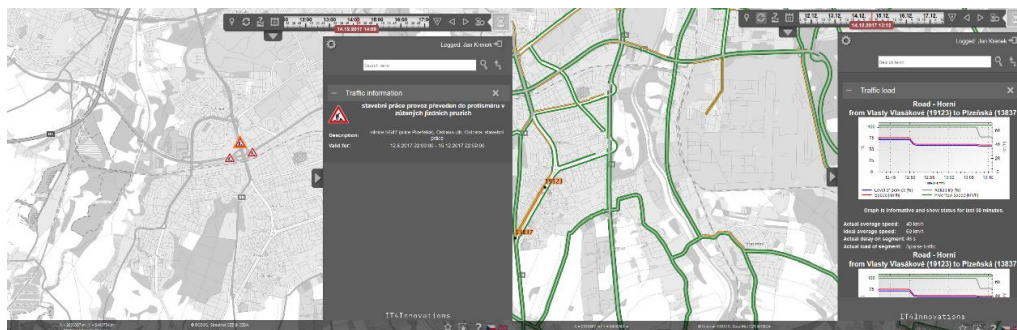


Fig. 4. FCD and traffic information

Traffic Monitoring and Modelling

In the domain of traffic monitoring and modelling, the system displays current and historical traffic situations, snapshots from the cameras located on the main crossroads of the City of Ostrava and provides the routing algorithm for route planning on the map and simulates traffic flow for a selected area with traffic-based What-If analysis.

Traffic Information and Floating Car Data

The Floreon+ system is able to visualize actual or historical traffic constraints and floating car data (FCD). The data for segments of routes comes from RODOS⁵ and data for Traffic Information from ŘSD⁶. The traffic constraints may be permanent (closure, other danger) or short term (accident, grass cutting). Floating car data is visualized as segments of streets in the map colored by actual or historical traffic load of these segments (see Figure 4). The segment can have one of these values: sparse traffic (Green), medium traffic (Orange), heavy traffic (Red).

Cameras

The user can select one or multiple cameras located at a crossroad and subsequently view the video stream from them in GUI of the Floreon+ system. Data from the cameras are provided by OVANET provider. The users working with the Floreon+ system can visually verify constipation where cameras are located.

Traffic Routing

The system uses its own routing algorithm, which takes information about the start and end points of the route (collected from the map in GUI) and the route parameters (choose shortest or fastest route) as the input parameters. The result from the selected parameters is shown in GUI as a vector layer. Extension of the routing algorithm that combines the route planning while avoiding the flooded roads during extraordinary events (floods) is under preparation.

Traffic Modelling

⁵ <http://www.centrum-rodos.cz/>

⁶ <https://www.rsd.cz/wps/portal/>

For traffic modelling in the Floreon+ system, the custom implementation of betweenness centrality (BC) algorithm from Ulrik Brandes (Brandes, 2001) is used. It is an algorithm based on the shortest paths with our vertex importance extension (Hanzelka, 2018) in the background. Input for this algorithm is the graph of the traffic network and importance of each vertex. This importance consists of selecting two properties that increase betweenness on the shortest paths from or to selected vertices.

Using this simulation, the user can select an area of interest through the web GUI, in which they can define impassable areas and set the road priorities in the selected sub-areas by polygonal selection. This simulation can also be based on an already computed simulation, which allows for more detailed specification of these crisis conditions and can exclude or include an additional area and sets its importance coefficients. If a newly executed simulation is based on some older one, the system is also able to show comparison between the old and the new simulation.

The result of simulation is saved and then visualized as a new map layer where the selected area can be seen with the resulting edge (road) evaluation as thickness. Thicker edges mean bigger betweenness score, which represents increased traffic flow on these edges (see Figure 6).

Using this approach, the user can see how traffic flow changes when a road is closed by removing some vertices from the graph of traffic network in definition of simulation. Another example can be modifying vertex importance of an area. This can simulate, for example, when a music festival ends and everybody leaves that place.

Mobility of Population

The Floreon+ system allows users to show information about the population in the region divided to square grid and population flow among the districts. This functionality allows the user to monitor travelling between districts in the region and actual concentration of people in the parts of the region.

The data processed in the Floreon+ system is acquired from mobile operators in anonymous and aggregated form. Then, calculations based upon the number of network events in a given location (phone calls, SMS events) are running over the data. Finally, the calculation data is stored and subsequently visualized in the system.

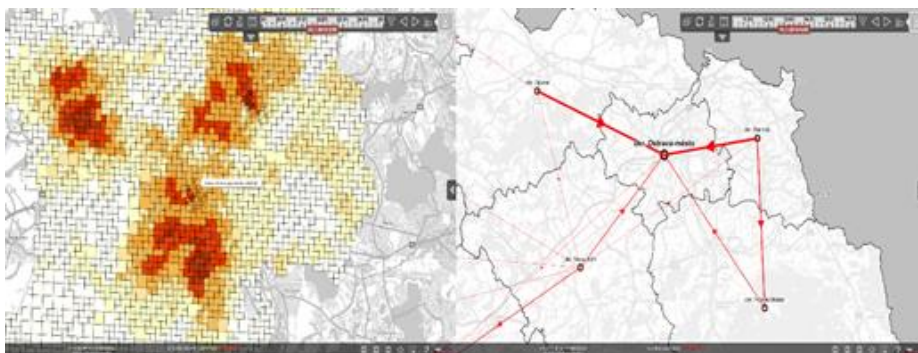


Fig. 5. Mobility events and Mobility flow for the Moravian-Silesian region

Mobility Concentration

Population concentration is visualized as a raster network. Depending on the value of individual concentration at a given moment, the given segment is displayed in individual color scales for each value. The detailed view of the individual raster segment shows actual concentration and indicated total mobile events on the hovered segment. The system also lets you view the concentration history for the segment and visualize that data in the graph. As an example of the use of this functionality, we can see actual individual concentration of the population in the part of the Moravian-Silesian region in the left part of Figure 5.

Mobility Flow

This visualization shows in what direction and how many users are going from the given location to the destination location and from the destination location to the given location. The amount is represented by thickness of the individual site interconnections. As an example of mobility flow functionality, we can mention commuting to work in the morning among the districts in the Moravian-Silesian region in the right part of Figure 5.

DIFFERENT DOMAIN INTERACTION

One of the main advantages of the Floreon+ system lies in the ability to combine different thematic areas. Possibly the main interaction of two different thematic domains is a combination of traffic modelling and hydrology modelling. The system is able to monitor and predict a hydrological situation in the Moravian-Silesian region and traffic modelling is able to work with the excluded or important road segments.

Figure 6 shows how traffic flow changes due to a road closures caused by the flooding. Left image shows the default traffic model output, and the right image shows the removed flooded area with different flow of traffic. Figure 6 shows how traffic model was changed and simulates how traffic flow increased around the affected area.



Fig. 6. Traffic modelling around the affected area

Because the traffic modelling method is able to work with fairly universal excluded roads or prioritized roads, the interaction with the toxic cloud pollution or mobility of the population is

also possible. These relevant areas (polluted parts of the city, closed roads during a concert, etc.) can be simply removed or changed in the graph of the traffic network that is used as input to traffic modelling analysis. The resulting analysis will show traffic flows for the original graph and for the graph with removed vertices. These two results can be then easily compared and, in the end, used for the route planning.

CONCLUSION AND FUTURE WORK

This article presented the Floreon+ system, a decision support system that integrates different thematic areas such as hydrological and traffic monitoring and modelling, toxic cloud pollution modelling, and mobility of the population. The system provides tools, analysis, and simulations from these thematic areas and aims to help the crisis staff in their decision making process during the critical events or to provide them with the possibility to simulate these situations beforehand.

It is important to mention that the system does not contain any decision making model, which would govern what should be done in case of some critical event. Throughout its results, the Floreon+ system provides additional information to the decision making process of crisis management staff or operational centers.

As the Floreon+ system is very extensive, this paper focuses mainly on the overview of the tools, methods and results in each thematic area that are available to the users of this system. From the data processing point of view, the system presents the current information about the hydrological, traffic and mobility situation. Moreover, it also offers the ability to execute user-defined on-demand simulations from these thematic areas that are utilizing the HPC infrastructure within the IT4Innovations National Supercomputing Center.

The future work will mainly focus on the fully automated process for the interaction of available thematic domains, thus enabling, for example, route planning based on the current hydrological, traffic, or mobility situation. The planned extension of the system involves new modules for flash floods and landslides.

ACKNOWLEDGEMENT

This work was supported by The Ministry of Education, Youth and Sports from the National Programme of Sustainability (NPU II) project "IT4Innovations excellence in science - LQ1602" and from the Large Infrastructures for Research, Experimental Development and Innovations project "IT4Innovations National Supercomputing Center – LM2015070". Part of the data available in the Floreon+ system is provided by "Transport Systems Development Centre" co-financed by the Technology Agency of the Czech Republic (reg. no. TE01020155).

REFERENCES

Brandes, U. (2001) A faster algorithm for betweenness centrality. *Journal of Mathematical Sociology*.

- Svatoň, V., Podhoranyi, M., Vavřík, R., Veteška, P., Szturcová, D., Vojtek, D., Martinovič, J. and Vondrák, V. (2017) Floreon+: a web-based platform for flood prediction, hydrologic modeling and dynamic data analysis. In Proceedings of the GisOstrava 2017, Dynamics in GIScience.
- Halmo, N. (2006) Flood protection program of Slovak republik In: International conference of flood protection, 4 – 7 December, High Tatras: Slovakia.
- CPD-68 (2010) HEC-RAS River Analysis System User's Manual Version 4.1. US Army Corps of Engineers Institute for Water Resources Hydrologic Engineering Center, Davis, CA.
- Ronovský, A., Brzobohatý, T., Kuchař, Š., Vojtek, D. (2017) Modelling of a Spread of Hazardous Substances in a Floreon+ System, AIP Conference Proceedings.
- CPD-74A (2010) Hydrologic Modeling System HEC-HMS User's Manual. U.S. Army Corps of Engineers Hydrologic Engineering Center, Davis, CA.
- Institute of Computer Science (ICS), The Czech Academy of Sciences. <http://www.medard-online.cz>, December 2016.
- Kubíček, P. and Kozubek, T. (2008) Mathematic-analytical Solutions of the Flood Wave and its Use in Practice (in Czech). VŠB-TU Ostrava, Ostrava, 150 p.
- Knebl, M.R., Yang, Z.-L., Hutchinson, K., Maidment, D.R. (2005) Regional scale flood modeling using NEXRAD rainfall, GIS, and HEC-HMS/RAS: a case study for the San Antonio River Basin Summer 2002 storm event. *Journal of Environmental Management* 75, 325-336.
- Hanzelka, J., Běloch, M., Martinovič, J., Slaninová, K. (2018) Vertex Importance Extension of Betweenness Centrality Algorithm. ICDMAI.

THE INFLUENCE OF MICRORELIEF ELEMENTS ON THE PASSABILITY OF THE AREA

Martin, HUBACEK¹; Filip, DOHNAL¹; Katerina, SIMKOVA¹

¹Department of Military Geography and Meteorology, Faculty of Military Technology, University of Defence in Brno, Kounicova 65, 662 10, Brno, Czech Republic

martin.hubacek@unob.cz; filip.dohnal@unob.cz; katerina.simkova@unob.cz

Abstract

Relief is one of the basic components of the landscape. Fragmentation of the relief creates the landscape and to some extent shapes the appearance of other landscape features in the area. Microrelief objects are an integral part of it. These objects can significantly influence the possibilities of vehicles moving and units maneuver when performing tactical tasks.

Detailed and accurate digital elevation models allowing to identify the location and shape of these microrelief objects already exist. The DMR 5 is that kind of a model and it covers the entire Czech Republic since 2016. When the technical parameters of the vehicles are compared with the parameters of the microrelief object, it is possible to identify the impassable microrelief objects. A procedure for analysing the influence of microrelief is designed as one of the steps of a complex model of passability. The proposed procedure uses the standard grid functions in ArcGIS data and DMR 5. The modelling results were verified in the field by army vehicles. In addition to verifying the results of modelling by vehicle rides, all tested microrelief objects were measured by an electronic tachymeter, and their shape was compared to the shape obtained from the DMR 5 data. The comparison confirmed the model's tendency to smooth out the terrain edges. When comparing terrain profiles measured in the field and detected from the raster model, the deviation in the critical value calculated for the measured profiles ranges from 10-25%. Further validation using vehicles is necessary to determine the more accurate reliability of the calculation process.

Keywords: microrelief, passability, cross-country movement, DEM (digital elevation model), military

INTRODUCTION

Relief is one of the basic components of the landscape. Fragmentation of the relief creates the landscape and to some extent shapes the appearance of other landscape features in the area. Relief is not unchanging, and its main form, as it is known today, has been created for millions of years on the basis of endogenous and exogenous processes (Colins 1998, Derbyshire et al 1981, Monkhouse 2014). Relief changes are happening even today. Endogenous forces usually act in a one-off fashion and fundamentally alter the main shapes of relief. Exogenous processes, including activities of water, wind, glaciers, gravitation, and humans, have been the long-term cause of flattening of relief and the creation of microrelief objects.

Different sources (Dictionary.com 2017, Oxford University Press 2017, Merriam-Webster 2017, VUGTK 2017) define these microrelief objects differently. In general, they agree, and microrelief

objects than can be defined as objects whose relative height is within a few meters. These microrelief objects are predominantly linear or point-like, and appear in particular in the form of streams, erosion engravings, terraces, excavations, pits and other objects.

In many cases, these microrelief objects are bound to watercourses and communication objects. They have a great impact, for example, on drainage conditions in the area and soil erosion (Freebairn and Gupta 1990, Römken, Helming and Prasad 2002, Rudolph, Helming and Diestel 1997). From the military point of view, microrelief objects have another meaning. Their shape, size and direction influence the possibilities of moving the units out of communication (Rybansky 2014, Talhofer, Mayerova and Hofmann 2016)). To plan the maneuver it is necessary to know the tactical technical parameters of the machines and the extent and shapes of the microrelief objects. On the basis of this knowledge, it is possible to decide whether or not vehicles are able to overcome microrelief objects of microrelief or if it is necessary to avoid them. The basic technical parameters of vehicles for determining the ability to overcome microrelief objects are (Rybansky 2009):

- type of chassis (wheeled, tracked);
- number of axles
- wheelbase;
- angles of approach;
- climbing ability - vertical step;
- ground clearance.

These values are usually well known and precisely quantified. Vehicle weight and other non-dimensional parameters may be neglected due to the sufficient engine power of all military vehicles. The second set of parameters describing the shape and size of the microrelief elements necessary to assess the impact of the microrelief on the passability of the area is described much less precisely. A few years ago, it was impossible to have precise descriptions of microrelief objects from large areas. Users typically only had maps or geodatabases where only the location of the microrelief objects, possibly added by their height, was recorded. This was also the case in the Czech Republic. Army users were provided with 1 : 25 000 topographic maps or microrelief layers of 1: 25 000 Digital Model of Territory. Microrelief objects registered in these products are the same, including information about them. The ability to evaluate the ability of vehicles to overcome to the relief based on these data is therefore minimal. Soldiers and military geographers, usually only based on the height of the microrelief element, can estimate whether the object will be an obstacle or not.

Detailed mapping of microrelief objects and the creation of high-precision digital relief models is essential for the detailed evaluation of microrelief objects. These models have been used for decades, in the Czech Republic the first since 1986 (Hubacek et al 2015), but their accuracy in case of coverage of large areas was insufficient. A significant change has been made with the use of airborne laser scanning technology. This technology allows you to quickly and efficiently

collect precise data about the location and height of the relief and the objects on it. In the years 2010 - 2013 this technology was used for the first nationwide scanning of the territory of the Czech Republic (Brazdil et al 2009).

As a result of a project involving the Czech Office for Surveying, Mapping and Cadastre, the Ministry of Defence and the Ministry of Agriculture are the new generation of the digital elevation models - DMR 4 and DMR 5 (Land Survey Office DMR4 2017, Land Survey Office DMR5 2017). The tests made by the creators as well as the independent verifications confirmed the high accuracy of these models (Hubacek et al 2015). These models, in particular DMR 5, shift the possibilities of modelling and field analyses in many areas, while also enabling them to be used in areas where it has been necessary to perform detailed geodetic measurements before starting analytical work (Sobotka 2012).

One of the new areas of use of DMR5 is the detailed analysis of microrelief objects and their evaluation of individual microrelief objects in terms of their ability to overcome vehicles and overall assessment of the passability of the area from the viewpoint of the overall impact of the microrelief.

THE EFFECT OF MICRORELIEF ON MOVEMENT

Microrelief objects can be overcome or to avoid (Rybansky 2009). In both cases, the progress of the units slows down, and in the latter case it is even necessary to maneuver. To measure the impact of these microrelief objects on the movement, it is possible to use detailed models of relief and GIS tools.

The proposed procedure is based on the analysis of the vehicle's limitations for crossing the microrelief objects and the determination of whether or not the terrain can be overcome by the selected vehicle. After some schematization and simplification of the problem, the following situations can happen to the wheeled vehicle:

- the perpendicular edge is higher than the vehicle climbing ability - vertical step (Fig 1a);
- a deep notch is wider than the vehicle's Crossing ability - trench width (Fig 1b);
- the angle between relief and microrelief is greater than the approach angle of the vehicle (Fig 1d);
- the angle of the upper edge of the microrelief object is less than twice the angle between the centre of the wheelbase and the lower edge of the tire on the axle (Fig 1c).

In the case of tracked vehicles, the situation is similar, except for the last case, that does not occur in this type of chassis.

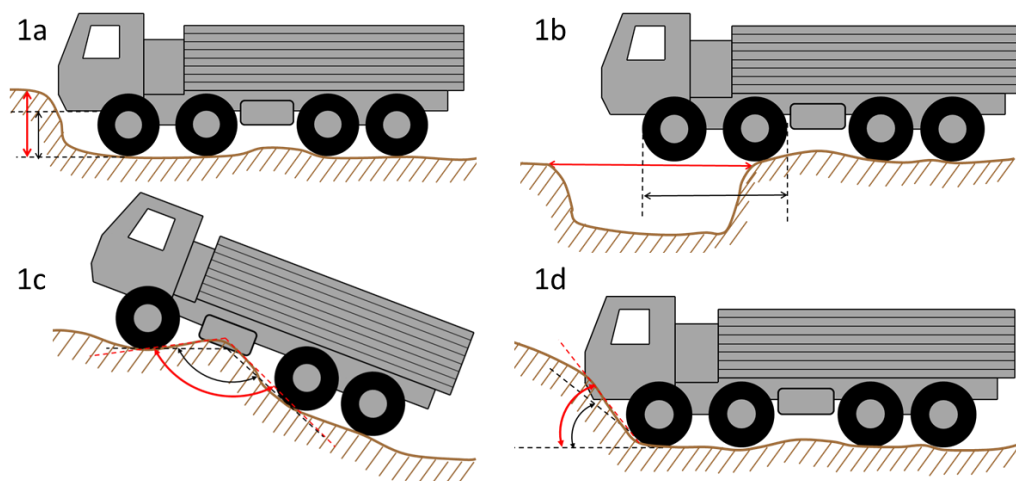


Fig. 1. Visualization of vehicle limit to overcome microrelief objects (black arrow)

METHOD OF EVALUATION OF MICRORELIEF OBJECTS

The proposed method for evaluating microrelief objects uses DMR 5 data. This model calculates a raster model with a pixel size of 0.5 meters. This value was chosen based on the DMR 5 error detection in the area of microrelief objects (Hubacek, Kovarik, Kratochvil 2016). The calculation is done in three separate steps that calculate the following properties of the model:

- difference in elevation of adjacent pixels;
- slope change value of two adjacent pixels;
- terrain edge detection;

The whole process is conducted in the ArcGIS programming environment and uses standard features. In case of differences in altitude values and slope values, the FocalStatistic function is used to find the highest values within the selected 3×3 pixel window. The elevation difference value is calculated from the elevation model grid. The slope difference value uses raster layer slope calculated from the relief model. The obtained values are compared with the vehicle's technical parameters (climbing ability - vertical step, angle of approach).

The procedure for detecting terrain edges is more complex. The calculation is parameterized for a particular type of wheeled vehicle and uses its technical parameters (ground clearance, wheelbase). When computing, the terrain altitude in the given location is compared to the calculated altitude of the centre of the vehicle when it is in the given location (Dohnal et al 2017). The calculation takes into account all possible directions of vehicle movement. The results of the calculation are shown in figure 2. Red pixel clusters represent detected microrelief objects impassable for a specific vehicle type (Land Rover Defender in this case). An example of the real shape of the microrelief objects can be seen in the height profile created along the blue line. Two impassable upper edges (Fig. 1c) are very well visible on this profile chart (Fig 2). The microrelief

object on the left is impassable due to its relative height exceeding the maximum height of the vehicle climbing ability (Fig 1a).

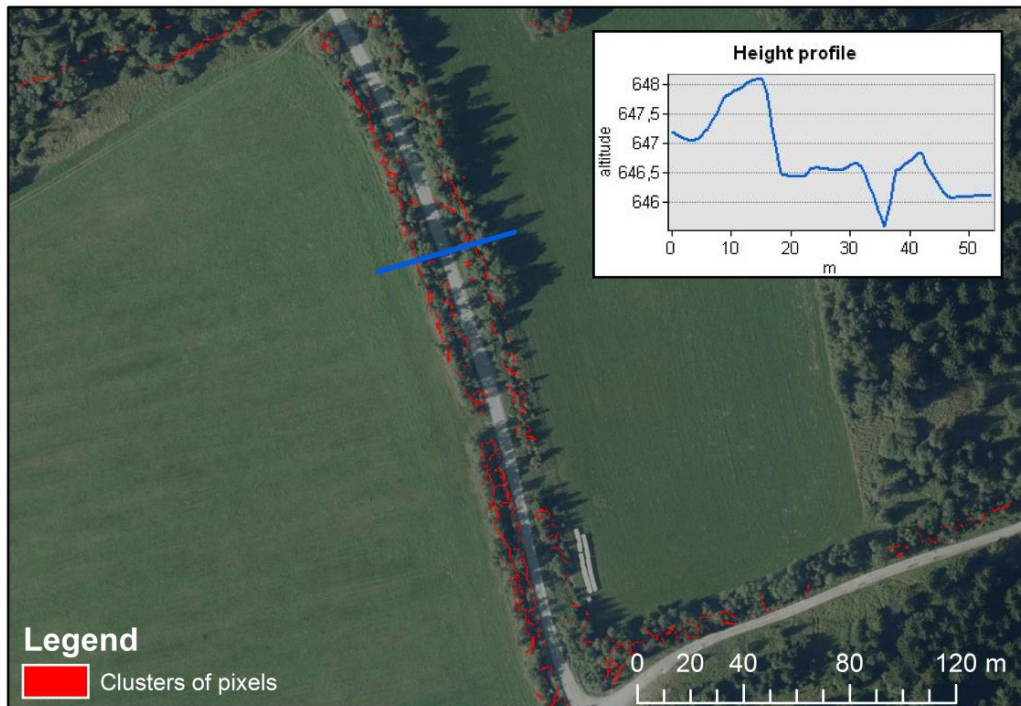


Fig. 2. The edges of the microrelief objects obtained by the described calculation

Detection of ditches from the point of view of crossing ability (trench width) has not yet been satisfactorily resolved and is the subject of further investigation. Therefore, it is not currently included in the model of influence of microrelief elements. As a result of the modelling of the effect of the microrelief, the layer containing microrelief objects non-passable for the given type of vehicle is included.

OPTIMIZATION OF CALCULATION AND VERIFICATION OF RESULTS

The above described procedure for detecting terrain edges is quite time consuming. That is why, there is effort to find the optimal method for terrain edges detection with implementation of parameterization for a particular vehicle. Based on the terrain elevation model, using the commonly available Curvature tool, convex or concave curvature of the terrain can be determined, which further influences the occurrence of the upper or lower edges of the microrelief elements. The function is used to calculate the values of the second derivation of the modelled relief pattern. However, these values must be parameterized for a particular vehicle type to detect the occurrence of non-passable edges. To find the limit value of the second derivation, a comparison of the calculated raster values with the edges detected by the method described above was performed. The comparison allowed division of the edges into passable and non-passable. For each vehicle, it is thus possible to determine the limit value of the second derivation that

divides edges into two sections. The initial results calculated for the Military Training Area (MTA) Libavá indicate that the limit value of the second derivation of elevation model for the determination of the non-passable pixel is around -0.5 (depending on the vehicle type). The spatial arrangement of pixels which value exceeds the detected value (depending on the vehicle type) forms visible line-type clusters. These then indicate the top edges of the non-passable (non-trafficable) microrelief elements in the field. This method is less demanding than previous, but its results are burdened with the same inaccuracy as the original calculation method from which it is derived.

The accuracy of the modelling is influenced by the overall accuracy of the altitude model used, the DMR 5 inaccuracies in the locations of the microrelief objects and the pixel size of the raster model. For this reason, it is necessary to verify the results based on field measurements. This activity is organizationally highly demanding. It is bound to choosing the right location, the possibility of moving the vehicles in this location and the availability of the tested vehicles. The deployment of military technology outside training facilities is in peacetime very problematic. Therefore, testing is only possible within the training areas. At the time of testing, it is necessary to have additional security (wrecker and medical) in addition to tested vehicles. Due to this fact, only partial verification has been performed. The ability of vehicles to overcome these microrelief objects was verified in the framework of comprehensive field tests at the MTA Libavá in May 2017.

Several microrelief objects were selected for verification, which were later on overcome by different types of vehicles (Fig 3). During overcoming microrelief objects by vehicles, there were found two kinds of errors:

- edge detection that the vehicle was able to overcome;
- not detecting sharp edges that vehicles were not able to overcome.



Fig. 3. Vehicles in overcoming microrelief objects during field test

In addition to verifying the results of modelling by vehicle rides, all selected microrelief objects were measured by an electronic tachymeter, and their shape was compared to the shape obtained from the DMR 5 data. The comparison was made on the measured profiles by calculating the deviations between the measured altitude and the altitude obtained from the DMR5. The

comparison confirmed the model's tendency to smooth out the terrain edges. When comparing terrain profiles measured in the field and detected from the raster model, the deviation in the critical value calculated for the measured profiles ranges from 10-25%. The magnitude of the deviation depends on the observed value, larger deviations occur in the case of perpendicular edge detection.

Currently, creating more accurate terrain model cannot be expected. In order to calculate the non-passable microrelief objects of the microrelief, it will be necessary to introduce an uncertainty in the detection of non-passable edges. However, the number of microrelief objects targeted and tested by technology is currently small for its parameterization. Therefore, it will be needed to carry out several more field verifications. At present time, the selection of suitable microrelief objects so as to affect as many representative samples of microrelief shapes as possible is carried out. The measuring is planned for the beginning of 2018.

Another significant finding that emerged from field tests was the demonstration of the driver's influence on the ability to overcome the microrelief object. Drivers with less experience in some cases have not been able to overcome some microrelief objects, even though the technical characteristics of the vehicle allow it. Parametrization of this problem will be significantly more difficult and it will not be possible without further tests using vehicles and a larger number of drivers.

DISCUSSION AND CONCLUSION

When evaluating the terrain, the landscape is assessed in its complexity. The evaluation method is dependent on the available geographic data, time options and the target audience of the results users. Different processing will be for the operational level of command during the planning of operations as opposed to processing for commander of tactical units using the results during combat control. The main elements, which contain communication, vegetation, water, settlements and relief will always be calculated. For lower levels, however, other influences are also important. These include, for example, microrelief objects. Knowledge of their spatial deployment and ability to overcome them can fundamentally influence decision-makers. Microrelief objects and the way they are deployed can be used to build barriers for defensive positions in order to direct the enemy's movements to locations suitable for focussed fire and destruction of technique, as well as to cover persons and vehicles.

New, more accurate relief models allow us to analyse the elements of the microrelief and thereby provide the commanders with the information they need to make decisions. Detecting microrelief edges and finding non-passable microrelief objects using these models is a promising way. By using the tools to calculate the curvature of the surfaces, the whole calculation was significantly speeded up. The largest time requirement is then the actual calculation of the input raster model from DMR 5 data.

The significance of the effect of the microrelief can be documented in Figure 4 and the numbers in the following indents. At the test site of 6 × 8 km area in the MTA Libavá, was for the LandRover Defender 110 calculated following:

- 6161 - detected non-passable edges longer than 2 meters
- 44 760 meters - total length of all non-passable edges
- 14.8 meters - average length of the non-passable edge
- 57 meters - maximum length of non-passable edge

Even though the DMR 5 achieves high internal accuracy, the discrepancies between the real state and the modelled reality were found in the results of microrelief modelling. Some detected microrelief objects were actually in passable, on the other hand, the suggested procedure did not detect all the non-passable objects of the microrelief. To eliminate these problems, it is necessary to determine the boundary of uncertainty in the contours of the detected microrelief objects. This approach requires measuring of microrelief objects and their comparison with the microrelief object shapes in the used terrain model. Measurements have shown so far that uncertainty values will vary according to the type of obstacle detected. The most problematic situation is in case of terrain levels detection. In this case, the model shows the biggest differences. These occur even when using a smaller pixel size in the calculation. The measurements made so far do not provide a large enough data set for determining uncertainty that range from 10 to 25%.

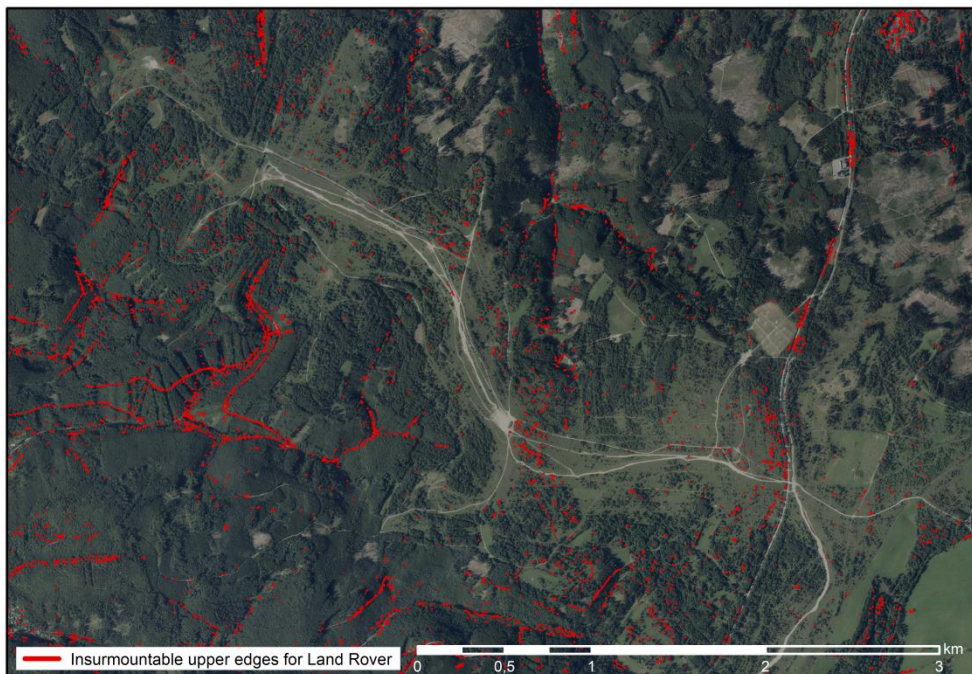


Fig. 4. Detected microrelief edges in the test area

The proposed procedure is applicable when the person analysing has an accurate digital terrain model and processes a small area (tens of kilometres or more). Problematic processing may be in the case of units deployed outside the Czech Republic. In these cases, only global elevation models such as DTED 2, SRTM or TRex are available. These models only capture microrelief objects in a very limited amount. A possible solution could be to determine the coefficients of

roughness depending on the overall roughness of the relief and the occurrence of other terrain elements such as watercourses and roads. These objects bind a significant occurrence of microrelief shapes. However, this issue will be the subject of further research to fully automate calculations and validate the uncertainty level setting in edge detection.

ACKNOWLEDGMENT

This paper is a particular result of the defence research project DZRO K-210 NATURENVIR managed by the University of Defence in Brno

REFERENCES

- Brazdil, K. et al. (2009), *Detail design elevation data processing. Technical report*, (in Czech), ZU, VGHMUr, Pardubice, Dobruska.
- Collins, J.M. (1998) *Military geography for professionals and the public*. Potomac Books, Sterling.
- Derbyshire, E., Hails, J. R., and Gregory, K. J. (1981). *Geomorphological Processes: Studies in Physical Geography*. Butterworth, London.
- Dictionary.com, www.dictionary.com/browse/microrelief, (December 15, 2017).
- Dohnal, F., Hubacek, M., Sturcova, M., Bures, M. and Simkova, K. (2017). Identification of microrelief shapes along the line objects over DEM data and assessing their impact on the vehicle movement. In: *International Conference on Military Technology (ICMT). Brno 31 May – 2 June*, IEEE, Brno, p. 262-267.
- Freebairn, D. M., and Gupta, S. C. (1990). Microrelief, rainfall and cover effects on infiltration. *Soil and Tillage Research*, 16(3), pp. 307-327.
- Hubacek, M., Kratochvil, V., Zerzan, P., Ceplova, L. and Brenova, M. (2015). Accuracy of the new generation elevation models. In: *International Conference of Military Technologies (ICMT), Brno, 19 – 21 May*. IEEE, Brno, pp. 289-294.
- Hubacek, M; Kovarik, V. and Kratochvil, V. (2016). Analysis of influence of terrain relief roughness on DEM accuracy generated from LIDAR in the Czech Republic territory. In: *Int. Arch. Photogramm. Remote Sens. Spatial Inf. Sci., Praha, 12-19 July*, ISPRS, Praha, pp. 25-30.
- Land Survey Office. DMR4, Digital Terrain Model of the Czech Republic of the 4th generation, <http://geoportal.cuzk.cz> (December 15, 2017).
- Land Survey Office. DMR5, Digital Terrain Model of the Czech Republic of the 4th generation, <http://geoportal.cuzk.cz> (December 15, 2017).
- Merriam-Webster, <https://www.merriam-webster.com/dictionary/microrelief> (December 15, 2017).
- Monkhouse, F. J. (2014). *Principles of physical geography*. Rowman & Littlefield. Lanham.
- Oxford University Press, <https://en.oxforddictionaries.com/definition/microrelief>, (December 15, 2017).
- Römken, M. J., Helming, K., and Prasad, S. N. (2002). Soil erosion under different rainfall intensities, surface roughness, and soil water regimes. *Catena*, 46(2), pp. 103-123.

- Rudolph, A., Helming, K., and Diestel, H. (1997). Effect of antecedent soil water content and rainfall regime on microrelief changes. *Soil technology*, 10(1), pp. 69-81.
- Rybansky M (2009) *The cross-country movement—the impact and evaluation of geographic factors*. CERM, Brno.
- Rybansky, M. (2014). Modelling of the optimal vehicle route in terrain in emergency situations using GIS data. In: *8th International Symposium of the Digital Earth, Kuching, 26-29 August*. IOP Publishing, Kuching, pp. 21- 31.
- Sobotka, J. (2012) Comparison of elevation data of the Czech Republic for design military constructions, *Advances in Military Technology*, 7(2), pp. 57-63.
- Talhofer, V., Hoskova, S. and Hofmann, A. (2016). Towards efficient use of resources in military: methods for evaluation routes in open terrain. *Journal of Security Sustainability Issues*, 6(1), pp. 53-70.
- VUGTK, https://www.vugtk.cz/slovník/5672_mikrorelief (December 15. 2017) in Czech